THE PATHOGENESIS OF SPONTANEOUS AUTOIMMUNE PERIPHERAL POLYNEUROPATHY: THE NOD.B7-2$^{-/-}$ MOUSE AS A MODEL FOR GUILLAIN BARRÉ SYNDROME

By

Barbie J. Gadsden

A DISSERTATION

Submitted to
Michigan State University
in partial fulfillment of the requirements
for the degree of

Comparative Medicine and Integrative Biology—Doctor of Philosophy

2016

ABSTRACT

THE PATHOGENESIS OF SPONTANEOUS AUTOIMMUNE PERIPHERAL POLYNEUROPATHY: THE NOD.B7-2$^{-/-}$ MOUSE AS A MODEL FOR GUILLAIN BARRÉ SYNDROME

By

Barbie J. Gadsden

Guillain Barré Syndrome (GBS) is a symmetrical ascending paralysis that often follows viral or bacterial infection. The foodborne pathogen *Campylobacter jejuni* is the most common infection that triggers GBS, but *C. jejuni* is mainly linked to one variant within a complex syndrome: Acute Motor Axonal Neuropathy (AMAN). One third of AMAN patients have IgG autoantibodies against neurogangliosides GM1 and GD1a; binding of these antibodies to peripheral nerves is thought to initiate nerve damage. Other GBS variants include Acute Inflammatory Demyelinating Polyneuropathy (AIDP), Acute Motor and Sensory Axonal Neuropathy (AMSAN), and Miller Fisher Syndrome (MFS). The triggers for these disorders are not known and a large number of potential infectious and noninfectious initiating causes have been implicated. In addition to *C. jejuni*, bacteria such as *Mycoplasma pneumonia* and *Haemophilus influenzae* and viruses such as Cytomegalovirus and Influenza have been associated with GBS.

GBS disease is monophasic; recurrence is rare, but has been reported. Patients in the initial stages of GBS report headache and joint pain. Tingling and numbness of extremities is followed by segmental ascending paralysis. Pain involving the extremities occurs later in the course of the disease and can be directly correlated with disease severity. The worst manifestation is paralysis of the muscles of respiration necessitating artificial respiration. Some GBS cases resolve, however, recent reports indicate that 20% of patients struggle with continuing disabilities. There is no cure and the death rate is ~5%. Currently, treatment is symptomatic and consists of plasmapharesis and

assisted ventilation for those patients with respiratory distress demonstrating the need for new approaches.

In the AMAN form of GBS, molecular mimicry is thought to play a role in the production of anti-ganglioside antibodies, which bind to and trigger attack on host nerve tissue. Both in humans and in animal models, the immune response to the bacterium results in production of anti-ganglioside antibodies that leads to damage of nerves and Wallerian-like degeneration; such “autoantibodies” have been shown to bind to motor neurons, nodes of Ranvier, and neuromuscular junctions. Little progress has been made in understanding the pathogenesis of GBS and even less in developing effective therapies, largely because of the lack of tractable animal models that mimic natural human disease.

Susceptible inbred mice would provide the ideal model in which the interplay of host and pathogen genetics in GBS pathogenesis could be explored. Non-Obese Diabetic (NOD) inbred mice have been documented to develop autoimmune diabetes mediated by auto-reactive T cells infiltrating the pancreas as well as autoimmune diseases of the salivary glands and thymus. Additionally, NOD mice deficient for the co-stimulatory molecule B7-$2^{-/-}$ are largely protected from autoimmune diabetes but develop a spontaneous autoimmune peripheral polyneuropathy (SAPP) called chronic inflammatory demyelinating polyradiculoneuropathy (CIDP) that resembles GBS.

A mouse model of Spontaneous Autoimmune Peripheral Polyneuropathy (SAPP) that mimics many aspects of human GBS has been identified. The short term goal of this body of work is to characterize the inflammatory responses that result in this spontaneous murine GBS with peripheral nerve lesions and to begin to determine mechanisms leading to this endpoint. The overarching goal is to use this mouse model to manipulate the onset and clinical severity of the disease, and screen new potential treatments for GBS that could reduce morbidity and mortality in human patients.

TABLE OF CONTENTS

LIST OF TABLES ix

LIST OF FIGURES x

KEY TO ABBREVIATIONS xiv

CHAPTER 1 1
INTRODUCTION 1
GUILLAIN BARRE SYNDROME OVERVIEW 2
Clinical Variants (Subtypes) of GBS 3
GBS Epidemiology 5
Pain in Guillain Barré Syndrome 5
Treatment Options for Guillain Barré Syndrome 6
Mechanism of Molecular Mimicry 8
Campylobacter jejuni and Guillain Barré Syndrome 8
Influenza Vaccine and Guillain Barré Syndrome 9
Clinical Trials for Guillain Barré Syndrome 10
Animal Models of Guillain Barré Syndrome 10
Remaining Gaps in GBS Research 11
Chronic Inflammatory Demyelinating Polyradiculoneuropathy 12
DISCUSSION 14
STUDY RATIONALE 15
SPECIFIC AIMS 17
Specific Aim 1 17
Experiment 1 17
Hypothesis 1 17
Hypothesis 2 17
Experiment 2 17
Hypothesis 17
Specific Aim 2 17
Experiment 3 17
Hypothesis 17
Experiment 4 17
Hypothesis 18
Specific Aim 3 18
Experiment 5 18
Hypothesis 18
Experiment 6 18
Hypothesis 18
Experiment 7 18
Hypothesis 18
BIBLIOGRAPHY 19

CHAPTER 2 24
NOD B7-2$^{-/-}$ Mice as a Working Model for Acute Inflammatory Demyelinating Polyneuropathy (AIDP): A Standardized Approach to Phenotyping Reveals New Clinical Features of Spontaneous Autoimmune Peripheral Polyneuropathy 24

ABSTRACT 25
INTRODUCTION 26
RATIONALE 30
Hypothesis 1 30
Hypothesis 2 30
RESULTS 32
Experiment 1 32
Experiment 2 33
Flow Cytometry 34
DigiGait 34
MATERIALS AND METHODS 35
Animals 35
Experimental Design 1. SAPP onset and frequency of disease. 35
Experimental Design 2. Targeted age screen study. 36
Open Field Test (OFT) 36
DigiGait 36
Euthanasia and Necropsy 37
Peripheral Nervous Tissue Removal Technique 38
Tissue Processing for Histologic Evaluation 39
Tissue Processing for Plastic Embedding 39
Evaluation of Axon Counts and Area of Large Myelinated Axons 40
Histopathology 40
Flow Cytometry 41
Statistical Analysis 42
DISCUSSION 43
ACKNOWLEDGEMENTS 47
APPENDIX 48
BIBLIOGRAPHY 59

CHAPTER 3 62
Blocking Cytokines and Crossing Strains 62
CHAPTER 3, SECTION 1 62
Get Lost Interleukin-17 and Interferon gamma! 63
INTRODUCTION 64
RATIONALE 67
Hypothesis 67
RESULTS 68
Open Field Test (OFT) 68
Grimace, Dyskinesia, and Tremors 69
DigiGait 70
Histopathology 72
Bone Scans 72
MATERIALS AND METHODS 73
Mouse Breeding and Handling 73
Cytokine Neutralizing Treatment Regiment 73
Intraperitoneal Injections 74
Open Field Test (OFT) 74
Histopathology 74
DigiGait 75
Bone Density and Architecture Measurement 75
Statistical Analysis 75

DISCUSSION 76
CHAPTER 3, SECTION 2 78
Let's Cross Over to the Dark Side 78
ABSTRACT 79
INTRODUCTION 80
RATIONALE 82
RESULTS 83
Clinical Disease 83
Open Field Test (OFT) 83
Hang Test 83
Histopathology 84
MATERIALS AND METHODS 85
Mouse Breeding and Handling 85
Hang Test 85
Open Field Test (OFT) 86
Assessing for Diabetes 86
Histopathology 86
DISCUSSION 87
ACKNOWLEDGEMENTS 89
APPENDIX 90
BIBLIOGRAPHY 145

CHAPTER 4 149
Altering the Intestinal Microbiota via Cecal Transfer 149
ABSTRACT 150
INTRODUCTION 151
RATIONALE 153
Hypothesis 153
RESULTS 154
Open Field Test (OFT) 154
Grip Test, Dyskinesia, and Grimace 154
Histopathology 155
Body Weight and Plasma Hormone Concentration 156
16s Sequencing 156
MATERIALS AND METHODS 158
Mouse Breeding and Husbandry 158
Preparation and Delivery of Cecal Inoculum 158
Cecal Content Inoculation 158
Open Field Test 159
Histopathology 159
Hormone ELISA Assays 160
Estradiol 160
Testosterone 160
MiSeq™ and Mothur Sequencing of Fecal Samples 161
DISCUSSION 162
ACKNOWLEDGEMENTS 165
APPENDIX 166
BIBLIOGRAPHY 183

CHAPTER 5 185
Investigating the Role of Sex Hormones in Spontaneous Peripheral Polyneuropathy: A pair of pilot studies 185
ABSTRACT 186
INTRODUCTION 187
RATIONALE 189
Ovariectomy 189
Hypothesis 189
Blocking Testosterone with Flutamide 189
Hypothesis 189
RESULTS 190
Ovariectomy Study 190
Open Field Test (OFT) 191
Histopathology 191
Testosterone 191
Flutamide Study 192
Open Field Test (OFT) 192
Histopathology 193
Estradiol 194
MATERIALS AND METHODS 195
Mouse Breeding and Handling 195
Ovariectomy 195
Open Field Test OFT) 196
Histopathology 196
Hormone ELISA Assays 197
Estradiol 197
Testosterone 198
Flutamide Preparation and Injection 198
Statistical Analysis 199
DISCUSSION 200
ACKNOWLEDGEMENTS 205
APPENDIX 206
BIBLIOGRAPHY 233

CHAPTER 6 235
FUTURE DIRECTIONS 235
Phenotype Tests with Quantitative Measures 236
Motor Function 236
Sensory Disturbances 237
Germfree Mice 238
Regulatory Cytokines 238
The Role of B7-2 238
Gene Expression Studies 239
Earlier Ovariectomy Timepoint 240
Castration for Removal of Testosterone Influence 240
Data Analysis (group vs individual) 240

LIST OF TABLES

Table 3.1	Experimental Groups for the Cytokine Blocking Study	91
Table 4.1	OTU and inoculum comparison	182

LIST OF FIGURES

Figure 2.1.	Clinical signs of SAPP	49
Figure 2.2	Histopathology of female peripheral nervous system	50
Figure 2.3	Histopathology of male peripheral nervous system	51
Figure 2.4	Histopathology of the peripheral nervous system of SAPP mice	52
Figure 2.5	Histopathology results for mice from the age screening study	53
Figure 2.6	Results of flow cytometry from 41-week-old B7-2$^{-/-}$ mice	55
Figure 2.7	Stance width in females as measured by DigiGait	56
Figure 2.8	DigiGait paw area in females	57
Figure 2.9	DigiGait stride length in females	58
Figure 3.1	Scatterplots of number of rears over time	92
Figure 3.2	Female mice rears compared by age	94
Figure 3.3	Male mouse rears compared by age	96
Figure 3.4	Dyskinesia in females	98
Figure 3.5	Dyskinesia in males	99
Figure 3.6	Facial grimace in females	100
Figure 3.7	Facial grimace in males	101
Figure 3.8	Tremors in females	102
Figure 3.9	Tremors in males	103
Figure 3.10	DigiGait front stance width	104
Figure 3.11	DigiGait hind stance width	106
Figure 3.12	Front stance comparison by treatment group in females	108
Figure 3.13	Front stance comparison by treatment group in males	109
Figure 3.14	Left hind paw area over time	110
Figure 3.15	Right hind paw area over time	112

Figure 3.16	Left forepaw area over time	114
Figure 3.17	Right forepaw area over time	116
Figure 3.18	Histopathology of males and females	118
Figure 3.19	Open field test rears over time in males and females	119
Figure 3.20	Rears, pairwise comparisons	120
Figure 3.21	Dyskinesia, males and females	122
Figure 3.22	Facial grimace, males and females	124
Figure 3.23	Hang test, males and females	126
Figure 3.24	Pairwise comparisons of hang time	127
Figure 3.25	Grip compensation on the hang test	129
Figure 3.26	Histopathology of the pancreas	130
Figure 3.27	Histopathology of the brachial plexus	131
Figure 3.28	Tremors, males and females	132
Figure 3.29	Body weight changes over time	134
Figure 3.30	Bone, trabecular number	135
Figure 3.31	Bone, trabecular thickness	136
Figure 3.32	Bone, trabecular separation	137
Figure 3.33	Bone volume fraction	138
Figure 3.34	Bone, average cortical thickness	139
Figure 3.35	Bone, cortical area	140
Figure 3.36	Bone, total cross sectional area inside the periosteum	141
Figure 3.37	Bone, marrow area	142
Figure 3.38	Bone, cortical area fraction	143
Figure 3.39	Femur length	144
Figure 4.1	Scatterplots of rears, weekly time points	167
Figure 4.2	Pairwise comparisons of rears	168

Figure 4.3	Grip test results	170
Figure 4.4	Grip deficits over time	172
Figure 4.5	Dyskinesia evaluation over time	173
Figure 4.6	Grimace responses	174
Figure 4.7	Facial grimace over time	176
Figure 4.8	Heat map showing of clinical signs	177
Figure 4.9	Scatterplot of histopathology	178
Figure 4.10	Mouse weights	179
Figure 4.11	PCA plot of fecal sample distribution and clustering	180
Figure 4.12	Plot showing bacterial OTU change	181
Figure 5.1	Ovariectomy setup	207
Figure 5.2	Number of rears over time	208
Figure 5.3	Rears at each time point	209
Figure 5.4	SAPP affected mouse clinical signs	211
Figure 5.5	Dyskinesia at each time point	212
Figure 5.6	Evaluation of hind limb grip at each time point	214
Figure 5.7	Evaluation of pain by facial grimace response	216
Figure 5.8	Heat map of combined phenotyping test results	218
Figure 5.9	Histopathology scores	219
Figure 5.10	Number of rears over time	220
Figure 5.11	Rears at each time point	221
Figure 5.12	Dyskinesia at each time point	223
Figure 5.13	Hind limb grip at each time point	225
Figure 5.14	Facial grimace response	227
Figure 5.15	Paw licking response	229
Figure 5.16	Heat map of combined phenotyping test results	231

Figure 5.17 Histopathology and Estradiol of Flutamide treated males 232

KEY TO ABBREVIATIONS

GBS	Guillain Barre Syndrome
CSF	Cerebrospinal fluid
CIDP	Chronic Inflammatory Demyelinating Neuropathy
AIDP	Acute Inflammatory Demyelinating Polyneuropathy
AMAN	Acute Motor Axonal Neuropathy
AMSAN	Acute Motor and Sensory Axonal Neuropathy
MFS	Miller Fisher Syndrome
LOS	Lipooligosaccharide
IgG	Immunoglobulin
PE	Plasma exchange
IVIgG	Intravenous Immunoglobulin G
EAN	Experimental Autoimmune Neuritis
EAE	Experimental Autoimmune Encephalitis
PNS	Peripheral Nervous System
AvIDP	Avian Inflammatory Demyelinating Polyneuropathy
MMN	Multifocal Motor Neuropathy
SAPP	Spontaneous Autoimmune Peripheral Polyneuropathy
DRG	Dorsal Root Ganglion
US	United States
MHC	Major Histocompatibility Complex
TCR	T Cell Receptor
T reg	T regulatory
IV	Intravenous
IDDM	Insulin Dependent Diabetes Mellitus

WT	Wild Type
AIRE	Autoimmune regulator
APECED	Autoimmune Polyendocrinopathy Ectodermal Dystrophy
ICAM 1	Intracellular Adhesion Molecule 1
FMT	Fecal microbial Transfer
IBD	Inflammatory Bowel Disease
IBS	Inflammatory Bowel Syndrome
GF	Germfree
SLE	Systemic Lupus Erythematosus
RA	Rheumatoid Arthritis
MS	Multiple Sclerosis
IL 1	Interleukin 1
IL 6	Interleukin 6
TNFa	Tumor Necrosis Factor alpha
TH2	T helper 2
TH1	T helper 1
OVX	Ovariohysterectomy

CHAPTER 1

INTRODUCTION

GUILLAIN BARRE SYNDROME OVERVIEW

In 1859, the first report of an ascending paralysis with poor prognosis was published. The French manuscript, written by Jean Baptiste Octave Landry de Thezillat, described the clinical picture and prognosis of ten patients who exhibited varying degrees of ascending paralysis, with or without the loss of pain sensation. Landry discussed the fact that there was not enough evidence to ascribe the clinical disease presentation to one particular etiology. After his initial report, such presentations were referred to as “Landry’s Paralysis (1, 2). The term “ascending paralysis was coined by Landry and ever since then, it has remained the classic clinical descriptor of what has since gone on to be known as Guillain Barré Syndrome (GBS). Fifty-seven years went by before there was another peer-reviewed report that described similar clinical findings to Landry’s 1859 report. In 1916, Georges Guillain, Jean-Alexandre Barré, and André Strohl published a paper describing acute onset of paralysis in two soldiers. Interestingly, they made no reference to Landry’s report in their findings. In fact, the authors stated that their disease had a much better prognosis than Landry’s report. Cerebrospinal fluid (CSF) obtained from a lumbar spinal tap of the case subjects contained an increased amount of albumin, but without the accompanying increase in absolute cell number (1, 2). This phenomenon is termed albuminocytologic dissociation, and is now accepted as a hallmark finding in GBS. Over the years, the GBS literature has grown, with the syndrome now distinctly characterized as different subtypes (variants) that often overlap, and make diagnosis and treatment difficult (3).

Guillain Barré Syndrome reported to occur symmetrically and often follows viral or bacterial infection. The disease course is variable, and although prognostic indicators are helpful, they are not 100% predictive. It is considered a neurologic emergency. Lumbar CSF tap and serial electrophysiological nerve conduction studies are the gold standard for a definitive diagnosis (4). GBS is monophasic. Recurrence is rare, but has been reported in 2-5% of affected individuals. Some patients have had up to 5 recurrent episodes (5). Death occurs in 5%

of patients (6). The average time for recurrences ranges from 4-8 years after the initial episode, with each recurrence occurring within a shorter interval of time. Patients less than 30 years of age are predisposed to repeated GBS episodes. Careful efforts must be made by medical personnel not to incorrectly diagnose GBS as Chronic Inflammatory Demyelinating Polyneuropathy (CIDP), or, fluctuations in GBS presentation secondary to treatment as a recurrent episode (5).

Clinical Variants (Subtypes) of GBS

GBS is divided into clinical variants where different mechanisms are at work to produce disease. It is important to remember that these forms can overlap, and may even progress to CIDP (7, 8). In North America and Europe, the most common variant of GBS is Acute Inflammatory Demyelinating Polyneuropathy (AIDP), with up to 90% of patients affected with this form. The axonal variants, Acute Motor Axonal Neuropathy (AMAN) and Acute Motor and Sensory Axonal Neuropathy (AMSAN) are only responsible for 5% of presenting cases. In Asia and Mexico, 30-65% of people develop AMAN, compared to only 6-7% in Spain (9, 10). Rare forms, or those referred to as “atypical GBS”, include Miller-Fisher Syndrome (MFS), and the Oropharyngeal variant. Both have a high association with autoantibodies to GQ1b and GT1a.

Acute Inflammatory Demyelinating Polyneuropathy (AIDP) is the most common GBS variant in America and West Europe. As the name implies, it is a demyelinating polyneuropathy that has been associated with Cytomegalovirus infection and circulating autoantibodies against GM2. The pathology that is presented dates back to the early descriptions published in the literature as Idiopathic Polyneuritis (11). The main target in AIDP is thought to be gangliosides located on the myelin sheath. The axons are damaged indirectly and suffer what is referred to as “bystander injury” (12). The light microscopic lesions are most well described for this variant of GBS. Characteristic pathology in the nerve is secondary to the infiltration of T lymphocytes and macrophages, with macrophages denuding and ingesting myelin. These lesions are seen in both

motor and sensory nerves, as well as the spinal roots (11, 13, 14). Pain, cranial nerve dysfunction, and autonomic nervous system complications are not uncommon (15).

Acute Motor Axonal Neuropathy (AMAN) occurs secondary to infections with certain strains of *Campylobacter jejuni* that contain lipo-oligosaccharide (LOS) similar to gangliosides found on human peripheral nerve axons (16, 17). In one third of patients, the clinical phenotype is accompanied by IgG antibodies against the peripheral nerve gangliosides GM1, and GD1a, and Gal-Nac-Gd1a (18). With the exception of 10% of patients, this subtype of GBS only affects the motor axons (19).

Acute Motor and Sensory Axonal Neuropathy (AMSAN) is considered to be a severe form of GBS with a very poor prognosis. Sensory and motor nerve fibers are affected in AMSAN. Pathologic lesions are present in the dorsal and ventral roots, and consist of Wallerian degeneration with large numbers of macrophages located at the Node of Ranvier (18).

Miller-Fisher Syndrome (MFS) primarily affects the cranial nerves that control eye movement—the abducens, trochlear, and oculomotor nerves. These nerves are rich in the ganglioside GQ1b, and 5% of MFS patients have circulating autoantibodies against GQ1b. They often also experience mild ataxia. The human monoclonal antibody Eculizumab, has been shown to block the onset of MFS by inhibiting the complement component C5 from being cleaved into C5a and C5b (20).

In 2014, Wakerly et.al. proposed a new classification scheme for GBS and MFS. Along with Nobuhiro Yuki, a pioneer in the field of GBS research, and several other experts, he believes that using a defined set of clinical features is more definitive than just a distinction between a primary demyelinating or axonal insult. They propose grouping the clinical disease presentation based on the presence or absence of ataxia and hypersomnolence, along with the anatomical pattern of weakness upon presentation to a medical facility. Nerve conduction studies and testing for anti-ganglioside antibodies are omitted from the criteria, as the authors

believe that these parameters are often inaccurate and can be misleading early in the disease presentation.

GBS Epidemiology

GBS occurs in 0.81-.089 per 100,000 people (15). In Western countries, 1-2 per 100,000 people develop GBS (6, 21). The incidence of Miller Fisher Syndrome (MFS) is a little less, with 0.4-0.6 individuals per 100,000 affected (3). Men and geriatric patients are preferentially affected (21-23). It is difficult to get obtain accurate data regarding the number of GBS cases because there is no specific biomarker for his syndrome and there are different criteria used for case definition (23). Seasonal occurrences have been reported in the literature, but no associating cause has been proven in most of those cases. In China, GBS has a seasonal summer occurrence; the onset is known to follow intestinal disease caused by drinking contaminated water (22). Brazil sees higher cases in the spring/summer months and the Netherlands have more reported cases in the winter months (24, 25). In a 2014 meta-analysis, Webb and colleagues identified preceding periods of diarrheal illness in all cases of AMAN. The authors mention a public health significance and the need to pinpoint the exact occurrences or favorable conditions in which the intestinal disease develops. If those conditions can be prevented, then it's possible that the number of GBS cases secondary to seasonal outbreaks will decrease (26).

Pain in Guillain Barré Syndrome

Many patients experience pain during GBS. However, there is not much research in the area of pain and its association to GBS. It's currently accepted that the immune system is directly responsible for pain secondary to inflammation in the peripheral nervous system, but the actual mechanisms haven't been completely explored. The way that pain presents during the course of the disease is variable and it changes as the disease progresses (27). Up to

89% of GBS affected people experience pain (15). At the beginning of the disease, the most commonly reported areas are the joints and lumbar region. The lumbar pain is attributed inflammation of the spinal roots (28). Headaches are reported uncommonly, but are often associated with Miller Fisher Syndrome. Moderate to severe pain involving the extremities and the back pain occurs later in the course of the disease. Some researchers believe that pain later in the disease can be directly correlated with disease severity. In an intensive longitudinal study using answers to survey questionnaires completed by attending neurologists, 170 GBS patients included in a prospective study reported their pain throughout the course of their GBS. In the early stages, pain was often first experienced two weeks before weakness occurred. In the recovery/chronic phases, it was reported at the same time that patients were experiencing fatigue. Pain was reported up to a year after the onset of disease in 1/3 of patients. The most common location was the arms and legs. Pain was present regardless of the variant of GBS that a person experienced, although it was more common in patients with sensory deficits. In atypical GBS cases (MFS), the neck and head were the most commonly reported locations (27, 29). The authors concluded that in addition to overt nerve pain, small c fibers may also have a role in the generation of the painful areas. Many patients that experienced pain also had abnormal results with heat and cold detection (30). The authors identify a study limitation as physicians not accounting for the mental state of the patient as the disease progressed. It is now known that there are mental derangements in the first several weeks after disease onset (31).

Treatment Options for Guillain Barré Syndrome

There is no cure for Guillain Barré Syndrome. A major impediment to a cure is the vast number of potential infectious and noninfectious initiating causes, along with an incomplete understanding of the pathogenesis. Up to 25% of patients experience respiratory complications and are placed on ventilators (6). Ventilator associated pneumonia secondary

to GBS is not an uncommon cause of death in these patients (9). Residual complications (fatigue, pain, and muscle weakness) are present in 20% of patients and 5-10% die (26, 32, 33).

Current treatment involves a combination of immunotherapy and supportive care. Plasmapharesis, also known as plasma exchange (PE) therapy, intravenous immunoglobulin (IVIg) therapy, and immunoabsorption are the three forms of immunotherapy used consistently to treat GBS.

The use of PE therapy was first published in 1978, and shortly thereafter, it became the gold standard of treatment for GBS. The results of this treatment are favorable, and patients show a significant improvement on the GBS disability scale, over the course of a year following completion of the treatment. The typical exchange treatment regimen ranges from 5-7.5 plasma exchanges over two weeks. During each treatment, the patient receives 1-1.5 plasma volume exchanges. This process rids the plasma of self-reactive antibodies and their accompanying inflammatory components. PE has its greatest favorable outcome if it's started within 2 weeks of GBS onset. Only two PE treatments are sufficient to decrease the time to motor recovery in patients that that are able to walk without assistance. The limitation to PE is that it is not available in all hospitals.

Intravenous Immunoglobulin G (IVIg) therapy was introduced as an immunotherapeutic treatment in 1988. The latest review shows that IVIg is just as effective as PE therapy. However, in contrast to PE therapy where treatment can be initiated within 4 weeks, there is less of a window with IVIg. It needs to be initiated within two weeks of the start of weakness. Five continuous days of IVIg therapy at a dose of 04g/kg is equivalent to two weeks of PE. In addition, the dose can be increased to 1g/kg body weight, which shortens the treatment course to 2 days. IVIg is now the preferred treatment of choice because its ease of administration and short dosing times has proven to be more effective. There is no scientific proof that a combined treatment of both PE therapy and IVIg are better than just one of the treatments alone(13).

The use of corticosteroids has also been employed in some cases. In higher doses, methylprednisone has been shown to be effective when used in combination with IVIg therapy. Patients are given this therapy when they are unable to walk for 10 minutes without assistance (15). The majority of treatment trials reported in the literature are in areas where AIDP is the most common subtype. The results should be interpreted, and conclusions should be made in light of the paucity of AMAN cases in the regions in which the studies were conducted.

Mechanism of Molecular Mimicry

Molecular mimicry is associated with many autoimmune diseases—those that are currently correlated with a previous infectious agent and those that aren't. Guillain Barré Syndrome, Systemic Lupus Erythematosus, Rheumatoid Arthritis, Myasthenia Gravis, and Multiple Sclerosis are just a surface scratch when identifying diseases that result secondary to a breakdown in central or peripheral tolerance, which subsequently allows lymphocytes to misdirect the inflammatory response. In central tolerance, naïve T cells in the developing thymus are exposed to self-antigens. Those that respond positively are deleted. In some cases, the amount of antigen presented is not enough to activate the cell, so it doesn't respond in neither the central, nor peripheral tolerance compartment. These cells are dubbed "ignorant", and since their activating antigen is unknown, it is referred to as "cryptic".

***Campylobacter jejuni* and Guillain Barré Syndrome**

Campylobacter jejuni is the most common antecedent infection associated with the development of GBS, specifically the AMAN subtype. It is a gram negative rod, found as a commensal in the chicken intestine. It causes gastrointestinal disease in humans and is

transmitted through the ingestion of undercooked chicken, contaminated water, or unpasteurized milk (33). Nyati and colleagues report that 25-40% of patients with GBS are infected with Campylobacter before the onset of neurologic symptoms (34). The currently

proposed mechanism is molecular mimicry between the lipooligosaccharide (LOS) present on the outer surface of the bacterial cell wall and the gangliosides located on the surface of human peripheral nerves. The onset of GBS begins 1-3 weeks after patients clear the Campylobacter infection. The host immune system is tricked into thinking that the bacteria is still present because T cells recognize epitopes from self-gangliosides as foreign. In addition to *C.jejuni*, *Mycoplasma pneumoniae* and *Haemophilus influenzae* are bacteria that have also been associated with GBS. Viruses implicated in cases of GBS include Cytomegalovirus and Influenza. The mechanisms of all of the antecedent infections have not been completely elucidated, and some causes cover a broad spectrum of disorders and leave the door open for much speculation.

Influenza Vaccine and Guillain Barré Syndrome

The most common viral pathogen associated with GBS is Influenza, both infection and vaccination. However, the effect of vaccination on the development of GBS is contradictory in the literature. The Spanish Flu of 1918 affected up to 40% of the world's population for two years. Isolated reports of "polyneuritis" followed this pandemic (19, 35). Increased reports of GBS surfaced in 1977 during the season of vaccination against "swine flu" strain A/NJ/76, but later proved to be of no concern (3, 6, 36, 37). In 2009, a similar concern arose regarding the H1N1 vaccine, but the incidence was determined to be only 1.6 per 1 million vaccinated people (15). It's currently accepted that the risk of GBS secondary to Influenza vaccine is low, but patients are still warned of the possibility. More recently, Martin and colleagues identified a significant increase associated with the risk of GBS secondary to vaccination (38).

GBS is 4-7 times more likely to follow Influenza infection than vaccination (39) . Two separate studies that assessed an Influenza database in the United Kingdom concluded that there is an increased incidence of GBS cases reported after an Influenza-like illness, but no association after vaccination (40, 41). Evidence of preceding infection has been identified via

serologic testing (35). The AMAN form has been reported after active H1N1 infection (42, 43). The proposed pathogenesis of GBS secondary to Influenza is similar to the molecular mimicry that occurs after *C. jejuni* infection. Additional antecedent infections that have been associated with GBS include cytomegalovirus and Epstein-Barr Virus (3).

Clinical Trials for Guillain Barré Syndrome

Patients are currently being recruited for the National Institutes of Health (NIH) International Guillain-Barré Syndrome Outcome Study (IGOS) (https://www.gbsstudies.org/home). This clinical trial focuses on the clinical and biologic factors that contribute to the disease, as well as the fate of the affected participants. This proposed body of works expects to obtain results useful for those who investigate GBS, as well as other researchers around the globe.

Animal Models of Guillain Barré Syndrome

To date, there are several rodent models of GBS in the literature. The most commonly studied is the Lewis rat, which can be induced to have Experimental Allergic Neuritis (EAN). It has the most longevity in GBS studies, as EAN is said to clinically mimic GBS. In 1979, it was first described as an inducible model, by injecting myelin proteins from various animals. It was a screening study to determine which species specific myelin would induce neuritis, separate from clinical signs induced in Lewis Rats with Experimental Autoimmune Encephalitis (EAE). Injections of whole peripheral nervous system (PNS) myelin were administered to the rats, along with Freund's incomplete adjuvant in the hind footpad. The same procedure was followed with other strains of rats (Wistar, Buffalo, Brown Norway, and Sprague-Dawley) that showed less severe clinical disease and were deemed not as good of a model as the Lewis rat. In addition to PNS myelin, myelin protein P2 has also been shown to induce EAN in Lewis Rats.

A cohort of juvenile white Leghorn chickens that were found be afflicted with a spontaneous inflammatory peripheral neuropathy were enrolled in a study to investigate the disease characteristics. Secondary to the identification of lymphocytes and histiocytes in the cranial nerves, and cervical and lumbrosacral nerve roots, the disease was given the name Avian Inflammatory Demyelinating Polyradiculoneuropathy (AvIDP). While on the surface, these birds look like a good model, there is no way to determine which chickens will develop disease (44). Other insufficient mouse models are being used in GBS research, but they come with complications such as additional autoimmune diseases and central nervous system lesions. This will further be discussed in Chapter 2.

As the understanding of peripheral neuropathy in rodents became clearer, other models began to be visible in the literature. In 2001, Salomon and colleagues first described an inflammatory condition in the peripheral nerves of NOD.B7-2 knockout mice. Beginning at 20 weeks of age, the female mice begin to exhibit gait deficits, manifested clinically as paralysis of the hind limbs, with an increasing severity that culminates in “generalized limb paralysis.” The reason for the gender bias in this disease is unknown, and to date, has not been investigated. SAPP does not affect the central nervous system. The B7-2 knockout mice have been found to have a high circulating autoantibody concentration of P0 protein by the time they reach 4 months of age. *In vivo* experiments showed that neonatal Schwann cells were autoreactive to P0 protein from mice at ages 4, 6, and 8 months(20). No autoreactivity was observed at 2 months.

Remaining Gaps in GBS Research

Because of the remarkable recovery rate of patients that experience GBS, tissues for histopathologic evaluation are scarce. Those patients that do succumb to the syndrome usually do not undergo an autopsy, as the cause of death is presumed to be GBS. However, the nerve lesions are well described, and are strikingly different for AIDP and

AMAN. AIDP is characterized by infiltration of the peripheral nerves, with lymphocytes and macrophages. Myelin degeneration is also evident. In AMAN, there is no presence either of lymphocytes and no evidence of an acute inflammatory response.

Chronic Inflammatory Demyelinating Polyradiculoneuropathy

One of the most common clinical copycats of GBS is Chronic Inflammatory Demyelinating Polyneuropathy. However, unlike GBS, CIDP is very treatable and is not necessarily considered an emergency. The prevalence rate is 1-9 per 100,000 individuals, and they experience either a relapsing or chronic progressive disease course (45). Like GBS, there are several different clinical variants (subtypes). The lines are often blurred with regard to a definitive diagnosis and classification into a particular subtype. CIDP phenotypic variants include sensory CIDP, motor CIDP, focal CIDP, Lewis –Sumner Syndrome, and Distal Acquired Demyelinating Symmetric Neuropathy. As is the case with many autoimmune diseases of the peripheral nervous system, an exact cause has yet to be identified (45, 46). Researchers in this area readily admit that differing clinical presentations along with different subtypes make it hard to study the pathogenesis. To complicate things even more, one of the main differential diagnoses for the motor form of CIDP is Multifocal Motor Neuropathy (MMN). Only a small number of patients diagnosed with CIDP are actually placed into this category, so there is some speculation that the motor variant may indeed be MMN (46). The proposed pathogenesis for CIDP is autoantibody deposition at the node of Ranvier, which causes 1) saltatory conduction interference or 2) direct destruction of the node secondary to complement deposition. The exact pathogenesis is proposed for the AMAN form of GBS (6). The targeted autoantigen in CIDP is neurofascin, which is a cellular adhesion molecule. In the AMAN for of GBS, the proposed targets are gangliosides GM1 and Gd1a. Treatment for CIDP is similar to GBS, and corticosteroids are especially effective (45, 46). Any type of peripheral neuropathy can mimic GBS—disorders of the neuromuscular junction, spinal cord injury, and botulism are a few in a long list of

differentials (47) .

DISCUSSION

The clinical presentation of GBS and all of its variants seems to be fairly well reported. That's not surprising, because all it entails just a matter of documenting what the patient reports and what is noted in daily charts by medical personnel as the disease progresses. Guillain Barré Syndrome will be 100 years old in 2016 and the difficulty with progress that has been made in understanding the pathogenesis lies in the fact that is still a "syndrome". The online Merriam-Webster medical dictionary (http://www.merriam-webster.com/medical/syndrome) defines a syndrome as a group of signs and symptoms that occur together and characterize a particular abnormality. The patient is given symptomatic treatment—in contrast to a disease, where the underlying known cause of the illness is treated. There has not been a specific infectious agent, genetic mutation, environmental factor, nor auto-antigen that is identified as being solely responsible for GBS. It is an undetermined mixture of all of the above, as well as potential variables that have yet to be identified. Some researchers think that there will never be a way to offer prophylaxis against GBS; thus, it's of the upmost importance to develop therapy that is effective in the acute stage (48).

STUDY RATIONALE

To date, there is a lack of tractable animal models for GBS. There are have been several different attempts at developing models, and claims for models that mimic the human clinical presentation. These “models” are not suitable because the nervous disease often has to be induced or they have more than one autoimmune disease present, which complicates interpretation of the data. There is also a belief that the number of animals used to validate animals as models of human disease is too small, and therefore, any experimental effect seen is also too small (49). We disagree. The proportion of humans affected with GBS is 0.81-.089 per 100,000 people—the number of mice that may show an experimental effect may indeed be small. For this reason, small, otherwise deemed “insignificant” changes should be viewed as worthy of follow up and further investigation. The goal is, at the very least, to identify a trend that allows for reasonable conclusions to be made, discussion to be had, and further investigations to be undertaken.

Evaluating pain in animal models of neuropathy is important and should not be overlooked. Oftentimes, mice are used for experiments at a young age. This can be faulty in clinical trials, especially those that seek to ameliorate diseases that predominantly occur in adults. Even worse, most studies don’t even report pain as an outcome that is measured during the course of the experiment (50). In studies presented in this thesis, the ethical dilemmas that arise with invoking pain in laboratory animals are avoided. Instead, the use of facial pain recognition in experimental mice is employed (51).

The NOD.B7-2$^{-/-}$ mouse develops a clinical peripheral neuropathy, Spontaneous Autoimmune Peripheral Polyneuropathy (SAPP) that mimics the clinical presentation of human AIDP. The spontaneity of the disease allows the natural course to take place without an investigator having to manipulate it, or “set it in motion”. The work presented in this thesis follows some preliminary strides made in the Mansfield lab secondary to the infection of the

NOD. B7-2$^{-/-}$ mice with *Campylobacter jejuni* strains isolated from patients with Guillain Barré Syndrome. SAPP comes with its own set of unknowns, most important of which is the fact that it has a female bias. The current work investigates the clinical presentation of SAPP and it's similarities to human AIDP in the NOD.B7-2$^{-/-}$ mouse. Specifically, several variables are manipulated in attempt to alter the time of disease onset and severity.

In addition, we present novel methodologies to harvest the murine peripheral nervous system and modified versions of clinical phenotyping test to keep track of clinical deterioration over time.

SPECIFIC AIMS

Specific Aim 1: To characterize the neurological disease in affected mice to determine how well these models mimic human symptoms and lesions of GBS.

Experiment 1: NOD.B7-2$^{-/-}$ mice develop SAPP in a time- and sex-dependent manner.

Hypothesis 1: NOD.B7-2$^{-/-}$ mice will exhibit clinical signs of peripheral neuropathy similar to those seen in humans with GBS.

Hypothesis 2: Inflammatory infiltrates will be consistent with that seen in the Acute Inflammatory Demyelinating Polyneuropathy (AIDP) form of the syndrome.

Experiment 2: Nerve lesions appear before the onset of clinical disease in SAPP

Hypothesis: NOD.B-2$^{-/-}$ mice will have inflammation in the DRG, sciatic nerve, and brachial plexus, shortly preceding the clinical onset of SAPP at 20 weeks.

Specific Aim 2: To investigate the role of key cytokines in SAPP using neutralizing antibodies, and to correlate B7-2 expression with clinical disease presence and severity.

Experiment 3: Interleukin-17 (IL-17) and/or Interferonγ (IFNγ) mediate development of nerve inflammation in NOD.B7-2$^{-/-}$ mice with SAPP.

Hypothesis: Blocking IL-17 and IFNγ in NOD.B7-2$^{-/-}$ mice at predetermined stages of disease will delay age of onset and decrease severity of disease compared to untreated mice. Specifically:

(1) Mice treated with anti-IL-17 antibody will not develop disease at all, or will experience delayed onset compared to untreated mice.

(2) Mice treated with anti-IFNγ antibody will be protected from disease.

(3) Mice treated with both anti-IL-17 and anti-IFNγ will not develop SAPP disease.

Experiment 4: The expression levels of B7-2 correlate with the onset/severity of clinical disease.

Hypothesis: NOD.B7-2$^{+/-}$ mice will have a lower disease incidence compared to female NOD.B7-2$^{-/-}$ mice.

Specific Aim 3: To determine the role of the intestinal microbiota and sex hormones in the development of SAPP.

Experiment 5: Male derived cecal microbiota is sufficient to block SAPP pathogenesis.

Hypothesis: Female NOD.B7-2$^{-/-}$ weanling mice inoculated with cecal contents from an adult male donor B7-2$^{-/-}$ mouse will be protected from the development of SAPP.

Experiment 6: Lack of estrogen is sufficient to confer protection against SAPP in female B7-2$^{-/-}$ mice.

Hypothesis: Ovariectomy will provide protection from SAPP in NOD.B7-2$^{-/-}$ mice.

Experiment 7: Determine whether an androgen receptor blocker abrogates protection from SAPP in female NOD.B7-2$^{-/-}$ mice.

Hypothesis: Blocking the binding of testosterone to its cognate receptor is sufficient to abrogate protection from SAPP in NOD.B7-2$^{-/-}$ male mice.

BIBLIOGRAPHY

BIBLIOGRAPHY

1. **Brody AJ, Sternbach G, Varon J.** 1994. Octave Landry: Guillain-Barre syndrome. The Journal of emergency medicine **12:**833-837.

2. **Afifi AK.** 1994. The landry-guillain-barre strohl syndrome 1859 to 1992 a historical perspective. Journal of family & community medicine **1:**30-34.

3. **Pithadia AB, Kakadia N.** 2010. Guillain-Barre syndrome (GBS). Pharmacological reports : PR **62:**220-232.

4. **Rinaldi S.** 2013. Update on Guillain-Barre syndrome. Journal of the peripheral nervous system : JPNS **18:**99-112.

5. **Kuitwaard K, van Koningsveld R, Ruts L, Jacobs BC, van Doorn PA.** 2009. Recurrent Guillain-Barre syndrome. Journal of neurology, neurosurgery, and psychiatry **80:**56-59.

6. **Yuki N, Hartung HP.** 2012. Guillain-Barre syndrome. The New England journal of medicine **366:**2294-2304.

7. **Mathey EK, Pollard JD.** 2013. Chronic inflammatory demyelinating polyneuropathy. Journal of the neurological sciences **333:**37-42.

8. **Wakerley BR, Yuki N.** 2015. Guillain-Barre syndrome. Expert Rev Neurother **15:**847-849.

9. **Bos Eyssen ME, van Doorn PA, Jacobs BC, Steyerberg EW, van der Voort PH, Zandstra DF, Horn J, Spronk PE, Hoedemaekers CW, Bakker J, van der Jagt M.** 2011. Selective digestive tract decontamination decreases time on ventilator in Guillain-Barre syndrome. Neurocritical care **15:**128-133.

10. **Devaux JJ, Odaka M, Yuki N.** 2012. Nodal proteins are target antigens in Guillain-Barre syndrome. Journal of the peripheral nervous system : JPNS **17:**62-71.

11. **Asbury AK, Arnason BG, Adams RD.** 1969. The inflammatory lesion in idiopathic polyneuritis. Its role in pathogenesis. Medicine (Baltimore) **48:**173-215.

12. **Willison HJ.** 2005. The immunobiology of Guillain-Barre syndromes. Journal of the peripheral nervous system : JPNS **10:**94-112.

13. **Hughes RA, Cornblath DR.** 2005. Guillain-Barre syndrome. Lancet **366:**1653-1666.

14. **Prineas JW.** 1981. Pathology of the Guillain-Barre syndrome. Ann Neurol **9 Suppl:**6-19.

15. **van den Berg B, Walgaard C, Drenthen J, Fokke C, Jacobs BC, van Doorn PA.** 2014. Guillain-Barre syndrome: pathogenesis, diagnosis, treatment and prognosis. Nature reviews Neurology **10:**469-482.

16. **Ang CW, Jacobs BC, Laman JD.** 2004. The Guillain-Barre syndrome: a true case of molecular mimicry. Trends in immunology **25:**61-66.

17. **Kuwabara S, Yuki N.** 2013. Axonal Guillain-Barre syndrome: concepts and controversies. Lancet Neurol **12:**1180-1188.

18. **Ho TW, Mishu B, Li CY, Gao CY, Cornblath DR, Griffin JW, Asbury AK, Blaser MJ, McKhann GM.** 1995. Guillain-Barre syndrome in northern China. Relationship to Campylobacter jejuni infection and anti-glycolipid antibodies. Brain **118 (Pt 3):**597-605.

19. **Howland GW.** 1919. The Nervous Conditions Associated with Influenza. Canadian Medical Association journal **9:**727-731.

20. **Kim HJ, Jung CG, Jensen MA, Dukala D, Soliven B.** 2008. Targeting of myelin protein zero in a spontaneous autoimmune polyneuropathy. Journal of immunology **181:**8753-8760.

21. **Ansar V, Valadi N.** 2015. Guillain-Barre Syndrome. Primary care **42:**189-193.

22. **Hughes RA, Rees JH.** 1997. Clinical and epidemiologic features of Guillain-Barre syndrome. The Journal of infectious diseases **176 Suppl 2:**S92-98.

23. **Sejvar JJ, Baughman AL, Wise M, Morgan OW.** 2011. Population incidence of Guillain-Barre syndrome: a systematic review and meta-analysis. Neuroepidemiology **36:**123-133.

24. **McGrogan A, Madle GC, Seaman HE, de Vries CS.** 2009. The epidemiology of Guillain-Barre syndrome worldwide. A systematic literature review. Neuroepidemiology **32:**150-163.

25. **Iqbal S, Li R, Gargiullo P, Vellozzi C.** 2015. Relationship between Guillain-Barre syndrome, influenza-related hospitalizations, and influenza vaccine coverage. Vaccine **33:**2045-2049.

26. **Webb AJ, Brain SA, Wood R, Rinaldi S, Turner MR.** 2014. Seasonal variation in Guillain-Barre syndrome: a systematic review, meta-analysis and Oxfordshire cohort study. J Neurol Neurosurg Psychiatry doi:10.1136/jnnp-2014-309056.

27. **Ruts L, Drenthen J, Jongen JL, Hop WC, Visser GH, Jacobs BC, van Doorn PA.** 2010. Pain in Guillain-Barre syndrome: a long-term follow-up study. Neurology **75:**1439-1447.

28. **Winer JB.** 2014. An update in guillain-barre syndrome. Autoimmune diseases **2014:**793024.

29. **Koga M, Yuki N, Hirata K.** 2000. Pain in Miller Fisher syndrome. Journal of neurology **247:**720-721.

30. **Umapathi T, Yuki N.** 2011. Pain in Guillain-Barre syndrome. Expert Rev Neurother **11:**335-339.

31. **Darweesh SK, Polinder S, Mulder MJ, Baena CP, van Leeuwen N, Franco OH, Jacobs BC, van Doorn PA.** 2014. Health-related quality of life in Guillain-Barre syndrome patients: a systematic review. J Peripher Nerv Syst **19:**24-35

.

32. **Allos BM.** 2001. Campylobacter jejuni Infections: update on emerging issues and trends. Clinical infectious diseases : an official publication of the Infectious Diseases Society of America **32:**1201-1206.

33. **Yuki N.** 2012. Guillain-Barre syndrome and anti-ganglioside antibodies: a clinician-scientist's journey. Proceedings of the Japan Academy Series B, Physical and biological sciences **88:**299-326.

34. **Nyati KK, Nyati R.** 2013. Role of Campylobacter jejuni infection in the pathogenesis of Guillain-Barre syndrome: an update. Biomed Res Int **2013:**852195.

35. **Lehmann HC, Hartung HP, Kieseier BC, Hughes RA.** 2010. Guillain-Barre syndrome after exposure to influenza virus. The Lancet infectious diseases **10:**643-651.

36. **Nelson DB, Holman R, Hurwitz E, Schonberger LB, Bregman DJ, Kaslow RA.** 1979. Results of the national surveillance for Guillain-Barre syndrome. Neurology **29:**1029-1032.

37. **Schonberger LB, Bregman DJ, Sullivan-Bolyai JZ, Keenlyside RA, Ziegler DW, Retailliau HF, Eddins DL, Bryan JA.** 1979. Guillain-Barre syndrome following vaccination in the National Influenza Immunization Program, United States, 1976--1977. American journal of epidemiology **110:**105-123.

38. **Arias.** 2015. Guillain-Barre syndrome and influenza vaccines: A meta-analysis. Vaccine **33:**3773-3778.

39. **Poland GA, Jacobsen SJ.** 2012. Influenza vaccine, Guillain-Barre syndrome, and chasing zero. Vaccine **30:**5801-5803.

40. **Stowe J, Andrews N, Wise L, Miller E.** 2009. Investigation of the temporal association of Guillain-Barre syndrome with influenza vaccine and influenzalike illness using the United Kingdom General Practice Research Database. American journal of epidemiology **169:**382-388.

41. **Tam CC, O'Brien SJ, Petersen I, Islam A, Hayward A, Rodrigues LC.** 2007. Guillain-Barre syndrome and preceding infection with campylobacter, influenza and Epstein-Barr virus in the general practice research database. PloS one **2:**e344.

42. **Chaari A, Bahloul M, Dammak H, Nourhene G, Rekik N, Hedi C, Chokri BH, Bouaziz M.** 2010. Guillain-Barre syndrome related to pandemic influenza A (H1N1) infection. Intensive care medicine **36:**1275.

43. **Kutlesa M, Santini M, Krajinovic V, Raffanelli D, Barsic B.** 2010. Acute motor axonal neuropathy associated with pandemic H1N1 influenza A infection. Neurocritical care **13:**98-100.

44. **Bader SR, Kothlow S, Trapp S, Schwarz SC, Philipp HC, Weigend S, Sharifi AR, Preisinger R, Schmahl W, Kaspers B, Matiasek K.** 2010. Acute paretic syndrome in juvenile White Leghorn chickens resembles late stages of acute inflammatory demyelinating polyneuropathies in humans. J Neuroinflammation **7:**7.

45. **Mathey EK, Park SB, Hughes RA, Pollard JD, Armati PJ, Barnett MH, Taylor BV, Dyck PJ, Kiernan MC, Lin CS.** 2015. Chronic inflammatory demyelinating polyradiculoneuropathy: from pathology to phenotype. Journal of neurology, neurosurgery, and psychiatry **86:**973-985.

46. **Nobile-Orazio E.** 2014. Chronic inflammatory demyelinating polyradiculoneuropathy and variants: where we are and where we should go. Journal of the peripheral nervous system : JPNS **19:**2-13.

47. **Wakerley BR, Yuki N.** 2015. Mimics and chameleons in Guillain-Barre and Miller Fisher syndromes. Pract Neurol **15:**90-99.

48. **Halstead SK, Zitman FM, Humphreys PD, Greenshields K, Verschuuren JJ, Jacobs BC, Rother RP, Plomp JJ, Willison HJ.** 2008. Eculizumab prevents anti-ganglioside antibody-mediated neuropathy in a murine model. Brain : a journal of neurology **131:**1197-1208.

49. **Hoke A, Simpson DM, Freeman R.** 2013. Challenges in developing novel therapies for peripheral neuropathies: a summary of The Foundation for Peripheral Neuropathy Scientific Symposium 2012. J Peripher Nerv Syst **18:**1-6.

50. **Mogil JS.** 2009. Animal models of pain: progress and challenges. Nat Rev Neurosci **10:**283-294.

51. **Langford DJ, Bailey AL, Chanda ML, Clarke SE, Drummond TE, Echols S, Glick S, Ingrao J, Klassen-Ross T, Lacroix-Fralish ML, Matsumiya L, Sorge RE, Sotocinal SG, Tabaka JM, Wong D, van den Maagdenberg AM, Ferrari MD, Craig KD, Mogil JS.** 2010. Coding of facial expressions of pain in the laboratory mouse. Nat Methods **7:**447-449.

CHAPTER 2

NOD B7-2$^{-/-}$ Mice as a Working Model for Acute Inflammatory Demyelinating Polyneuropathy (AIDP): A Standardized Approach to Phenotyping Reveals New Clinical Features of Spontaneous Autoimmune Peripheral Polyneuropathy

Barbie J. Gadsden, Ankit Malik, Hahyung Kim, Julia A. Bell, and Linda S. Mansfield

Prepared for the Journal of the Peripheral Nervous System

ABSTRACT

Guillain Barré Syndrome (GBS) is the world's leading cause of acute neuromuscular paralysis. Acute Inflammatory Demyelinating Polyneuropathy (AIDP) is the most common form of GBS in the United States. Limited progress has been made in understanding the pathogenesis of GBS and in developing therapies largely because of the lack of good, tractable animal models. NOD B7-2$^{-/-}$ mice develop spontaneous autoimmune peripheral neuropathy starting at 20 weeks of age. It is known that female mice have higher rates and more severe of disease than male mice. We hypothesized that NOD.B7-2$^{-/-}$ mice have disease and lesions that mimic the AIDP form of GBS. In a closed, specific pathogen free colony of NOD B7-2$^{-/-}$ mice, female mice had higher rates of inflammatory peripheral nerve disease than male mice. This disease correlated with the presence of inflammation in the dorsal root ganglion, the brachial plexus, and the sciatic nerve, which in rare cases, was present in mice younger than 20 weeks of age. Flow cytometry revealed distinct differences in cellular composition between NOD B72$^{-/-}$ mice and NOD wild type controls. NOD B7-2$^{-/-}$ mice had significantly increased numbers of myeloid cells, B cells and neutrophils. Based on our studies, we defined novel phenotypic and pathologic characteristics of SAPP in NOD B7-2$^{-/-}$ mice that include flipped hind limbs, overgrown toenails, and the presence of neutrophils under light microscopy. We have concluded that SAPP most closely resembles the AIDP form of GBS. Thus, the NOD.B7-2$^{-/-}$ mouse can be used to further investigate GBS research.

INTRODUCTION

Guillain-Barré Syndrome (GBS) is an autoimmune symmetrical ascending paralytic disorder that often follows bacterial or viral infection, most commonly *Campylobacter jejuni* or Influenza (25). It is the world's leading cause of acute neuromuscular paralysis with an incidence of 1.3 cases per 1000 in the US annually (17, 22). In most cases, disease onset begins approximately 2–3 weeks after preceding infections and is considered a neurologic emergency. Limb weakness is rapidly followed by symmetrical ascending paralysis. Most GBS patients make a full recovery, with 15–20% experiencing residual effects and life-long disability. This syndrome is mostly monophasic in presentation; recurrence is rare, but has been reported in 2-5% of affected individuals (24). Currently, there is no cure for this debilitating syndrome; treatment is symptomatic and consists of intravenous immune globulin, plasma exchange, and assisted ventilation for patients with respiratory distress (14, 25). Secondary complications that often arise include the formation of blood clots due to immobility and fatigue. Unresolved cases of GBS can progress to Chronic Inflammatory Demyelinating Polyneuropathy (CIDP) with permanent neurologic dysfunction. New treatments are needed to shorten the disease course and hasten recovery time. However, because of the critical nature of this dysfunction, few clinical trials have been conducted to address potential therapeutic options for GBS. The presence of different forms of GBS further complicates screening of new drugs in patients.

The currently accepted mechanism of GBS associated axon and myelin damage is the theory of molecular mimicry. It is hypothesized that self-peptides on the myelin and on the axon (at the node of Ranvier) are recognized as foreign by the immune system. Subsequently, anti-self-antigen antibodies are produced and the tissue is destroyed by inflammatory cells. The type of inflammatory cells that are present depends on the particular variant of GBS found in the patient. Acute Inflammatory Demyelinating Polyneuropathy (AIDP) is the most common variant of GBS in America and Western Europe (1). It has been

associated with Cytomegalovirus infection and is characterized by circulating auto-antibodies against the neuronal ganglioside GM2 (14). Histopathologic changes are characterized by lymphocytes and plasma cells in the anterior spinal roots and motor nerve fibers causing weakness (6). Additional architectural changes increase with severity and include demyelination and axonal degeneration. Acute Motor and Axonal Neuropathy (AMAN) is associated with antecedent *Campylobacter jejuni* infection. In AMAN, histopathologic lesions in the sciatic nerve are primarily axonal, and there is a distinct absence of lymphocytes and plasma cells. Macrophages are the main cell type found. The clinical phenotype is accompanied by IgG antibodies against peripheral nerve gangliosides GM1, GD1a, and Gal-Nac Gd1a. Neurofascin-186 and gliomedin proteins found at the Node of Ranvier are thought to induce inflammation leading to autoreactivity (5). Because GBS encompasses a wide range of forms, animal models that mimic each form are needed to study underlying mechanisms and screen for efficacious drugs.

Many published animal models are described as models of Guillain Barré Syndrome (2). Chicken, rabbits, mice, and rats have all been used in experiments investigating the host response and sequence of events occurring in GBS and CIDP neuropathy (2, 18, 21). In a 2010 report, juvenile White Leghorn Chickens, ranging from 5 to 13 weeks of age developed spontaneous paresis and inflammatory neuropathy around the age of sexual maturity (2, 13). However, in longer studies conducted with these birds, they were found to have increasing levels of IL-10 gene expression, which correlated with cessation of clinical signs. Lewis rats are another familiar model of AIDP, whereby Experimental Autoimmune Neuropathy (EAN) is induced by injection of bovine peripheral nerve myelin or myelin components (7). Yet, neither of these animal models follows the natural course of AIDP onset. Mouse models of spontaneous GBS/CIPD include TCR-Tg (POT) transgenic mice, L31/CD4$^{-/-}$ mice, NOD.Aire$^{GW/+}$ mice, and the NOD.B7-2$^{-/-}$ mice (10, 15, 16, 23). Of these four strains, the AIRE$^{+/-}$ mice also get diabetes and the L31/CD4$^{-/-}$ mice develop central nervous system (CNS)

lesions, which does not occur in AIDP patients. Although the TCR-Tg (POT) mice do not develop any other autoimmune disease, they do not develop spontaneous neuropathy unless they are transferred with CD-25 depleted T cells. That leaves the B7-2$^{-/-}$ mouse as the true spontaneous model within this disease category that best resembles AIDP without other organ involvement, and therefore, is likely to be more suitable model to study its pathogenesis and for therapeutics discovery.

Mice on the NOD genetic background have various immunological derangements, which make them a suitable model for autoimmune disease research. In NOD wild type mice, the majority of the adult females develop Type 1 diabetes, with 80% reported to be affected by 24 weeks of age and some even developing disease as early as 15 weeks of age. Males are affected later than females, and with a much lower incidence of 20% affected (9) . Adult NOD.IL10$^{-/-}$ mice develop spontaneous colitis. IL-10 deficiency leaves mice unable to mount a suppressive immune response against bacteria in the gut that are otherwise commensal flora. The NOD.B7-2$^{-/-}$ mice lack the costimulatory molecule B7-2 on the surface of dendritic cells. These mice develop spontaneous peripheral nerve disease called Spontaneous Autoimmune Peripheral Polyneuropathy (SAPP) (15).

SAPP was first reported in NOD.B7-2$^{-/-}$ mice in 2001 as a model for Chronic Inflammatory Demyelinating Polyneuropathy (CIDP)(15). At 20 weeks of age, mice began to exhibit hind limb weakness and difficulty walking (15). By the time the mice reached 32 weeks of age, it was reported that 100% of females and 30% of males were affected. Mice do not recover from this disease. Tissues evaluated under light microscopy revealed mononuclear cell inflammation in the dorsal root ganglia and sciatic nerves. In the B7-2$^{-/-}$ mouse, the target for the autoimmune inflammation shifted from the beta cells of the pancreas (where it appears in NOD WT mice affected with diabetes) to the sciatic nerve (3, 15) of AIDP. Because this spontaneous disease is clinically and histologically similar to the AIDP variant of GBS, NOD.B7-2$^{-/-}$ mice are an attractive strain to study its pathogenesis. Published studies have

focused on identifying the mechanisms underlying development of SAPP in NOD.B7-2$^{-/-}$ mice. In support of molecular mimicry as the theorized mechanism, myelin protein zero (P0) was implicated as the target antigen present on the nerve in SAPP. In NOD.B7-2$^{-/-}$ mice, circulating autoantibodies to P0 were detectable beginning at about 16 weeks of age (8). To date, two key cytokines, Interleukin-17 (IL-17) and Interferon gamma (IFNγ) have been reported to have vital roles in the onset and disease course of SAPP. Splenic gene expression of IL-17, a cytokine produced during the T-helper 17 (TH17) immune response, is elevated to peak levels in the spleens of B7-2$^{-/-}$ mice at approximately 16 weeks of age, which is 4 weeks before the earliest published reports of clinical disease onset in the mice. IFNγ gene expression was shown to rise in the spleen between 16 and 24 weeks of age, and reached its peak at 32 weeks of age, which was the published age at which all female mice and 30% of male mice were affected (15). Previous literature describing the pathology and known immunopathogenesis showed similarities to human AIDP. Thus, we hypothesized that NOD.B7-2$^{-/-}$ mice affected with SAPP mimic the AIDP form of GBS.

RATIONALE

The rationale for the screening study was that if we were going to investigate SAPP as a model for AIDP in the B7-2$^{-/-}$ mouse, using mice in the Mansfield Colony, we would have to provide a comprehensive descriptive summary of the clinical signs and histopathological description of the affected portions of the PNS in the mice present therein. The results from the preliminary screen would provide familiarity of what the disease looks like in the colony. Subsequent study results could then be related back to what is known to be true from unmanipulated mice.

Objectives in the first screening study were:

1) to accurately describe preclinical changes and the clinical phenotype in detail, as they related to mice housed in the specific pathogen free (SPF) Mansfield Colony

2) to determine the lesion distribution during development of SAPP

3) to characterize the major nerve lesions and predominant inflammatory cell types present.

4) to assess the presence of inflammation in the dorsal root ganglion, the sciatic nerve, and the brachial plexus, before the onset of clinical disease.

5) to employ the use of the Digigait^{TM} to identify early subtle gait changes.

Hypothesis 1: NOD.B7-2$^{-/-}$ mice will exhibit clinical signs similar to those seen in humans with GBS.

Hypothesis 2: Inflammatory infiltrates will be consistent with those seen in AIDP.

The rationale for the age screen study was that if mice were to be use as models of inducible GBS after infection with *Campylobacter jejuni*, then identifying the time at which mice develop spontaneous peripheral nerve inflammation was essential.

The objectives of this study were:

1) to determine of inflammatory infiltrates were present within the nerve before 20 weeks of age

2) to determine if the severity of PNS inflammation increased with time

RESULTS

Experiment 1

The open field test was used to phenotype the mice on a weekly basis. Observation of clinical signs were made daily. In the early stages of disease, affected mice exhibited a disrupted gait pattern and reluctance to rear on the side of the cage in the open field test. As the disease progressed, the mice remained in one area within the open field test, with increased respiratory movements (tremors). They also exhibited the hind limb clasping reflex and rapid, involuntary movements of all four limbs when suspended by their tail. Severely affected mice exhibited overgrown toenails, flipped hind limbs and an intermittent foot drag when walking (Figure 2.1). SAPP itself was not fatal; however, some mice were severely debilitated and no clinical recovery phase was ever observed. A humane endpoint was reached when the mice were no longer able to support themselves on their hind limbs to reach food and water.

In a cohort of 11 females between the ages of 20 and 32 weeks of age, 9% (1/11) developed mild inflammation, 18% (2/11) developed moderate inflammation, and 36% (4/11) developed severe inflammation. No inflammatory cells were noted in the remaining 36% (4/11) of females. Of particular interest is the older cohort of females between the ages of 34 and 44 weeks old, in which only 31% (10/32) of the females had an overall histopathologic categorization of severe. 34% (11/32) of female mice had a moderate inflammatory score and 25% (8/32) were placed in the mild category. No inflammation was seen in 9% (3/32) females. The male mice had much lower scores. In the cohort of males between the ages of 20-32 weeks, 50% (4/8) had mild inflammation in the dorsal root ganglion, brachial plexus, and sciatic nerve. Moderate inflammation was present in 13% (1/8) males. No inflammation was seen in 38% (3/8) males (Figure 2.2 and 2.3).

Regardless of age of the cohort, we consistently found that female mice had higher inflammation scores than male mice. When each section of tissue was evaluated separately (dorsal root ganglion, brachial plexus, sciatic nerve), the female mice had higher inflammation

scores than males. Although the differences were not statistically significant, there was an increasing trend of higher scores among the females, as they aged, whereas the males' scores remained relatively constant throughout life. Noteworthy was that there was a background of mild inflammation present in both male and female and male mice between the ages of 17 and 19 weeks, with 20% (1/5) female mice having a severe overall inflammatory score and 17% (1/6) males having a moderate overall score.

Light microscopic changes in the dorsal root ganglion of affected mice included mild numbers of scattered and clustered infiltrates of small lymphocytes, with rare plasma cells. The sciatic nerve and brachial plexus contained a more heterogeneous population of lymphocytes, plasma cells, and fewer neutrophils (Figure 2.4). In addition, macrophages with intracytoplasmic, Luxol Fast Blue positive, vacuolated material were present in moderate numbers. Other architectural changes included varying degrees of myelin loss, most significant in sections of the sciatic nerve. Severe cases showed axonal swelling and occasional areas of replacement fibrosis.

Thick toluidine blue stained sections of sciatic nerve taken from 7 females and 10 males between the ages of 17 and 22 weeks of age showed no difference in either the number or the area of the large myelinated axons, as measured with Image J software (data not shown).

Experiment 2

In this time course study, 23% (3/13) of female mice that were sacrificed between the ages of 15 and 19 weeks of age (before the onset of clinical disease) showed some degree of inflammation in the dorsal root ganglion, brachial plexus, or the sciatic nerve. They all had low numbers of cells within the DRG, and 2 out of the three had low numbers within the brachial plexus. In the sciatic nerve, one mouse had a low score, one had a high score, and one had no inflammation at all. Out of 14 female mice in the 20-24 week old age cohort, 14% (2/14) had

severe overall histopathologic scores and 14% (2/14) had scores that fell within the moderate category. In the mild disease category, there were 21% (3/14) females. Half of this cohort (7/14) has no detectable inflammation. Overall scores for the two 41-week-old mice were in the mild and moderate category (Figure 2.5, A-C). As noted in the previous study, there was an increasing trend toward higher inflammatory scores as the age of the females increased. Statistical significance ($p>0.01$) of brachial plexus scores was detected between the 15-19 week old cohort and the 20-24 week old cohort (Figure 2.5, D-E). Seven male mice between the ages of 15 and 21 weeks were included in this study and none of them had any histologic evidence of disease (data not shown). The cellular infiltrate was typical of SAPP and similar to that described in the previous study.

Flow Cytometry

Inflammatory cells collected from the sciatic nerves of three 41-week old female NOD B7-2$^{-/-}$ mice from the age screen study, as well as 3 NOD wild type mice serving as adult controls were analyzed by flow cytometry (Figure 2.6). There were significant differences in the numbers of neutrophils (P= 0.0218), dendritic cells (P=0.0116), and myeloid cells (P=0.0258) in the sciatic nerve of the B7-2$^{-/-}$ mice, compared to wild type mice.

DigiGait

The stance width, paw area, and stride length were evaluated and the data were compared between female age cohorts of 16-19 weeks and 20-24 weeks. The mean of the forelimb stance varied slightly between groups, but there was no significant difference detected. There were no differences between the cohort means with regard to paw area and stride length (Figures 2.7-2.9).

MATERIALS AND METHODS

Animals

Approvals from the Michigan State University Institutional Animal Care and Use Committee were obtained for mouse husbandry practices and all experimental procedures (approval number 06/12-107-00). All mice used in the experiments described here were of the NOD.129S4CD86$^{-/-}$ genotype and were originally obtained from The Jackson Laboratory (Bar Harbor, Maine). Hereafter, they are referred to as the NOD B7-2$^{-/-}$genotype. Mice were bred and reared in a specific pathogen free (SPF) colony and tested to determine that they were free of bacteria known to elicit chronic inflammation in the gastrointestinal tract (12). PCR assays obtained from Jackson Laboratories were used to confirm mouse genotypes both before and after experiments ((http://jaxmice.jax.org/pub-cgi/protocols/protocols.sh?objtype=protocol&protocol_id=346). Some mice were studied within the breeding colony and some were transported to an SPF containment facility where neurological phenotyping was possible. In all cases mice were housed individually in sterile, filter topped cages with sterilized bedding. Their cages were changed in a laminar flow hood. All mice were fed irradiated Harlan Teklad 6% fat diet 7913 and given sterile water ad libitum.

Experimental Design 1. SAPP onset and frequency of disease.

We expected SAPP to develop in NOD.B7-2 $^{-/-}$ mice as previously described (15). We expected that NOD.B72$^{-/-}$ mice would begin to develop peripheral neuropathy at 20 weeks of age, with females being affected at a higher rate than males. The study consisted of a total of 82 mice: 60 females and 22 males. The mice were placed in the open field test weekly for photo and video documentation of a neurologic phenotype. Clinical observations were made on a daily basis by observing mice in their home cages on the static rack.

Experimental Design 2. Targeted age screen study.

We expected that inflammatory cells present within the nerve are responsible for the outward clinical manifestation of neurologic signs; therefore, we expected that the presence of such cells would precede the onset of clinical signs. The objective of this study was to determine if there are inflammatory lesions present within the nerve before onset of disease, which was expected at ~ 20 weeks of age. We also intended to determine if lesion severity increased over time. The study followed 40 female and 11 male mice for development of peripheral nerve disease using weekly phenotyping with the open field test and DigiGait tests. Mice were observed daily and randomly selected for sacrfice at predetermined time points, ranging from 15–24 weeks, with 3 female mice being carriedout to 41 weeks. A randomly selected subpopulation of mice were allowed to reach 41 weeks of age as a maximum for the final evaluation.

Open Field Test (OFT)

Open field testing was performed according to a published protocol with modifications (4). Mice were placed in a standard sized rat cage and videotaped for one minute, using a Sony Handycam Digital Video Recorder (model DCR-SX41). At the end of the open field videotaping, they were assessed for hind limb clasping by holding them gently upside down by the tail a foot above the countertop, and capturing the reaching reflex on video (20) . The videos were then blinded and evaluated by a trained operator using a neurological clinical scoring sheet that documented gait abnormalities including, rearing, foot splay/drag, intermittent bunny hopping, and crossed forelimbs.

DigiGait

DigiGait (Mouse Specifics, Inc., Quincy, MA), a treadmill with a high quality video camera, was used to capture subtle gait deficits in experimental mice. Raw data files were transferred directly to a computer analysis program with software designed to identify early,

subtle changes in mouse gait, which cannot be seen with the naked eye. Before each experiment, the mice were trained on the DigiGait apparatus three times per week for 1–2 weeks to determine optimum running speed, and to identify those mice that were incapable of providing usable data. Mice that became unable to complete 5 second uninterrupted runs on the DigiGait treadmill were removed from the study group during the training period. This did not affect group size, as more mice than needed were trained in anticipation of some uncooperative behavior, which included failure to run consistently and jumping, and riding the treadmill belt until they contacted the bumpers.

Once the mice were placed on the clear DigiGait treadmill belt, the front and rear bumpers were adjusted to ensure that the animal remained within the field of vision for the duration of the run. The mice were exercised at three speeds, 20, 30, and 40 centimeters per second (cm/s), for a minimum of 3 seconds with their snouts facing in the same direction to facilitate accurate comparisons. The treadmill was stopped briefly to adjust the speed between runs. The DigiGait Imager software recorded the raw video files. The raw video was then reduced to no less than 500 frames, and saved for analysis. After manual processing as specified by the manufacturer (https://mousespecifics.com/digigait/), each video was analyzed for various parameters, including, but not limited to, stride length, paw angle, stance width, animal length, animal width, stride length variability, and stride width variability. These parameters were measured on each limb for every mouse.

Euthanasia and Necropsy

At the end of the study or at specific humane endpoints, mice were humanly euthanized with slow filling of the CO_2 chamber. Death was confirmed by physical examination. All euthanasia procedures were carried out in accordance with the 2013 AVMA guidelines for the euthanasia of animals. https://www.avma.org/KB/Policies/Documents/euthanasia.pdf. The liver, spleen, pancreas, kidneys, heart, and lungs were removed from the carcass and placed in 10%

phosphate buffered formalin, pH 7.0 (Thermo Fisher Scientific, Waltham, MA, USA) to fix for 48 hours. They were then transferred to a 60% EtOH solution. Thereafter, peripheral nerves and the brain and spinal cord were removed and fixed for histologic evaluation.

Peripheral Nervous Tissue Removal Technique

After euthanasia and removal of internal organs, the axillary region was dissected to allow exposure of the brachial plexus. The forelimbs were separated from the carcass by transecting the nerves at the level of the scapula. Remaining muscle was carefully removed to expose the nerve. Mice were then placed in ventral recumbency and the remaining pelt was reflected upward and removed. The head was dislocated from the skeleton by cutting between the foramen magnum and the first cervical vertebra (atlas). Bilaterally, the muscle over the sciatic nerve was reflected back and the sciatic nerve was dissected up to the level of the spinal cord. Then, with the aid of a dissecting microscope, muscle was cleaned from the vertebral column and a dorsal laminectomy was performed to expose the spinal cord. Beginning at the most rostral aspect of the vertebral column, small cuts were made on both sides of the lateral aspect of each vertebra, until the entire length of the spinal cord was exposed. The carcass was stored in 10% neutral buffered formalin for 48 hours and then switched to 60% ethanol until the nerves and roots were harvested. The sciatic nerve was removed in its entirety, from its most distal aspect, where it branches into the tibial and common peroneal nerves, up to its dorsal roots at the spinal cord (L3, L4, L5). The nerves of the brachial plexus were also removed and embedded *en bloc*. All harvested tissues were placed in a tissue cassette between two slips of lens paper, with two cassette sponges for stabilization, and stored in 60% ethanol until further processing.

Tissue Processing for Histologic Evaluation

Samples of the sciatic nerve, brachial plexus, and dorsal root ganglion previously fixed in 10% neutral buffered formalin were processed and vacuum infiltrated with paraffin on a ThermoFisher Excelsior tissue processor; followed by embedding with the ThermoFisher HistoCentre III embedding station. Once blocks were cooled, excess paraffin was removed from the edges, and they were placed on a Reichert Jung 2030 rotary microtome (City, state) and faced to expose tissue sample. The block was then faced, cooled, and finely sectioned at 4–5 microns. Sections were dried at 56°C in a slide incubator to ensure adherence to the slides for 2 – 24 hours. Slides were removed from the incubator and stained with a routine Hematoxylin and Eosin method as follows: Two changes of xylene – 5 minutes each, two changes of absolute ethanol – 2 minutes each, two changes of 95% ethanol – 2 minutes each, running tap water rinse for 2 minutes, endure Hematoxylin (Cancer Diagnostics Inc. City, NC) for 1 ½ minutes, followed directly by a 10–15 second differentiation in 1% aqueous glacial acetic acid and running tap water for 2 minutes to enhance nuclear detail. Slides were placed in one change of 95% ethanol – 2 minutes, 1% Alcoholic Eosin-Phloxine B – 2 minutes to stain cytoplasm, one change of 95% ethanol for 2 minutes, four changes of 100% ethanol – 2 minutes each, four changes of Xylene – 2 minutes each, followed by coverslipping with synthetic mounting media for permanent retention and visualization with light microscopy. This work was carried out at the Investigative Histopathology Laboratory, Division of Human Pathology, Department of Physiology, Michigan State University. Stained sections were observed using an Olympus BX41 microscope, and photographed with an Olympus DP71U-TV0.5XC-3 camera.

Tissue Processing for Plastic Embedding

Once the sciatic nerve was removed, it was fixed in 2.5% glutaraldehyde/ paraformaldehyde in 0.1M cacodylate buffer, overnight at 4°C. After fixation, the samples

underwent three, 10 minute washes in 0.1M cacodylate buffer. Then, they were post fixed in osmium tetroxide in 0.1M cacodylate buffer. They were then stored overnight at 4°C, after which they were washed again three times, for 10 minutes in 0.1M cacodylate buffer. After the washes were complete, the samples were processed through a graded ethanol series for dehydration (30–100%) in the microwave at 40 watts for 5 minutes. The samples were then infiltrated with an acetone-resin (PolyBed 812) ratio until the resin amount was at 100%, after which, they were placed in an oven for 48 hours to allow the resin to polymerize. Sections were cut at 500 nm thickness, mounted onto a slide and stained with Toluidine Blue.

Evaluation of Axon Counts and Area of Large Myelinated Axons

Toluidine Blue stained sections of the sciatic nerve were examined at 40X magnification and evaluated using the ImagePro software (Media Cybernetics, Rockville, Md). Cross sections of large myelinated axons were enumerated by placing a click mark in the center of each neuron. Thereafter, a line was drawn around each large myelinated axon to measure the area. The entire area of the nerve section was counted. Numerical data was imported to an Excel spreadsheet for statistical analysis.

Histopathology

Hematoxylin and eosin stained sections of tissue from the dorsal root ganglion, brachial plexus, and sciatic nerve were examined. Scoring was based on the degree of inflammation present in each section. Those sections that had a mild degree of inflammation were assigned the number 1. Moderate inflammation was given a score of 2, and severe inflammation was given a score of 3. Cells composing the infiltrate were recorded along with any other architectural changes, such as myelin loss. Scores from the tissues were added together for a final histopathology score. Each mouse was then given an overall histopathology score as follows: A total score of 1-3 was classified as mild, 4-6 as moderate, and 7-9 as severe. Luxol

Fast Blue staining of a separate section was used to confirm the loss of myelin. Two veterinary pathologists, including a neuropathologist, and one human neuropathologist reviewed the nerve scoring criteria. The slides were blinded and read by an ACVP board certified veterinary pathologist (BJG).

Flow Cytometry

The right sciatic nerve was quickly harvested from the mouse carcass during necropsy. The tissue was then transferred into a glass vial containing 2-3 mls of collagenase buffer and incubated in an orbital shaker. The tissue was then filtered into phosphate buffered saline (PBS) through a 40um cell strainer and incubated for 40 minutes at 37C. The PBS mixture was centrifuged at 800 x g for 5 minutes. The supernatant was removed and discarded and the cell pellet was resuspended in 10ml of 40% Percoll buffer. A density gradient was made by very slowly combining the 40% Percoll cell mixture to a 50 ml conical tube with 80% Percoll. The gradient was allowed to settle for five minutes and then centrifuged for 20 min at 1000 xg. The band of cells at the gradient interface was carefully collected by pipette, washed with PBS, and resuspended in 1ml of R10 media, and immunostained. The following monoclonal antibodies (eBiosciences) were used: anti-CD3 (clone 145–2C11), anti-CD4 (clone RM 4-5), preincubated for 20 minutes with anti-CD16/CD32 to block Fc receptors, then washed and labeled with appropriate mixture of isotype matched controls for 30 minutes, centrifuged at 650g, and resuspended in FACS buffer. To exclude dead/dying leukocytes, cells were gated according to forward and side scatter. For intracellular cytokine staining, cells were restimulated for 4 hours with cell stimulation cocktail (eBioscience) and fixed and permeabilized using fixation and permeabilization solution (eBioscience). All cells were analyzed on a LSRII flow cytometer (BD Biosciences) and data processed using FlowJo software (Tree Star) (11).

Statistical Analyses

Histologic scoring was evaluated using Kruskal-Wallis with Dunn's post test for tests evaluating time as a single factor. A 2-way ANOVA with Sidak post test was used when analyses comparing gender and age were compared.

DISCUSSION

These studies added significant new information to what is already known about SAPP in NOD B7-2$^{-/-}$ mice especially pertaining to newly observed clinical features and parameters of early gait deficits (or lack thereof). From observation of mice during our preliminary screening study, we were well aware of the clinical features of SAPP, and were confident in being able to document its progress using the Open Field Test. Newly identified features included occasional knuckling and crossing over of the forelimbs, overgrown toenails, flipped hind limbs, and dyskinesia of all four limbs. In our experimental mice, Spontaneous Autoimmune Peripheral Polyneuropathy (SAPP) began with the mice appearing unsteady in their gait. As the disease progressed, they began to exhibit a foot splay and intermittent, correctable flipped hind limbs in moderate disease, which became non-correctable in severe disease. Overgrown toenails observed in moderate to severely affected mice during the open field test were the result of not being able to normally move the affected leg(s) to wear the nails down. Severely affected mice were reluctant to move in the open field test and had increased respiration, but no mouse was ever in respiratory distress.

Humans with GBS ultimately endure respiratory embarrassment and have to be mechanically ventilated; in that regard, SAPP is different. There are future plans under way to assess the phrenic nerve, which supplies the diaphragm, for presence of inflammatory cells. From our clinical observations, some mice progress with SAPP at a faster rate than others. Even female mice from the same litter may have varying degrees of disease severity, with different ages of onset. The histopathologic changes observed in the B7-2$^{-/-}$ mice are distinct from those observed in the working inducible model of GBS secondary to *Campylobacter jejuni* infection, where the primary histopathologic lesion consists of scattered macrophages with intracytoplasmic Luxol Fast Blue positive material.

In contrast to previously published studies, our mice did not all succumb to SAPP at 32 weeks of age. In fact, 3 female mice in the older group cohort of 34-44 weeks did not have evidence of inflammation in the dorsal root ganglion, the brachial plexus, nor the sciatic nerve. While the absence of B7-2 predisposes the mice to the development of SAPP, these findings support the fact that the clinical penetrance of this autoimmune disease has varying, unknown host factors involved in the age of onset and degree of clinical disease.

The method of nerve dissection used in these studies allowed for assessments to be made along the complete length of the sciatic nerve and brachial plexus, as well all sciatic dorsal nerve roots (L3-L5). This *en bloc* embedment allowed information to be gathered regarding not only severity of inflammation, but also to confirm that in the early stages of disease, the lesion distributions within the brachial plexus and sciatic nerves is often multifocal to locally extensive, with progression to diffuse involvement in severe cases. Lastly, it ensured that identical tissues from each mouse were being evaluated in order to make accurate comparisons and meaningful correlations from statistical analyses. The microscopic infiltrates of lymphocytes, plasma cells, and macrophages, along with associated demyelination and clinical disease presentation are similar to the human variant of GBS known as Acute Inflammatory Demyelinating Polyneuropathy (25).

We found that nerve lesions preceded the onset of clinical signs of SAPP. Although mice usually show clinical disease around 20 weeks, there were several mice that had inflammation in all three tissues examined before then. While only a small percentage of mice experienced nerve lesions prior to 20 weeks of age, we realize that, as often as is the case in research, that all mice in a particular treatment group will not behave the same way. That does not negate the positive information that is gathered from the data, and in some cases such as this, are worthy of following up on. This subset of data may have implications on the application of early

intervention and treatment protocols with GBS in the form of antibody blocking therapy or competitive inhibition in the form of carbohydrate (ganglioside) binding.

Previous work has shown that SAPP also induces sensory changes. Ubogu and colleagues found a decrease in dorsal caudal tail (DCT) conduction velocity in female SAPP affected mice that peaked at 32-35 weeks of age (19). In our studies, it was noted that as mice began to show signs of clinical SAPP, they tried to get away very quickly from the handler if the dorsal portion of their tail was touched while being coaxed to move in the Open Field Test. This was interpreted as hypersensitivity. As the mice aged and the disease progressed, the perceived hypersensitivity stopped. After the initial screening study, mice were not touched once they were placed in the testing cage, except to remove them and place them back in their home cage.

The DigiGait was used in a time course fashion to identify subtle changes in gait that may occur before SAPP becomes visible to the observer with the naked eye. Although the measurements for the stance width, paw area, and stride length were not significant in this study, we don't discount the DigiGait as a useful tool to pick up these changes—we interpret this data in light of the fact that the mice were put down at ages before the reported onset of clinical disease (16-19 weeks) and early disease onset (20-24 weeks).

In previous SAPP studies, the inflammation in the peripheral nerve has been described as mononuclear. In the closed colony of mice, there were also noticeable numbers of neutrophils present via light microscopy, especially in sections of the sciatic nerve and the brachial plexus—none were noted in the DRGs. This finding translated over the flow cytometry data, in which there was a statistically significant difference in the number of neutrophils recovered from the sciatic nerve of the B7-2$^{-/-}$ mice when compared to the wild type mice. While neutrophils are mostly thought of as key players in innate immunity, they also have a role in adaptive immunity—more specifically in chronic inflammation and autoimmune diseases. SAPP is considered an autoimmune disease and in some cases the inflammation is longstanding.

What is not yet understood is whether or not neutrophils actively contribute to the nerve damage via tissue destruction, or if their presence is more related to cellular trafficking of additional leukocytes via secretion of IL-17. Dendritic cells can function as immunoregulatory cells to dampen in the inflammatory response, but in this case, they are believed to perpetuate the inflammation through presentation of self-antigens such as myelin proteins to T cells, with subsequent activation of autoreactive CD4+ cells, or proinflammatory cytokine release to drive the differentiation of cells locally. The increased number of macrophages labeled as CD11b+MHCII+ represent macrophages. They can also be seen on light microscopy with intracytoplasmic myelin debris.

Lastly, the single factor that seems to be overlooked in the ongoing research of SAPP is the female bias toward disease development. Gender is rarely discussed and in some other GBS/CIDP mouse models of autoimmune peripheral neuropathy, there is no discussion of this lopsided occurrence. There is major focus on the immunopathogenesis of this disease, but research on other host specific factors that may play a significant role on the front end (onset and severity) is scarce. Several factors should be considered, including, but not limited to gender specific hormones and the intestinal microbial community. We have studies under way to evaluate the role of these factors in development of SAPP in the NOD.B7-2$^{-/-}$ mouse.

One limitation that we acknowledge is the unbalanced number of female to male specimens. This imbalance arose because the female NOD.B7-2$^{-/-}$ mice consistently had litters that were predomonantly female. However, the large variation between the males and females does not present a problem, since the females are the ones that mainly develop disease. This is also supported by the fact that some of our later studies have equal numbers of male mice per expriemental group, and the the disease penetrance still exhibits the female bias. None of the mice in the study died before the endpoint due to SAPP.

ACKNOWLEDGEMENTS

We would like to thank Dr. Alicia Pastor Withrow for her expertise in the plastic embedding and thick sectioning. We would also like to thank Amy Porter and Kathy at the MSU Investigative Histopathology Lab for special care with our specimens, and Drs. Jon Patterson and Howard Chang for critical review of the histopathology scoring methodology.

APPENDIX

Figure 2.1. Clinical signs of SAPP. Mice affected with SAPP exhibit twisting of the body and clasped limbs (A), abnormal limb placement and movement (B), markedly overgrown toenails (C), hind limb foot splay (D), flipped hind limbs (E), and malaligned body position secondary to abnormally placed forelimbs (F).

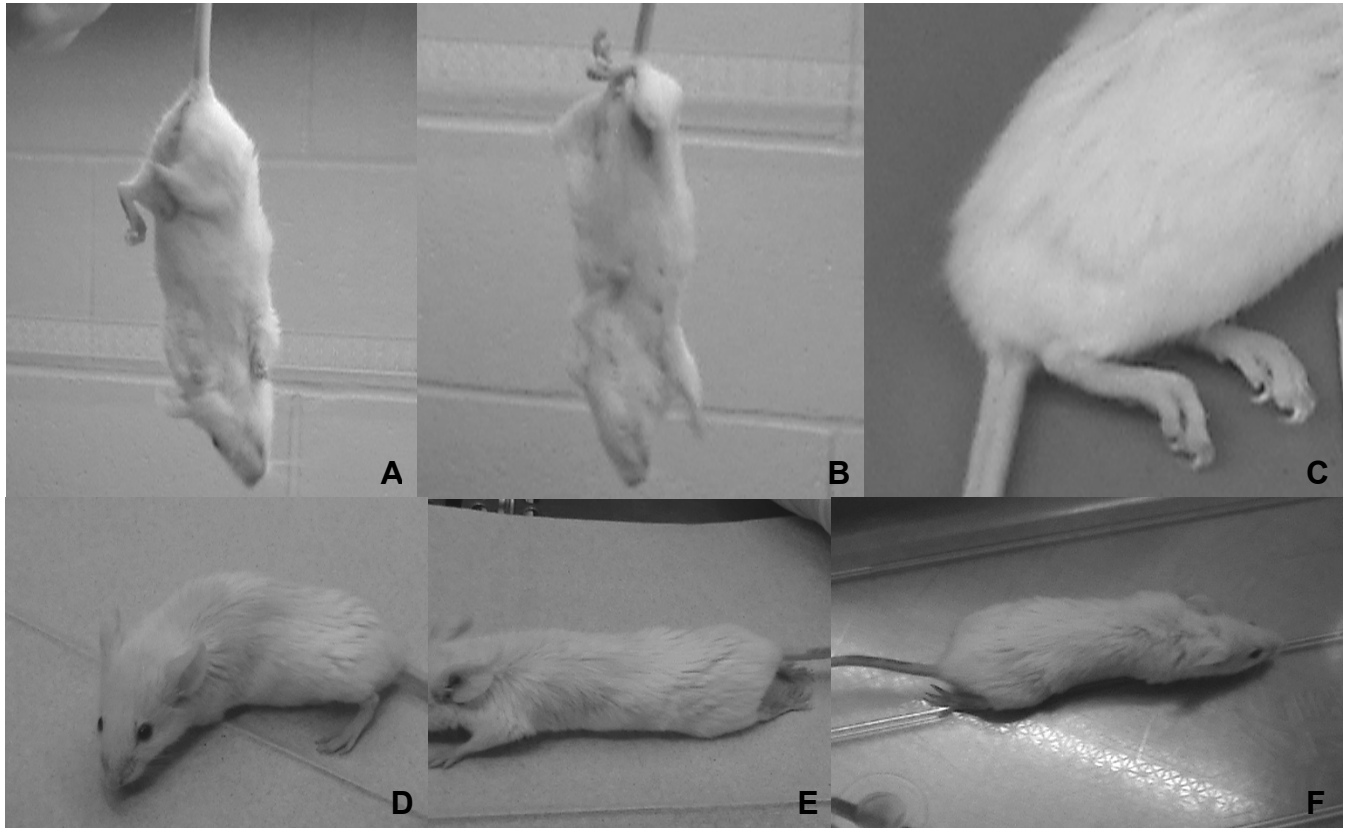

Figure 2.2 Histopathology of female peripheral nervous system. (A) Total scores (B) Dorsal root ganglion (C) Brachial plexus (D) Sciatic nerve

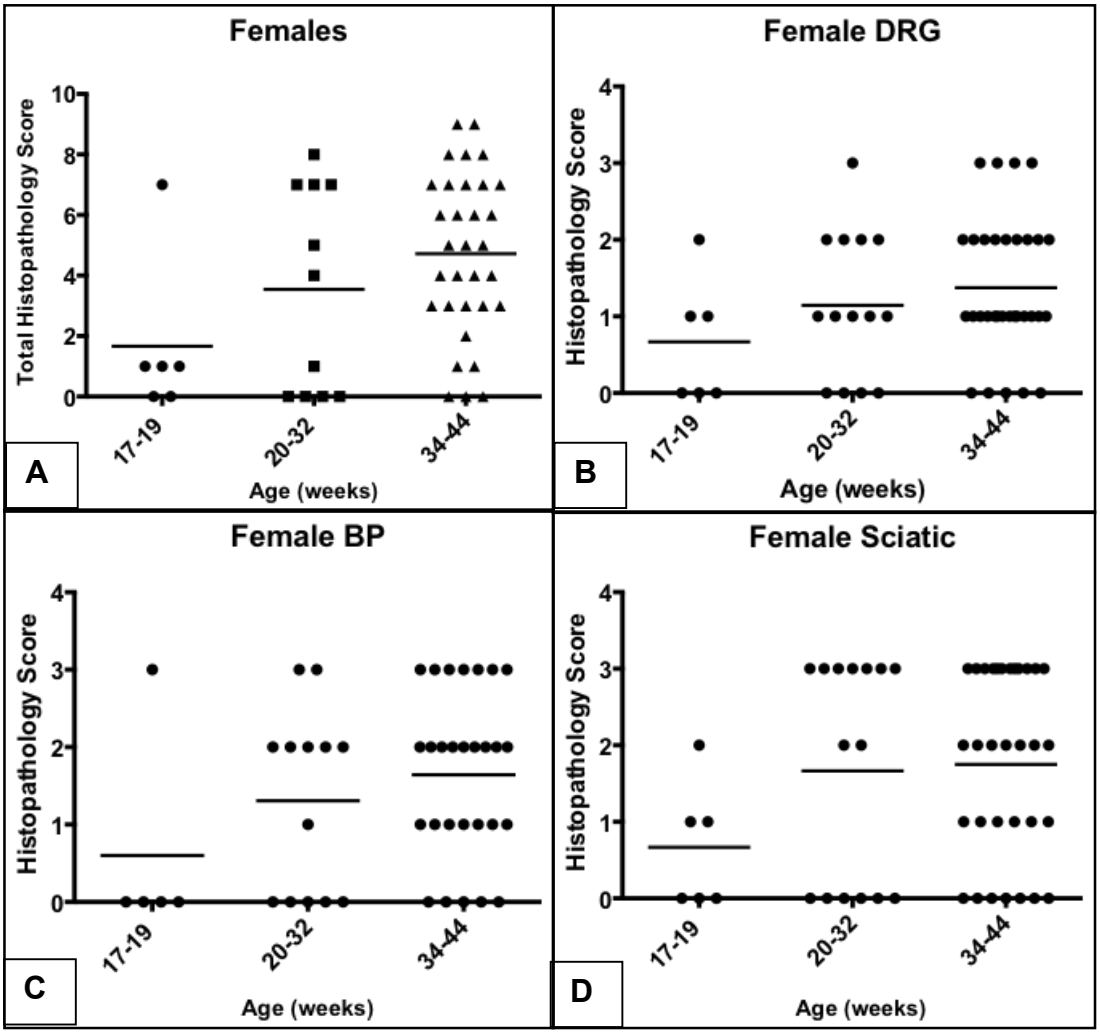

Figure 2.3 Histopathology of male peripheral nervous system. (A) Total scores (B) Dorsal root ganglion (C) Brachial plexus (D) Sciatic nerve

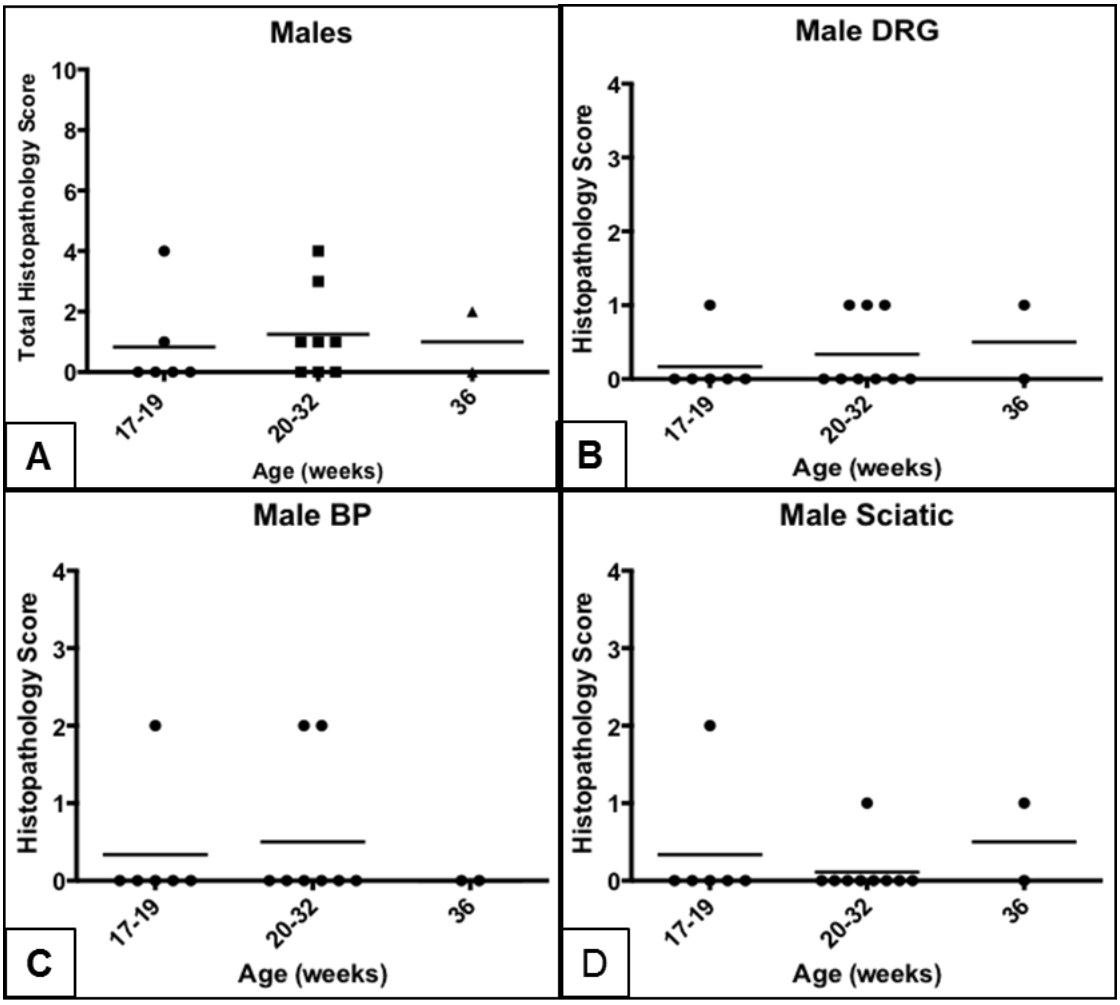

Figure 2.4 Histopathology of the peripheral nervous system of SAPP mice. (A) DRG from an unaffected mouse (B) DRG from affected mouse (C) sciatic nerve from unaffected mouse (D) sciatic nerve from affected mouse. The tissues from affected mice contain clusters and scattered infiltrates of lymphocytes and plasma cells. Loss of myelin and edema (clear space) can be seen in the sciatic nerve section).

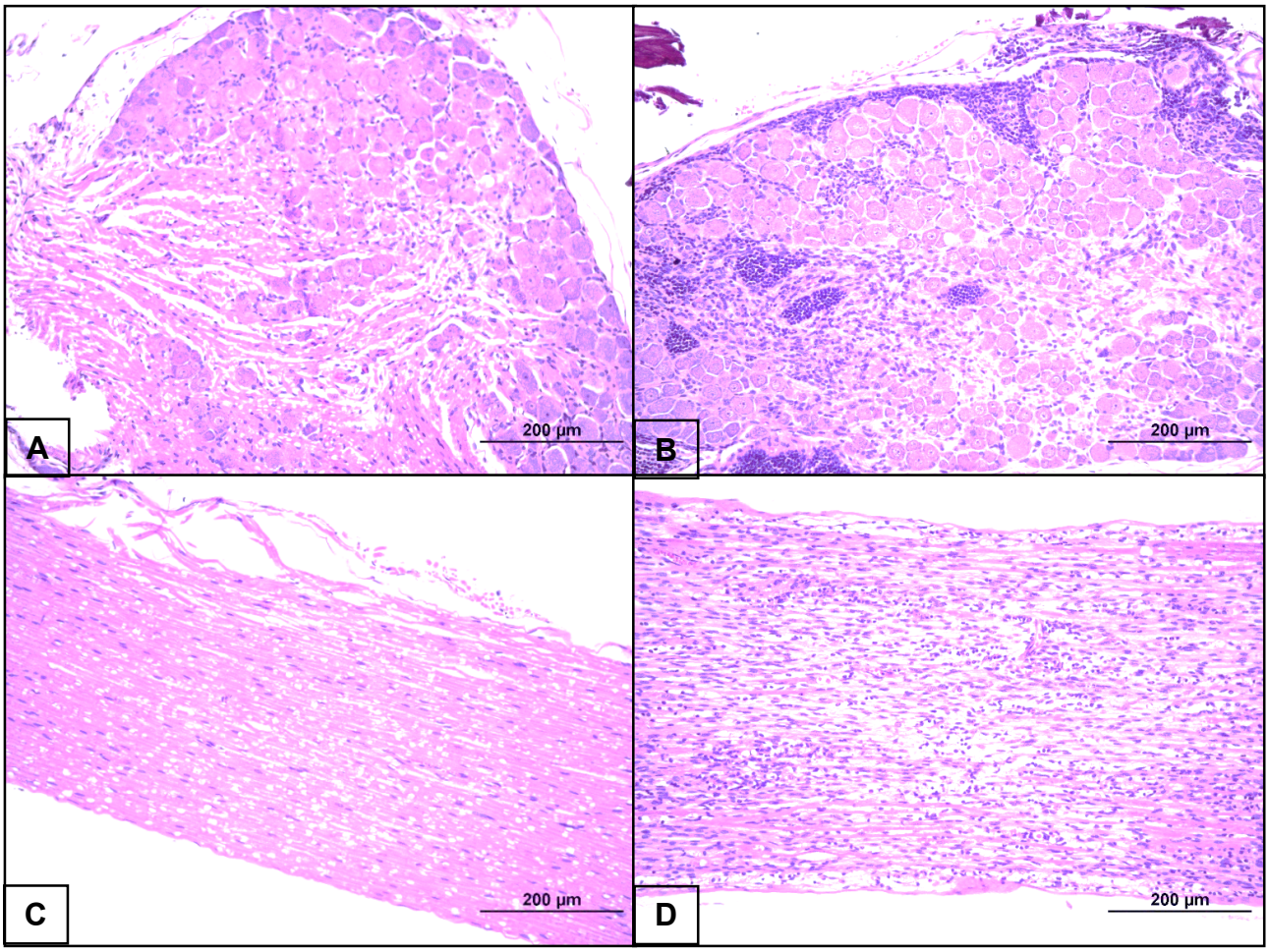

Figure 2.5 Histopathology results for mice from the age screening study. (A) 15-19 weeks, before the appearance of clinical signs (B) 20-24 weeks, after the onset of clinical disease (C) 41 weeks, past the age at which information for SAPP is published.

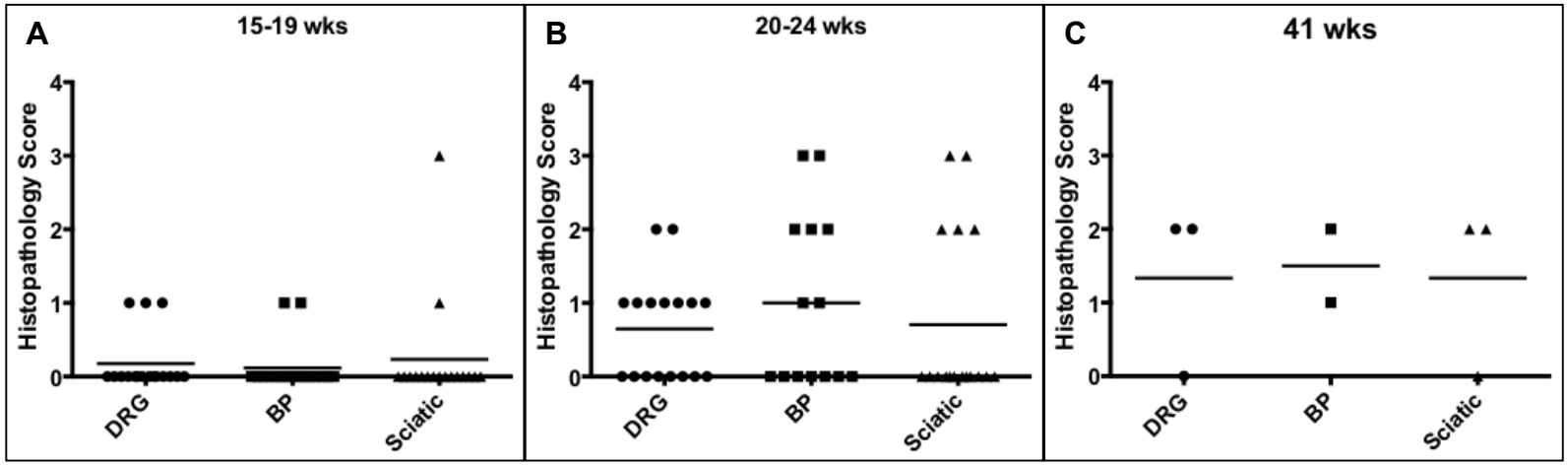

Figure 2.5 (cont'd) Comparisons of each part of the peripheral nervous system between age cohorts. (D) Dorsal root ganglion (E) brachial plexus (F) sciatic nerve. The mean histo score of the brachial plexus is significantly increased at 20-24 weeks, compared to 15-19 weeks.

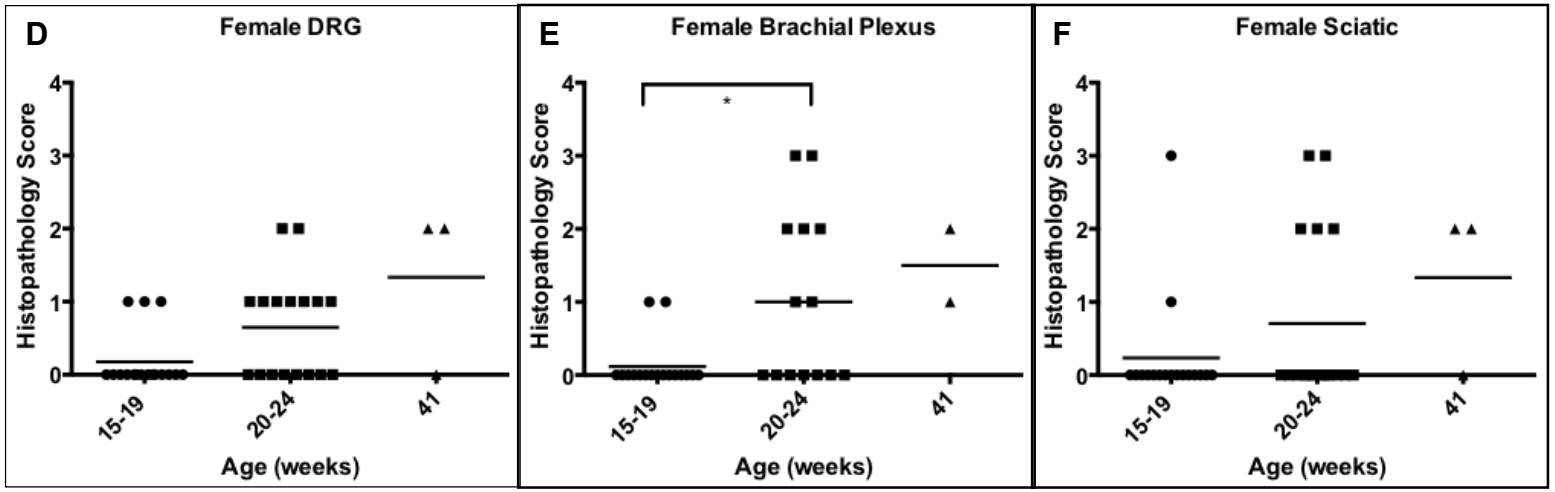

Figure 2.6 Results of flow cytometry from 41-week-old B7-2$^{-/-}$ mice. Significant increases in the mean cell number were seen in (C) myeloid cells, P=0.0258 (D) neutrophils, P=0.0218 (E) dendritic cells, P=0.0116

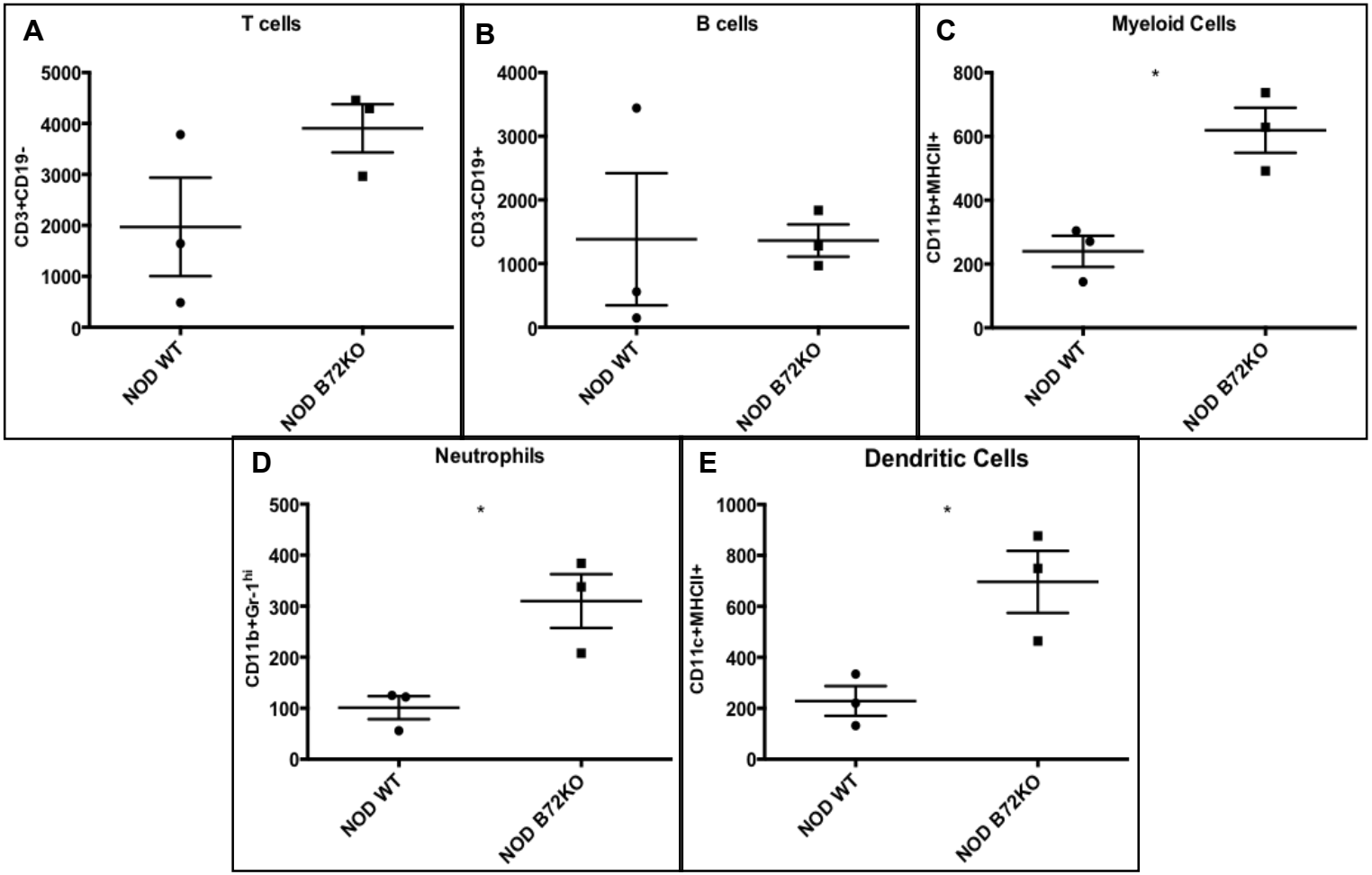

Figure 2.7 Stance width in females as measured by DigiGait. There is a significant increase in the mean of the 20-24 week cohort, as compared to the 16-19 week cohort.

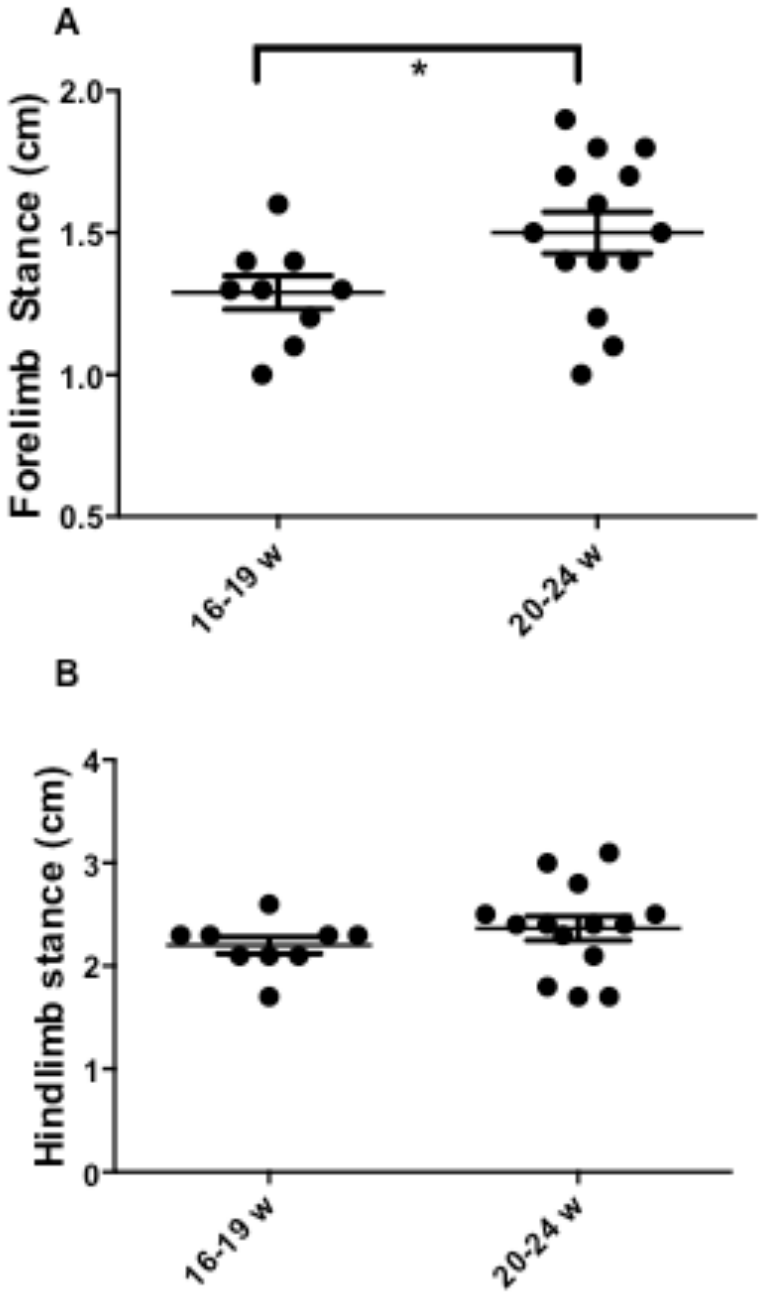

Figure 2.8 DigiGait paw area in females. No significant differences or trends are observed.

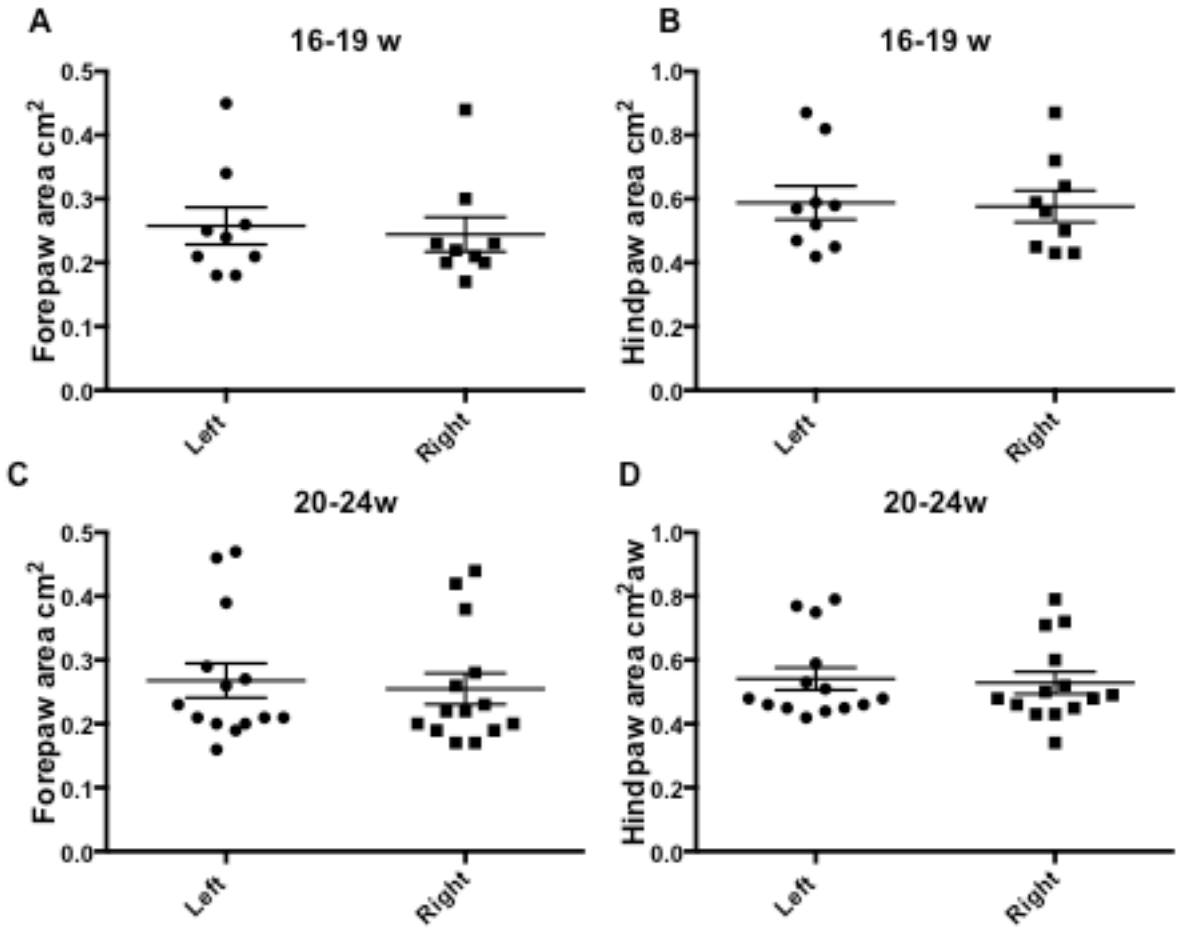

Figure 2.9 DigiGait stride length in females. No significant differences or trends are observed.

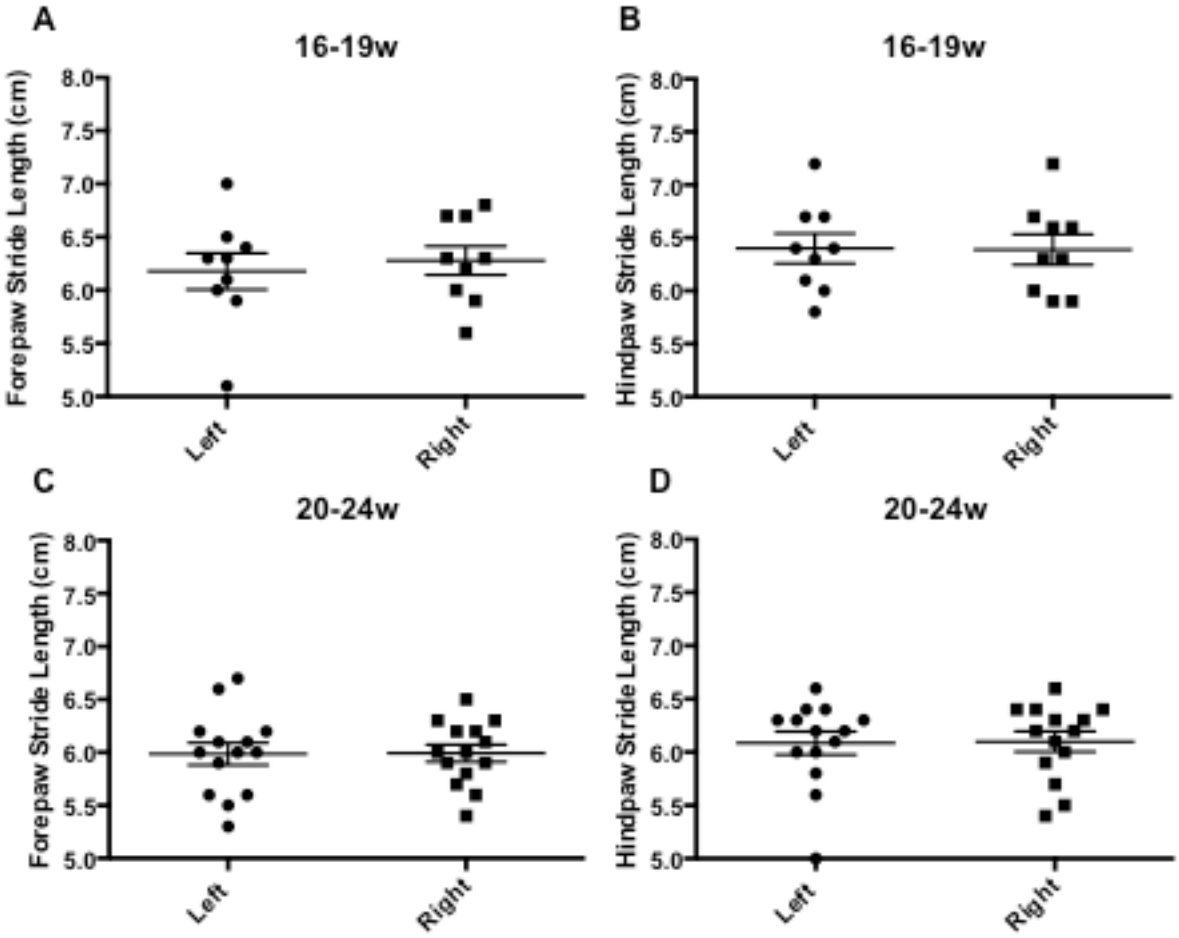

BIBLIOGRAPHY

BIBLIOGRAPHY

1. **Arcila-Londono, X., and R. A. Lewis.** 2012. Guillain-barre syndrome. Semin Neurol **32:**179-186.

2. **Bader, S. R., S. Kothlow, S. Trapp, S. C. Schwarz, H. C. Philipp, S. Weigend, A. R. Sharifi, R. Preisinger, W. Schmahl, B. Kaspers, and K. Matiasek.** 2010. Acute paretic syndrome in juvenile White Leghorn chickens resembles late stages of acute inflammatory demyelinating polyneuropathies in humans. J Neuroinflammation **7:**7.

3. **Bour-Jordan, H., H. L. Thompson, and J. A. Bluestone.** 2005. Distinct effector mechanisms in the development of autoimmune neuropathy versus diabetes in nonobese diabetic mice. J Immunol **175:**5649-5655.

4. **Brooks, S. P., and S. B. Dunnett.** 2009. Tests to assess motor phenotype in mice: a user's guide. Nat Rev Neurosci **10:**519-529.

5. **Devaux, J. J., M. Odaka, and N. Yuki.** 2012. Nodal proteins are target antigens in Guillain-Barre syndrome. J Peripher Nerv Syst **17:**62-71.

6. **Hughes, R. A., R. D. Hadden, N. A. Gregson, and K. J. Smith.** 1999. Pathogenesis of Guillain-Barre syndrome. J Neuroimmunol **100:**74-97.

7. **Keceli, S. A., A. Willke, G. S. Tamer, O. B. Boral, N. Sonmez, and P. Cagatay.** 2014. Interaction between caspofungin or voriconazole and cefoperazone-sulbactam or piperacillin-tazobactam by in vitro and in vivo methods. APMIS **122:**412-417.

8. **Kim, H. J., C. G. Jung, M. A. Jensen, D. Dukala, and B. Soliven.** 2008. Targeting of myelin protein zero in a spontaneous autoimmune polyneuropathy. J Immunol **181:**8753-8760.

9. **Lenschow, D. J., S. C. Ho, H. Sattar, L. Rhee, G. Gray, N. Nabavi, K. C. Herold, and J. A. Bluestone.** 1995. Differential effects of anti-B7-1 and anti-B7-2 monoclonal antibody treatment on the development of diabetes in the nonobese diabetic mouse. J Exp Med **181:**1145-1155.

10. **Louvet, C., B. G. Kabre, D. W. Davini, N. Martinier, M. A. Su, J. J. DeVoss, W. L. Rosenthal, M. S. Anderson, H. Bour-Jordan, and J. A. Bluestone.** 2009. A novel myelin P0-specific T cell receptor transgenic mouse develops a fulminant autoimmune peripheral neuropathy. J Exp Med **206:**507-514.

11. **Malik, A., D. Sharma, J. St Charles, L. A. Dybas, and L. S. Mansfield.** 2014. Contrasting immune responses mediate Campylobacter jejuni-induced colitis and autoimmunity. Mucosal Immunol **7:**802-817.

12. **Mansfield, L. S., J. S. Patterson, B. R. Fierro, A. J. Murphy, V. A. Rathinam, J. J. Kopper, N. I. Barbu, T. J. Onifade, and J. A. Bell.** 2008. Genetic background of IL-10(-/-) mice alters host-pathogen interactions with Campylobacter jejuni and influences disease phenotype. Microb Pathog **45:**241-257.

13. **Nyati, K. K., and R. Nyati.** 2013. Role of Campylobacter jejuni infection in the pathogenesis of Guillain-Barre syndrome: an update. Biomed Res Int **2013:**852195.

14. **Pithadia, A. B., and N. Kakadia.** 2010. Guillain-Barre syndrome (GBS). Pharmacol Rep **62:**220-232.

15. **Salomon, B., L. Rhee, H. Bour-Jordan, H. Hsin, A. Montag, B. Soliven, J. Arcella, A. M. Girvin, J. Padilla, S. D. Miller, and J. A. Bluestone.** 2001. Development of spontaneous autoimmune peripheral polyneuropathy in B7-2-deficient NOD mice. J Exp Med **194:**677-684.

16. **Su, M. A., D. Davini, P. Cheng, K. Giang, U. Fan, J. J. DeVoss, K. P. Johannes, L. Taylor, A. K. Shum, M. Valenzise, A. Meloni, H. Bour-Jordan, and M. S. Anderson.** 2012. Defective autoimmune regulator-dependent central tolerance to myelin protein zero is linked to autoimmune peripheral neuropathy. J Immunol **188:**4906-4912.

17. **Takahashi, M., M. Koga, K. Yokoyama, and N. Yuki.** 2005. Epidemiology of Campylobacter jejuni isolated from patients with Guillain-Barre and Fisher syndromes in Japan. J Clin Microbiol **43:**335-339.

18. **Tan, X. D., Y. C. Dou, C. W. Shi, R. S. Duan, and R. P. Sun.** 2009. Administration of dehydroepiandrosterone ameliorates experimental autoimmune neuritis in Lewis rats. J Neuroimmunol **207:**39-44.

19. **Ubogu, E. E., N. Yosef, R. H. Xia, and K. A. Sheikh.** 2012. Behavioral, electrophysiological, and histopathological characterization of a severe murine chronic demyelinating polyneuritis model. J Peripher Nerv Syst **17:**53-61.

20. **van den Akker, E., M. Reijnen, J. Korving, A. Brouwer, F. Meijlink, and J. Deschamps.** 1999. Targeted inactivation of Hoxb8 affects survival of a spinal ganglion and causes aberrant limb reflexes. Mech Dev **89:**103-114.

21. **Vriesendorp, F. J.** 1997. Insights into Campylobacter jejuni-induced Guillain-Barre syndrome from the Lewis rat model of experimental allergic neuritis. J Infect Dis **176 Suppl 2:**S164-168.

22. **Willison, H. J.** 2005. The immunobiology of Guillain-Barre syndromes. J Peripher Nerv Syst **10:**94-112.

23. **Yang, M., A. Rainone, X. Q. Shi, S. Fournier, and J. Zhang.** 2014. A new animal model of spontaneous autoimmune peripheral polyneuropathy: implications for Guillain-Barre syndrome. Acta Neuropathol Commun **2:**5.

24. **Yuki, N.** 2001. Infectious origins of, and molecular mimicry in, Guillain-Barre and Fisher syndromes. Lancet Infect Dis **1:**29-37.

25. **Yuki, N., and H. P. Hartung.** 2012. Guillain-Barre syndrome. N Engl J Med **366:**2294-2304.

CHAPTER 3

Blocking Cytokines and Crossing Strains

CHAPTER 3, SECTION 1

Get Lost Interleukin-17 and Interferon gamma!

INTRODUCTION

There is a lack of treatment options that address the cellular immunity of GBS. The two main treatments PE and IVIg (discussed in Chapter 1) address alleviation of the humoral arm of the disease by clearing the patients' plasma of self-reactive and pathogenic autoantibodies. However, there are no current therapies that target the production and/or effector action of inflammatory cytokines. Cytokine release is the "third" step in initiating the adaptive arm of the immune response. The first step is antigen presentation by professional or nonprofessional antigen presenting cells, and the second step is costimulation between the antigen peptide on the major histocompatibility complex (MHC) and the T cell receptor (TCR). Cytokines "direct Immune cell traffic" in the sense that they call in certain cells to ramp up or calm down the immune response. They also have the ability to inflict direct injury on tissues. The reason for no current therapy for cellular immunity in GBS could relate to the fact that there is no "smoking gun" in terms of the predictability of IFNγ in certain disease states. High levels of circulating neutralizing antibodies to IFNγ are associated with patient recovery in GBS according to one study, but other studies have refuted that claim, even claiming that IFN does not play a role in the pathogenesis at all (6, 9, 20).

For the purpose of this body of work, the spotlight is on the actions of Interleukin-17 (IL-17) and Interferon gamma (IFNγ). The role of IL-17 and IFNγ in autoimmune disease is both an interesting and conflicting area of research. Both of these cytokines cause free radical and nitric oxide release in peripheral nervous tissue. These substances are toxic to both Schwann cells and myelin, and cause demyelination if their production is unregulated. IFNγ was also found to induce Schwann cells to present myelin protein P2 to an antigenic specific T cell line, through the upregulation of MHC molecules (7). In addition to a "disease-promoting" effect, another function of IFNγ is to assist in converting CD4 T cells into T regulatory cells (Treg) (10).

Even in animal models of autoimmune disease, the roles of key cytokines are up for discussion. In a study conducted in a rat model of EAN, IFNγ was found to reduce disease

severity when given orally. However, IV administration resulted in marked disease. When neutralizing antibodies were given, the disease was alleviated (8). In the NOD wild type mouse, a strain that readily and reliably develops type 1 insulin dependent diabetes mellitus (IDDM), IFNγ has been identified as a key cytokine for disease maintenance. However, when these mice were given recombinant IFNγ, they were protected from diabetes and had more pancreatic islets present via light microscopy, when compared to their non -treated counterparts (23). In 2005, Bour-Jordan and colleagues investigated the role of IFNγ in SAPP, in the female NOD.B7-2$^{-/-}$ mice. They crossed the NOD.B7-2$^{-/-}$ mice with NOD-IFNγ$^{-/-}$ mice to create a double knockout mouse. They reported that at up to 40 weeks of age, 100% of the female double knockout mice remained free of the disease. They concluded that IFNγ was necessary in the development of SAPP in the NOD.B7-2$^{-/-}$ mice. Interestingly SAPP could not be reproduced in mice on the B6 background (22).

In 2008, Kim and colleagues were able to pinpoint the age at which splenic gene expression of IL17 and INFγ peaked in the spleen of NOD.B7-2$^{-/-}$ mice. They used age-matched, NOD WT mice as controls for expression levels, and showed autoreactivity of T cells *in vivo* to myelin protein P0. The NOD.B7-2$^{-/-}$ mice have circulating autoantibodies to P0 as early as 8 weeks of age (22) . An overarching goal of this thesis is to conduct studies that can contribute information to be used in the generation of therapeutics in GBS research and clinical trials. With all of the work that has been done to date with GBS and the EAN mouse, it still remains a question as to whether or not cytokines such as IFNγ can be targeted for therapy (25).

In this study, the role of IL-17 and IFNγ is investigated, both separately, and in concert, as they relate to SAPP in the NOD.B7-2$^{-/-}$ mouse. Although the exact role of IL-17 in GBS remains incompletely understood, we hoped to extrapolate information from the following experiments to discuss potential therapeutic options for AIDP. The purpose of the following study was to determine whether IL-17 and/or Interferon gamma mediate development of nerve

inflammation in the NOD.B7-2$^{-/-}$ mice with SAPP. Prevention or delay of disease due to diminished levels of these cytokines would indicate clearer paths toward elucidating the underlying mechanisms of the AIDP variant of GBS.

RATIONALE

Splenic gene expression of IL-17 peaks before the clinical onset of SAPP, and IFNg peaks after the disease onset. The rationale for this study was that if the implicated cytokines were neutralized in the mice around the time that they are reported to be at their highest levels, then the disease occurrence could be dampened down and/or abolished.

Hypothesis: Blocking IL-17 and IFNγ in NOD.B7-2$^{-/-}$ mice at predetermined stages of disease will delay age of onset and decrease severity of disease compared to untreated mice. Specifically:

(1) Mice treated with anti-IL-17 antibody will not develop disease at all, or will experience delayed onset compared to untreated mice.

(2) Mice treated with anti-IFNγ antibody will be protected from disease.

(3) Mice treated with both anti-IL-17 and anti- IFNγ will not develop SAPP disease.

RESULTS

Open Field Test (OFT)

Female mice treated with neutralizing antibody against IL-17 showed a statistically significant decrease in rears at 24-26 weeks of age and 28-30 weeks of age, when compared to 12-14 weeks of age (Figure 3.1, C). The number of rears at 24-26 weeks were significantly lower than those at both 12-14 weeks and 16-18 weeks in the IL-17 neutralized male mice (Figure 3.1,D).

Both male and female mice treated with IFNγ blocking antibody had a statistically significant decrease in the number of rears at 24-26 weeks, when compared to 16-18 weeks of age (Figure 3.1, E and F). In addition, males also showed a statistically significant decrease between 12-14 weeks and 28-30 weeks.

Mice that were treated with both neutralizing antibodies showed similar clinical parameters as those that were treated with either anti-IL-17 or anti-IFNγ. In females, a statistically significant decrease was seen at 24-26 weeks when compared with12-14 and 16-18 weeks (Figure 3.1,G). In male mice, when compared to 12-14 weeks, there was a statistically significant decrease in the number of rears at 24-26 weeks and 28-30 weeks (Figure 3.1, H).

Female mice in the control group showed no significance over time among themselves (Figure 3.1,A). However, male mice had a significant decrease in rears at 24-26 weeks, compared with 12-14 weeks (Figure 3.1,B).

The means of the rears of experimental groups are compared to the mean of control mice and every other treatment group.

Female mice did not have any differences among the means between experimental groups at any time point (Figure 3.2). At 12-14 weeks of age, male mice treated with neutralizing antibodies against IFNγ and the IL-17/IFNγ had significantly increased means compared to the control treated mice (Figure 3.3,A). Significant increases in rear means between control treated and IFNγ blocked males were also present at 16-18 weeks 20-22

weeks (Figure 3.3, C and D). In addition, at 18-20 weeks, mice that were being treated with antibodies against IL-17 had significantly increased rear means. At 20-22 weeks of age, male mice that had both cytokines blocked had significantly decreased rear means compared to mice treated with only IFNγ neutralizing antibodies (Figure 3.3, E). At the conclusion of the study, male mice treated with the antibody blocking study had a statistically significant decrease in rear means compared to mice received only IFNγ blocking antibodies.

Grimace, Dyskinesia, and Tremors

Regarding uncontrolled limb movement (dyskinesia), the earliest signs appeared in female mice age 18-20 weeks, in all groups except the combo treated group (Figure 3.4,A). Female mice treated with the IL-17/IFNγ blocking combo did not have dyskinesia until 22-24 weeks of age (Figure 3.4,C). It is worthy to note that within the sham group of mice, there were always a greater percentage of females with uncontrolled limb movement compared to males during any given week (data not shown-graphed as a percentage).

In the sham treated male mice, dyskinesia was first observed at 20-22 weeks in the control mice and mice that were being treated with IL-17 neutralizing antibody (Figure 3.5,B). There were affected male mice in all groups at the conclusion of this study (Figure 3.5,F).

In female mice, the facial grimace was a prominent feature of the disease; it first appeared in female mice being treated with IL-17 blocking antibodies at 20-22 weeks (Figure 3.6,B)—they went on to have 100% positivity for the facial grimace at the conclusion of the study (Figure 3.6,F). Only 33% of control mice had evidence of pain (facial grimace) at the end of the study.

Male mice treated with the IL-17/ IFNγ blocking antibody combo had the longest consecutive streak of grimace (6 weeks) among treatment groups (Figure 3.7,B). Surprisingly, control treated mice had the highest percentage of mice with a facial grimace, at 24-26 weeks of age (Figure 3.7,D).

Tremors were observed in all groups of mice, except those in the double blocked group. From 22-24 weeks, until the end of the experiment, female mice from all treatment groups showed tremors (Figure 3.8,C-F)

In male mice, the first sign of tremors were observed at 20-22 weeks of age, in all treatment groups except the IFNγ blocked grouped (Figure 3.9,B). As the experiment progressed, tremors remained present in each treatment group. The occurrence of tremors (in the contingency table) at 26-28 weeks is significantly different among the groups (Figure 3.9,E).

DigiGait

Note: At any given week, the number of mice represented are different, as all mice did not provide 3 second runs at each testing time.

At 22-24 weeks of age, the female mice in the sham group and the α-IL17 group did not provide 3 second runs. Groupwise comparisons and comparisons over time did not show any significant differences over time (Figures 3.10-3.13). However, males with neutralized IFNγ showed a trend toward increase numbers of rears over time (Figure 3.10,F).

When mice were compared to one another over time with regard to the left hind paw area, there was a statistically significant increase in the mean from 12-14 weeks to 16-18 weeks in males treated with IL-17 blocking antibody (Figure 3.14,D) . Males that were treated with both IL-17 and IFNγ blocking antibodies had statistically significant increase in paw area from 12-14 weeks of age to 1-18 weeks and 28-30 weeks (Figure 3.14, H). There was also significance over time in the control male group; however, the software and statistical analysis did not pick up which time points the differences occurred between (Figure 3.14,B).

Statistical significance was observed over time for the right hind paw among the control male mice, but the test did not specify where the differences occurred (Figure 3.15,B). The males treated with IL-17 blocking antibody had a statistically significant increase in the mean

from 12-14 weeks to 16-18 weeks of age (Figure 3.15,D). Furthermore, male mice treated with both α-IL-17 and α-IFNγ blocking antibody had a significant increase in rears from 12-14 weeks to 28-30 weeks of age (Figure 3.15,H).

Control male mice had a significant difference in the left forepaw area mean over time—the double treated males and females did as well (Figure 3.16, B and H). Left forepaw area in the females treated with α-IL17 was significantly increased from12-14 weeks to 28-30 weeks of age (Figure 3.16,C). Increased means were also noted from 12-14 weeks to 16- 18 weeks in IL17 neutralized males and IFNγ neutralized males (Figure 3.16, D and F). Double treated mice from both groups showed an overall significant change in rears over time (Figure 3.16, G and H).

The right forepaw of the following groups experienced significant changes over time, where the change was not specified in the multiple comparison analysis: control males and males neutralized with IFNγ blocking antibody (Figure 3.17, B and F). In male mice treated with IL17 neutralizing antibody, there was a significant increase in right paw area in mice 16-18 weeks was seen when compared to measurements taken at 12-14 weeks (Figure 3.17,D). Males treated with both neutralizing antibodies had a significantly increased mean compared to the last time point at 28-30 weeks of age (Figure 3.17,H).

Significance was only found in one data set from all four limbs, in both male and female mice, from all four treatment groups. There was significance between the means of the left fore limb stride length in male mice at 22-24 weeks of age (data not shown).

Histopathology

The differences discussed below are done so in terms of trends.

In this experiment, the female mice that were treated with the IL17/ IFNγ neutralizing antibody combo had histopathologic scores that were less than the sham treated mice (Figure 3.18) Female mice treated with only IFNγ blocking antibody had mean histopathology scores similar to the sham treated group. Female mice treated with IL17 neutralizing antibody had an interesting histopathological profile. Half of the mice (3/6) had histopathology scores that placed them in the severe range, while the other half had scores that placed them in the mild category. There were minimal fluctuations up and down between the male treatment groups: groups treated with the IL17/ IFNγ neutralizing antibody combo and IL17 antibody only, had a slightly lower mean score than the sham group. The group treated with IFNγ blocking antibody had a slightly increased mean increased mean compared to the control mice.

Bone Scans

The following parameters for bone morphology were measured: trabecular number and thickness, trabecular separation, bone volume fraction, average cortical thickness, cortical area, total cross-sectional area inside the periosteum, marrow area, cortical area fraction, and femur length. There was no significant difference across groups, or between male and females within any of the treatment groups. Trabecular and cortical bone parameters are similar in both male and female mice, regardless of treatment group. All bone figures are presented in the Appendix.

MATERIALS AND METHODS

Mouse Breeding and Handling

All experimental protocols and procedures were approved by the Institutional Animal Care and Use Committee at Michigan State University (06-12-107-00).The mice were from a specific pathogen free colony and singly house at a containment facility in sterilized, filter-topped cages that were changed one a week. Mice were fed a diet of Irradiated Harlan Teklad 7913 chow (Harlan Teklad, Indianapolis, Indiana, USA) and given free access to sterilized water. Animal technicians and experimental handlers wore standard personal protective equipment for non-infectious animals any time they were handling mice, and their gloves were disinfected using 70% ethanol between cages.

Cytokine Neutralizing Treatment Regimen

Experimental NOD.B7-2$^{-/-}$ mice were randomized and separated into four treatment groups. The control (sham) injected group received intraperitoneal injections of Rat Gamma Globulin (Jackson Immunoresearch, West Grove, PA). A second group received neutralizing antibodies against IL-17A (BioXCell, West Labanon, New Hampshire, USA). The third group was injected with antibodies against IFNγ (BioXCell, West Lebanon, New Hampshire, USA). The final group received two consecutive series of injections (IL-17 and IFNγ). The injections were time to coincide with the time that peak levels of gene expression for the B7-2$^{-/-}$ mice had been reported by Kim (11). The sham treated group received injections for as long as the other groups were treated. Injections for the IL-17 group began when the mice were 12 weeks of age, so that by the time they reached 16 weeks of age, there would be considerable depletion of circulating levels of IL-17. The IFNγ group received injections from 16-20 weeks of age. The group that was treated with IL-17 and IFNγ neutralizing antibodies received IL-17 blocking antibodies from 12-16 weeks, immediately followed by IFNγ neutralizing antibodies from 16-20 weeks.

Intraperitoneal Injections

Injections were delivered in accordance with standard laboratory animal practice, as described in The Laboratory Mouse (1). Mice were injected every three days and left and right sides were alternated each time to minimize tissue sensitivity.

Open Field Test (OFT)

Mice were placed in the open field test and observed every two weeks for signs of motor deficits. The test was performed with modifications (5). The mice were videotaped for 60 seconds while they moved freely about the field (plastic rat cage). At the end of the 60 seconds, they were help up by their tails and evaluated for dyskinesia, which included the clasping reflex. The open field was disinfected using 70% ethanol in between each mouse.

Presence or absence of a facial grimace was evaluated from the open field test videos. This protocol was modified from Langford, et.al (12). The mice received a score of 0 if there was no grimace present, and a score of 1 if there was a grimace. A grimace was identified by the following features: squinted eyes, flattened ears, and puffed cheeks. Tremors were also evaluated as a measure of pain. Mice with without tremors received a score of zero, and mice with tremors received a score of 1.

Histopathology

The sciatic dorsal root ganglia (L3-L5), the brachial plexus, and the sciatic nerve were evaluated under light microscopy, using (insert scope here). All samples were taken from the left side of the mouse and were stored in 60% ethanol until processing. The slides were evaluated blindly using the standard peripheral nerve scoring sheet.

DigiGait

The mice were placed on the Digigait treadmill once every two weeks and run at speeds of 20, 30, and 40 centimeters per second. The following parameters were evaluated: hind stance width, stride length, and paw area.

Bone Density and Architecture Measurement

Femurs were fixed in 10% formalin for 24 hours and scanned using a GE Explore Locus microcomputed tomography (μCT) system at a voxel of 20 μm obtained from 720 views. The beam angle increment was 0.5 and beam strength was set at 80 peak kV and 450 μA. Each run consisted of control and treated bones and a calibration phantom to standardize gray scale values and maintain consistency. On the basis of auto-threshold and iso-surface analyses of multiple bone samples, a fixed threshold of 600 was used to separate bone from bone marrow. Bone measurements were blinded. Trabecular bone was analyzed in the region between the distal epiphysis to the growth plate. Trabecular bone mineral content, bone volume fraction, thickness, spacing, and number values were computed by GE Healthcare MicroView software application for visualization and analysis of volumetric image data. Cortical measurements were performed in a 2 x 2 x 2 mm cube centered midway down the length of the bone.

Statistical Analysis

The open field test over time, within groups was analyzed using a Kruskal-Wallis, with Dunn's multiple comparisons test. Dykinesia, grimace, and tremors were analyzed using Chi square test for trend. Histopathology and ELISA data were analyzed with Kruskal-Wallis, with Dunn's multiple comparison test. All statistical tests were performed using GraphPad Prism, version 6 (La Jolla, CA, USA).

DISCUSSION

We expected that blocking IL-17and IFNγ would reduce disease severity, and as a result, the mice would 1) have the motor strength to ambulate normally and 2) be free from pain, which would allow them to want to move. When evaluating the rears in the mice, an increased activity in all of the groups compared to the sham inoculated mice was expected, throughout the duration of the experiment. Instead, there was a gradual decline in the number of rears in all of the treatment groups over time, in both male and female mice. Since 20 weeks of age is the reported time of onset, there was a special interest in the time points of 20 weeks to the end of the experiment—specifically, if there was a statistically significant or trending decrease in the number of times that mice were able to stand on their hindlimbs.

The fact that there was no increase in activity within the open field test over time, compared with no significant differences in histopathology scores between the treated groups can be used to support the fact that the blocking antibodies did not completely alleviate the clinical signs of SAPP.

The mean histopathology scores in the group treated with both IL-17 and IFNγ blocking antibody is in line with what was expected. It makes sense that if both the initiating cytokine (IL-17) and maintenance cytokines (IFNγ) are blocked at critical time points necessary for disease initiation, the resulting decrease in disease severity would be obvious upon histopathologic evaluation. It was surprising to find elevated cell numbers in the group of mice in which IFNγ was blocked. This cytokine is reported to be necessary to maintain the disease. Although there were no statistically significant decreases, the trends were interpreted with the small sample size of mice in mind.

IFNγ is known to have both a perpetuating and a protective effect in Guillian Barré Syndrome (15). This may also be the case for the SAPP, and it is a likely possibility that its role would depend on both the duration of the disease, as well as the composition of the cytokine millieu in the microenvironment.

It is concluded that female mice treated with the IL-17 and IFNγ blocking combination were the most protected from disease. In both female and male mice, treatment with IFNγ blocking antibody alone yielded results similar to sham treated mice. To confirm the conclusions of this current study, an attempt was made to rescue the SAPP phenotype of mice in the breeding colony. SAPP affected mice were identified and a given a treatment regimen to neutralize IFNy. Two weeks into this study, the dyskinesia prevented safe IP injection of the mice and the study was discontinued.

Experimental Note: *Two female mice were removed from the data set of the control group because they began circling after the experiment started; one began at 16 weeks, and the other, at 22 weeks. One mouse was removed from the IFNγ data for the same reason. It is noteworthy that the circlers came from groups of mice that were NOT receiving any IL-17 blocking antibody. In other words, they had a full complement of IL-17 present. Both of the females that were removed had the heaviest brain weights of the group (.66g and .6g). They were also littermates. The one mouse taken from the IFNγ group had a brain weight of .57g, the second highest in the group. The mice were kept until the end of the experiment; however, their data was omitted from the statistical analysis and graphs. Histopathological evaluation of the circlers revealed no inflammation in the dorsal root ganglia, brachial plexus, or sciatic nerves. While there is no direct connection between IL-17, brain weight, and circling in the NOD mice, this is a fact that should not be completely disregarded, especially since the remaining females in the treatment groups from which these mice were in had severe histopathology scores.*

CHAPTER 3, SECTION 2

Let’s Cross Over to the Dark Side

ABSTRACT

NOD. B7-2$^{-/-}$ mice develop spontaneous autoimmune peripheral polyneuropathy. B7-2 is a key receptor on the surface of antigen presenting dendritic cells. Mice with their full complement of B7-2 genes develop diabetes. We bred for NOD B7-2$^{+/-}$ heterozygote mice by crossing NOD WT mice with NOD.B7-2$^{-/-}$ mice. The B7-2$^{+/-}$ mice were genotyped at the beginning and then end of the experiment confirmed to be heterozygotes. The rationale was that if the complete lack of B7-2 results in SAPP, then the presence of one functional allele will reduce the incidence of disease in both female and male mice. Early in the course of the experiment, female mice began to develop diabetes; the male mice soon followed. This unexpected event occurred earlier than is typical for diabetes to be seen in NOD wild type mice in the Mansfield Colony. Female mice that did not develop diabetes went on to develop SAPP, at a rate and severity that is normally observed in NOD.B7-2$^{-/-}$ mice.

INTRODUCTION

Mice on the NOD background have inherent defects in immunoregulatory cell numbers. They lack the full complement of $FOXP3^+$ T regulatory cells, which renders them are defective at signaling to quell an excessive immune response. NOD wild type mice develop diabetes, with a gender bias toward females (https://www.jax.org/strain/004762). The NOD B7-$2^{-/-}$ mice develop Spontaneous Autoimmune Peripheral Neuropathy, which also mainly affects females. It has been proven that the absence of B7-2 (also known as CD86 costimulatory molecule) promotes an inflammatory phenotype in the peripheral nerves of these mice (22). This disease could not be replicated in mice on the B6 background. As mentioned earlier, B7-s2 is just one of many immunomodulatory molecules that have been shown to be responsible for the induction of peripheral inflammatory neuropathies in mice. The exact relationship between costimulatory molecules, AIRE, and thymic medullary epithelial cells in central tolerance remains a mystery. However, as research on mouse models of inflammatory neuropathies makes its way to the forefront of GBS research, it is becoming increasingly clear that a defect in a wide variety of molecules can predispose mice to an inflammatory neuropathy, if it is involved in the pathway of central tolerance. Of course the ideal place to start an investigation into autoimmune disease pathogenesis is with AIRE, the transcription factor that allows some tissue specific antigens to be presented to early thymocytes. The presentation of most tissue specific antigens are dependent upon AIRE, while a small percentage is AIRE-independent (2). Mice with defects in AIRE develop peripheral neuropathy and diabetes(3). Mice that completely lack AIRE develop a multi-organ inflammatory phenotype, secondary to T cell reactivity to a plethora of self-antigens. This disease is similar to the human condition, Autoimmune Polyendocrinopathy-Candidiasis-Ectodermal Dystrophy (APECED), in which AIRE defects are inherited in an autosomal recessive fashion(21).

There has also been consideration for the fact that the defect may lie in the autoantigen itself. Myelin P0 protein has been investigated for this reason, and it has been found that genetic

mutations in the gene for P0 offer two similar, yet strikingly different presentations of peripheral neuropathy. Mice with homozygous gene mutations for P0 quickly develop a demyelinating phenotype in the PNS that is noticeable as early as 4 weeks after birth. However, those mice with a heterozygous P0 mutation develop gait deficits that progress to paralysis, beginning at 20 weeks of age (19). Intracellular adhesion molecule 1 (ICAM1), a leukocyte adhesion molecule and costimulatory molecule is protective against diabetes in NOD mice. However, the lack of ICAM1 results in a peripheral neuropathy, characterized by inflammation of the peripheral nerves with mononuclear cells (17). The clinical and histopathologic phenotype of this disease is similar to SAPP, with the exception of the age of onset: SAPP begins at 20 weeks, and the ICAM1 deficient neuropathy begins at 28 weeks of age. This study seeks to shift the disease phenotype of SAPP, by adding back half of the complement of the B7-2 costimulatory molecule.

RATIONALE

NOD mice that are homozygous knockouts for B7-2 develop spontaneous autoimmune peripheral nerve disease. The rationale for this study is that if NOD wild type and NOD B7-$2^{-/-}$ mice are crossed, the resulting heterozygotes will have at least partial action of B7-2, which may decrease the inflammatory phenotype seen in the peripheral nerves.

Hypothesis: NOD.B7-$2^{+/-}$ mice will have a lower disease incidence compared to female NOD.B7-$2^{-/-}$ mice.

RESULTS

Clinical Disease

Throughout the duration of the experiment, mice were lost to diabetes. Female mice reached a humane endpoint for diabetes as early as 17 weeks of age. Males were also affected; their humane endpoint was as early as 25 weeks of age. At the conclusion of the study, 36% (5/14) of female mice and 74% (13/14) male mice remained. Throughout the course of the experiment, four female mice and four males developed diabetes. Diabetic mice had excessively wet bedding, which emitted a sweet smelling ketotic odor, as is classically described for the disease. Additional findings observed included a “tucked-up” appearance, enlarged abdomen, and rough haircoat.

Open Field Test (OFT)

Both female and male mice had significantly decreased rears over time (Figure 3.19). Pairwise comparisons showed statistical differences between the mean rears of male and female mice at 20, 24, and 27 weeks of age (figure 3.33, B,D,E). Both female and male mice exhibited dyskinesia, and a significant difference between occurrences was seen at 20 weeks (Figure 3.34,B). The facial grimace was present more in male mice in this study, fist appearing at 17 weeks. The females didn't start to show a grimace until 3 weeks later, at 20 weeks of age Figure (3.35).

Hang Test

When male mice were compared to themselves longitudinally, there was a significant difference in hang time (Figure 3.23). No significant difference in time spent hanging was noted when females were compared to themselves over time. In pairwise comparisons between males and females, there was a significant difference at 28 weeks of age (Figure 3.24, E). In some

cases, SAPP affected mice would slip their SAPP-affected, clasped hind paw through the bars to compensate for lack of toe/grip strength (Figure 3.25).

Histopathology

Under light microscopy, clinically diabetic mice had pancreatic lesions consistent with diabetes (Figure 3.26). Normal pancreatic islet architecture was effaced and obliterated by varying degrees of scattered and clustered small lymphocytes and plasma cells. Beta cells in affected islets were difficult to identify. There were mild infiltrates of a similar mononuclear cell population in peri-islet areas. The following morphologic diagnosis given was: Moderate to severe, multifocal to locally extensive, lymphoplasmacytic pancreatic insulitis and peri-insulitis.

Mice affected by SAPP had a heterogeneous population of inflammatory cells in the brachial plexus, and peripheral nerves. The inflammation was a mixture of lymphocytes, plasma cells, neutrophils, and macrophages. In the dorsal root ganglion, the predominant cell type was small lymphocytes. The character of the inflammation was similar to that observed in previous SAPP experiments. The brachial plexus had more severe inflammatory scores among the three tissues examined, but there was no statistically significant difference (data not shown). A masson trichrome was used to confirm the presence of increased compact collagen replacing normal myelinated axon morphology (Figure 3.27, A and B).

Histopathologic evaluation of the dorsal root ganglia, brachial plexus, and peripheral nerves of male mice revealed no tissue architectural changes, nor infiltration of inflammatory cells in all but one mouse. The affected mouse had a total score of 2, with fibrosis noted in the brachial plexus (Figure 3.27,C).

MATERIALS AND METHODS

Mouse Breeding and Handling

The study began with 14 female mice and 17 male mice. The study concluded when the mice were 33 weeks of age. All experimental protocols and procedures were approved by the Institutional Animal Care and Use Committee at Michigan State University (06-12-107-00). NOD wild type mice were mated with NOD B7-2$^{-/-}$ mice to create the F1 generation. The mice were from a specific pathogen free colony and singly housed in sterilized, filter-topped cages, on corn cob bedding. The cages were changed once a week. Mice were fed a diet of Irradiated Harlan Teklad 7913 chow (Harlan Teklad, Indianapolis, Indiana, USA) and given free access to sterilized water. Animal technicians and experimental handlers wore standard personal protective equipment for non-infectious animals any time they were handling mice, and gloves were disinfected using 70% ethanol between cages.

Hang Test

Mice were placed right side up on the wire cage rack of their home cage. Once their paws were gripped onto to rack, it was slowly rotated upside down above their cage. The timer was started. The mice were given three separate trials, and the average was taken of the three times. The maximum time for hanging per trial was 2 minutes. If a mouse reached the 2-minute mark, they were removed from the rack and allowed to rest for 30 seconds before the next trial began. If they were unable to hold on for at least 10 seconds, they were listed as not having a successful trial, and a time of zero was recorded.

Open Field Test (OFT)

Mice were placed in the open field test and observed weekly for signs of motor deficits. The mice were videotaped for 60 seconds while they moved freely about the field (plastic rat cage). At the end of the 60 seconds, they were held up by their tails and evaluated for dyskinesia, which included the clasping reflex. The open field cage was disinfected using 70% ethanol in between each mouse.

Presence or absence of a facial grimace was evaluated from the open field test videos. This protocol was modified from Langford, et.al (12). The mice received a score of 0 if there was no grimace present, and a score of 1 if there was a grimace. A grimace was identified by the following features: squinted eyes, flattened ears, and puffed cheeks. Tremors is a known sign of pain in mice. Mice that showed tremors in the open field test were given a score of 1; absence of tremors was given a score of 0.

Assessing for Diabetes

Mice that had excessively soaked corn cob bedding were confirmed to have diabetes using Ketostix Bayer Reagent Strips. A pink sticker labeled “Diabetes” was placed on the cage card and affected mice were monitored closely until a human endpoint was reached.

Histopathology

The sciatic dorsal root ganglia (L3-L5), the brachial plexus, and the sciatic nerve were evaluated under light microscopy. All samples were taken from the left side of the mouse and fixed in 10% neutral buffered formalin for 48 hours. They were then transferred into 60% ethanol until processing. The slides were evaluated blindly using the standard peripheral nerve scoring sheet. Sections of pancreas, liver, heart, and kidney were also screened for evidence of inflammation or architectural changes

DISCUSSION

At the inception of this study, the aim was to 1) decrease the severity of SAPP or 2) protect the mice from developing SAPP. Some mice were protected from SAPP, but they went on to succumb from diabetes. One male mouse, out of 17, had a high histopathology nerve score. In previous experiments involving male mice, there was always a background population of male B7-2 knockout mice with inflammation in the nerves. It is possible that having half of the complement of B7-2 is able to partially redirect the inflammation in the males away from the nerve and to the pancreas. This thought is supported by the number of male mice that developed diabetes in this study, when it historically has a female bias.

The fact that the female mice with high histopathology scores didn't have a grimace response in the open field test is perplexing. The grimace was also absent in the females that had diabetes. The 3 females mice that did show a grimace at some point in the study, all had histopathologic scores of zero. When inflammatory cells enter the nerve, they secrete cytokines and other inflammatory mediators as chemoattractants for additional cells. The nerves, both motor and sensory, often suffer bystander injury. As a result, it was expected that the mice would experience pain. Recently published studies acknowledge more than one pain pathway in the peripheral nervous system—specifically one that has been found to involve crosstalk between microglial cells and neurons, which is further discussed in Chapter 5 (4, 24).

The facial grimace has been reliably used as a pain indicator in trial studies and observation of other SAPP affected mice to ensure accurate documentation. In addition, it has also been used successfully to assess pain mice after ear-notching, vasectomies, as well as the effectiveness of post-operative pain medication (13, 16, 18). A recent publication highlights the potential for variation in "live" scores (right at the moment) versus those scored from still images (18). It is worth reiterating here that all mouse grimace scores were taken from live, video-recorded images that can be revisited at any time.

Throughout the study, diabetic mice were euthanized when they reached a humane endpoint. This decreased the sample size significantly, especially in the females. There was no foresight that they would succumb to diabetes as early as they did. The experiment began with 31 mice, which included 14 females and 17 males. At the end of the study, there were 5 females and 14 males. Rarely is diabetes seen in the Mansfield colony of NOD wild type mice. When it is present, it's typically in females greater than 25 weeks of age (lab personnel communication). In this particular study, 8 mice developed diabetes.

The hang test times declined as the mice became ill, but it is believe that they would have been shorter had the mice not learned to adapt. Normal behavior is for mice to move around and explore on the bar while hanging upside-down. Rather than just falling back into their home cage when they could no longer hang on, some mice stuck their paws through the bars and remained immobile until the two minutes time limit for the trial was up. This falsely elevated the averages in some cases, and the data was interpreted in light of that fact. The male and female mice had similar average hang times until 26 weeks of age. That is when the males started to hang longer than the females, and it remained that way until the conclusion of the study.

Despite the fact that the desired outcome was not reached, it was concluded that in addition to being a costimulatory molecule, B7-2 plays a major role in central tolerance, quite possibly by helping to shape the T cell repertoire to a particular PNS antigen, most like myelin protein zero (MPZ). It is known that at least one of the autoantigens in SAPP is MPZ (11, 14). This conclusion was reached by seeing an overall shift in the clinical phenotype of SAPP in the heterozygote mice.

ACKNOWLEDGEMENTS

We would like to thank Dr. Ankit Malik for his expertise in cytokine neutralization and assistance with flow cytometry. In addition, we thank Leslie Dybas and Dr. Julia Bell for the generation of the F1 mice for use in heterozygote experiment. We would also like to thank Dr. Laura McCabe and Regina Irwin for the technical assistance with micro-computed tomography of the mouse femurs.

APPENDIX

Table 3.1 Experimental Groups for the Cytokine Blocking Study

Treatment Group	No. of males/females	Timing of treatments
Anti-IL-17 Antibody	6 females, 7 males	12-16 weeks of age
Anti-IFNγ Antibody	6 males, 6 females	16-20 weeks of age
Anti-IL-17 and IFNγ Antibody	6 females, 6 females	12-16 weeks (α-IL17) followed by 16-20 weeks of age (α-IFNγ)
Control IgG	5 females, 6 males	

Figure 3.1 Scatterplots of number of rears over time, within individual treatment groups. Tables beneath the plots show times when statistical significance between testing time points were significant.

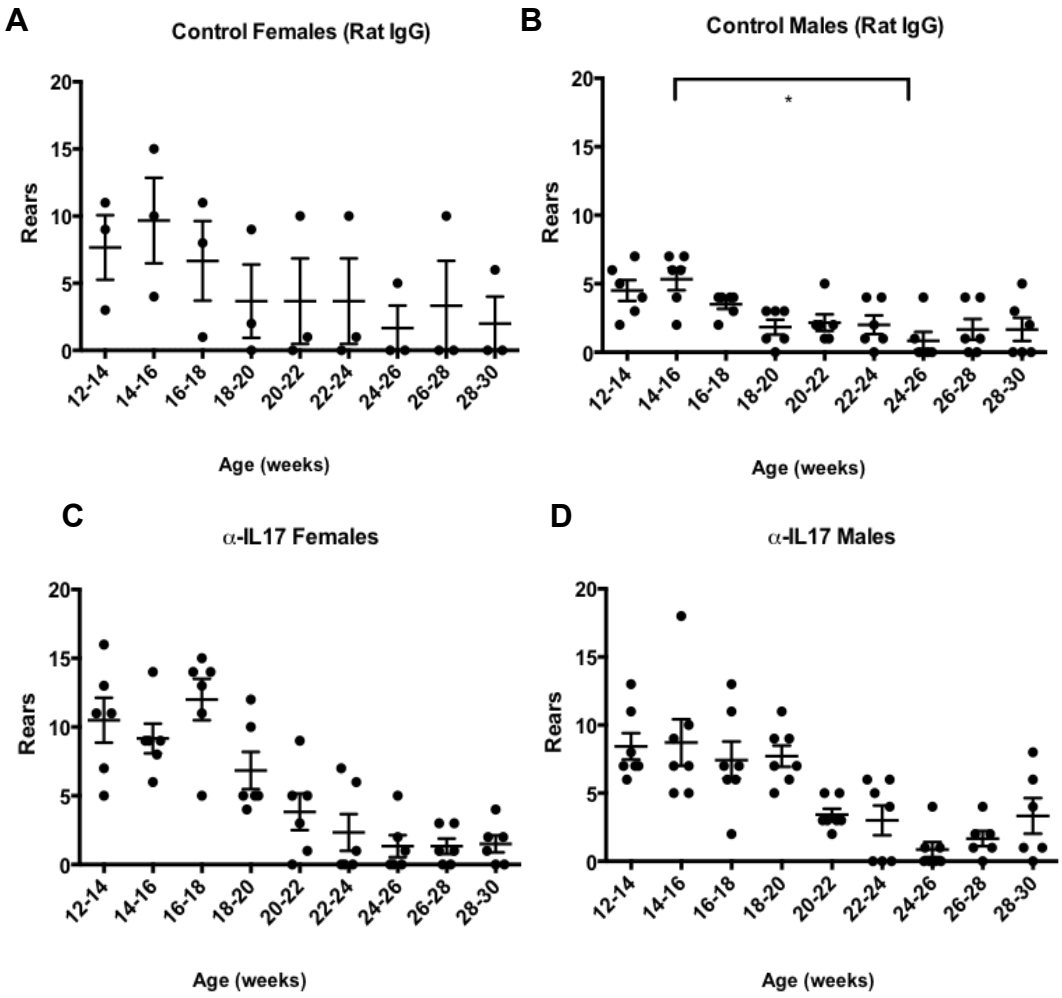

α-IL17

Age (weeks)	Significance
12-14 vs 24-26	*
12-14 vs 26-28	*
16-18 vs 22-24	*
16-18 vs 24-26	**
16-18 vs 26-28	*
16-18 vs 28-30	*

α-IL17

Age (weeks)	Significance
14-16 vs 24-26	**
16-18 vs 24-26	*
18-20 vs 24-26	**

Figure 3.1 (cont'd)

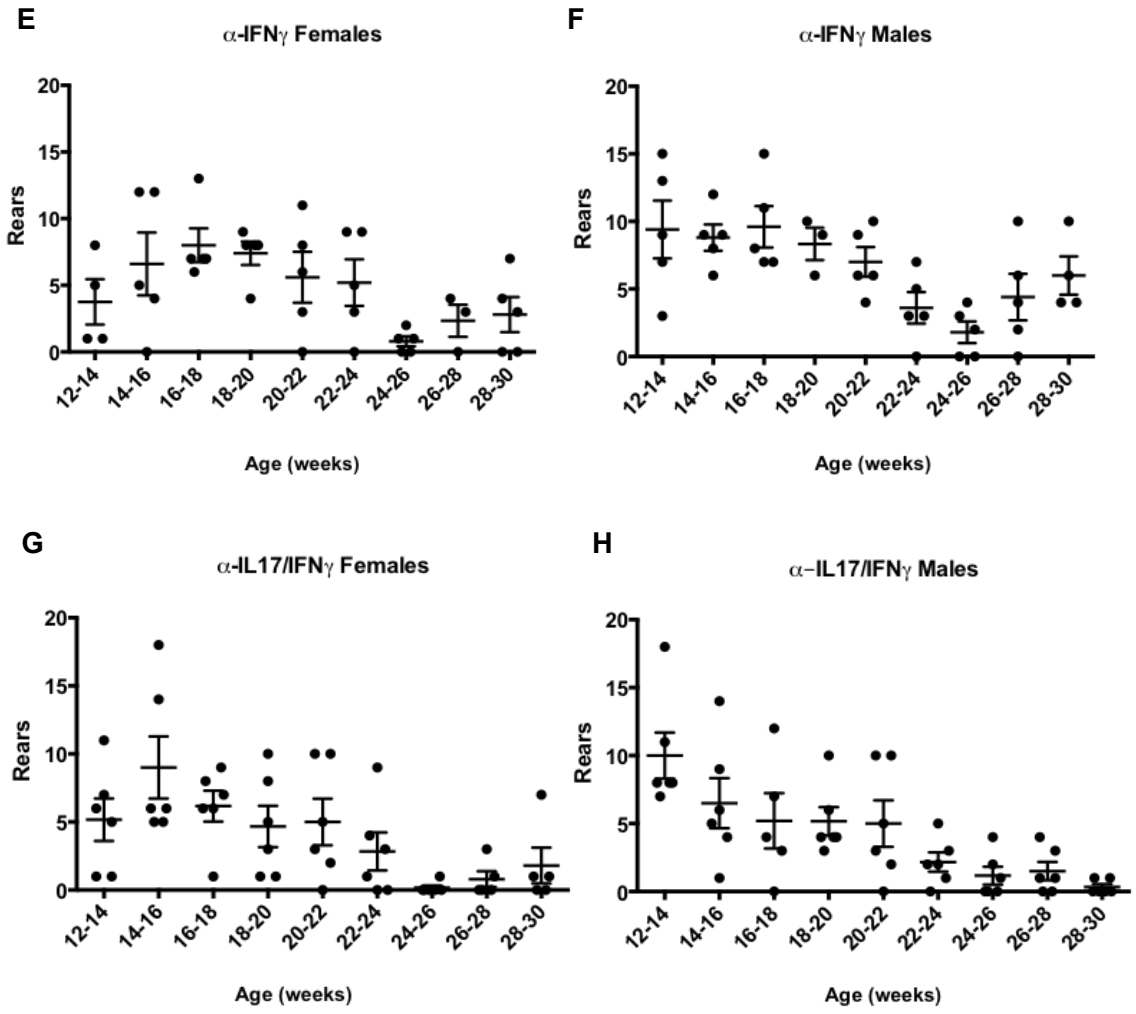

α-IFNγ

Age (weeks)	Significance
14-16 vs 24-26	*
16-18 vs 24-26	*

Age (weeks)	Significance
16-18 vs. 24-26	*

Age (weeks)	Significance
12-14 vs 24-26	*
12-14 vs 26-28	*
12-14 vs 28-30	**

Figure 3.2 Female mouse rears compared by age. No statistically significant differences in means were observed.

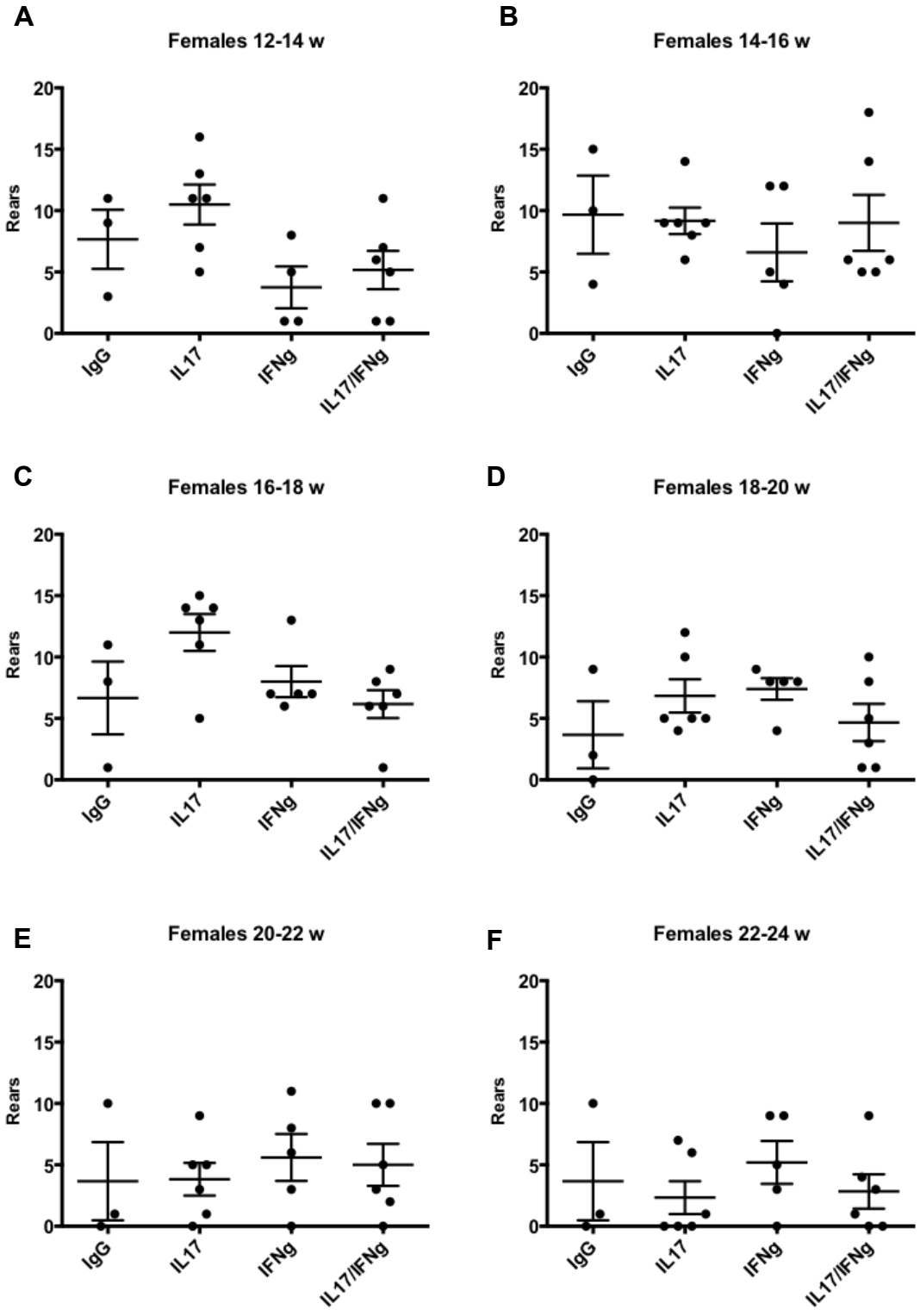

Figure 3.2 (cont'd)

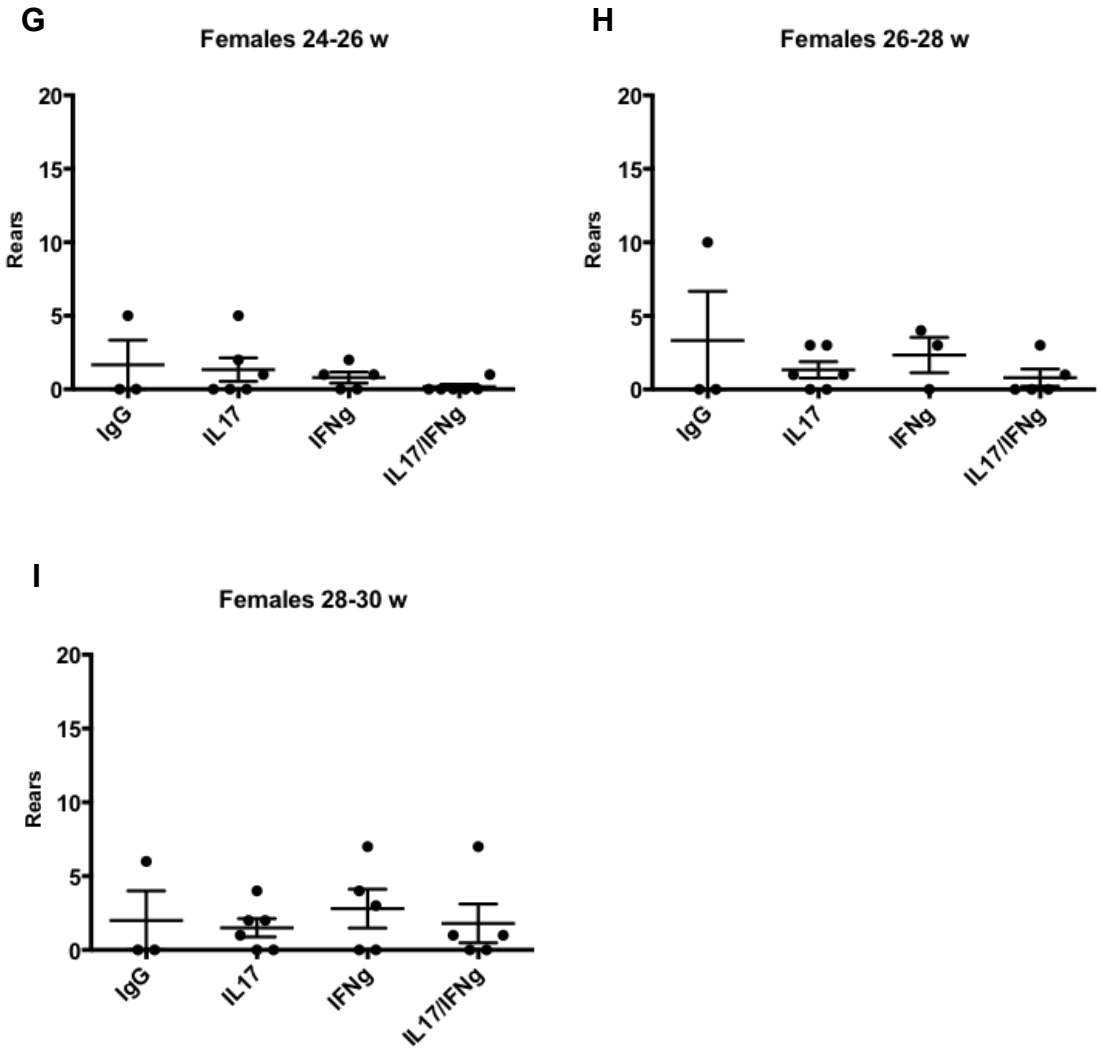

Figure 3.3 Male mouse rears compared by age. Multiple differences are seen between treatment groups at various time points. Most commonly, significantly increased rear means are noted between the control group and mice treated with antibodies to IFNγ.

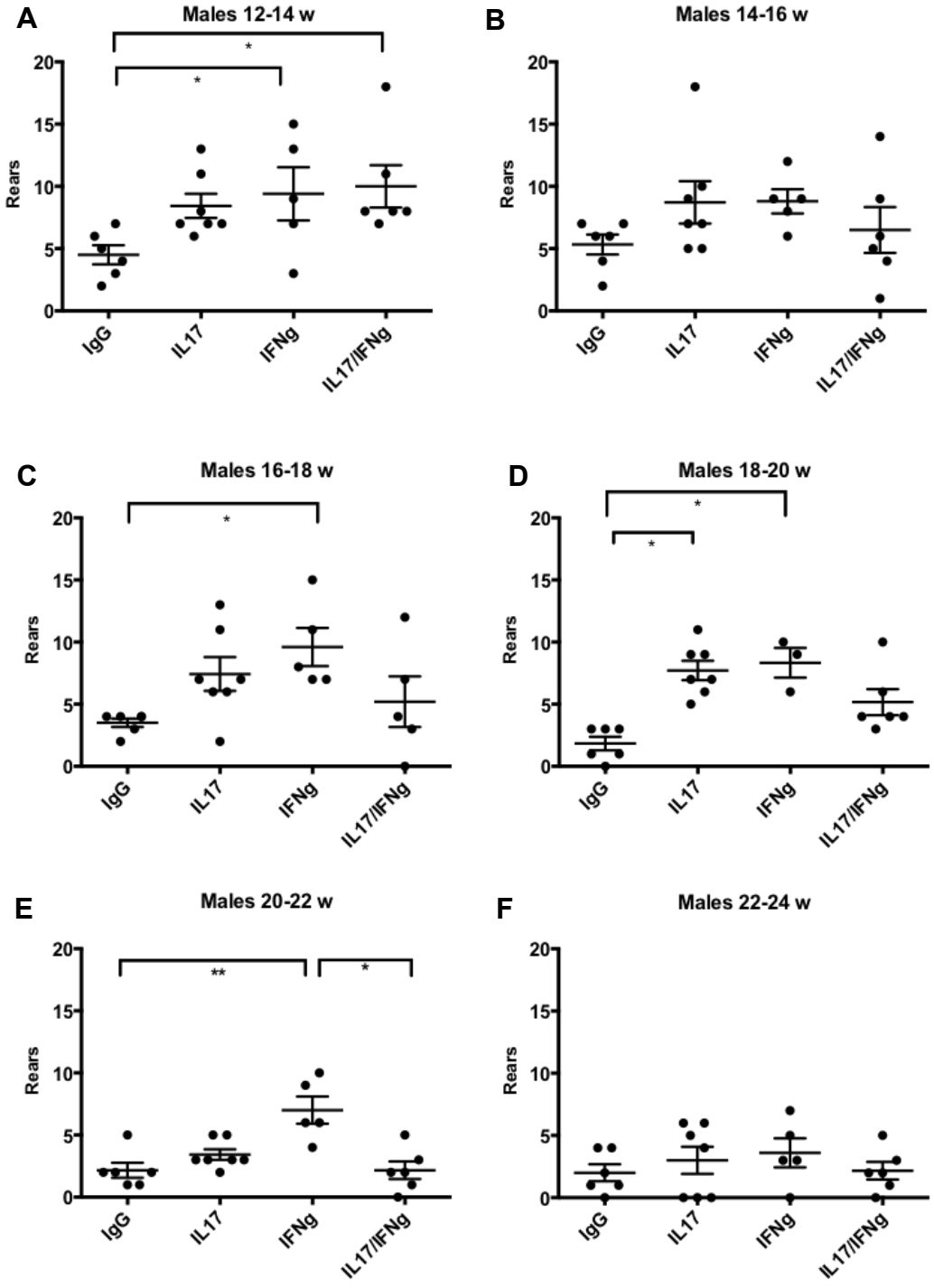

Figure 3.3 (cont'd)

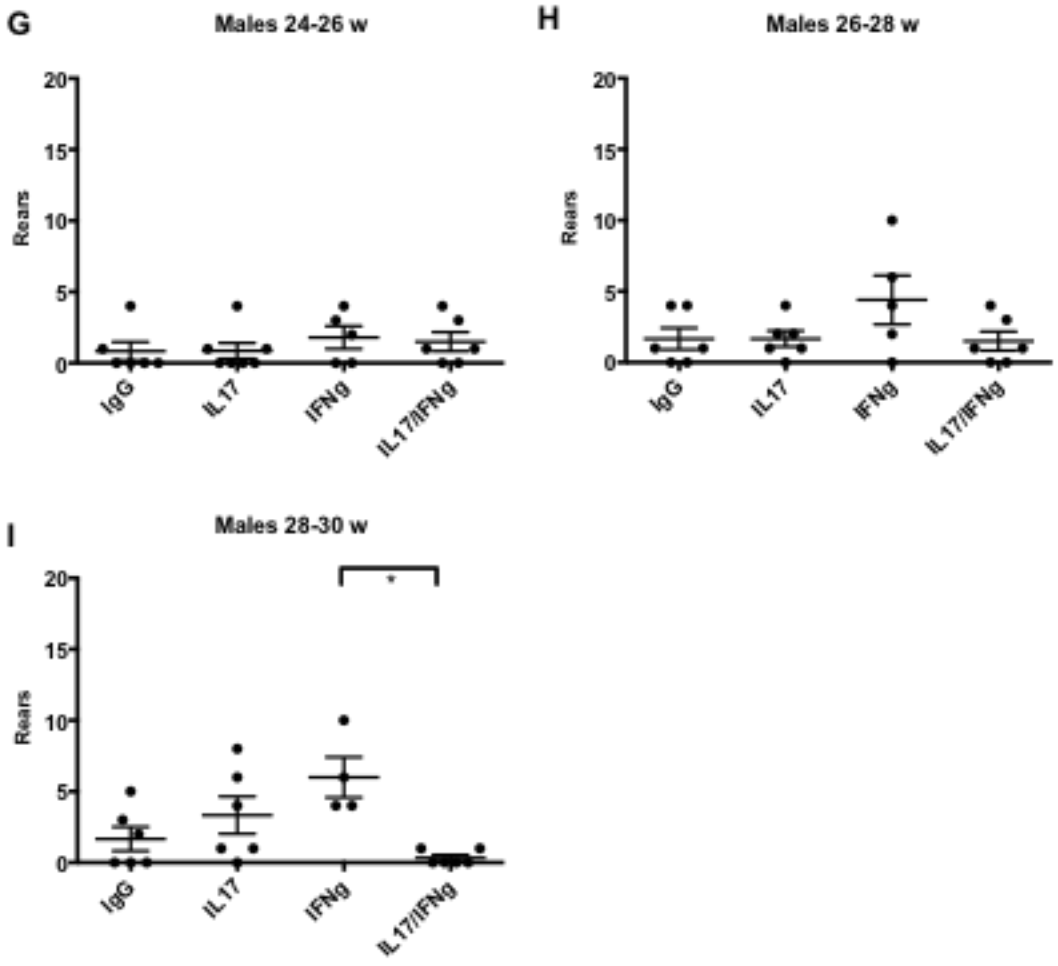

Figure 3.4 Dyskinesia in females was a prominent clinical feature in all female treatment groups.

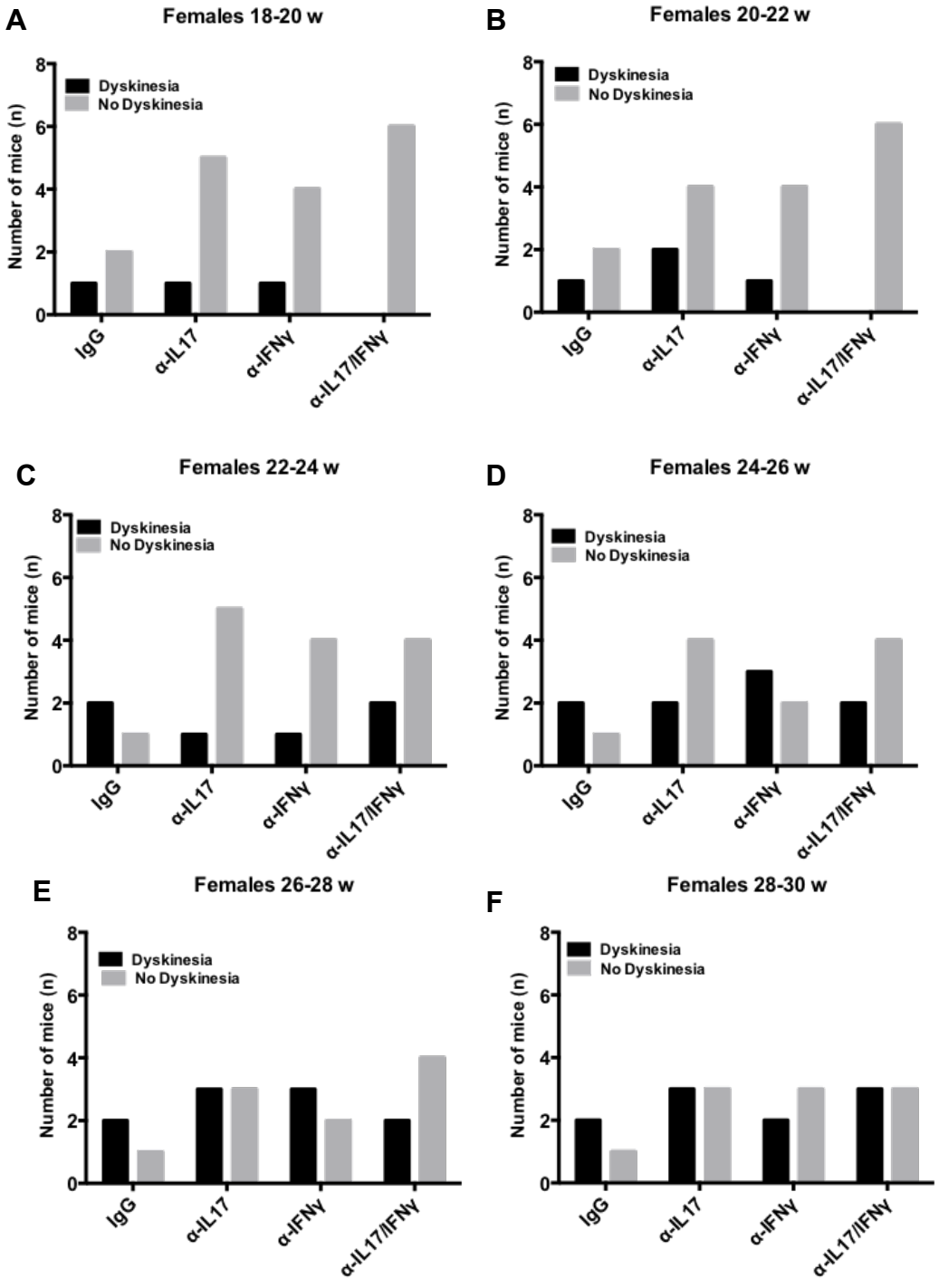

Figure 3.5 Dyskinesia in males was present in all experimental treatment groups at the end of the experiment.

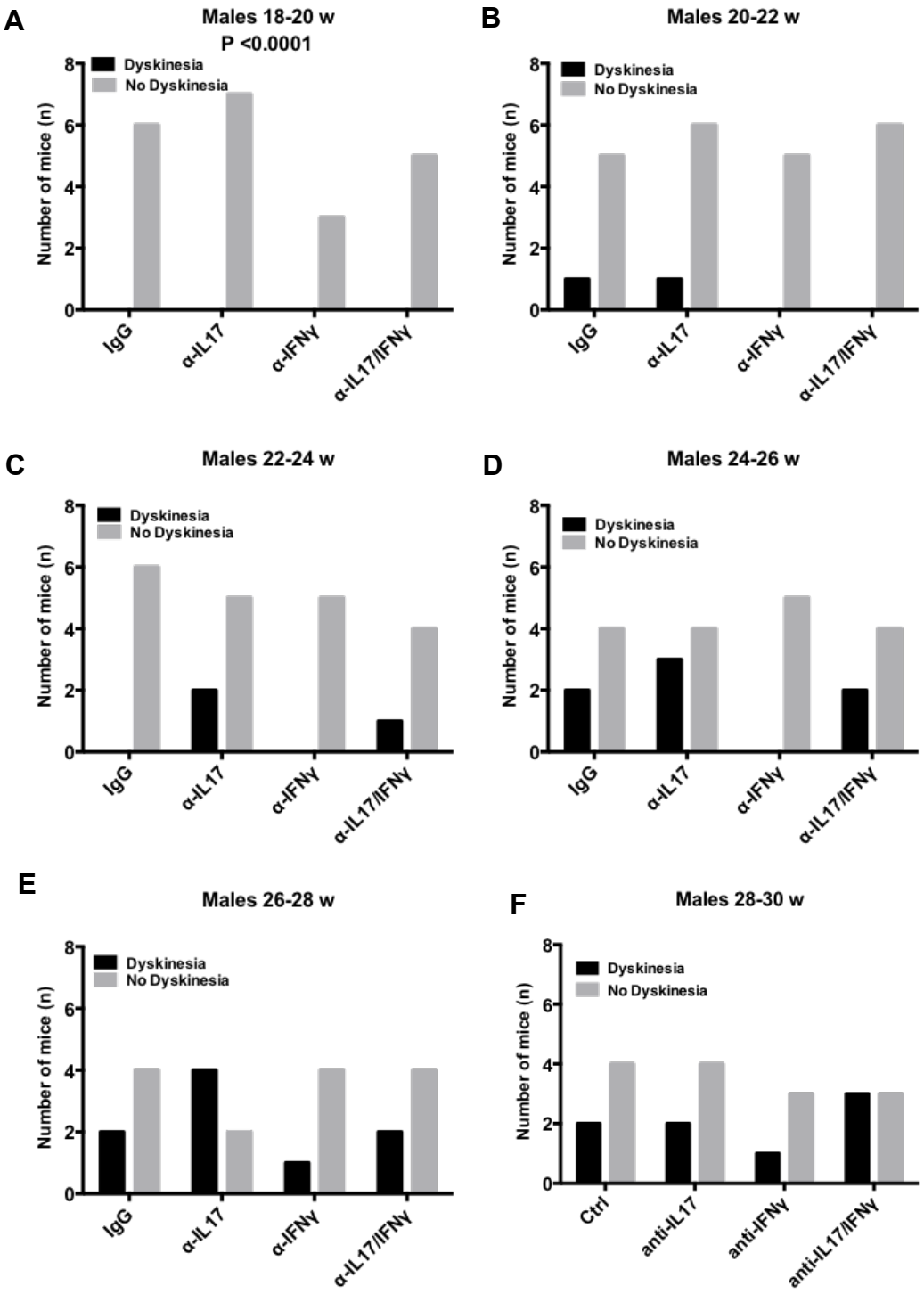

Figure 3.6 Facial grimace in females. Female mice treated with neutralizing antibodies against IL-17 had 100% of mice affected at the conclusion of the experiment (F).

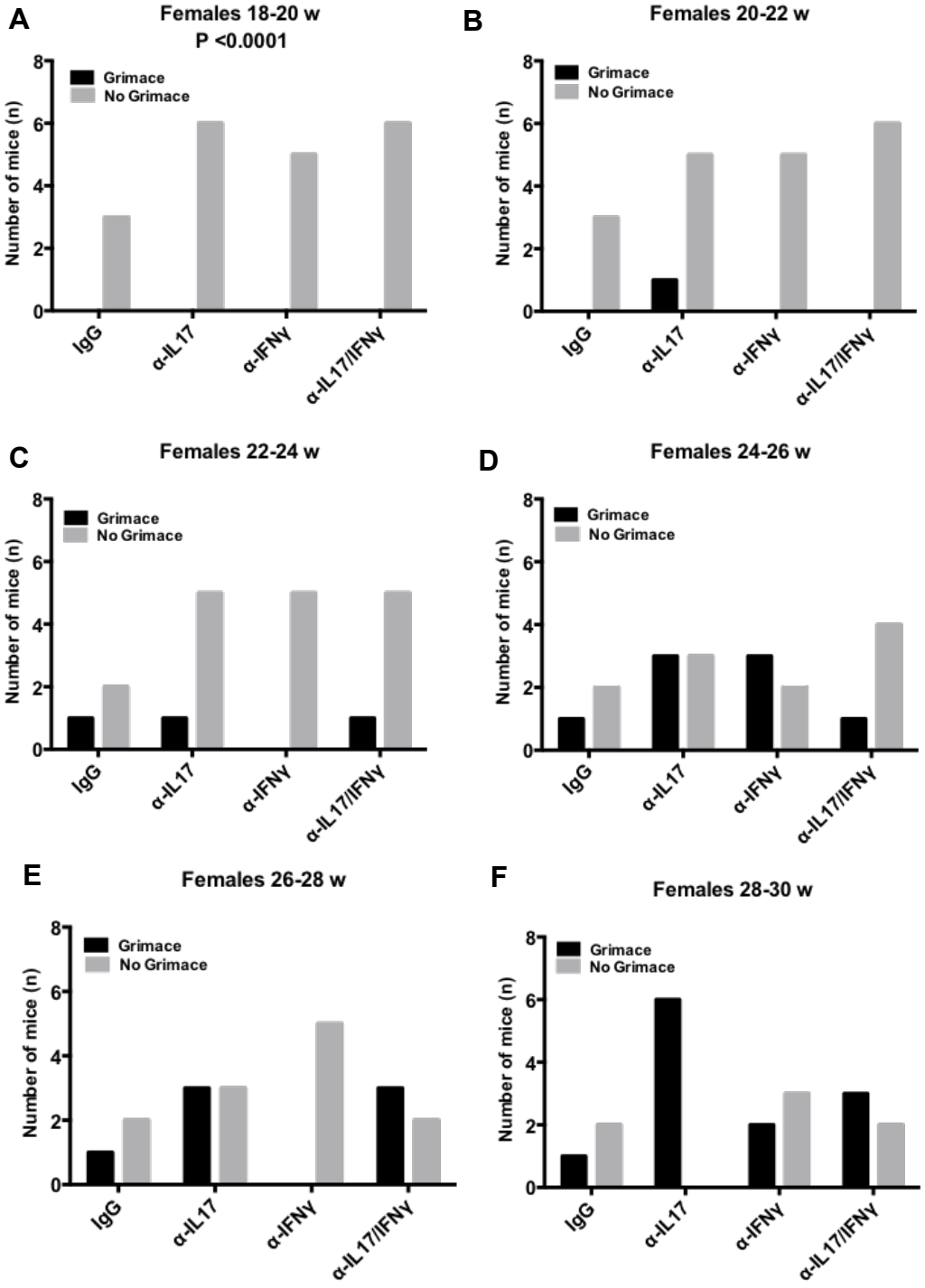

Figure 3.7 Facial grimace in males. The longest grimace streak was present in mice treated with both cytokine neutralizing antibodies.

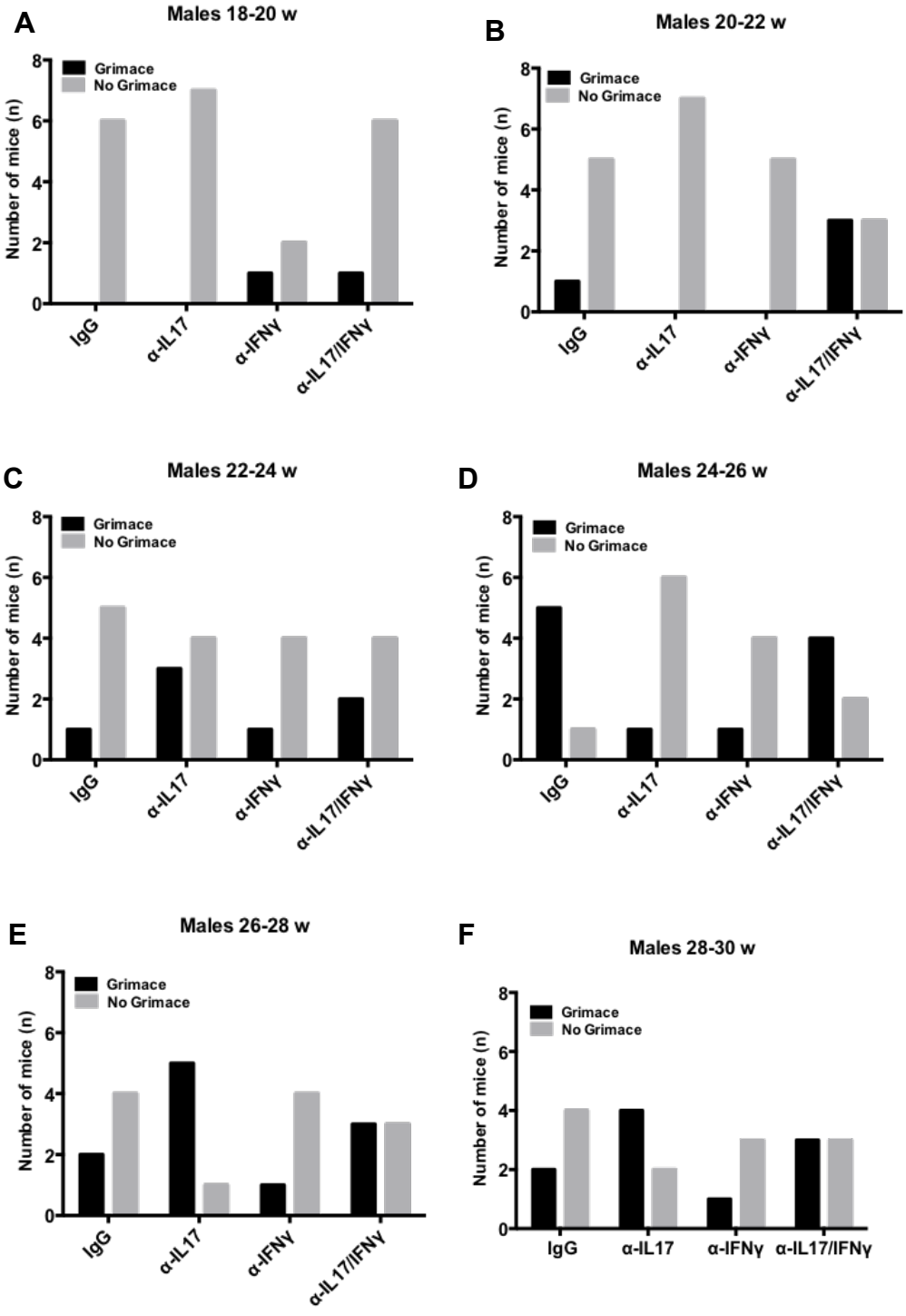

Figure 3.8 Tremors in females. Although there was not a constant presence of tremors throughout out the experiment, mice in all groups experienced tremors at some point throughout the experiment.

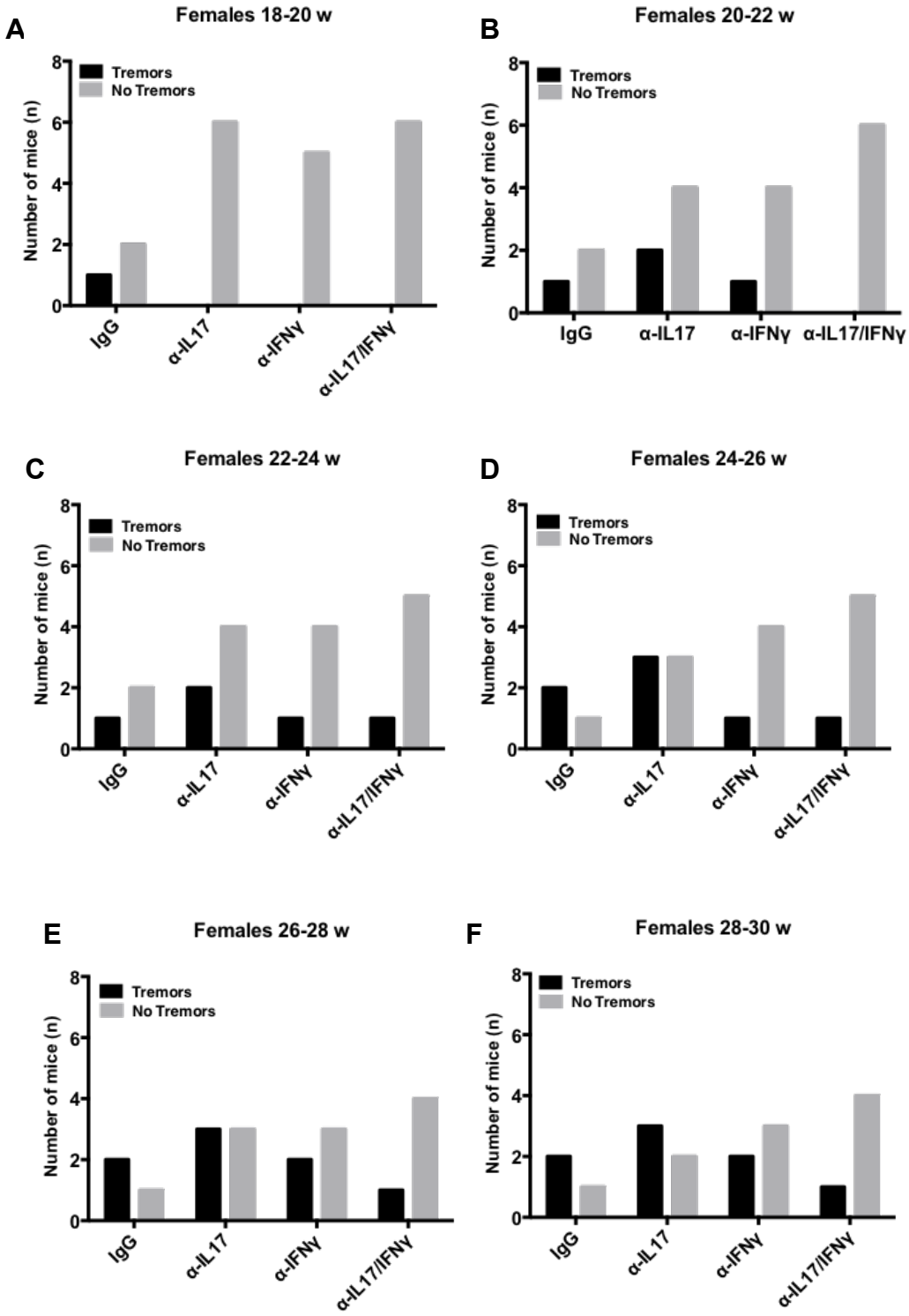

Figure 3.9 Tremors in males. Male mice had a statistically significant difference in the occurrence of tremors at 26-28 weeks with groupwise comparison (E).

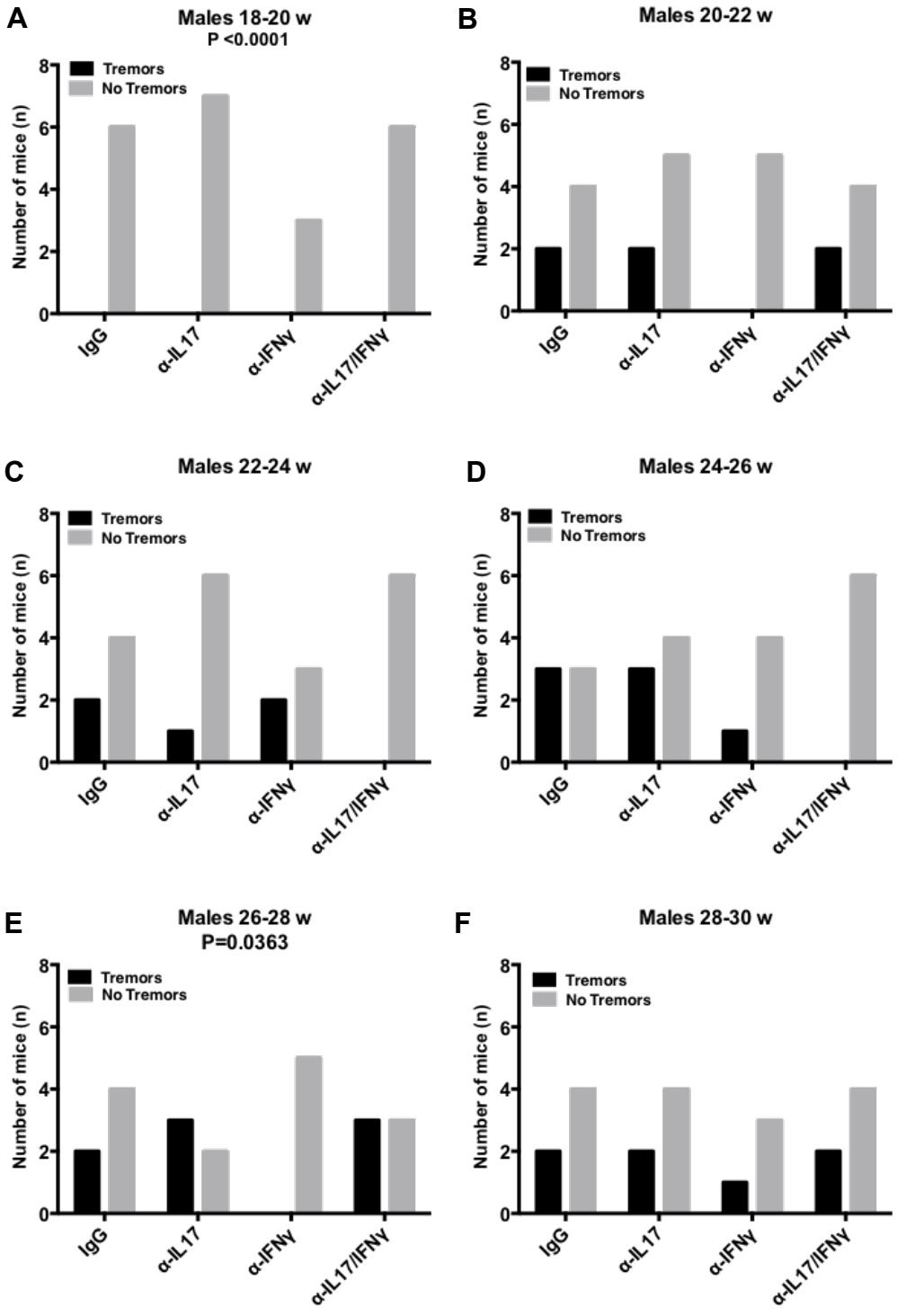

Figure 3.10 DigiGait front stance width. There is no statistical significance in front stance width over time in any treatment groups, male or female.

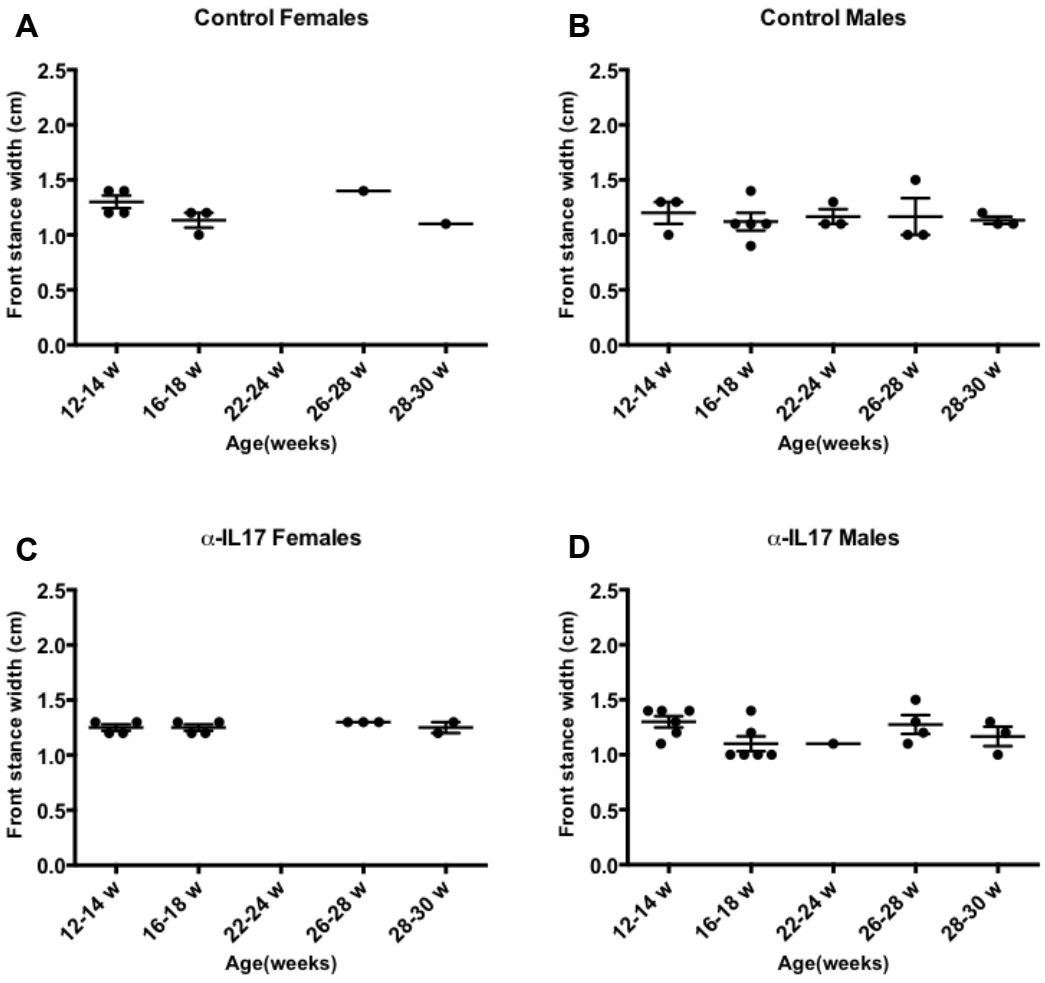

Figure 3.10 (cont'd)

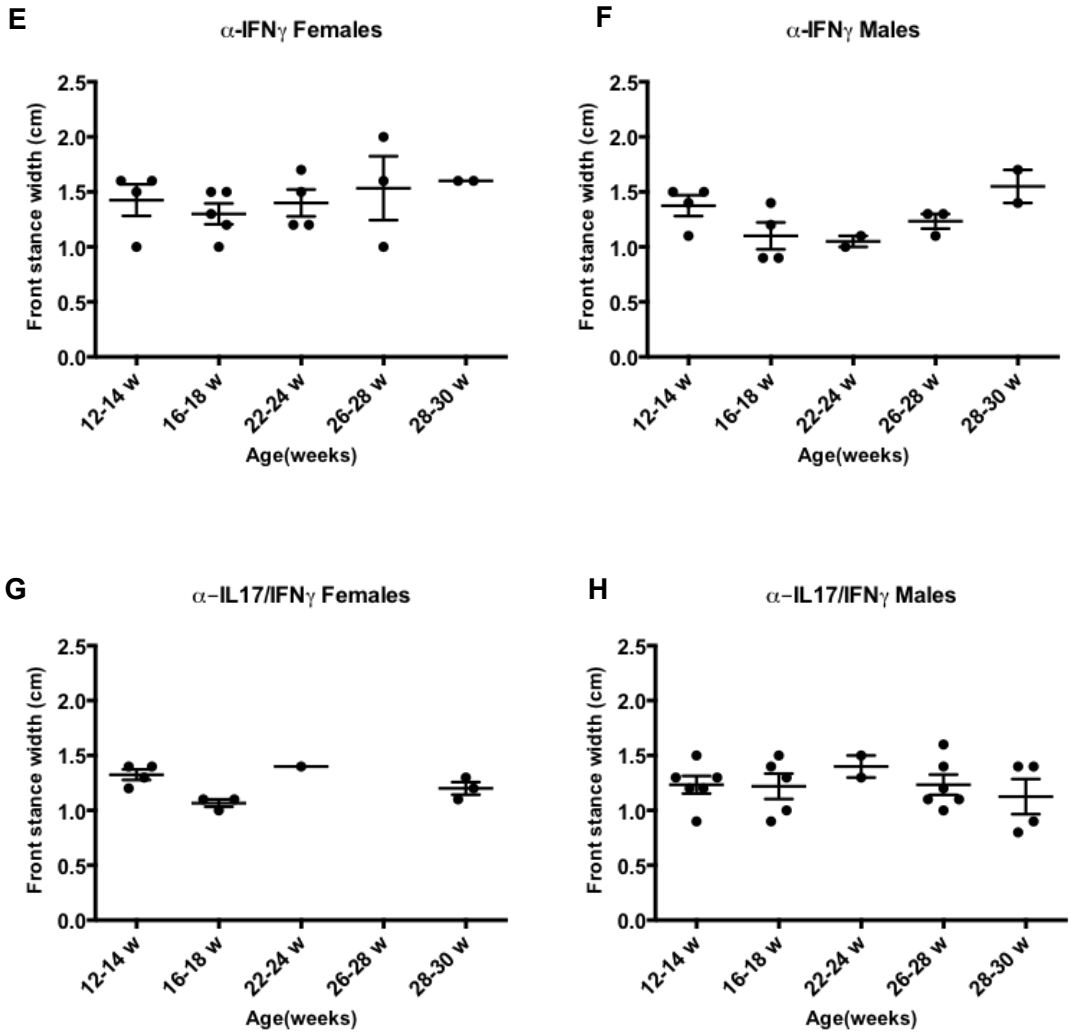

Figure 3.11 DigiGait hind stance width. There is no statistical significance in hind stance width over time in any treatment groups, male or female.

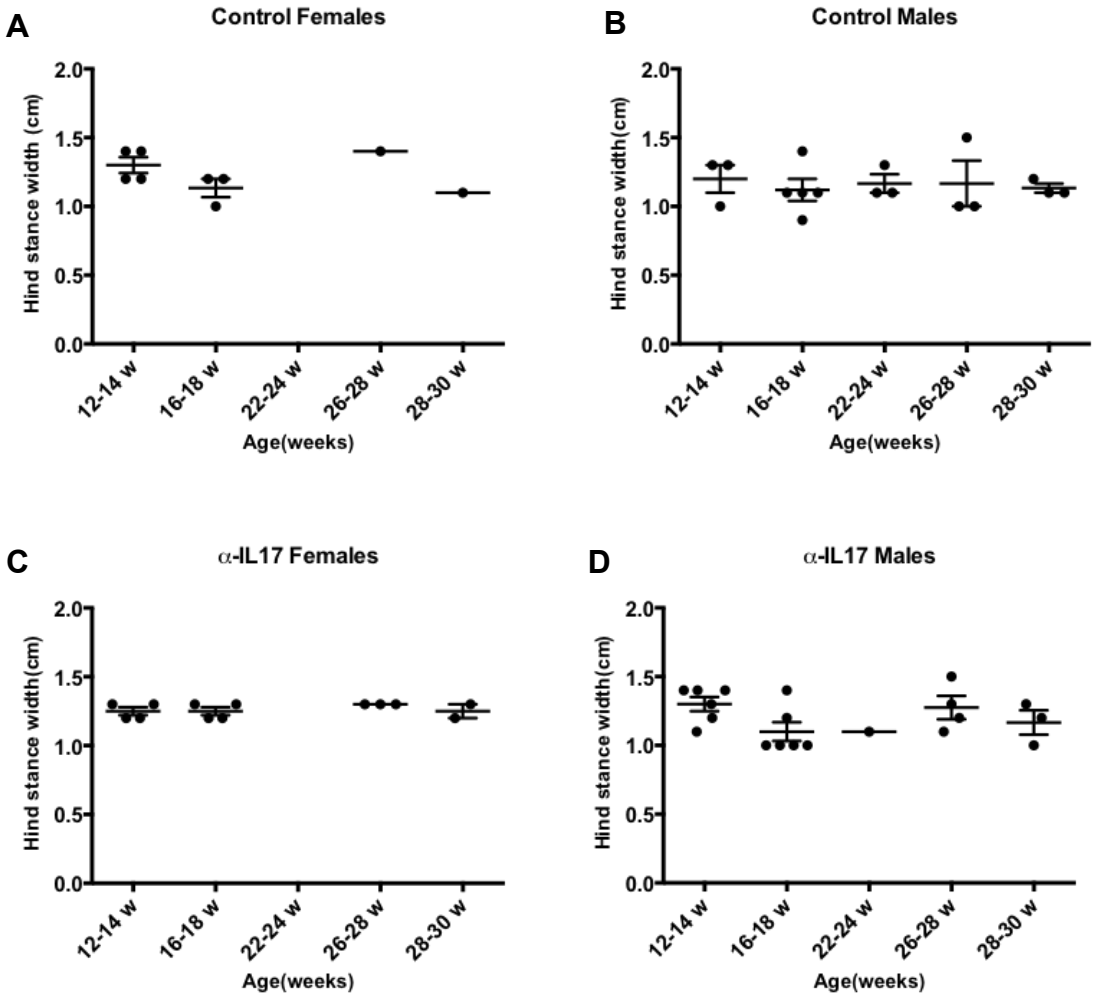

Figure 3.11 (cont'd)

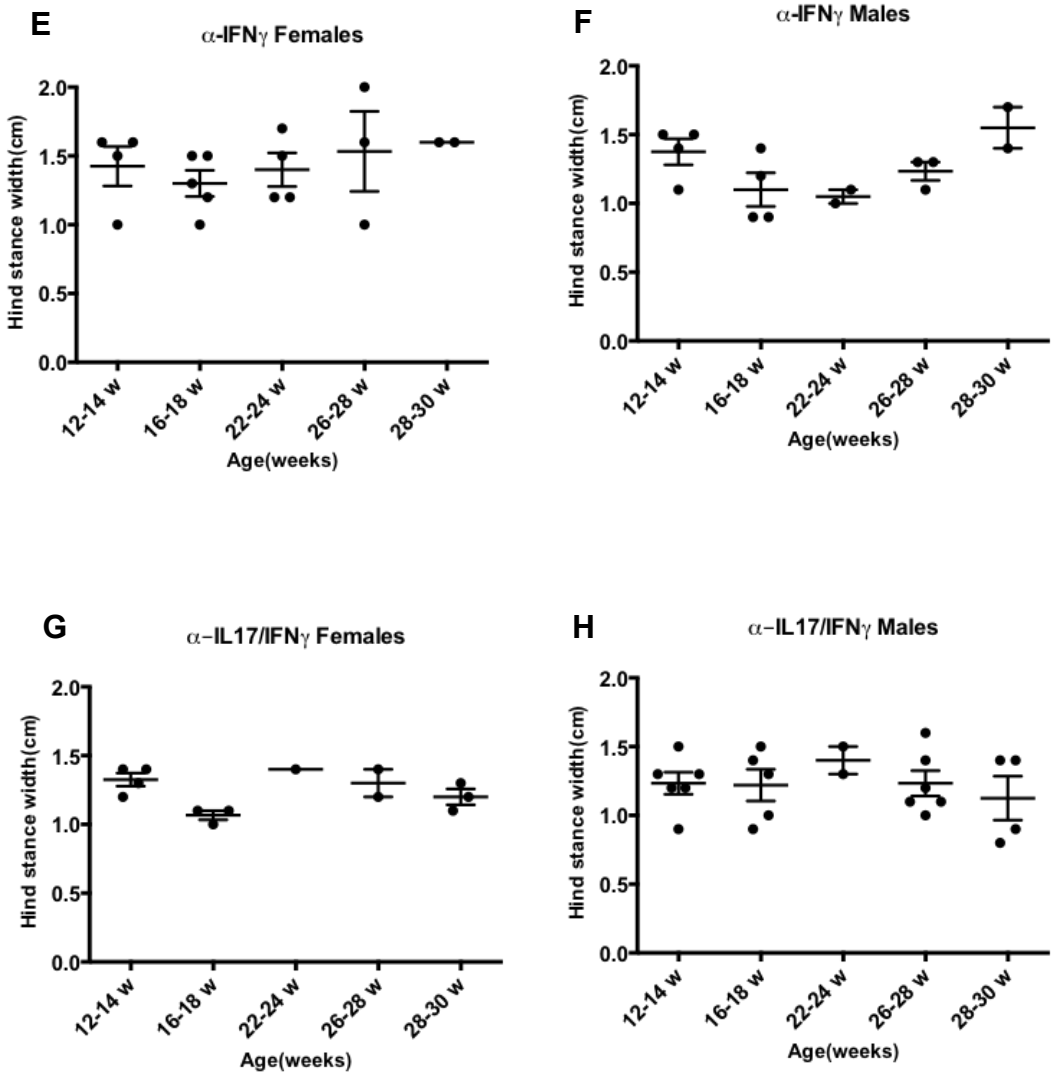

Figure 3.12 Front stance width comparison by treatment group in females. There were no statistically significant differences between groups.

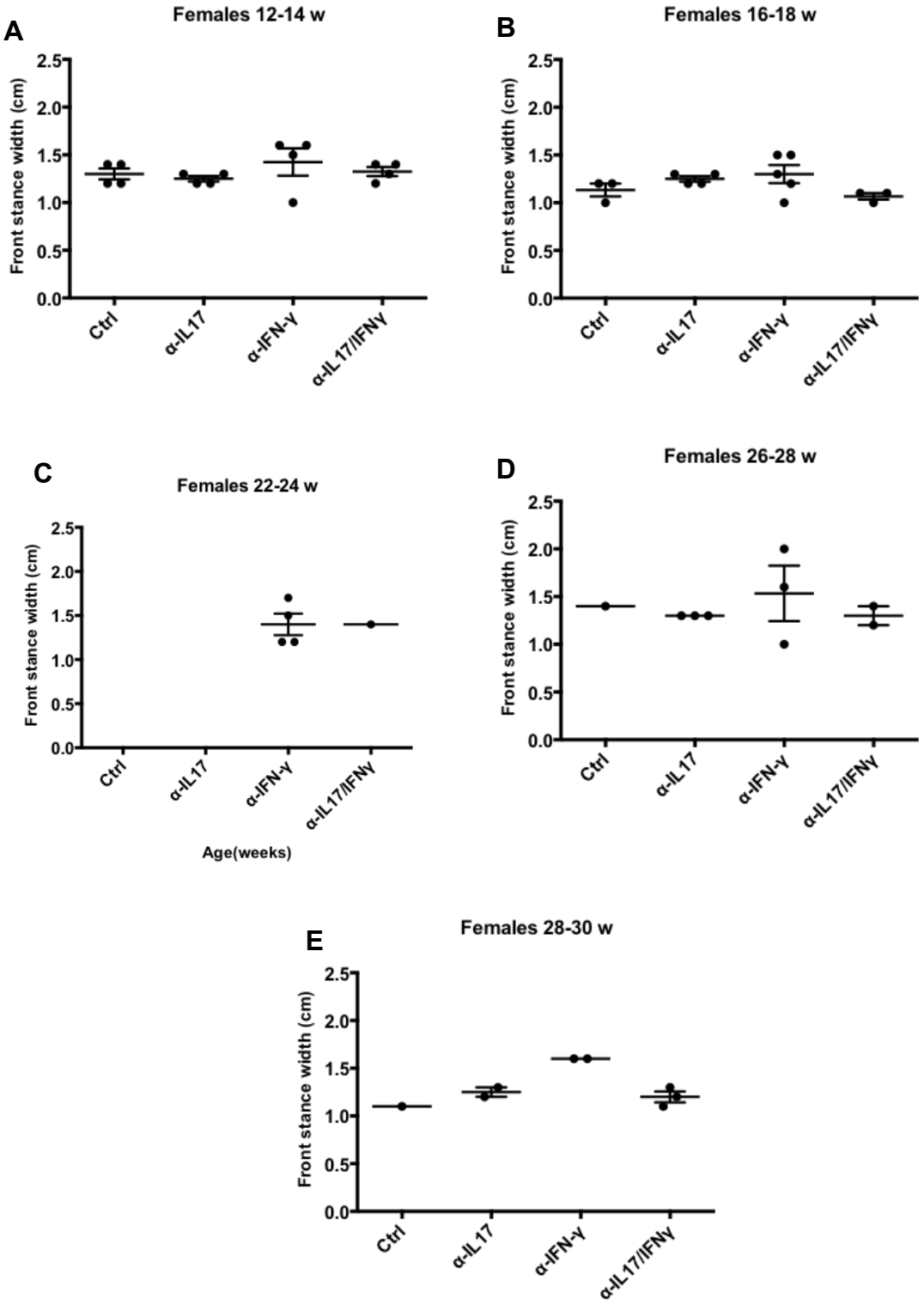

Figure 3.13 Front stance width comparison by treatment group in males. There were no statistically significant differences between groups.

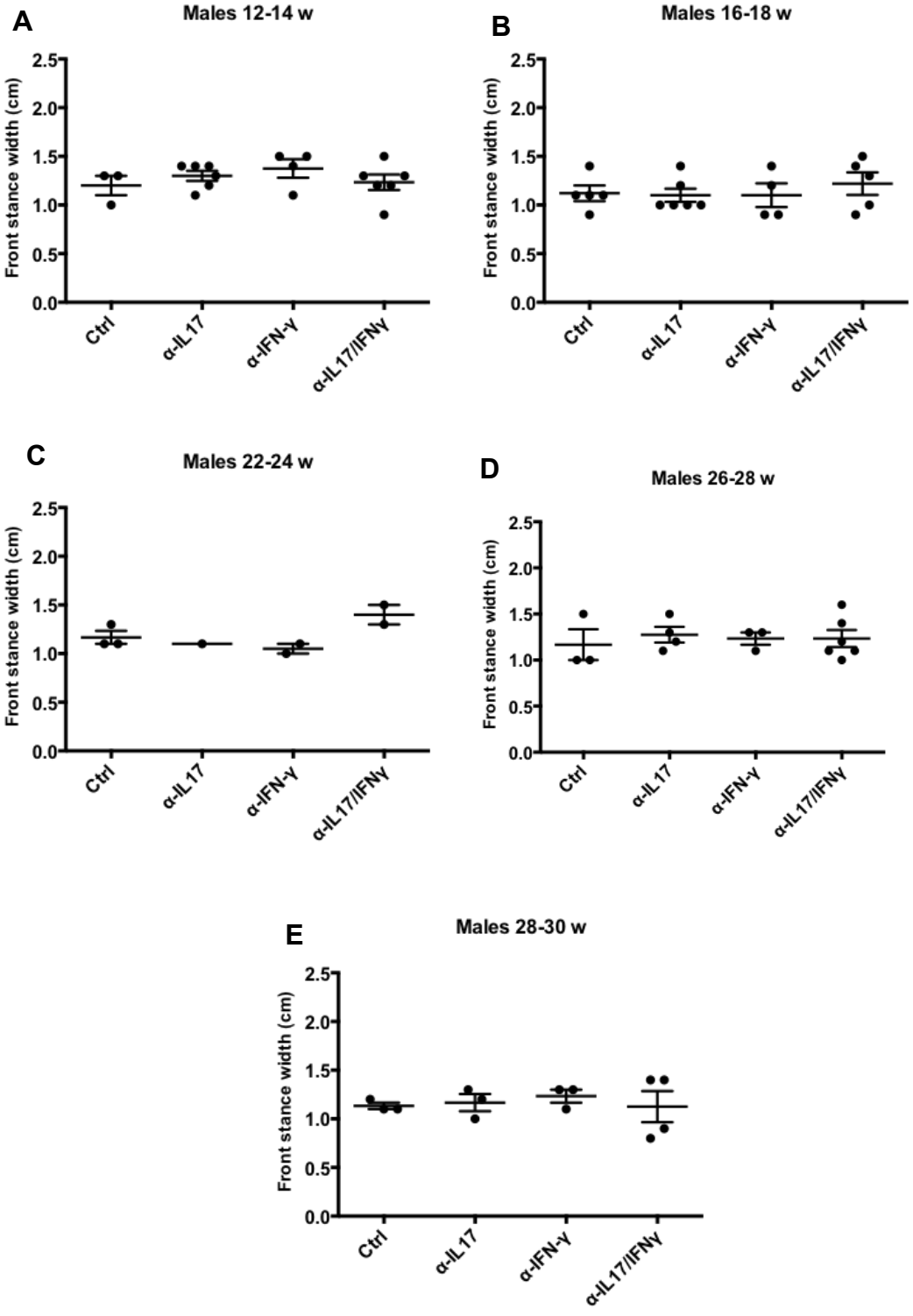

Figure 3.14 Left hind paw area over time.

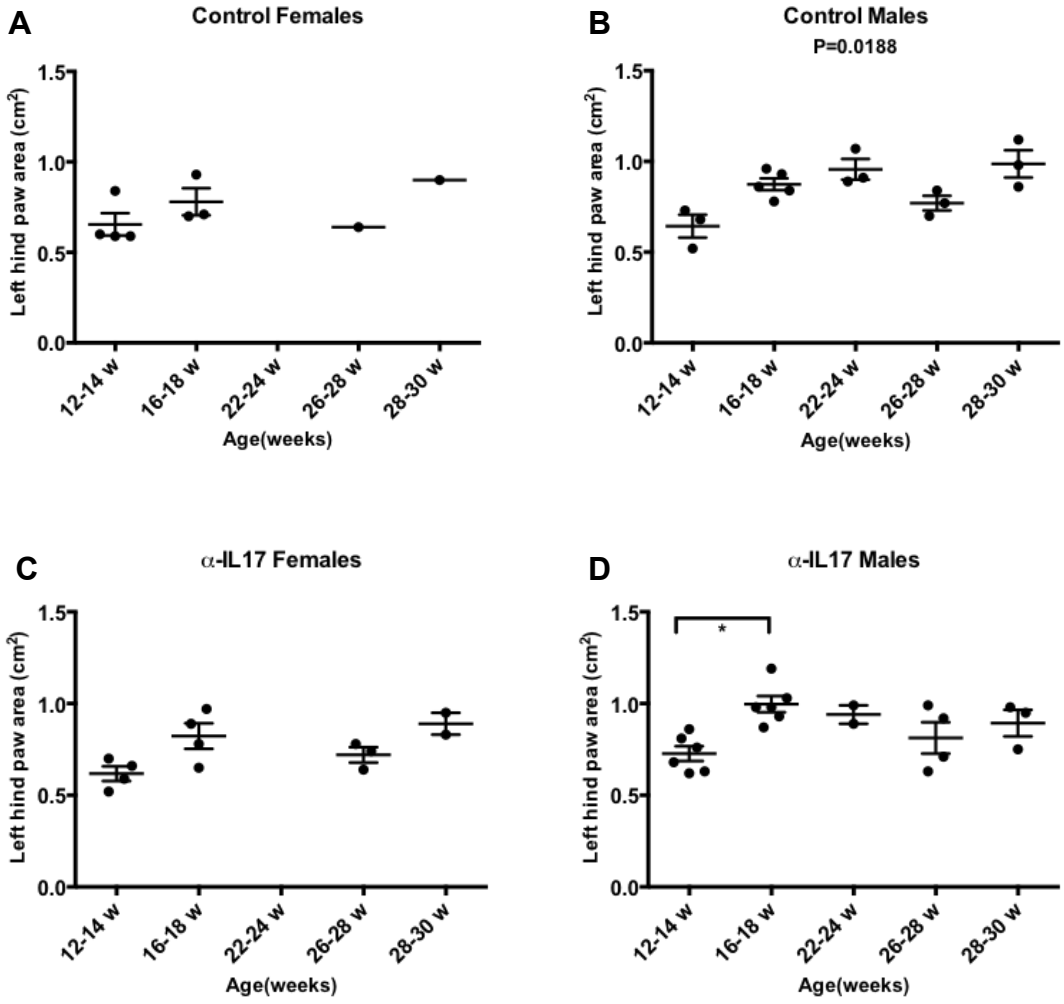

Figure 3.14 (cont'd)

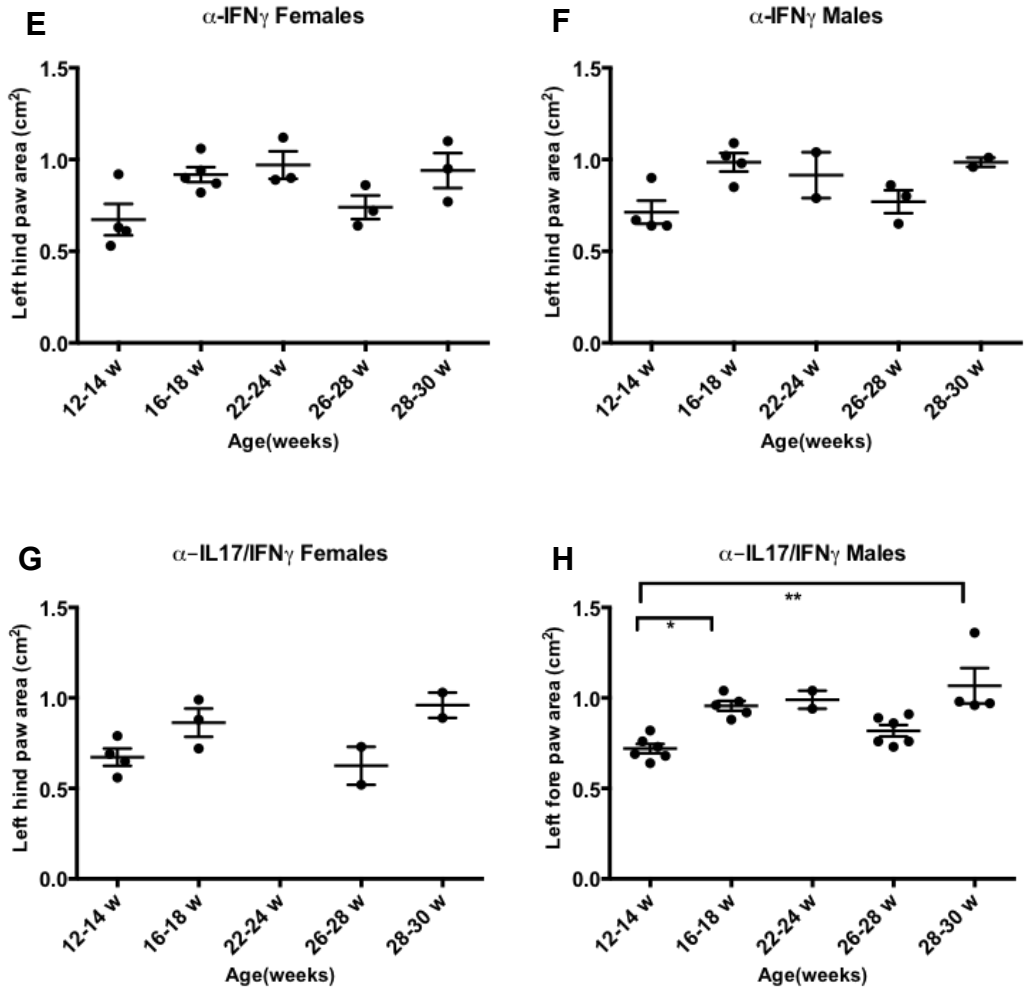

Figure 3.15 Right hind paw area over time.

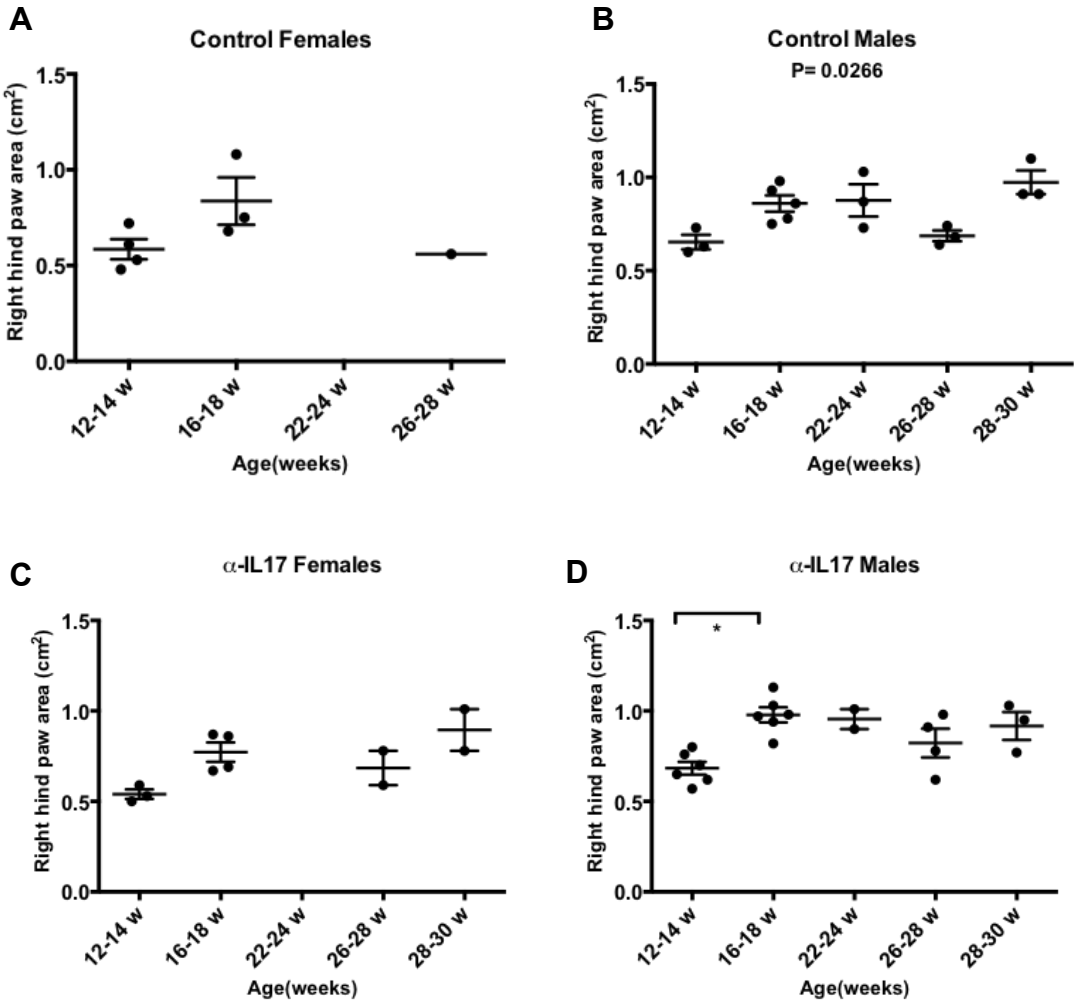

Figure 3.15 (cont'd)

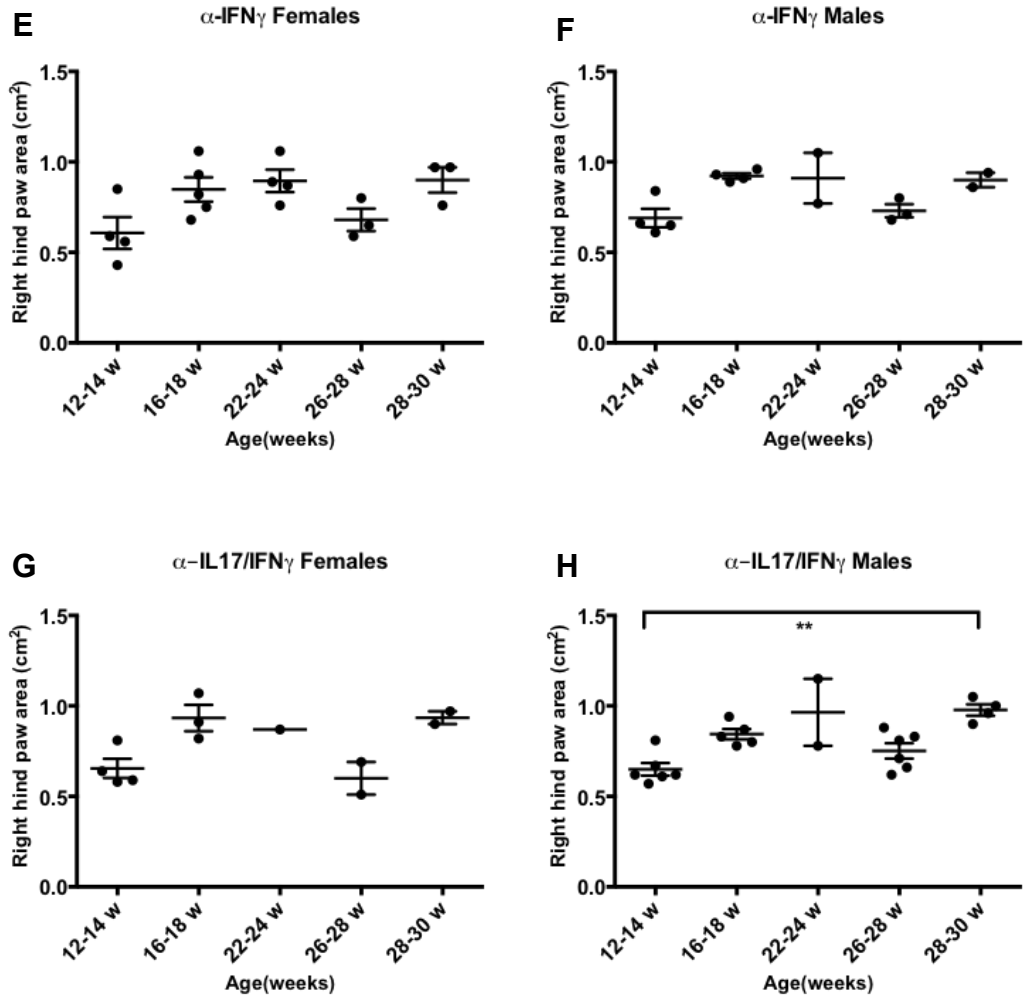

Figure 3.16 Left forepaw area over time

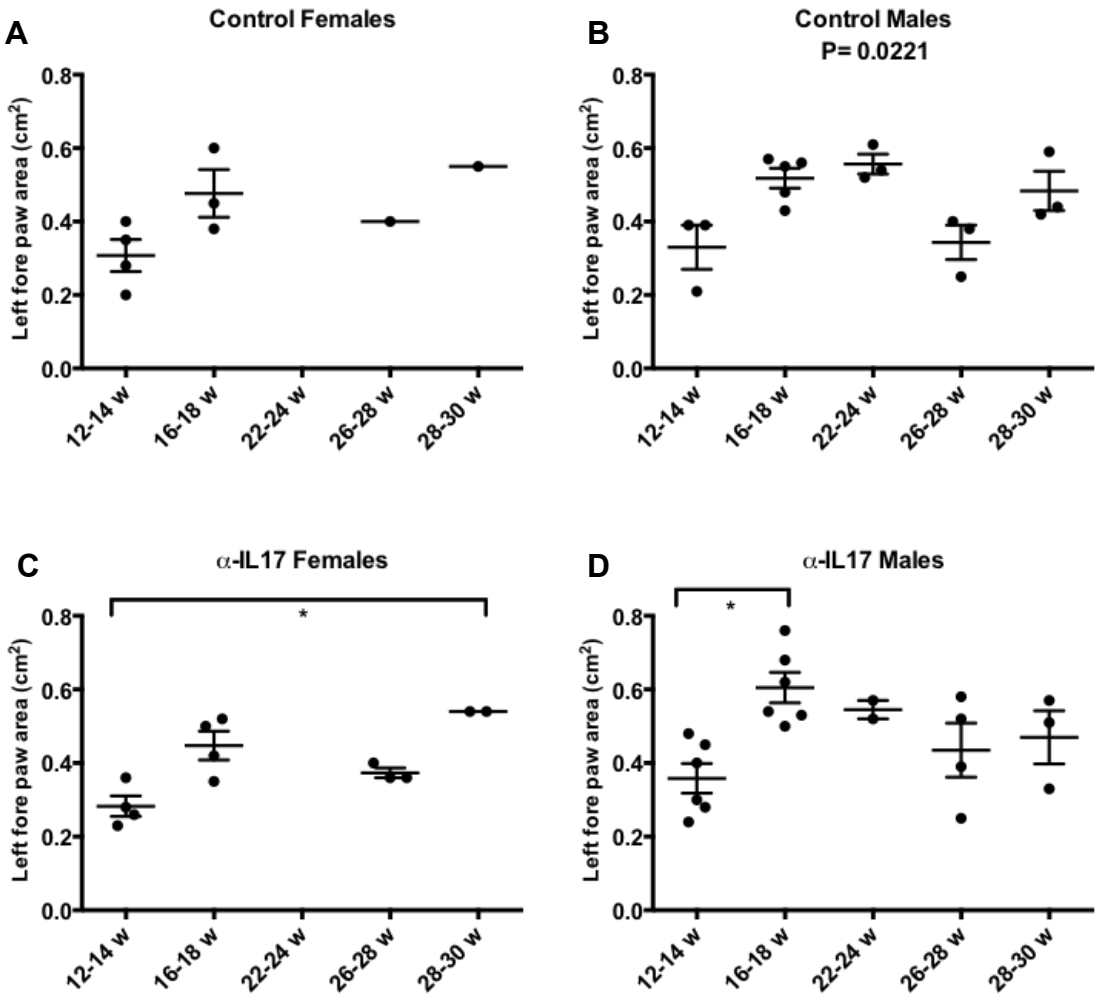

Figure 3.16 (cont'd)

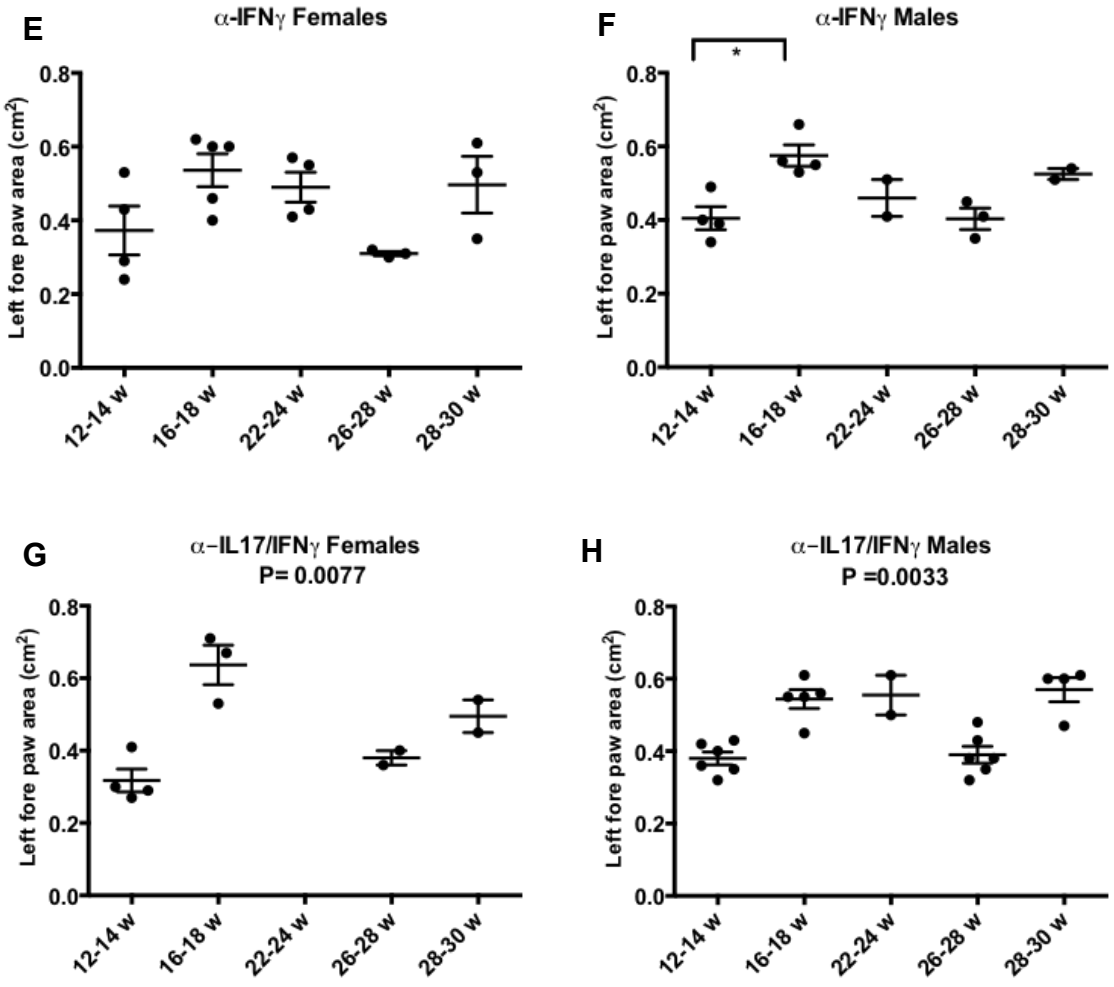

Figure 3.17 Right forepaw area over time

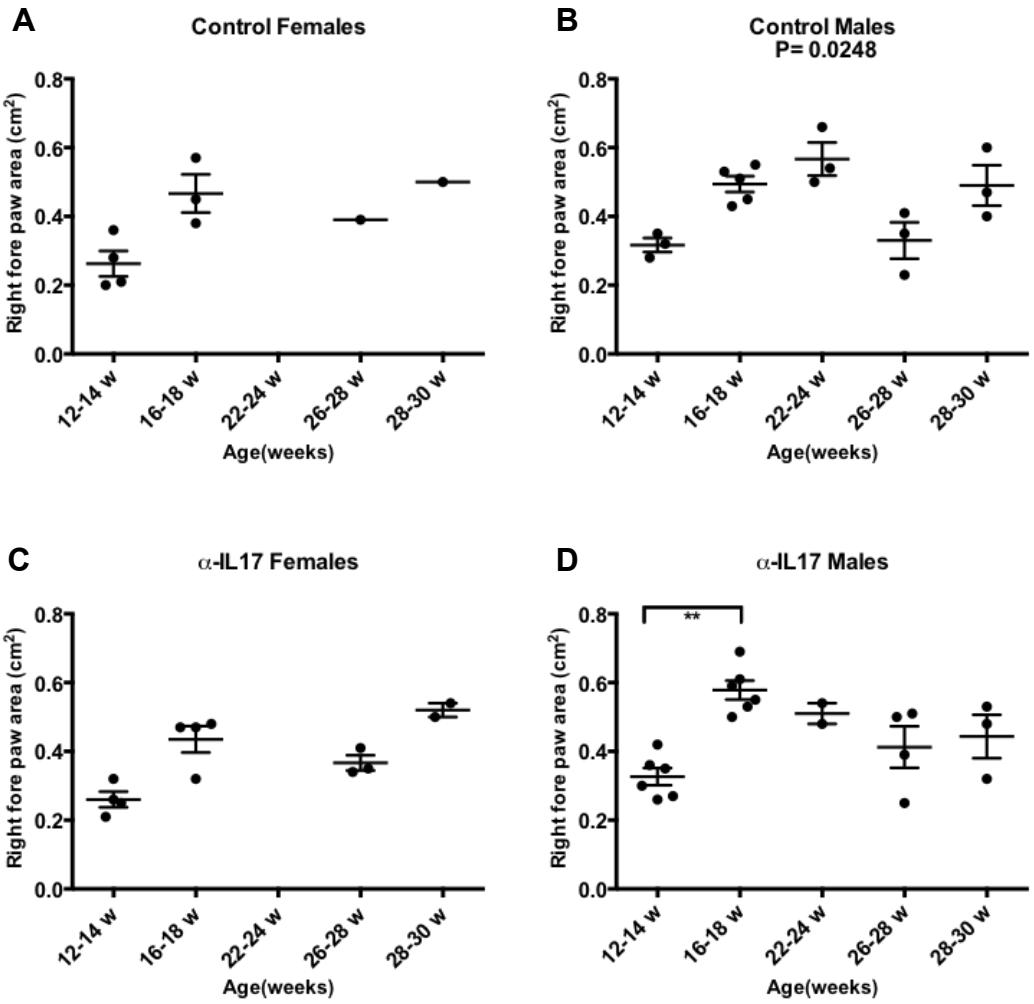

Figure 3.17 (cont'd)

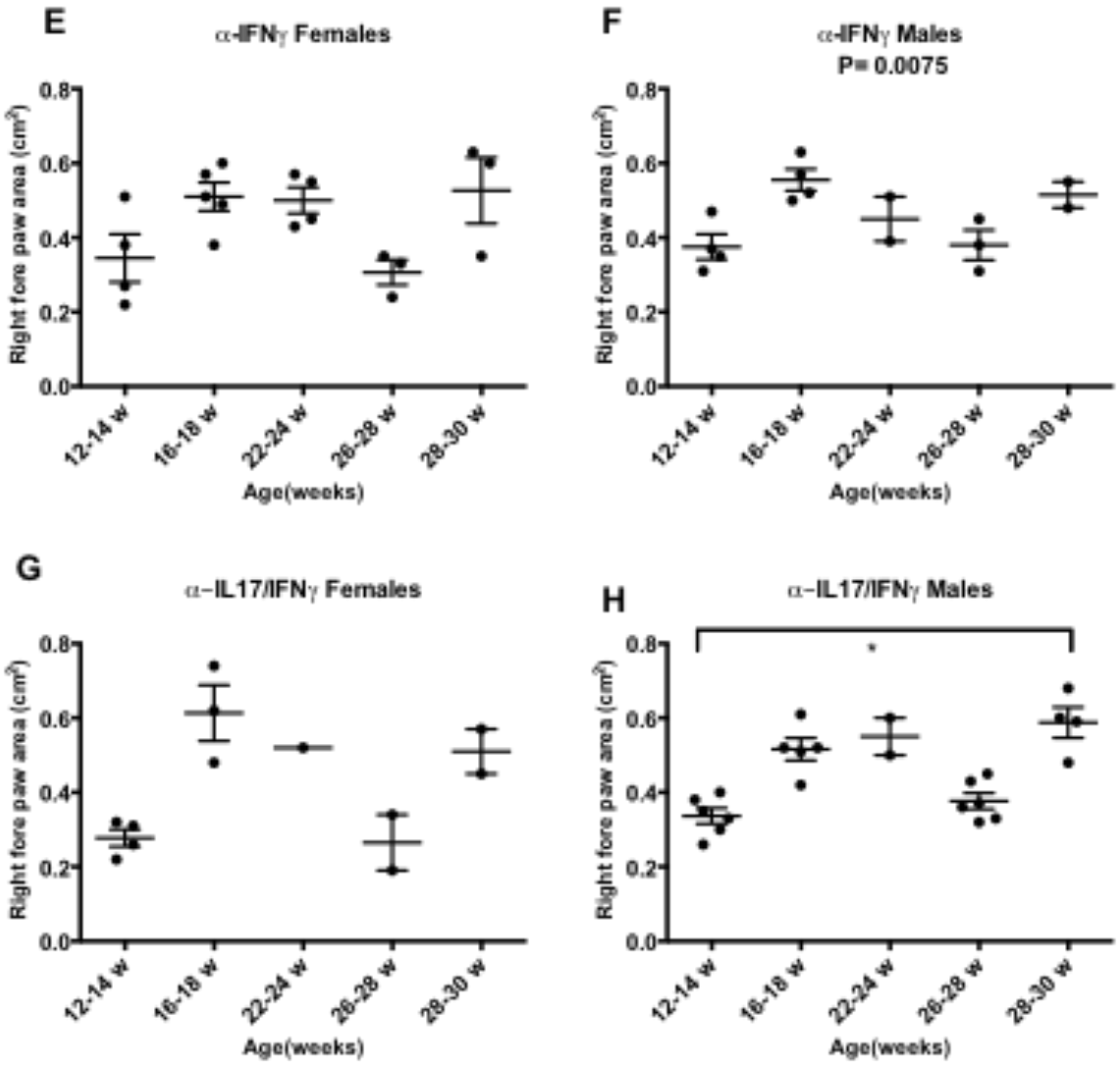

Figure 3.18 Histopathology of males and females. Combined score of the dorsal root ganglion, brachial plexus, and sciatic nerve.

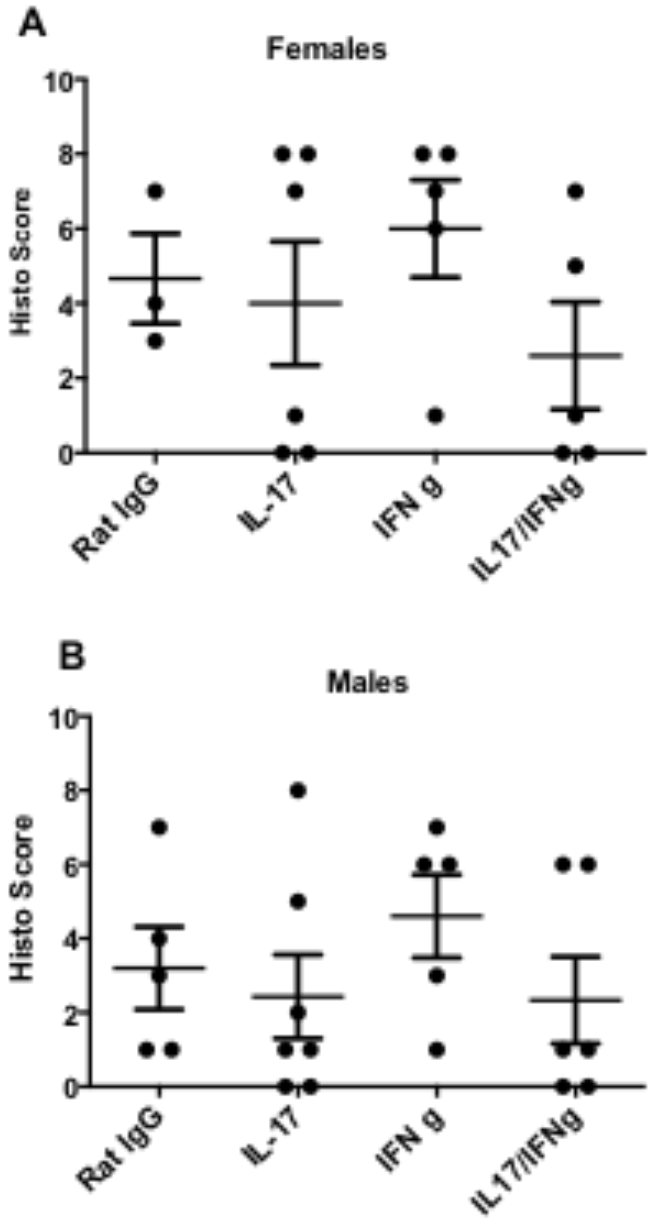

Figure 3.19 Open field test rears over time in males and females.

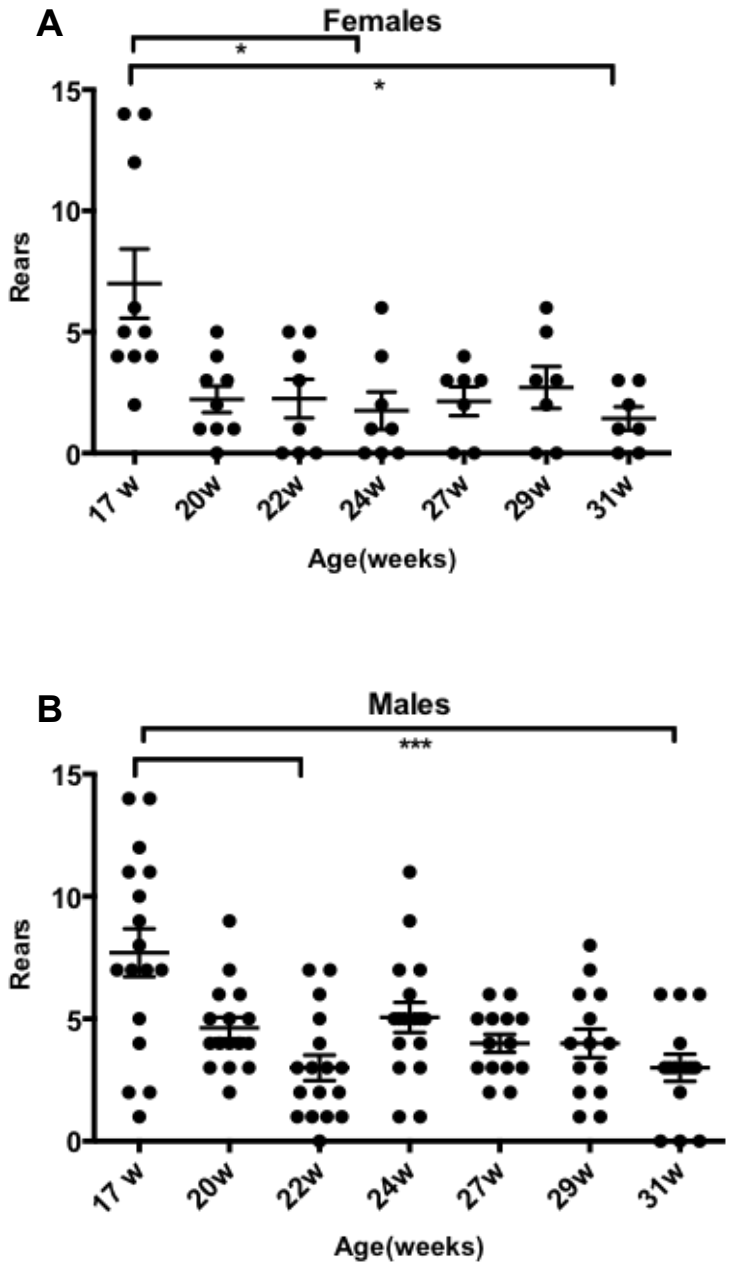

Figure 3.20 Rears, pairwise comparisons. Statistical significance is seen between males and females at 20 weeks (B), 24 weeks (D), and 27 weeks of age (E).

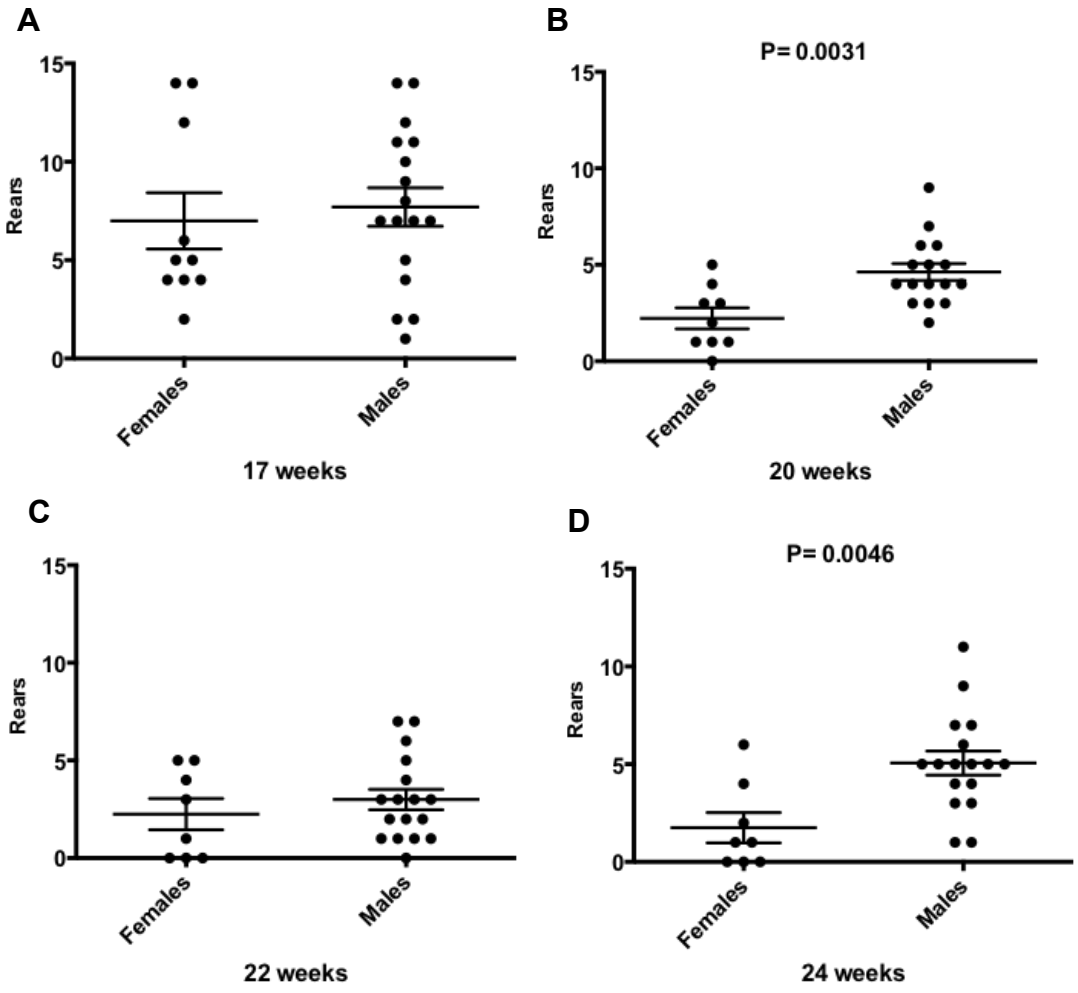

Figure 3.20 (cont'd)

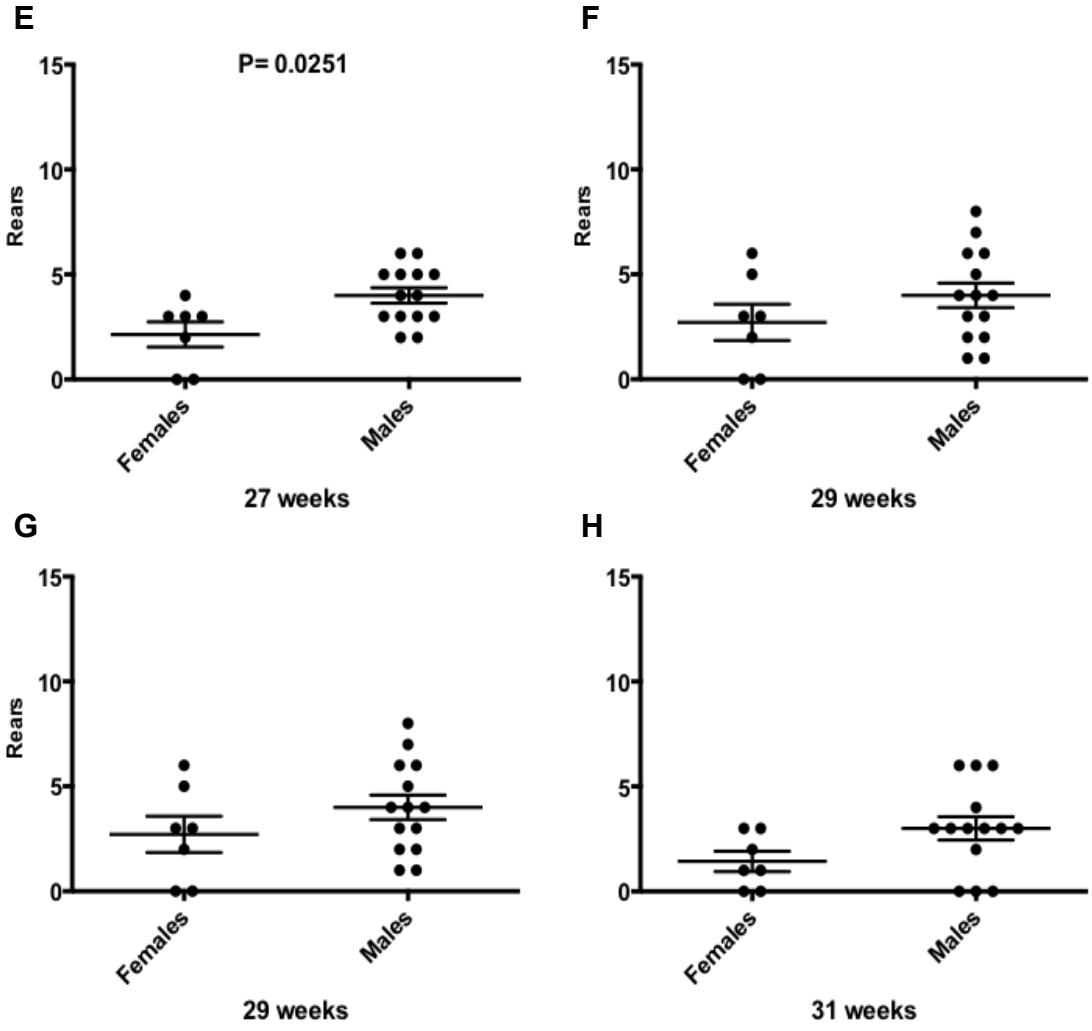

Figure 3.21 Dyskinesia, males and females. Significance in occurrence between males and females is seen at 20 weeks (B),

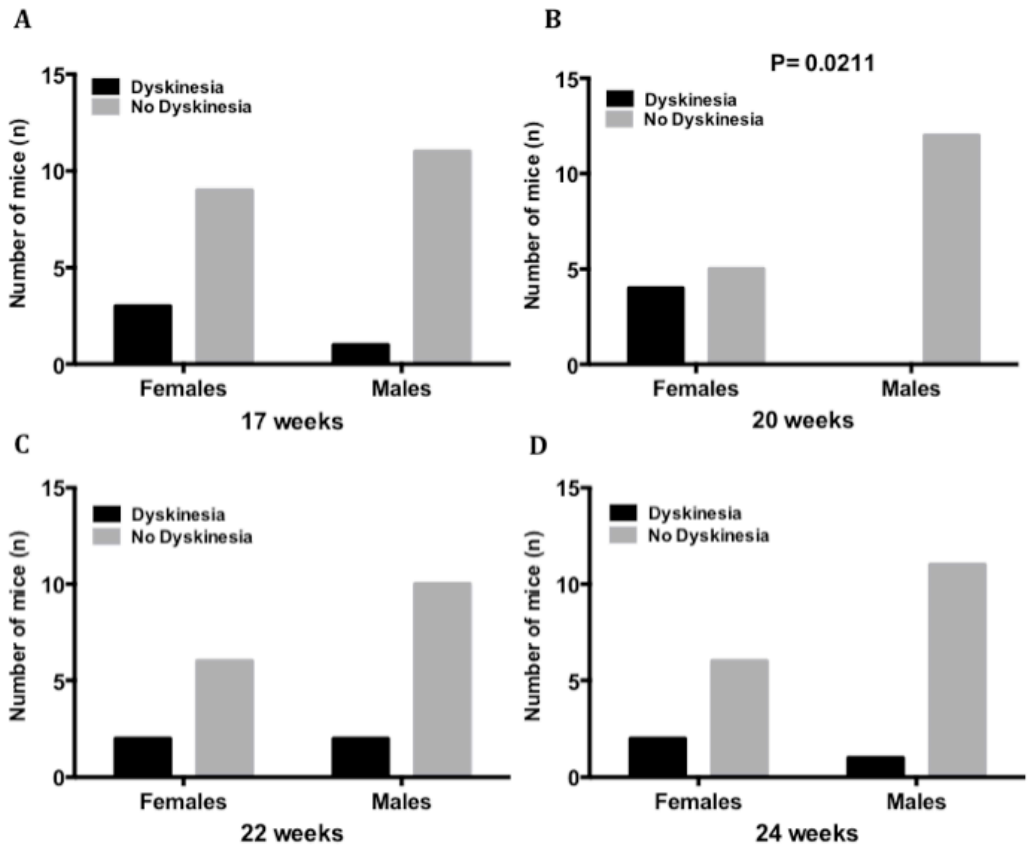

Figure 3.21 (cont'd)

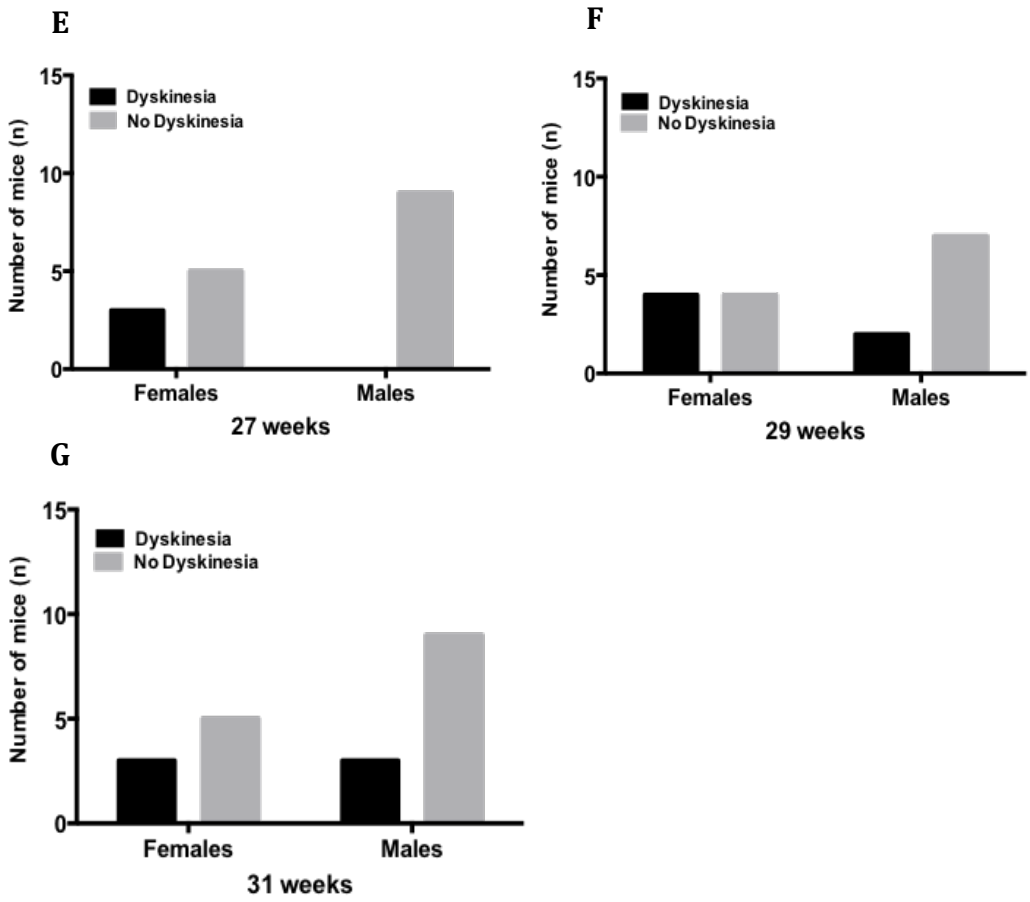

Figure 3.22 Facial grimace, males and females. Facial grimace was seen in males and females throughout the duration of the experiment.

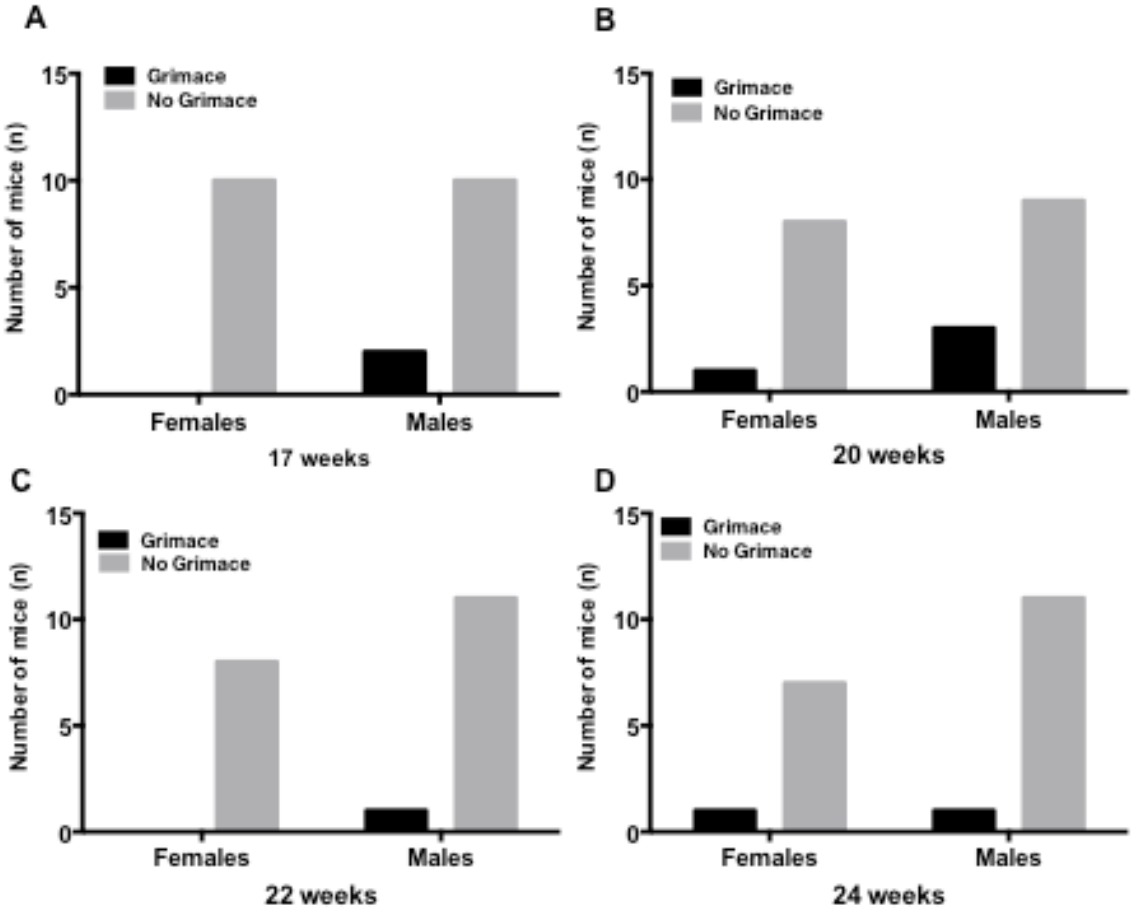

Figure 3.22 (cont'd)

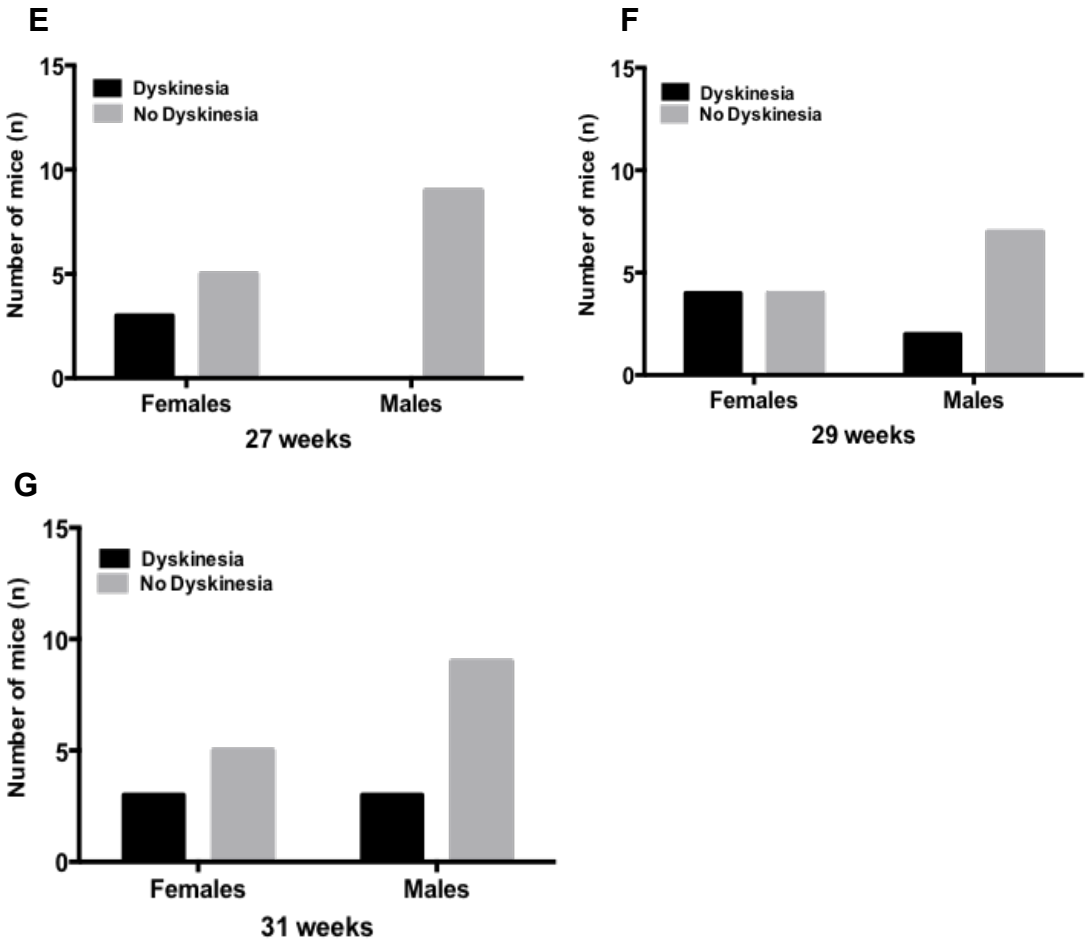

Figure 3.23 Hang Test, males and females.

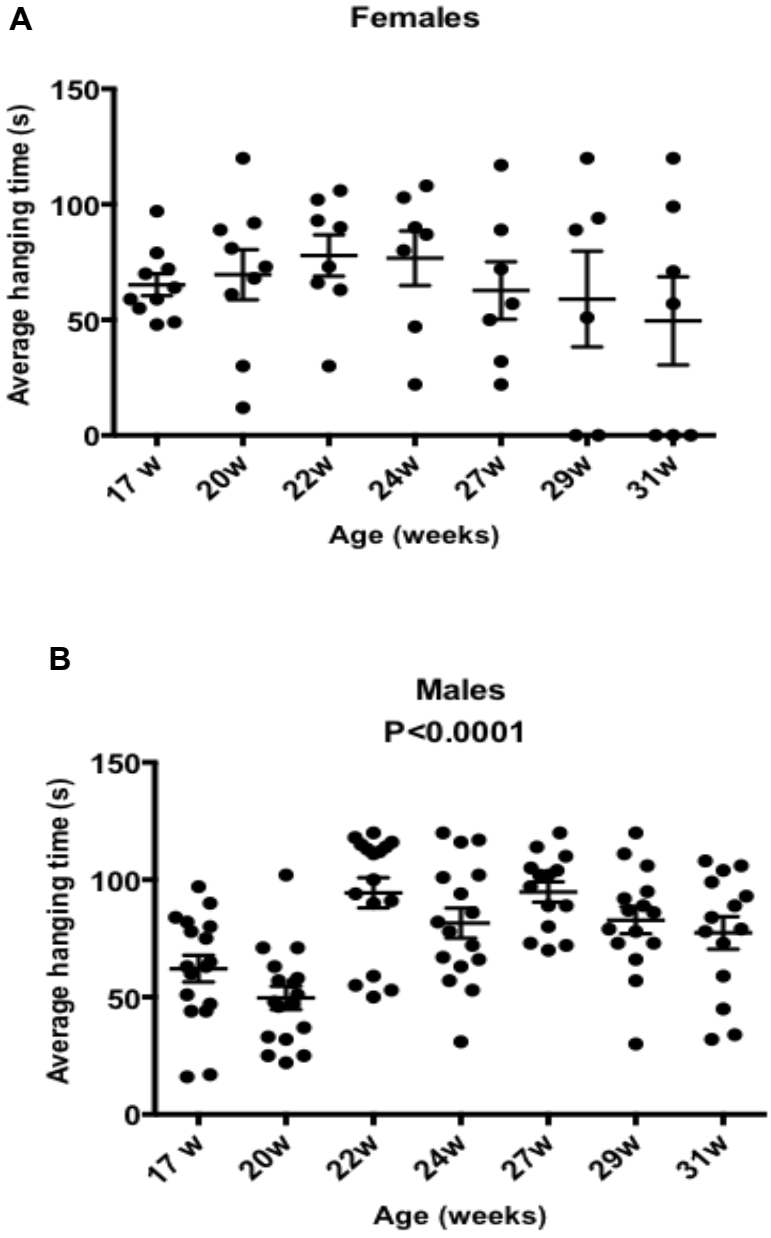

Figure 3.24 Pairwise comparisons of hang time between males and females over time.

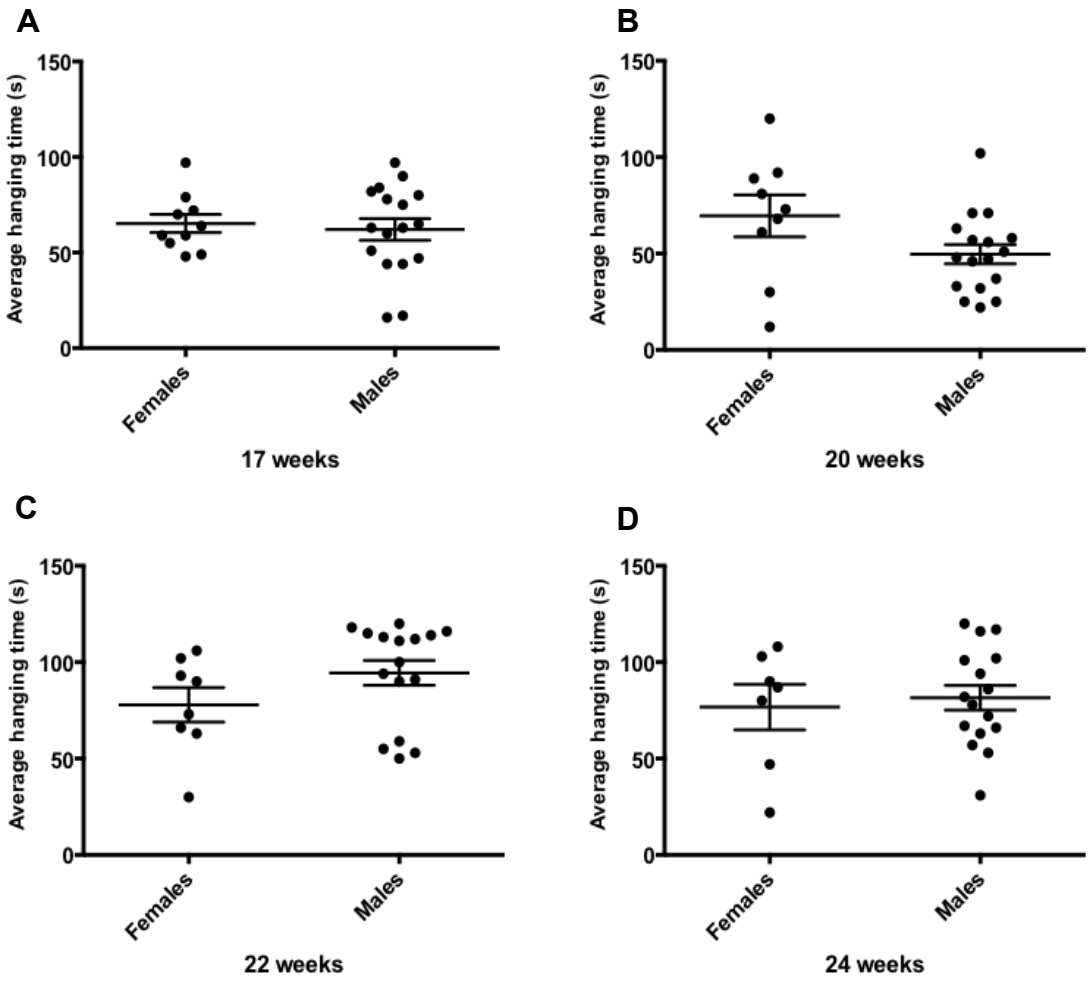

Figure 3.24 (cont'd)

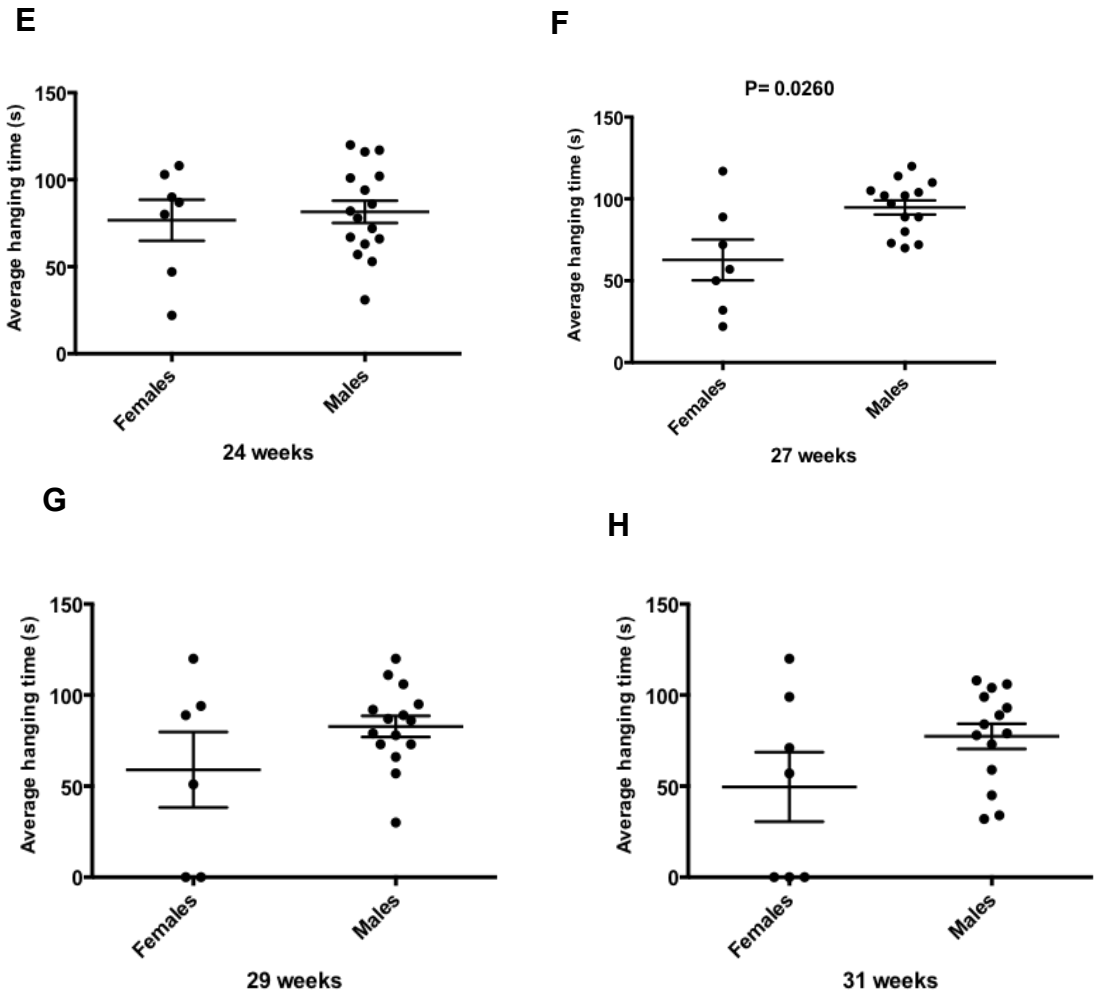

Figure 3.25 Grip compensation on the hang test by SAPP-affected mice.

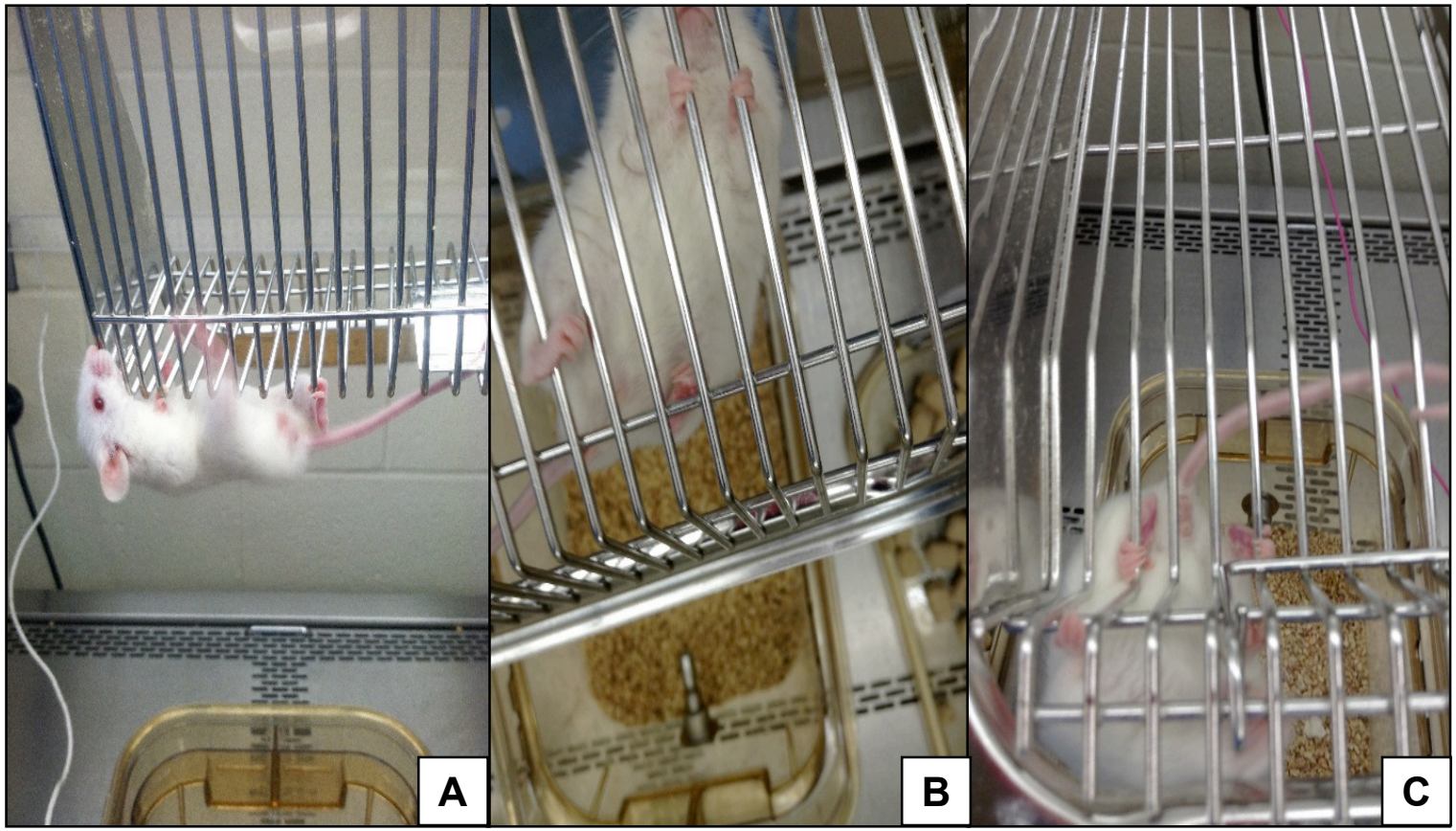

Figure 3.26 Histopathology of the pancreas. A,C Unaffected pancreatic islets from non-diabetic mice. B,D Infiltration of pancreatic islets by lymphocytes. These lesions are classic for Type 1 Insulin Dependent Diabetes Mellitus in NOD m

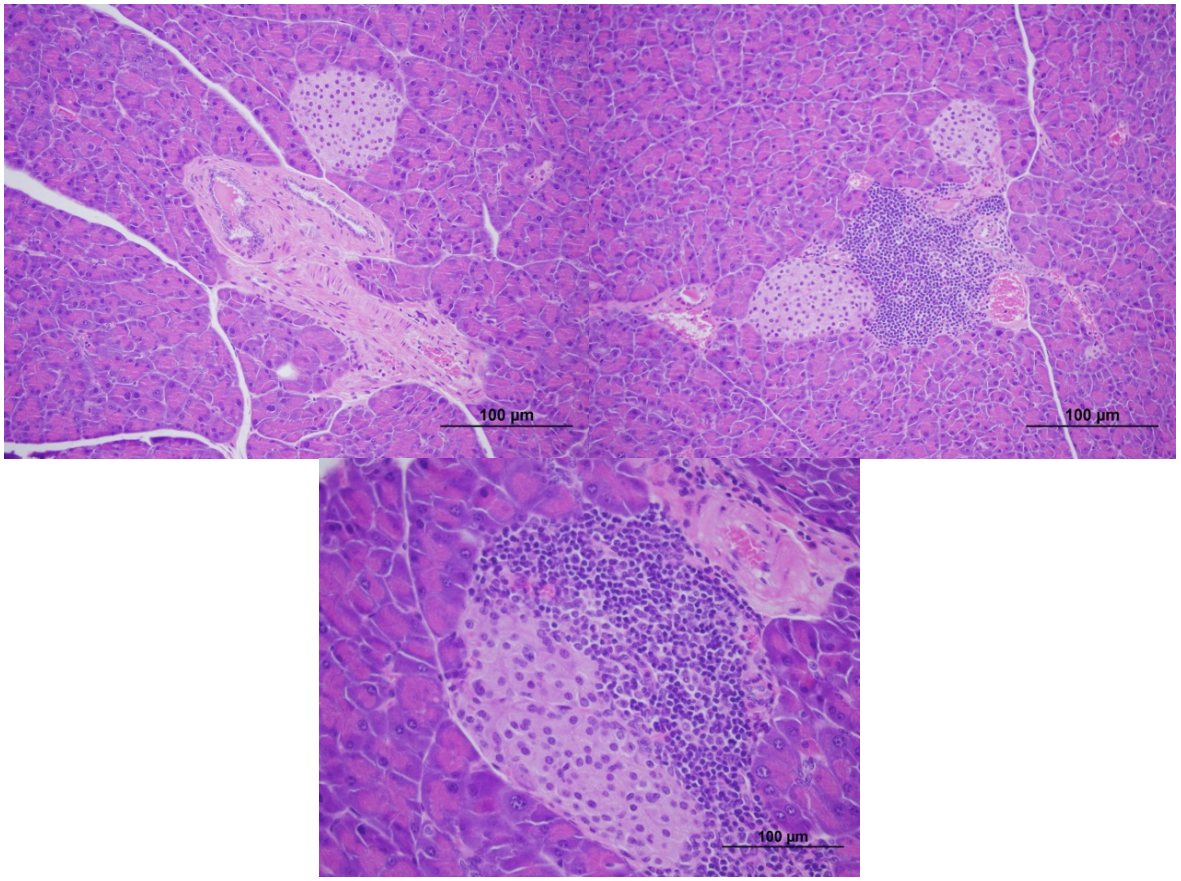

Figure 3.27 Histopathology of the brachial plexus in SAPP affected mice

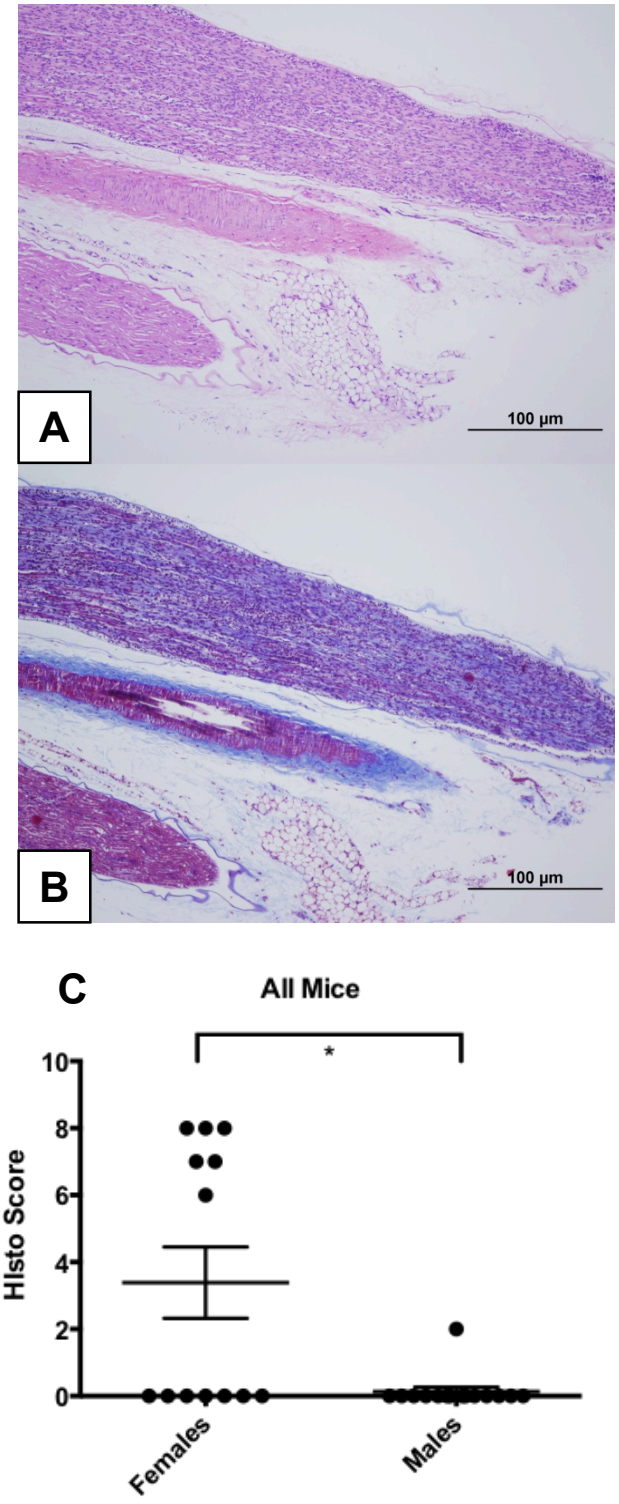

Figure 3.28 Tremors, males and females. Tremors were not a prominent feature of the disease until the very end, where both males and females were affected.

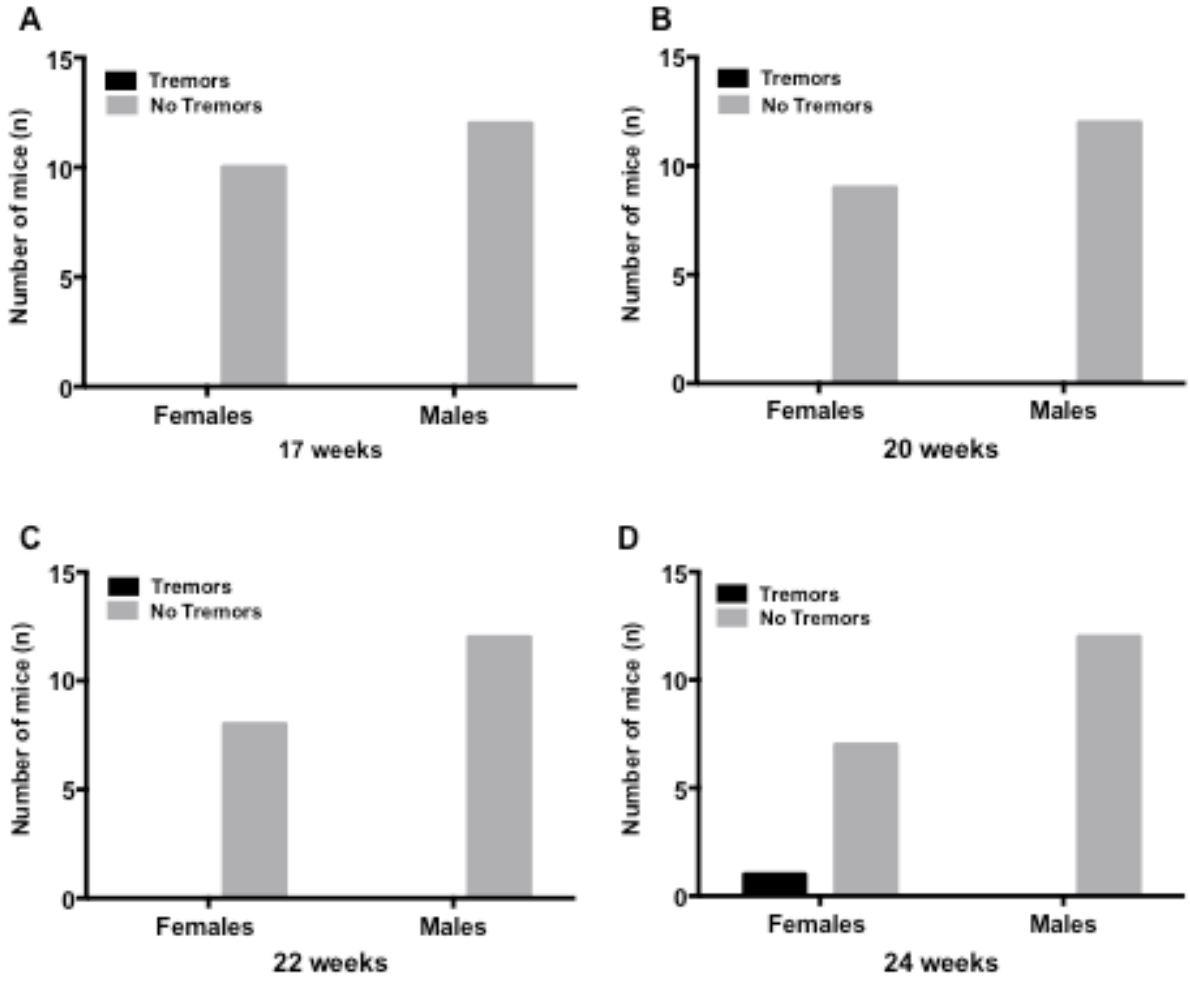

Figure 3.28 (cont'd)

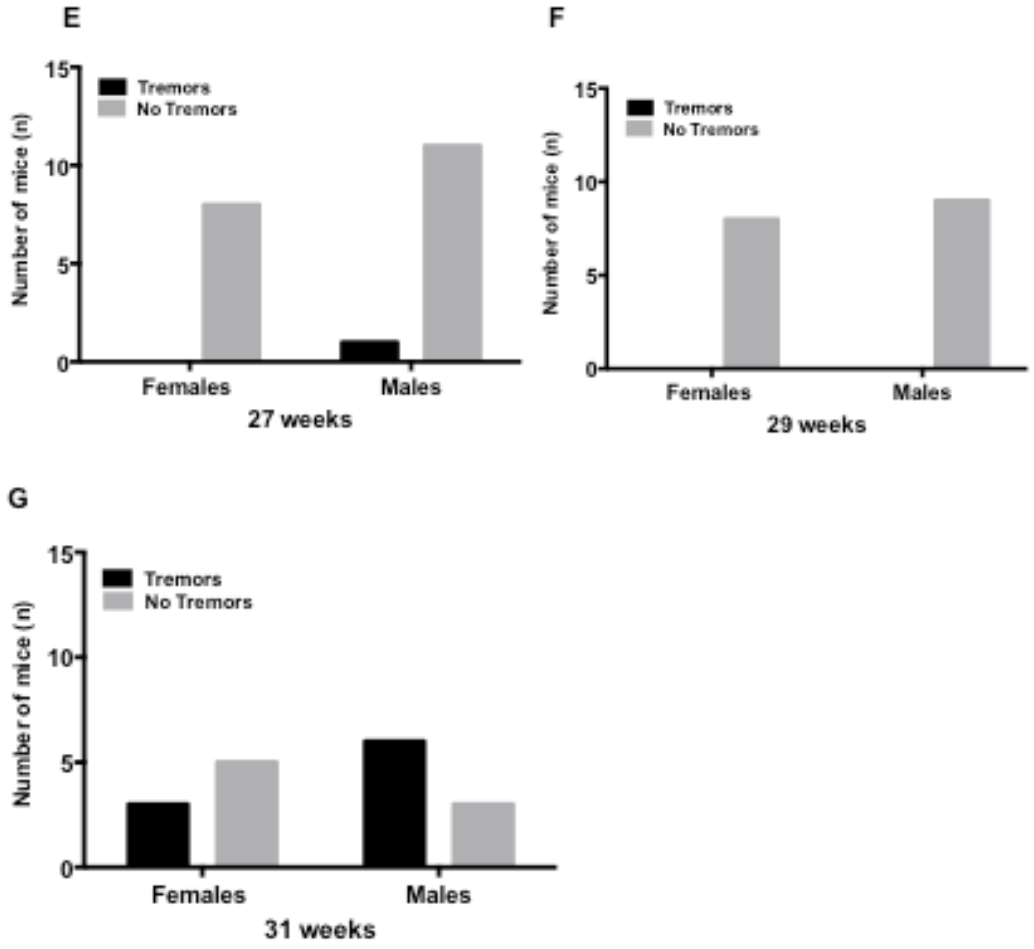

Figure 3.29 Body weight changes over time.

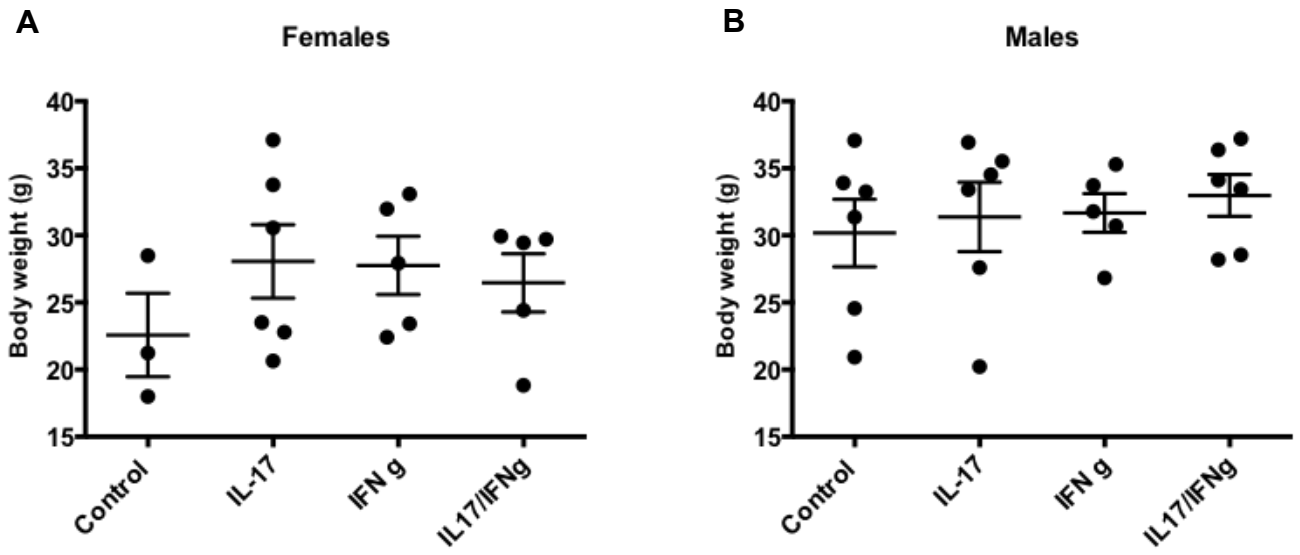

Figure 3.30 Bone, Trabecular number

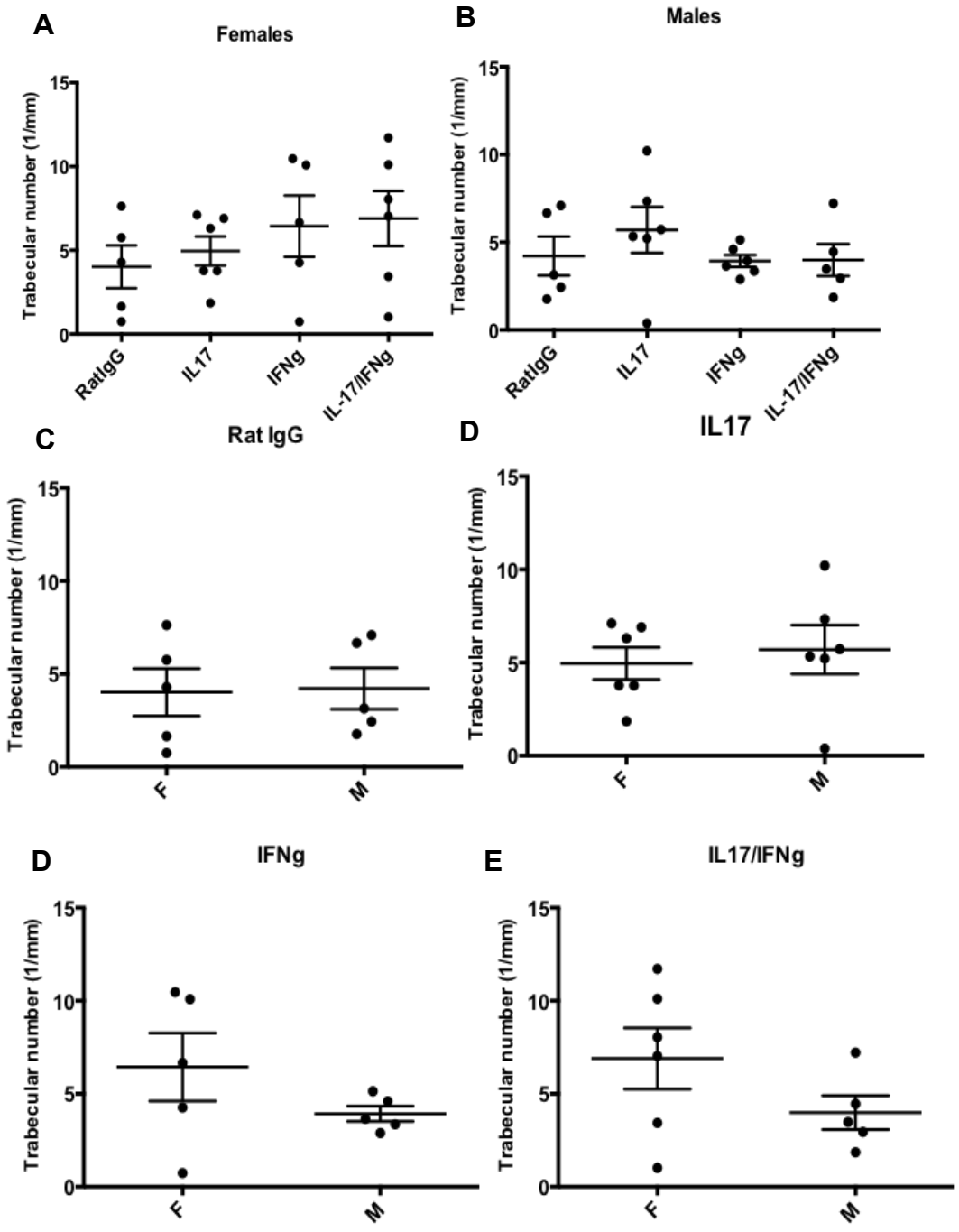

Figure 3.31 Bone, Trabecular thickness

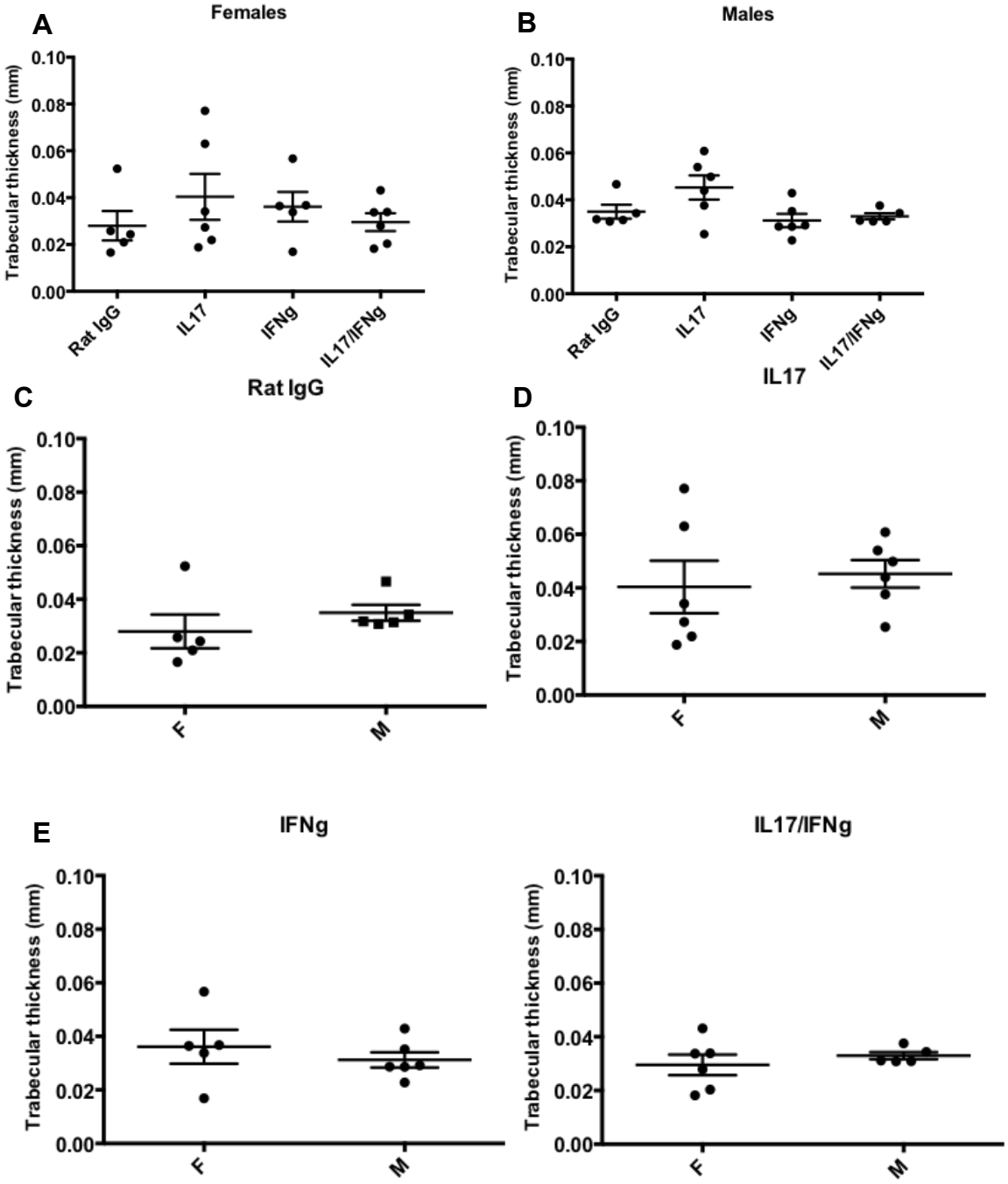

Figure 3.32 Bone, Trabecular separation

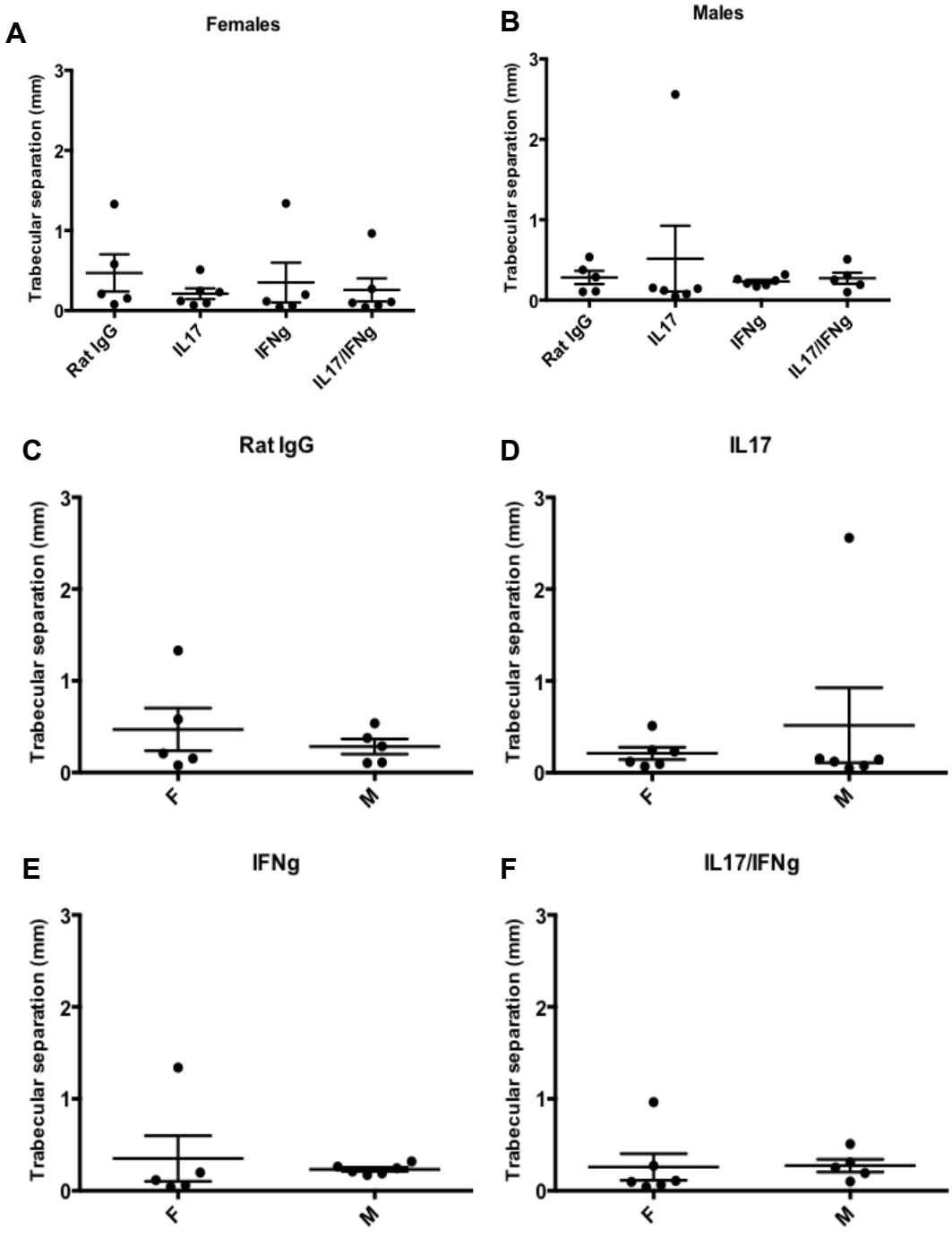

Figure 3.33 Bone volume fraction

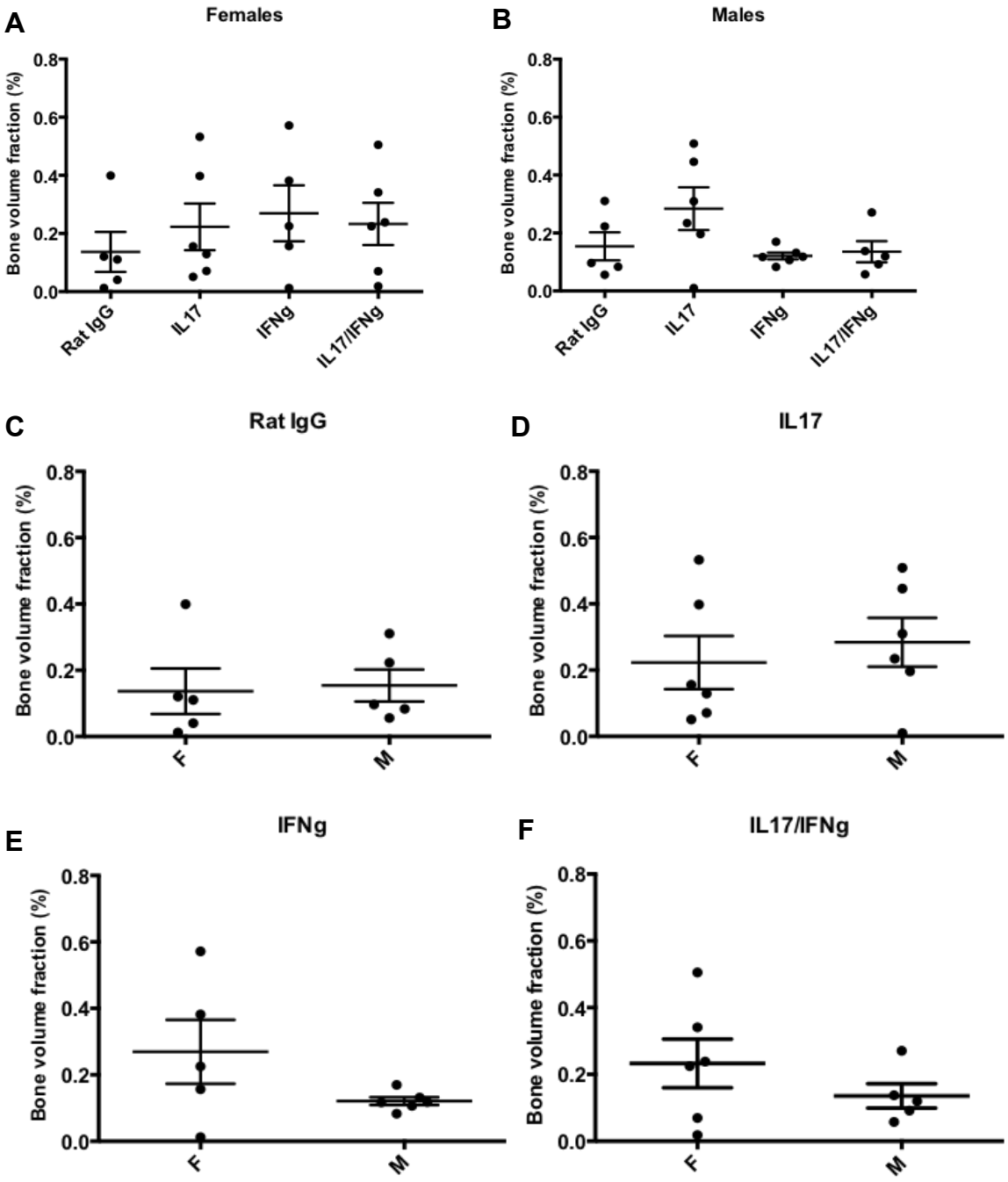

Figure 3.34 Bone, Average cortical thickness

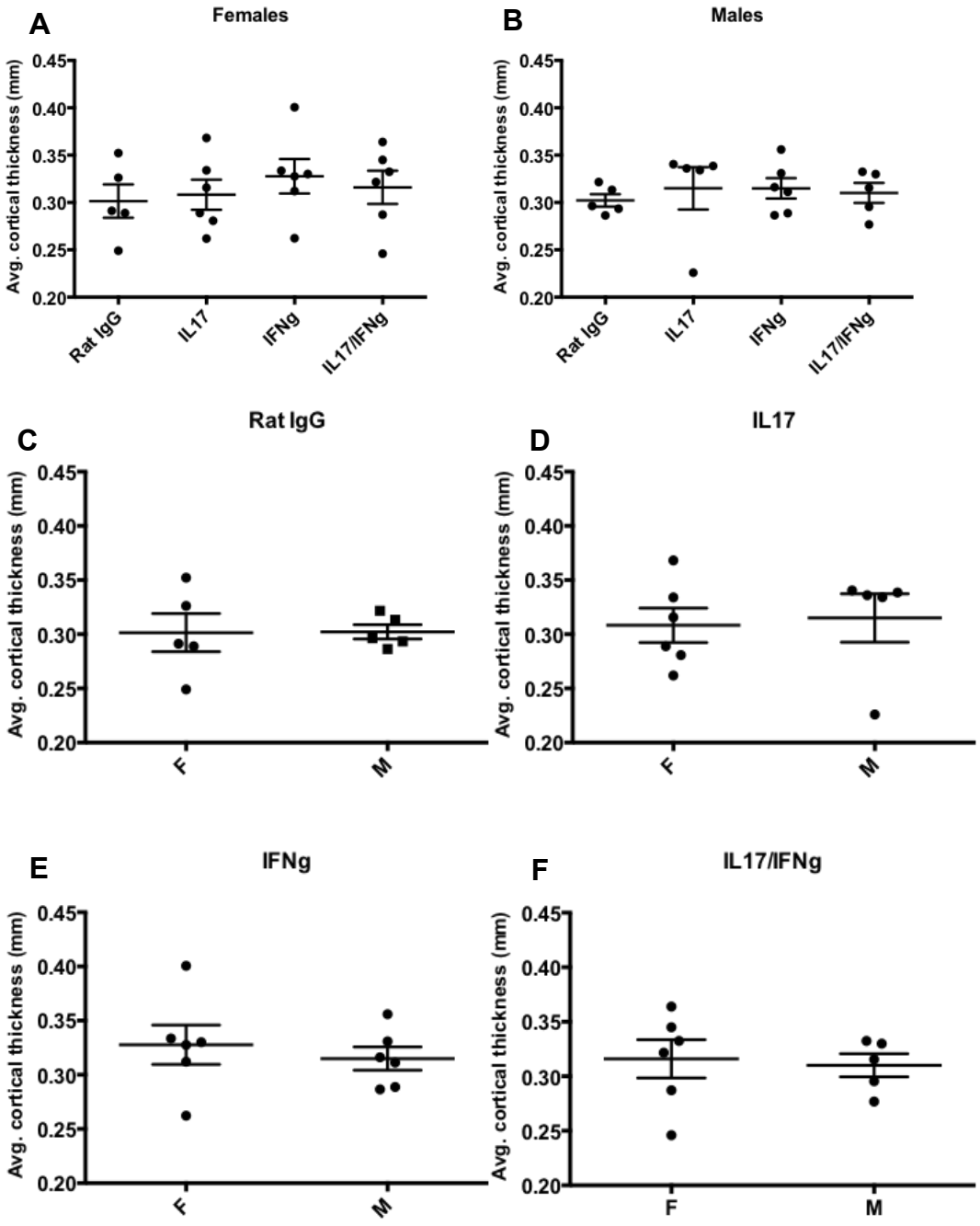

Figure 3.35 Bone, Cortical area

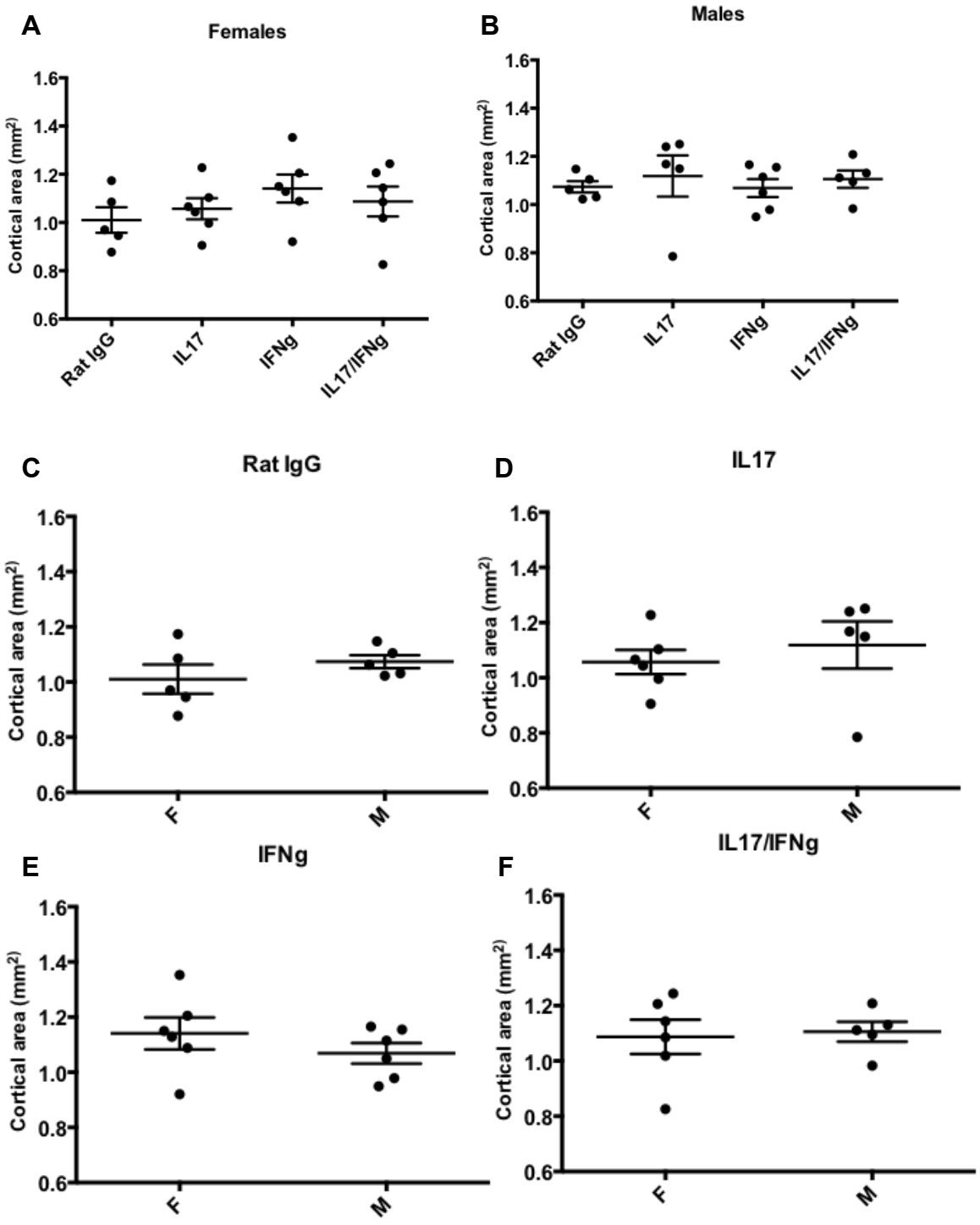

Figure 3.36 Bone, Total cross sectional area inside the periosteum

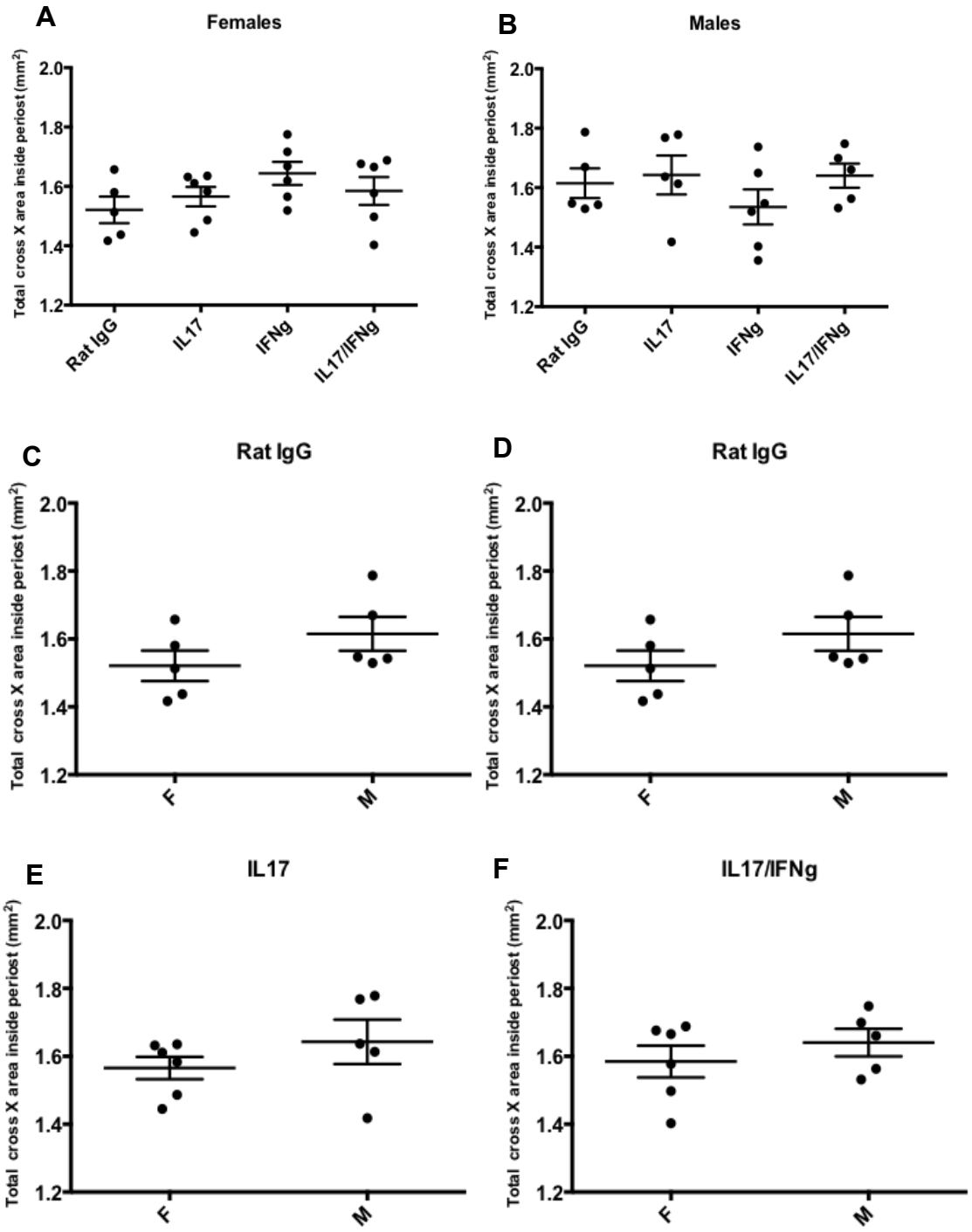

Figure 3.37 Bone, Marrow Area

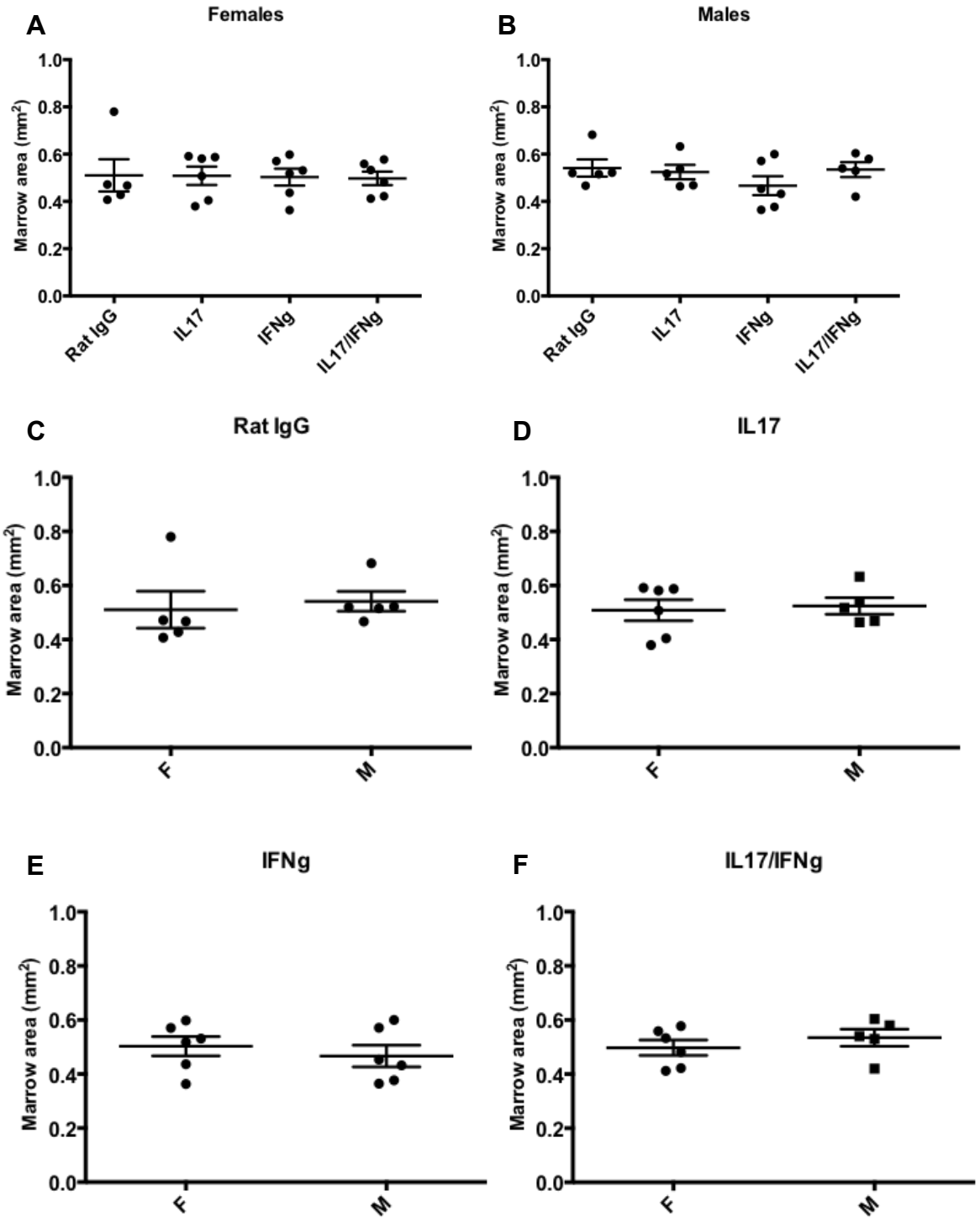

Figure 3.38 Bone, Cortical area fraction

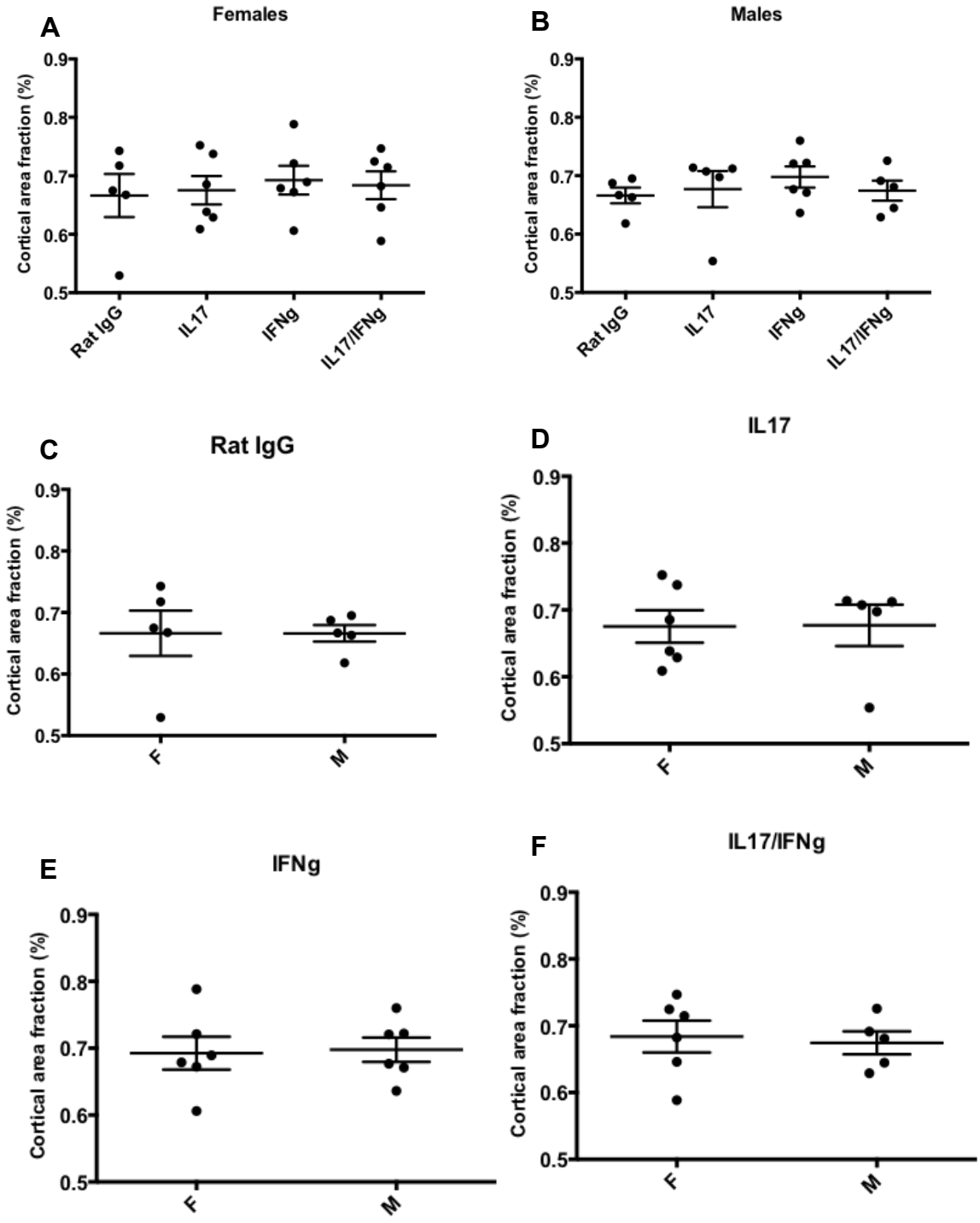

Figure 3.39 Femur length. Points in red indicate estimated volume due to missing primal aspect of femur.

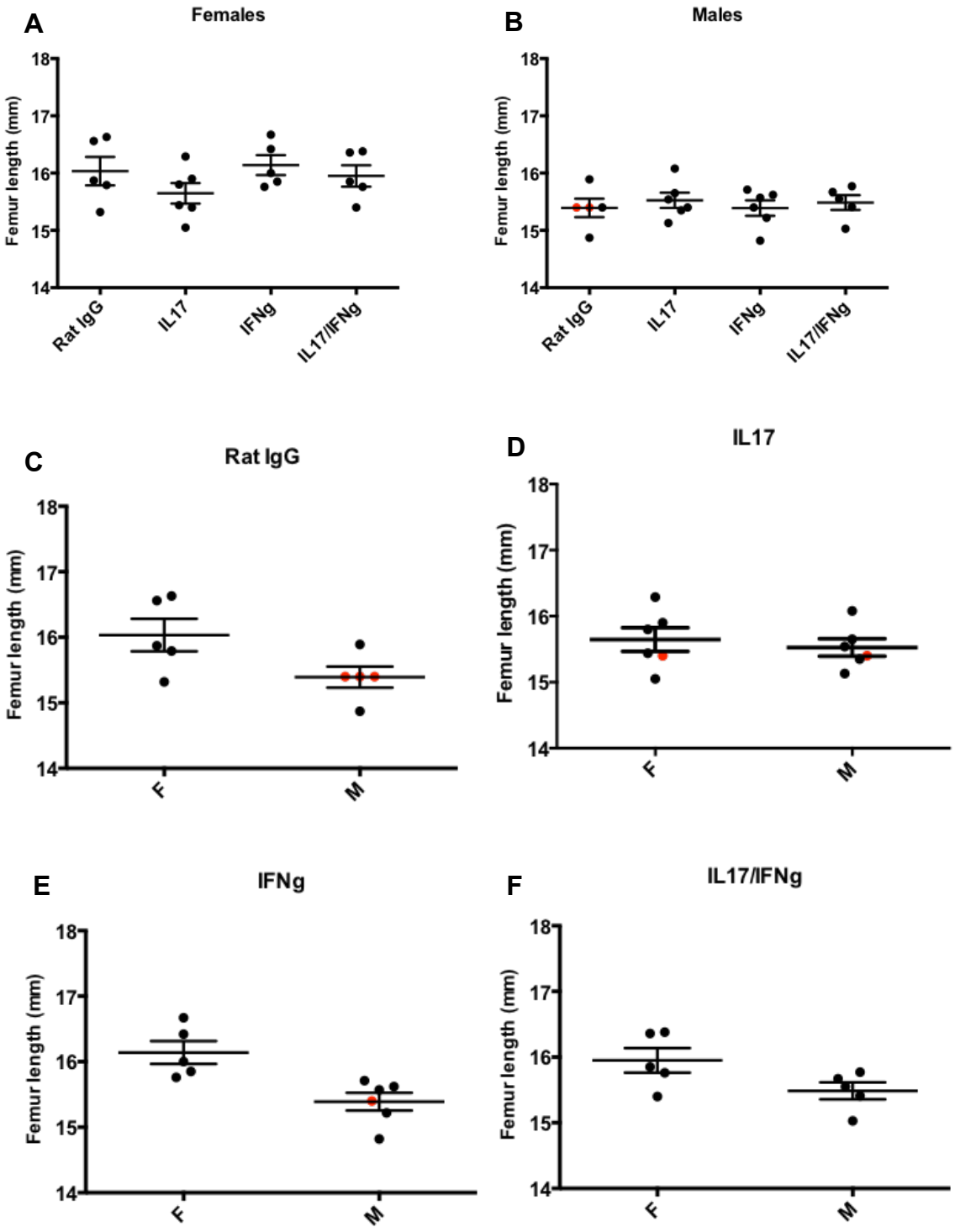

BIBLIOGRAPHY

BIBLIOGRAPHY

1. 2004. The Laboratory Mouse, 1st ed. Elsevier.

2. **Alvarez, I., J. A. Collado, R. Colobran, M. Carrascal, M. T. Ciudad, F. Canals, E. A. James, W. W. Kwok, M. Gartner, B. Kyewski, R. Pujol-Borrell, and D. Jaraquemada.** 2015. Central T cell tolerance: Identification of tissue-restricted autoantigens in the thymus HLA-DR peptidome. J Autoimmun **60:**12-19.

3. **Ansar, V., and N. Valadi.** 2015. Guillain-Barre Syndrome. Prim Care **42:**189-193.

4. **Bordon, Y.** 2015. Neuroimmunology: A painful difference between the sexes. Nat Rev Immunol **15:**469.

5. **Brooks, S. P., and S. B. Dunnett.** 2009. Tests to assess motor phenotype in mice: a user's guide. Nat Rev Neurosci **10:**519-529.

6. **Elkarim, R. A., C. Dahle, M. Mustafa, R. Press, L. P. Zou, C. Ekerfelt, J. Ernerudh, H. Link, and M. Bakhiet.** 1998. Recovery from Guillain-Barre syndrome is associated with increased levels of neutralizing autoantibodies to interferon-gamma. Clin Immunol Immunopathol **88:**241-248.

7. **Gold, R., K. V. Toyka, and H. P. Hartung.** 1995. Synergistic effect of IFN-gamma and TNF-alpha on expression of immune molecules and antigen presentation by Schwann cells. Cell Immunol **165:**65-70.

8. **Hartung, H. P., B. Schafer, P. H. van der Meide, W. Fierz, K. Heininger, and K. V. Toyka.** 1990. The role of interferon-gamma in the pathogenesis of experimental autoimmune disease of the peripheral nervous system. Ann Neurol **27:**247-257.
9. **Horiuchi, I., H. Ochi, H. Murai, M. Osoegawa, M. Minohara, H. Furuya, and J. Kira.** 2001. Th2 shift in mononeuritis multiplex and increase of Th2 cells in chronic inflammatory demyelinating polyneuropathy: an intracellular cytokine analysis. J Neurol Sci **193:**49-52.

10. **Huang, S., L. Li, S. Liang, and W. Wang.** 2009. Conversion of peripheral CD4(+)CD25(-) T cells to CD4(+)CD25(+) regulatory T cells by IFN-gamma in patients with Guillain-Barre syndrome. J Neuroimmunol **217:**80-84.

11. **Kim, H. J., C. G. Jung, M. A. Jensen, D. Dukala, and B. Soliven.** 2008. Targeting of myelin protein zero in a spontaneous autoimmune polyneuropathy. J Immunol **181:**8753-8760.

12. **Langford, D. J., A. L. Bailey, M. L. Chanda, S. E. Clarke, T. E. Drummond, S. Echols, S. Glick, J. Ingrao, T. Klassen-Ross, M. L. Lacroix-Fralish, L. Matsumiya, R. E. Sorge, S. G. Sotocinal, J. M. Tabaka, D. Wong, A. M. van den Maagdenberg, M. D. Ferrari, K. D. Craig, and J. S. Mogil.** 2010. Coding of facial expressions of pain in the laboratory mouse. Nat Methods **7:**447-449.

13. **Leach, M. C., K. Klaus, A. L. Miller, M. Scotto di Perrotolo, S. G. Sotocinal, and P. A. Flecknell.** 2012. The assessment of post-vasectomy pain in mice using behaviour and the Mouse Grimace Scale. PLoS One **7:**e35656.

14. **Louvet, C., B. G. Kabre, D. W. Davini, N. Martinier, M. A. Su, J. J. DeVoss, W. L. Rosenthal, M. S. Anderson, H. Bour-Jordan, and J. A. Bluestone.** 2009. A novel myelin P0-specific T cell receptor transgenic mouse develops a fulminant autoimmune peripheral neuropathy. J Exp Med **206:**507-514.

15. **Lu, M. O., and J. Zhu.** 2011. The role of cytokines in Guillain-Barre syndrome. J Neurol **258:**533-548.

16. **Matsumiya, L. C., R. E. Sorge, S. G. Sotocinal, J. M. Tabaka, J. S. Wieskopf, A. Zaloum, O. D. King, and J. S. Mogil.** 2012. Using the Mouse Grimace Scale to reevaluate the efficacy of postoperative analgesics in laboratory mice. J Am Assoc Lab Anim Sci **51:**42-49.

17. **Meyer zu Horste, G., A. K. Mausberg, S. Cordes, H. El-Haddad, H. J. Partke, V. I. Leussink, M. Roden, S. Martin, L. Steinman, H. P. Hartung, and B. C. Kieseier.** 2014. Thymic epithelium determines a spontaneous chronic neuritis in Icam1(tm1Jcgr)NOD mice. J Immunol **193:**2678-2690.

18. **Miller, A. L., and M. C. Leach.** 2015. Using the mouse grimace scale to assess pain associated with routine ear notching and the effect of analgesia in laboratory mice. Lab Anim **49:**117-120.

19. **Miyamoto, K., S. Miyake, M. Schachner, and T. Yamamura.** 2003. Heterozygous null mutation of myelin P0 protein enhances susceptibility to autoimmune neuritis targeting P0 peptide. Eur J Immunol **33:**656-665.

20. **Press, R., V. Ozenci, M. Kouwenhoven, and H. Link.** 2002. Non-T(H)1 cytokines are augmented systematically early in Guillain-Barre syndrome. Neurology **58:**476-478.

21. **Ramsey, C., O. Winqvist, L. Puhakka, M. Halonen, A. Moro, O. Kampe, P. Eskelin, M. Pelto-Huikko, and L. Peltonen.** 2002. Aire deficient mice develop multiple features of APECED phenotype and show altered immune response. Hum Mol Genet **11:**397-409.

22. **Salomon, B., L. Rhee, H. Bour-Jordan, H. Hsin, A. Montag, B. Soliven, J. Arcella, A. M. Girvin, J. Padilla, S. D. Miller, and J. A. Bluestone.** 2001. Development of spontaneous autoimmune peripheral polyneuropathy in B7-2-deficient NOD mice. J Exp Med **194:**677-684.

23. **Sobel, D. O., J. Han, J. Williams, J. W. Yoon, H. S. Jun, and B. Ahvazi.** 2002. Gamma interferon paradoxically inhibits the development of diabetes in the NOD mouse. J Autoimmun **19:**129-137.

24. **Sorge, R. E., J. C. Mapplebeck, S. Rosen, S. Beggs, S. Taves, J. K. Alexander, L. J. Martin, J. S. Austin, S. G. Sotocinal, D. Chen, M. Yang, X. Q. Shi, H. Huang, N. J. Pillon, P. J. Bilan, Y. Tu, A. Klip, R. R. Ji, J. Zhang, M. W. Salter, and J. S. Mogil.** 2015. Different immune cells mediate mechanical pain hypersensitivity in male and female mice. Nat Neurosci **18:**1081-1083.

25. **Zhang, H. L., L. Wu, X. Wu, and J. Zhu.** 2014. Can IFN-gamma be a therapeutic target in Guillain-Barre syndrome? Expert Opin Ther Targets **18:**355-363.

CHAPTER 4

Altering the Intestinal Microbiota via Cecal Transfer

ABSTRACT

Many host factors play a role in the onset and maintenance of autoimmune diseases. Since SAPP has a predominant female bias in occurrence in the NOD.B7-2$^{-/-}$ mouse, it is reasonable to examine those factors that differ between females and males, namely estrogen and testosterone. Increased levels of testosterone in female NOD wild type mice are protective against Type I diabetes. The testosterone increase is regulated through the gut, but the exact mechanism of increase in unknown. The purpose of this study was to examine the capability of the male microbiota to shift the sex hormone profile in NOD.B7-2$^{-/-}$ mice from estrogen to testosterone, and evaluate whether or not the shift would result in protection from SAPP. Female weanling mice were given male donor cecal contents via oral gavage. Transferred mice developed more severe disease than mice that were sham inoculated. There was no difference in plasma estradiol concentration. That finding does not confirm that the gut has no action on the levels; it suggests that earlier time points may be critical to uncovering shifts in plasma hormone concentration, as well as early shifts in the mouse gut flora after cecal transfer.

INTRODUCTION

In this study, the goal was to alter the microbiota of weanling female NOD.B7-2$^{-/-}$ mice, to resemble that of adult male mice. To do so, a modified version of the cecal transfer procedure used in human medicine was employed. Fecal microbial transfer (FMT) is on the rise as treatment for many diseases, including, but not limited to Inflammatory Bowel Disease (IBD), Irritable Bowel Syndrome, (IBS) and *Clostridium difficile* infection. It is defined as "infusion of a fecal suspension from a healthy individual into the gastrointestinal tract of an individual with colonic disease." The expected outcome is that the patient will accept the community and intestinal homeostasis will ensue (1, 6). The exact way that FMT works is not completely understood—there are some cases that can be cured, while others are not (6). The first report of successful FMT therapy was published in 1958, when it was used to treat patients with pseudomembranous colitis (2) . One researcher believes that this therapy should be classified as an organ transplant because of the transplanted material's ability to reshape the gut microbiota (1).

As the treatment becomes more popular, the focus is shifting to treatment of extra-intestinal diseases such as allergic conditions, metabolic diseases and autoimmune disease. SAAP, the disease being studied in our lab in the NOD B-72$^{-/-}$ mice, is an autoimmune disease (5). NOD wild type mice were a given a similar treatment to alleviate Type 1 Diabetes. In 2013, Markle and colleagues reduced the occurrence of diabetes in female NOD WT mice. The weanling mice had been transferred (transplanted) with cecal contents from adult male mice. They were able to prove that the microbial composition people are exposed to at an early age can influence testosterone levels and alter the development of autoimmune disease. At the end of the study, they concluded that the donor mouse transplant was able to raise the plasma testosterone concentration, and protect the mice from disease. They confirmed the action of testosterone by treating transferred mice with flutamide, an androgen receptor blocker. The protective effects of the cecal transfer were abrogated in those mice (4). Based on promising

literature of alleviating various diseases in humans using FMT, as well as the recent murine cecal transfer success, we sought to understand if similar mechanisms regulated the development of SAPP.

RATIONALE

The rationale was that since the diseases in congenic WT and B7-2$^{-/-}$ mice are both biased toward females, autoimmune in nature, and appear histologically similar (in different target organs), we expect that transferring cecal microbiota from a donor male will have similar effects in abrogating onset of SAPP in female NOD.B7-2$^{-/-}$mice. Since SAPP has a predominantly female bias, we only used females for this experiment.

Hypothesis: Female NOD.B7-2$^{-/-}$ weanling mice inoculated with cecal contents from an adult male donor B7-2$^{-/-}$ mouse will be protected from the development of SAPP.

RESULTS

Open Field Test (OFT)

Over the course of the entire experiment, the group of mice that were transferred with cecal contents from male donors had a constant decline in the number of rears in the open field test, compared to their sham inoculated counterparts (Figure 4.1). Transferred mice also had a consistently low/poor performance at the last three experimental testing time points. Pairwise comparisons between experimental groups revealed a trend toward decreased numbers of rears in the transferred mice, compared to the sham mice at 21-22 weeks and 31-32 weeks (Figure 4.2, B and F).

Grip Test, Dyskinesia, and Grimace

The transferred mice showed a greater deficit than the sham treated mice in the ability control their limbs and grip the pen that was placed on their abdomen. Data analyzed within the groups indicated that the treated mice showed significant differences over time as the weeks progressed (Figure 4.4, B). There was no significance over time in the sham treated group. The earliest grip deficit was recorded at the first week of testing in both groups, when the mice were 19-20 weeks of age (Figure 4.3, A). The highest percentage of mice with grip deficits in the transferred group occurred when the mice were between 31-32 weeks of age, with 86% (6/7) of mice affected at 31-32 weeks (Figure 4.2, H). In the sham group, 60% (3/5) was the highest, and it occurred between 31-32 weeks (Figure 4.2 F). At the conclusion of the study, 83% (5/6) of the treated mice had grip deficits, compared to 40% (2/5) of sham mice.

The transferred mice also had more incidence of dyskinesia, also known as involuntary limb movement. Both groups of mice had significant differences over time within the groups, but the significance was greater in the transferred mice (Figure 4.6). Mice given donor cecal contents had dyskinesia present at the first testing trial (19-20 weeks); the sham mice did not show dyskinesia until the third trial (23-24 weeks). In the transferred group, at 31 weeks of age,

100% (6/6) mice had dyskinesia that was present at each testing trial until the study concluded (Figure 4.5, F). This 100% occurrence was observed after two mice from the transferred group a humane endpoint and were euthanized. At no time during the experiment did the sham mice reach 100% occurrence for dyskinesia. The highest percentage for those mice was 80% (4/5), and that did not occur until the final week of testing, when the mice were 35-36 weeks of age (Figure 4.4, H).

In this particular study, the facial grimace was not a prominent feature of the disease presentation. In the transferred mice, the first facial grimace was recorded at 28-29 weeks of age, compared to the very last week of testing (35-36 weeks) for the sham group. The highest percentage of mice with a grimace in the transferred groups occurred at the last testing trial, with 33% (2/6) affected (Figure 4.6, H). In the sham mice, 40% (2/5) were affected in the last week. Both cohorts had significance over time within their respective groups (Figure 4.7).

A heat map with all clinical parameters combined shows that, collectively, more severe clinical signs were observed in transferred mice than sham inoculated mice (Figure 4.8)
Note: One mouse in the sham group was not included in the phenotypic analysis because of missing data points. That makes the "n" for the sham group 5.

Histopathology

Every mouse that was given cecal contents from the male donors had some degree of inflammation in the dorsal root ganglion, sciatic nerve, or brachial plexus (Figure 4.9). Of the 8 mice in the treated group, 25% (2/8) had a severe score, 63% (5/8) had a moderate score, and 12% (1/8) had a mild score. In the sham inoculated group, 33% (2/6) had a severe score, 16% (1/6) had a moderate score, and 16% (1/6) had a mild score. There were 33% (2/6) of mice that did not have any inflammation in any of the examined tissues. Architectural changes included myelin loss with axonal swelling and the presence of large numbers of macrophages with intracytoplasmic myelin accumulation. The description for one of the mice in the treated group

was noted as “striking vacuolation” in the sciatic nerve. Fibrosis was observed in 33% (2/6) mice the sham treated group an in 75% (6/8) of transferred mice.

Body Weight and Plasma Hormone Concentration

Treated mice had a significant decrease in body weight from the 20 week time point to necropsy (Figure 4.10). Sham inoculated mice had a slight decrease, but there was no significance. When the groups were compared to each other at the three time points (baseline-weanling age), 20 weeks, and necropsy, there was no difference in the mean body weight.

There was no significant difference in estradiol or testosterone plasma concentration between the groups (data not shown).

16s Sequencing

Sequencing reads generated by MiSeq and analyzed by Mothur and PAST revealed significant differences in Operational Taxonomic Units (OTU) in the gut microbial community (figure 4.11). Both the sham and treated groups had significantly different microbial gut flora, compared to the inoculum, before it was delivered. At 20 weeks of age, the age at which SAPP begins to occur, the mice that were given the donor cecal contents had a gut community that was still significantly different from the inoculum, while the sham treated mice did not.
The differences noted occurred in several different families of bacteria (Table 4.1). At all three sampling times, the unclassified Clostridia were always significantly different from the inoculum. The number of Lactobacilli in the control mice had a trend toward greater quantities when compared to the treated mice at all three sampling points, including the initial time point. The majority of the mice cluster together in a Principal Component Analysis (PCA) plot at the time of initial sampling. At the midpoint (20 weeks) and necropsy time points, the groups are still distinguishable from one another, but they do not separate into distinct clusters (Figure 4.11).

They do not form their own clusters to show distinct evolution of the gut microbiota from the original inoculum. Bacterial OUT changes are shown in Figure 4.12 and Table 4.1.

MATERIALS AND METHODS

Mouse Breeding and Husbandry

All experimental protocols and procedures were approved by the Institutional Animal Care and Use Committee (IACUC) at Michigan State University (06-12-107-00). The mice were from a specific pathogen free colony and singly house in sterilized, clear plastic disposable cages, supported by an Innovive rack. The cages were changed once a week. HEPA-filtered air was delivered through the top of each cage. Mice were fed a diet of Irradiated Harlan Teklad 7913 chow (Harlan Teklad, Indianapolis, Indiana, USA) and given free access to sterilized water. Animal technicians and experimental handlers wore standard personal protective equipment for non-infectious animals any time they were handling mice, and their gloves were disinfected using 70% ethanol between cages.

Preparation and Delivery of Cecal Inoculum

Two adult male NOD.B7-2$^{-/-}$ donor mice were sacrificed and then transferred into an anaerobic chamber. A midline incision was made and the cecum was exposed. The tip of the cecum was cut using a pair of sterile scissors. Forceps were slid along the length of the cecum to extract and pool the cecal contents into a falcon tube. 15% PBS/glycerol solution was added to the sample to bring the volume up to 12mls. The inoculum was vortexed at 1000rpm for 5 minutes. The supernatant was collected, passed through a filter, and aliquoted into 2ml cryo vials and snap frozen.

Cecal Content Inoculation

Mice were gavaged twice, two days apart, with 250µl of the inoculum each time. The inoculum was delivered into their mouths using sterile pipette tips, with the distal end of the tips cut off by a razor. The sham inoculated group was given the vehicle PBS and glycerol. The mice

were inoculated the same day that they were weaned (21 days). Only females were used in this experiment. There were 6 mice in the sham group and 8 in the infected group.

Open Field Test (OFT)

Mice were placed in the open field test and observed every two weeks for signs of motor deficits. The test was performed with modifications from (ref). The mice were videotaped for 60 seconds while they moved freely about the field (plastic rat cage). At the end of the 60 seconds, they were help up by their tails and evaluated for dyskinesia, which included the clasping reflex. The rat cage was disinfected using 70% ethanol in between each mouse.

The grip test was performed by placing a pen on the abdomen of the mouse as it was held up by its tail. This test of controlled motor function evaluated the mouse by its ability to wrap its hind limbs around the pen. Mice received a score of zero (0) if there were no deficits, and a score of one (1) if the mouse was unable to grip the pen.

Presence or absence of a facial grimace was evaluated from the open field test videos. This protocol was modified from Langford, et.al (3). The mice received a score of 0 if there was no grimace present, and a score of 1 if there was a grimace. A grimace was identified by the following features: squinted eyes, flattened ears, and puffed cheeks.

Histopathology

The sciatic dorsal root ganglia (L3-L5), the brachial plexus, and the sciatic nerve were evaluated under light microscopy. All samples were fixed in 10% NBF for 48 hours and transferred to 60% ethanol. Samples were taken from the left side of the mouse and were stored in 60% ethanol until processing. The slides were evaluated blindly using the standard peripheral nerve scoring sheet. Stained sections were observed using an Olympus BX41 microscope, and photographed with an Olympus DP71U-TV0.5XC-3 camera.

Hormone ELISA Assays

ELISA assays for estradiol and testosterone were performed on thawed plasma. The assays were provided in kits from CALBIOTECH (Spring Valley, California, USA). Blood was collected at necropsy and centrifuged at 10rpm for 120 seconds. The plasma was removed with a pipette, aliquoted into 50µl samples to avoid multiple freeze-thaw cycles, and stored at -80ºC until it was time to run the assay. The samples were run in duplicates.

Estradiol

The samples were thawed on wet ice prior to use, and all reagents were removed from the refrigerator and brought to room temperature prior to use. 25 µL of the standards and samples were dispensed into their respective wells. Estradiol enzyme conjugate in the amount of 100µL was then added and the wells were gently mixed on a shaker for 20 seconds. The samples were incubated at room temperature for 2 hours, and the liquid was subsequently removed from the wells. The wells were washed with wash buffer 3 times and blotted on absorbance paper after each wash. Then, 100µL of tetramethylbenzidine (TMB) reagent was added to the wells and incubated at room temperature for 30 minutes. The reaction was halted by the addition of 50µL of Stop Solution in each well. The wells were mixed gently on the shaker for 30 seconds. The absorbance was read at 450 nm with A Universal EL800 Microplate Reader (BioTek Instruments, Inc., Winooski, VT). The absorbance values were interpolated and fitted to the standard curve using GraphPad Prism 6.

Testosterone

The samples were thawed on wet ice prior to use. 25 µL of the standards and samples were dispensed into their respective wells. 100µL of Testosterone-HRP Conjugate Reagent was placed into wells, followed by 50µL of rabbit anti-Testosterone. The samples were mixed well using a shaker, and incubated at room temperature for 1 hour. The wells were then rinsed with wash buffer 3 times, followed by the addition of 100µL of TMB reagent. The samples were mixed gently for 5 seconds and allowed to incubate for 15 minutes at room temperature. Stop

Solution was added to the wells and mixed on the shaker for 30 seconds. The absorbance was read at 450 nm with A Universal EL800 Microplate Reader (BioTek Instruments, Inc., Winooski, VT). The absorbance values were interpolated and fitted to the standard curve using GraphPad Prism 6.

Mi Seq™ and Mothur Sequencing of Fecal Samples

DNA was extracted from fecal pellets using a routine extraction protocol. Bacterial DNA concentration was confirmed by the nanodrop. Samples were sequenced by the Illumina MiSeq™ platform at the Research Technology Support Facility (RTSF) at Michigan State University. The raw 16s data was placed into the Mothur platform for gene sequencing analysis (http://www.mothur.org). The subsequent bioinformatics data was statistically analyzed via experimental group comparisons using PAST statistical software.

DISCUSSION

Transferring male cecal contents into female weanling mice altered the microbial gut flora (for a period of time) and made clinically worse in transferred mice. A statistically significant change over time was demonstrated in regards to the presence and numbers of bacterial members of the gut microbial community in the treated group compared to the inoculum that they were given. At the 20 week time point, the sham inoculated group showed no differences from the inoculum, meaning that their gut community had stabilized and reflected what is normally seen in adult B7-2$^{-/-}$ mice. However, the interactions in the gut between the transferred microbial inoculum and the normal host flora caused microbial interactions that favored growth of certain bacterial populations and stunted growth of others in the treated mouse group. Although there was no statistically significant difference in the amount of Lactobacillus present between sampling times, the increasing trend toward notable differences, with more bacteria present in the control mice than the transferred mice, cannot be overlooked.

Lactobacillus reuteri was found to cause increased levels of testosterone in geriatric mice, but the authors did not speculate about the mechanism. We interpret all of these microbial ecology results while bearing in mind that the 16s RNA sequencing analysis done in this study only provides a picture of the quantity of different microbial community members present in the sample; it does not provide what genes are expressed at any given time point. In essence, it is clear “who” is present, but not “what” they’re doing. In addition, mothur does not contain a list of all bacteria that exist, hence sequential data for a number of unclassified organisms is also present.

Two of the mice in the treated group had to be humanely euthanized, due to SAPP, before the conclusion of the study. Clinical disease appeared earlier in the treated mice, and a higher percentage of them had moderate to severe inflammation in dorsal root ganglion, brachial plexus, and sciatic nerves. Motor deficits evaluated with the grip test and the presence

of dyskinesia, were prominent in both groups of mice. However, it is evident that more severe clinical signs were seen in treated mice (heat map).

The grimace evaluation was not a very useful tool in this study. From our previous knowledge with the NOD.B7-2$^{-/-}$ mice, a facial grimace was expected in the control mice, as the disease progressed. With the number of lymphocytes and the amount of nerve damage present, there should have been clinically measurable evidence of pain. The fact that it has been shown that rodents are able to mask pain was considered; however, the grimace has been a feature of this disease that has been consistently present in the past.

The phenotype was indeed altered, just not in the direction that was hypothesized. Milder disease was expected in the treated mice,, and it was expected to also be associated with increased plasma testosterone. Just as there are microbes in the gut that can be indirectly protective to the development of autoimmune diseases via upregulation of sex hormone production, there are some that can be causative and exacerbate the disease onset (5).

No difference in the concentration of estradiol or testosterone was present in these mice. It is probably because the concentrations of both hormones were normalized by the time the disease reached its peak. In the Markle paper, testosterone was elevated in the mice given donor cecal contents at 7 and 14 weeks of age, but not at 34 weeks (4). In hindsight, it is thought that a difference in estradiol and testosterone levels between the groups would have been seen in a time course study; more specifically, 4-6 weeks after the transfer. It's not far-fetched to think that rather than testosterone being elevated, it could be estradiol, which could induce the production of proinflammatory mediators (discussed in Chapter 5).

The ideal experimental conditions to investigate the role of the microbiota in SAPP would be to derive germfree NOD.B7-2$^{-/-}$ mice. Despite all of the supporting literature for the use of germfree (GF) mice in the investigation autoimmune diseases, King and Sarvetnik made the claim that the prohibition of specific flora is responsible for the alleviation of diabetes. In their study of diabetes in GF mice, they discovered that mice that were housed in an isolator

contaminated with *Bacillus cereus* had delayed diabetes onset and decreased disease severity (2). If there are specific microbes responsible for priming the immune system to induce autoimmunity in the PNS, GF female mice will be protected from disease. Currently, we have a germfree project started. So far, we have embryos frozen, ready to be transplanted and cesarean rederived.

In conclusion, transferring cecal contents from donor male mice into female weanling mice made the disease worse in the transferred group. The reason for this change is unknown at this time. The major limitation in conducting a time course study is that it eliminates the ability to track clinical data on a single mouse over time. There is no way to predict which mouse will develop clinical disease, other than to follow them out clinically and evaluate phenotypic parameters. Our hypothesis is rejected, while realizing that a time course study, coupled with gene expression studies, will shed additional light on early microbial changes that may influence estradiol and testosterone production, which can then be correlated with inflammatory peripheral nerve lesions.

ACKNOWLEDGEMENTS

We thank Dr. Phillip Brooks and Dr. Julia Bell for assistance with processing the sequencing, analyzing the resulting sequences, and creating the accompanying plots. We appreciate the healthy discussion and interpretation of the results.

APPENDIX

Figure 4.1 Scatterplots of rears, weekly time points. The transferred mice had a decrease in rears that was significant over time, while the sham treated mice did not.

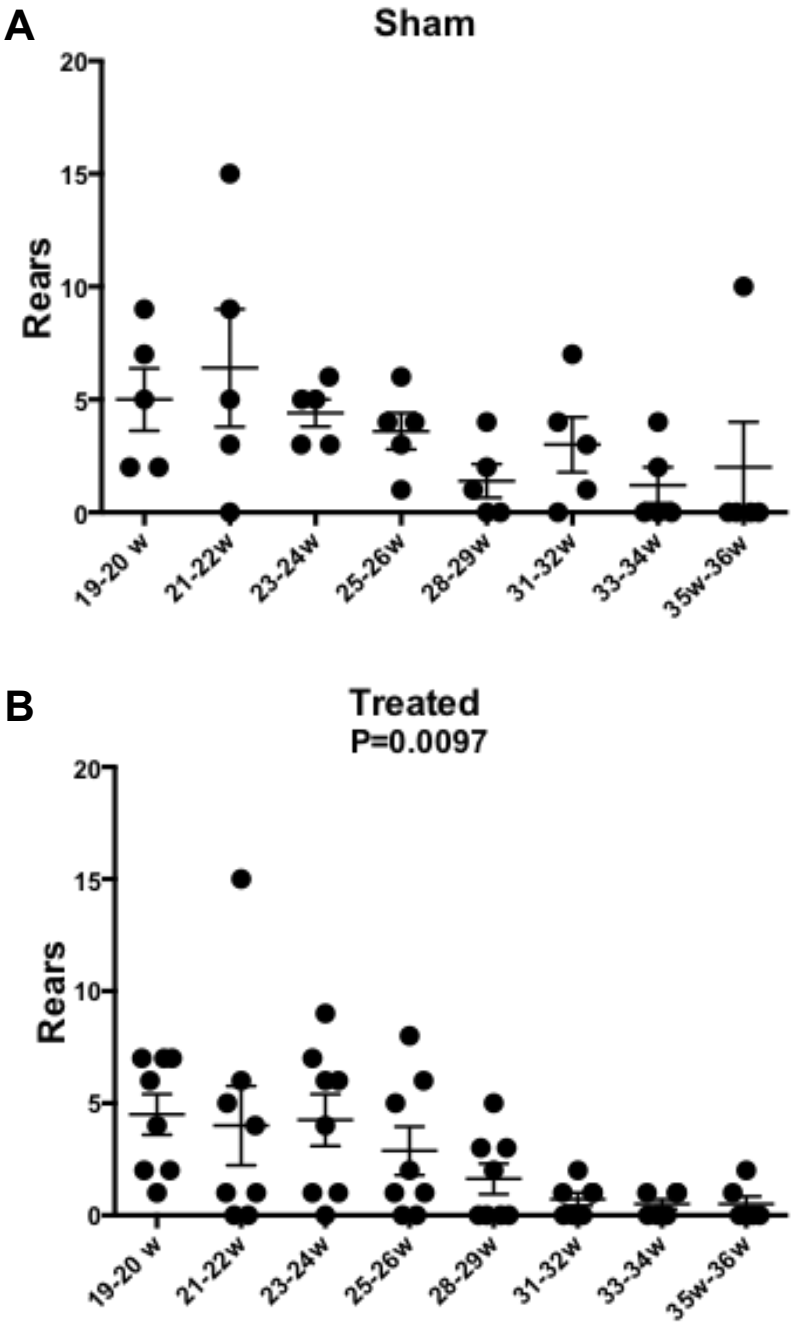

Figure 4.2 Pairwise comparisons of rears between sham and treated mice at each testing time point. The treated group had a trend toward decreased rears at 31-32 weeks of age.

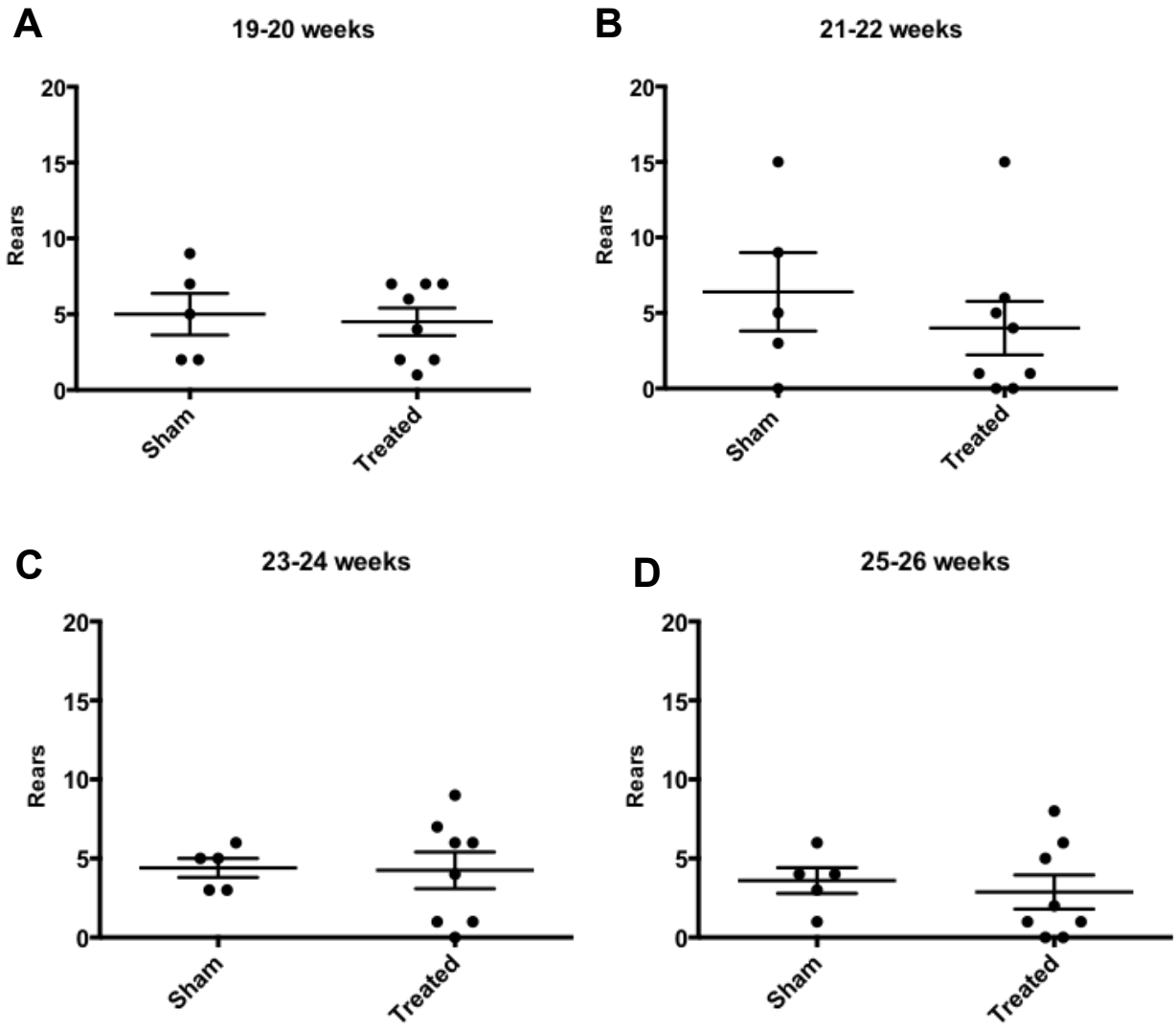

Figure 4.2 (cont'd)

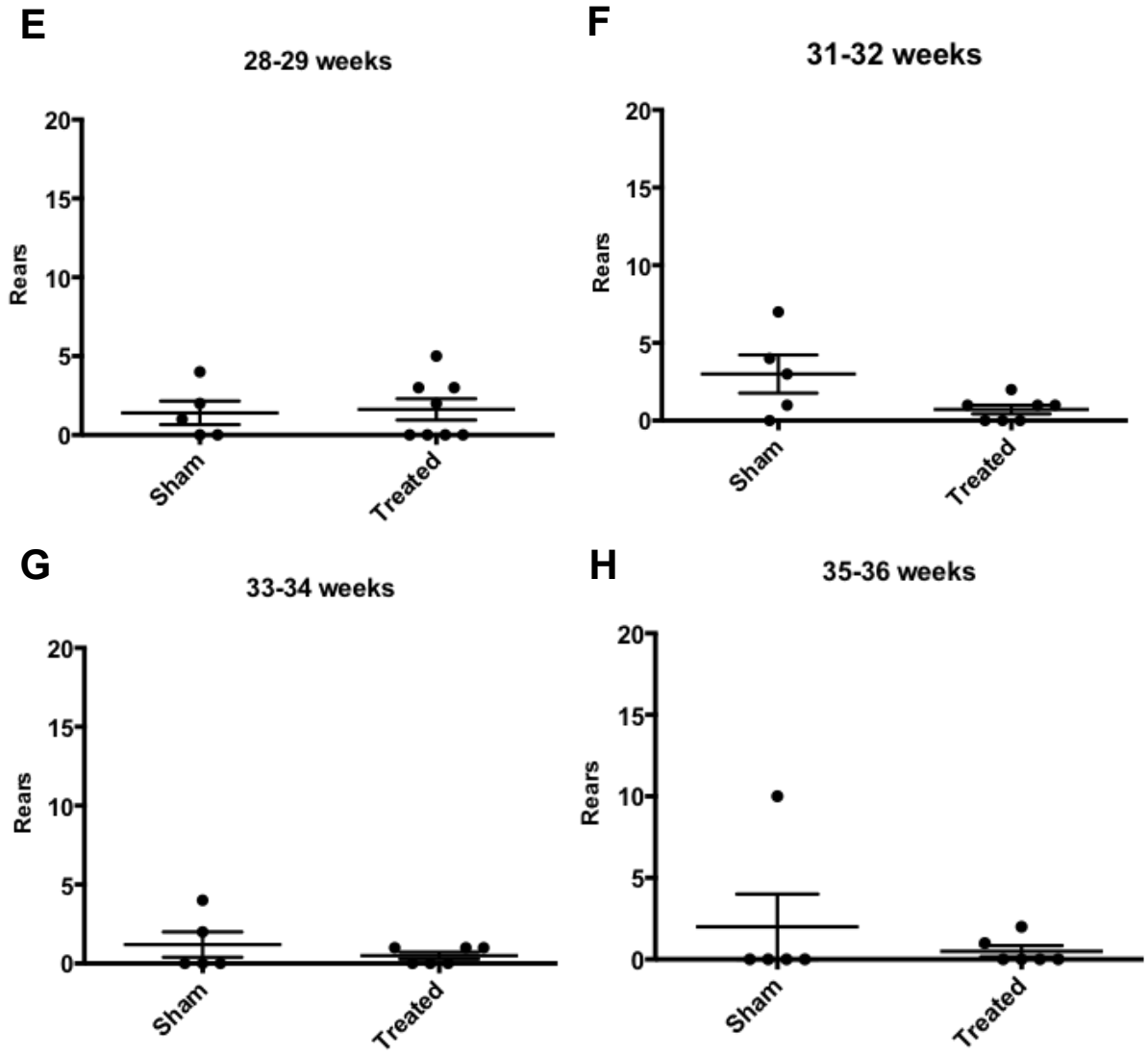

Figure 4.3 Grip test results. Sham and treated mice compared at each time point. Except for the sham treated mice at 21-22 weeks of age, there was evidence of a grip deficit at every time point.

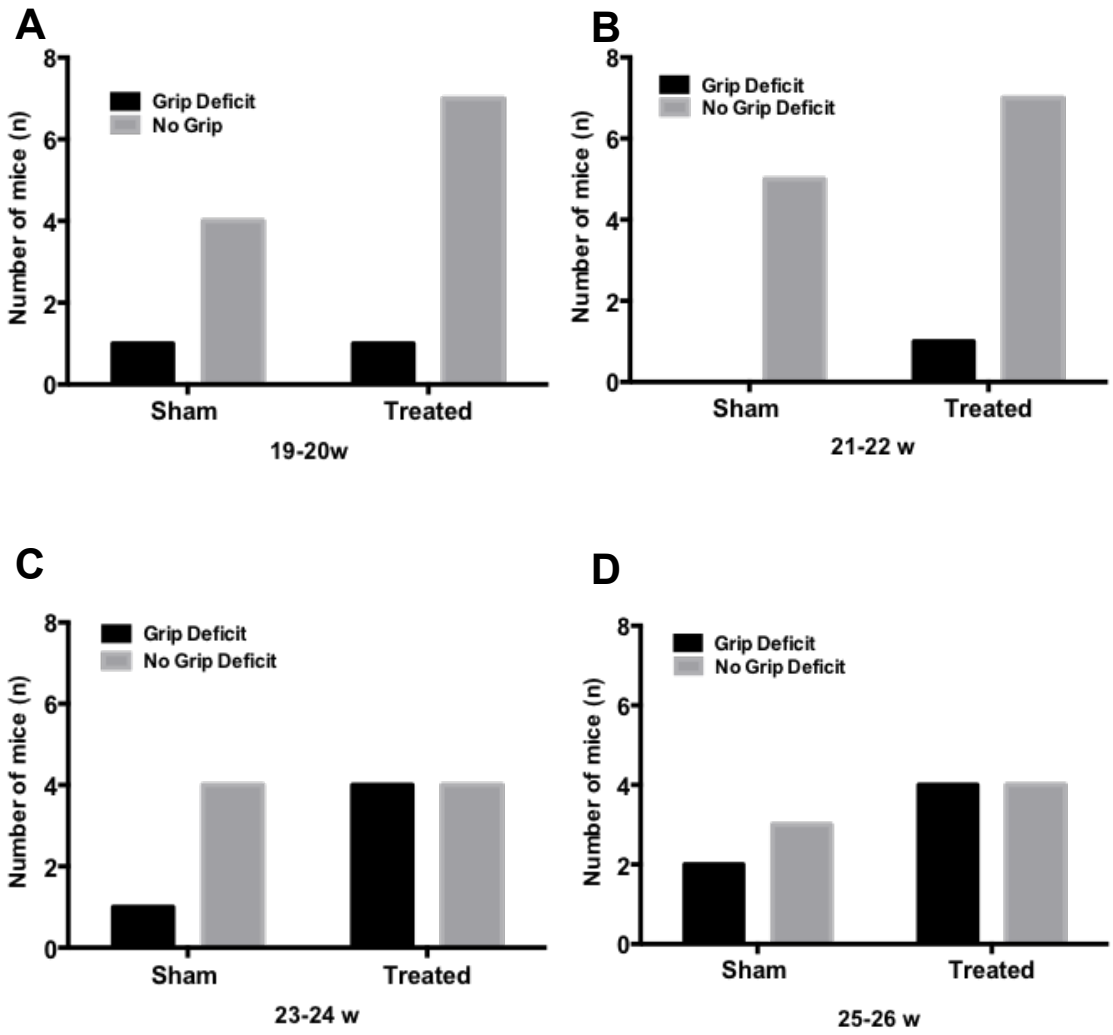

Figure 4.3 (cont'd)

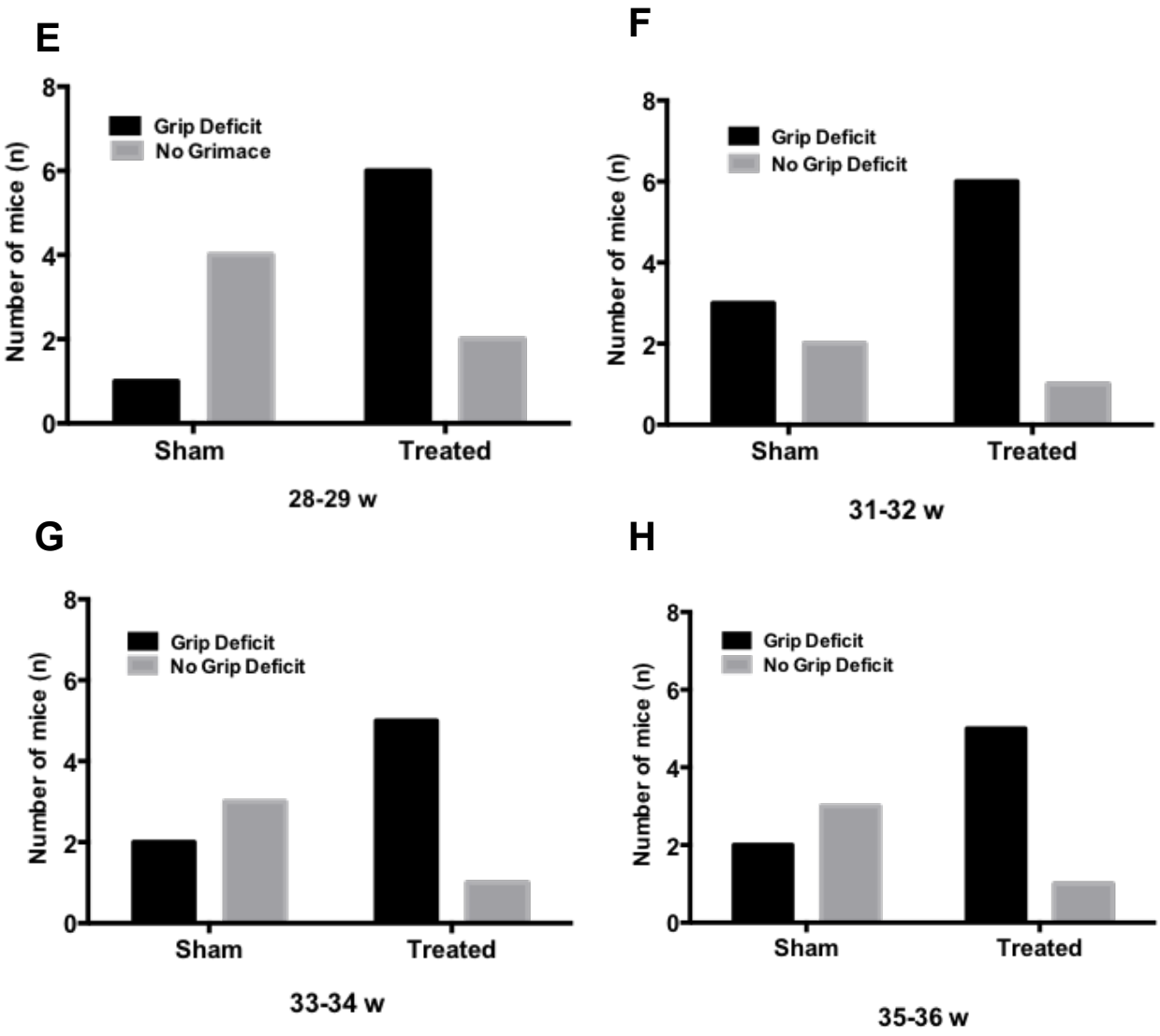

Figure 4.4 Grip deficits over time. Sham (A) and treated (B) mice

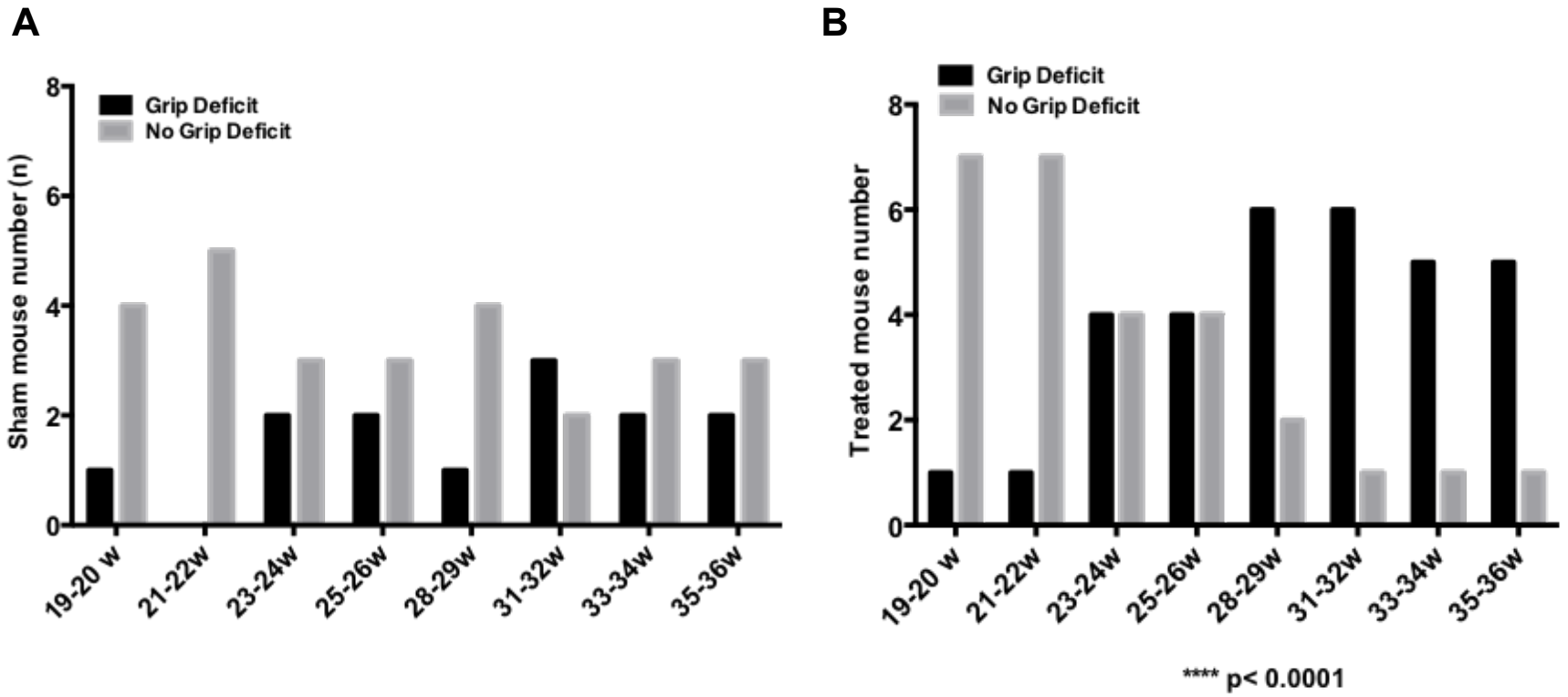

Figure 4.5 Dyskinesia over time. Sham vs treated mice.

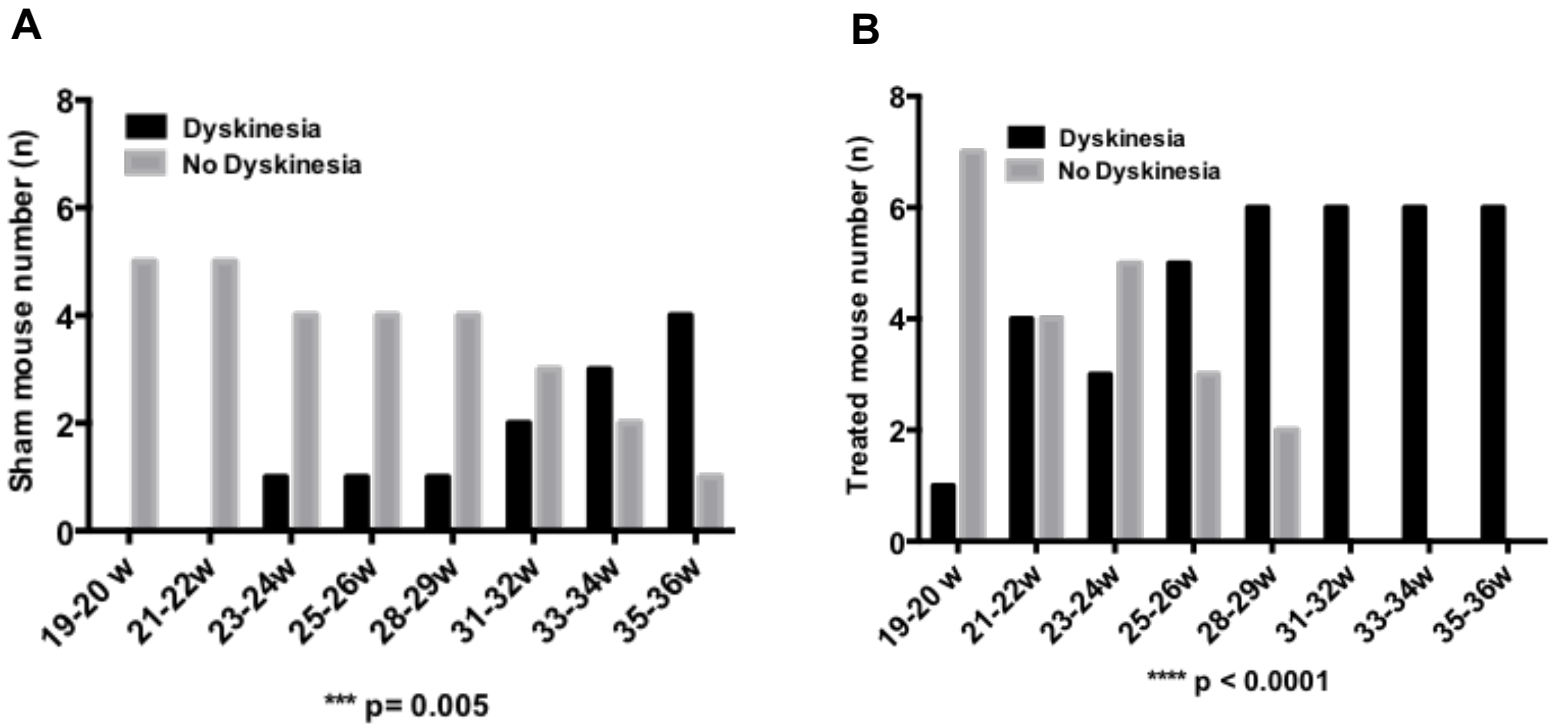

Figure 4.6 Grimace responses. The grimace first appeared in the treated mice at 28-29 weeks of age (E). It wasn't apparent in the sham mice until 35-36 weeks of age (H).

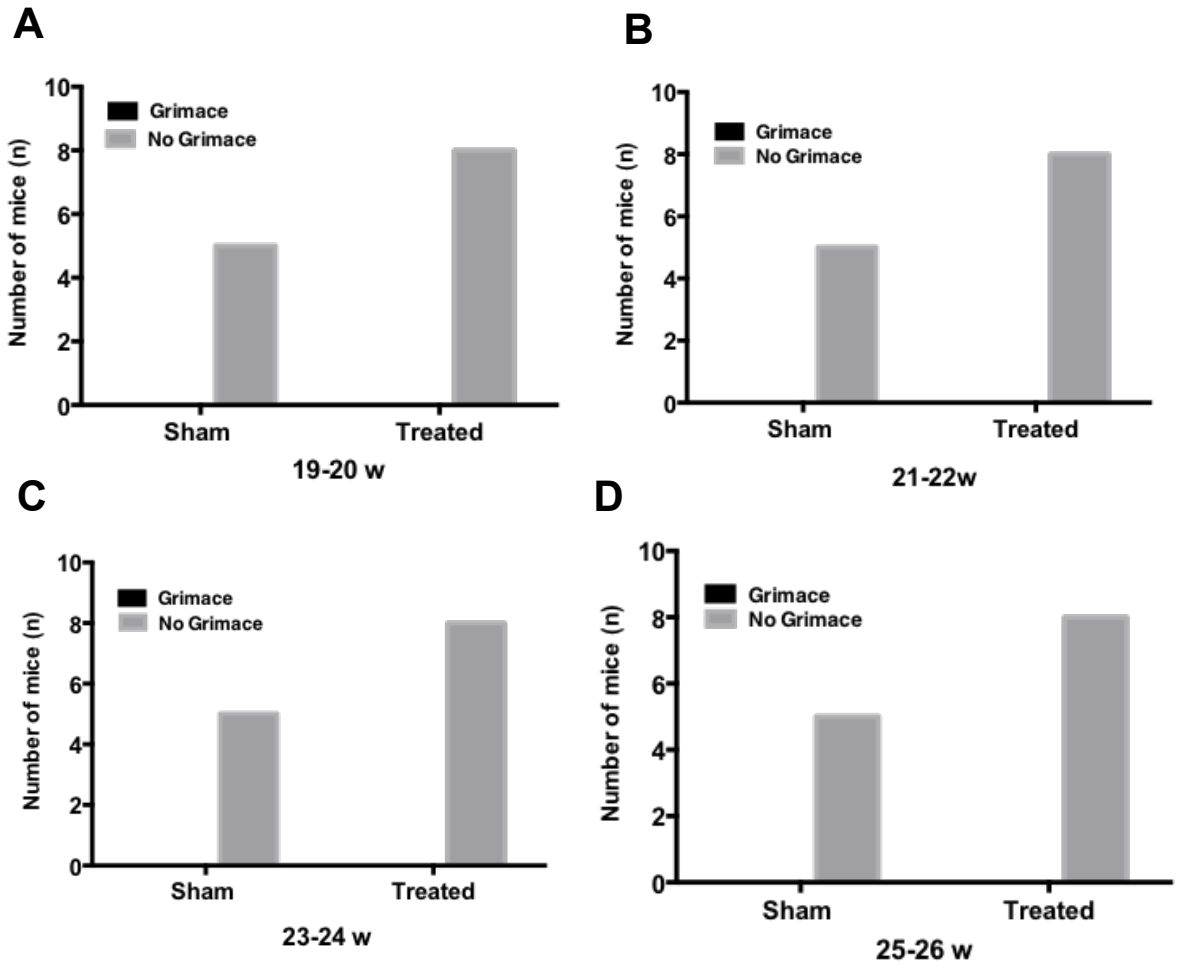

Figure 4.6 (cont'd)

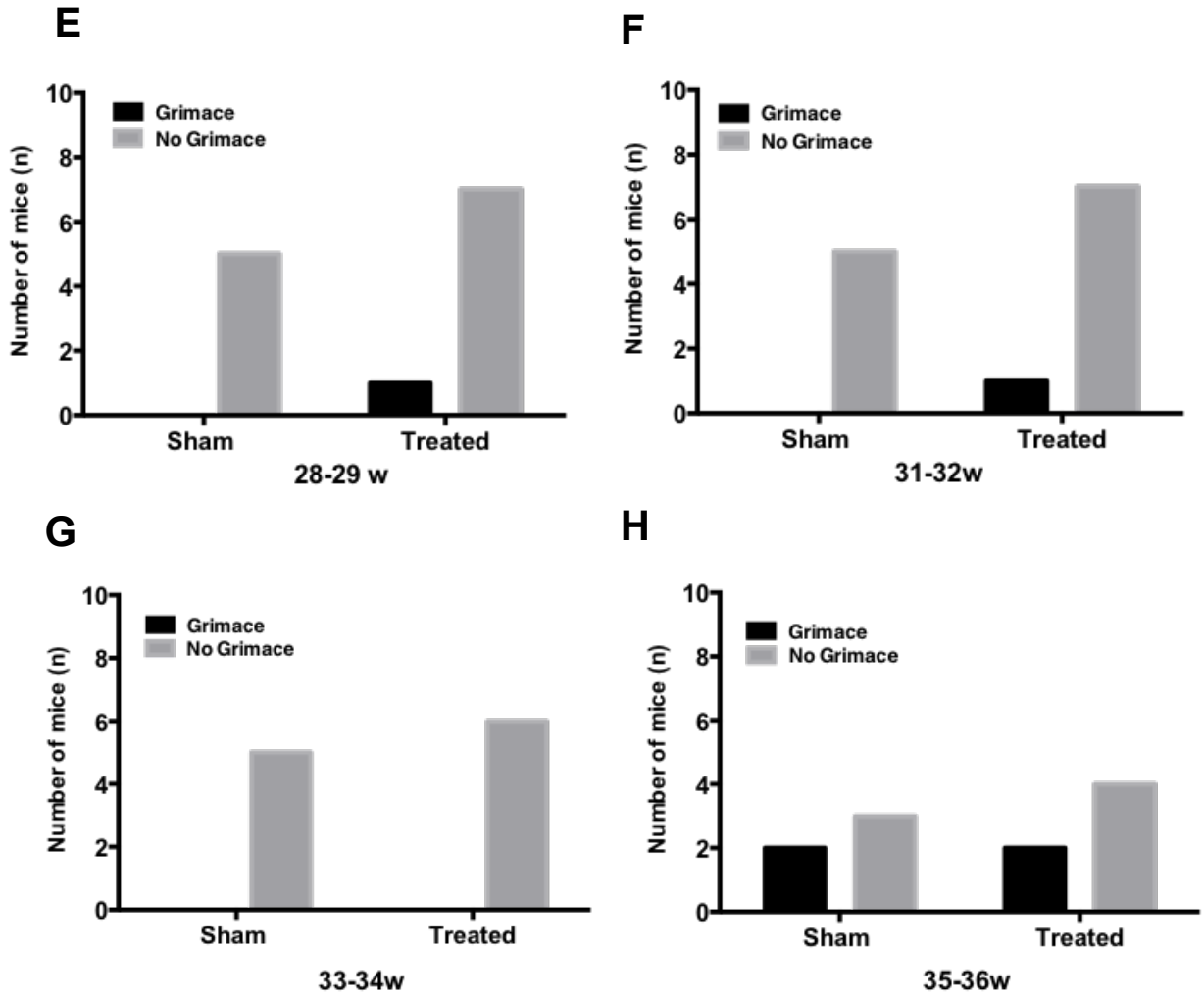

Figure 4.7 Facial grimace over time.

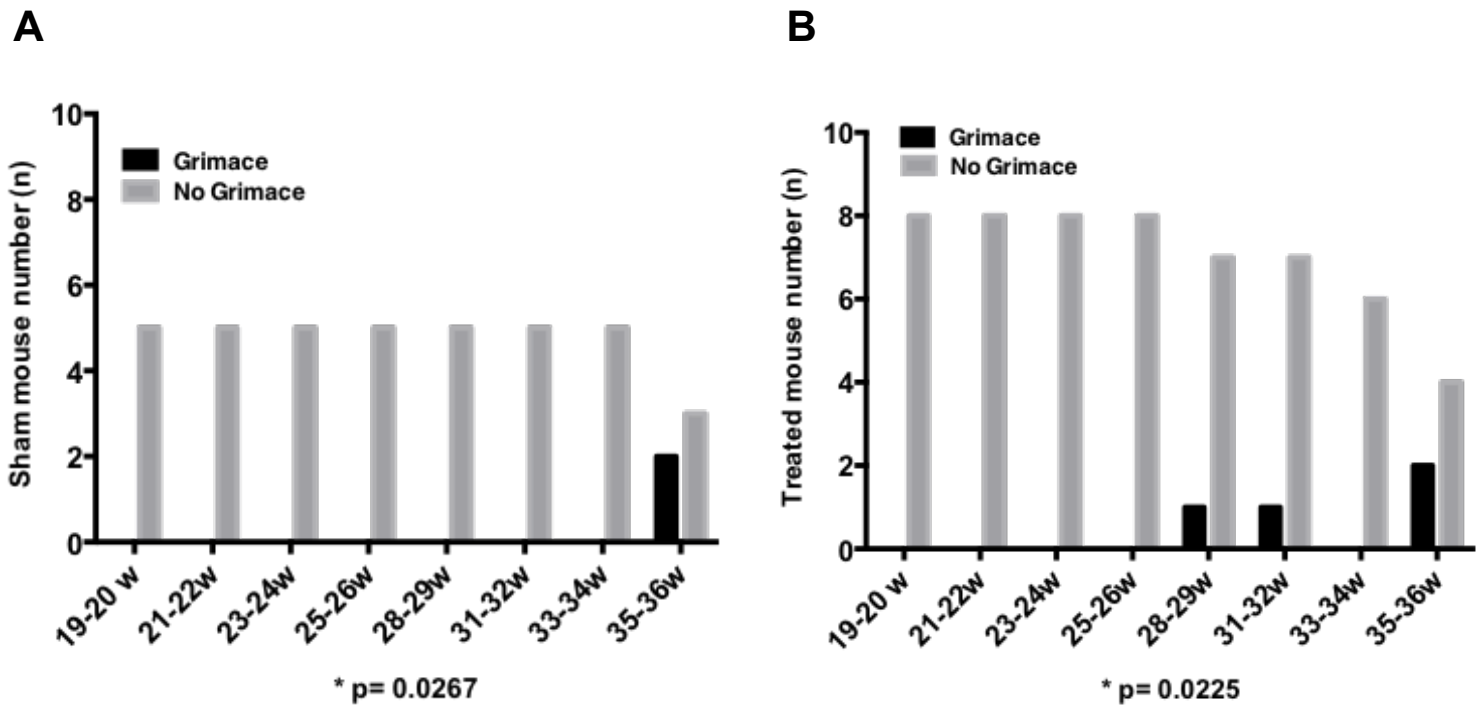

Figure 4.8 Heat map of clinical signs at each time point. The map includes grip deficits, dyskinesia, and the facial grimace. The black boxes indicated that a mouse was no longer in the experiment (reached a humane endpoint).

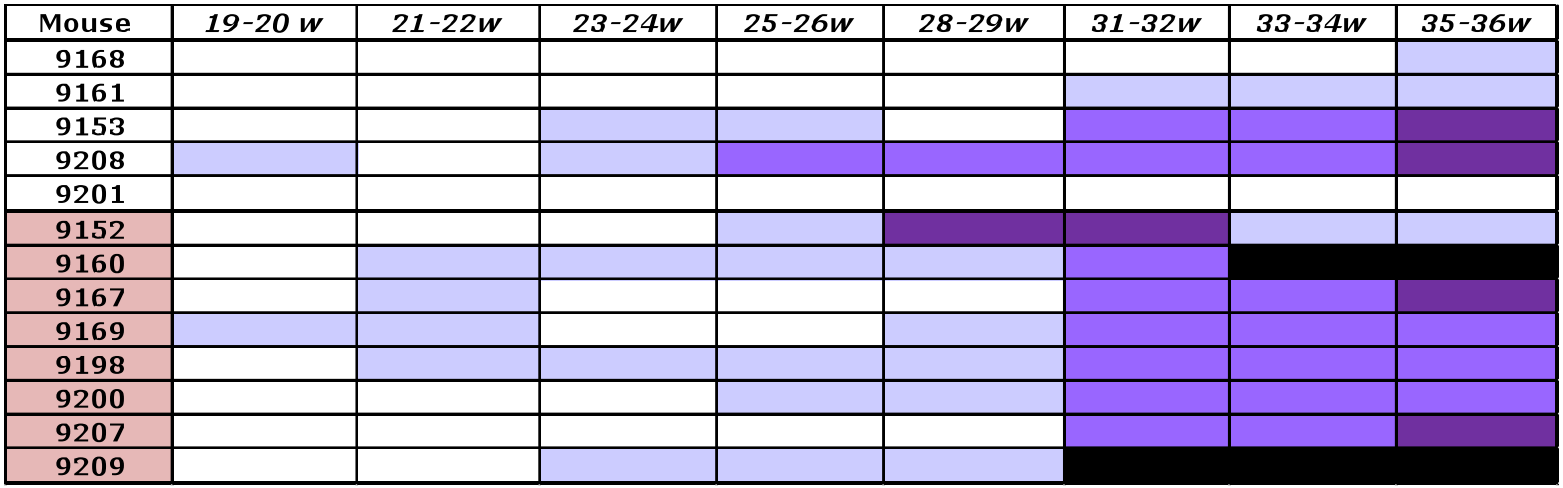

Color	# of signs
	1
	2
	3

Figure 4.9 Scatterplot of histopathology scores for sham and treated transferred mice. Note the trend toward higher histopathology scores in the treated group of mice. There are also two mice in the sham treated group with scores of zero. There were no unaffected mice in the treated group.

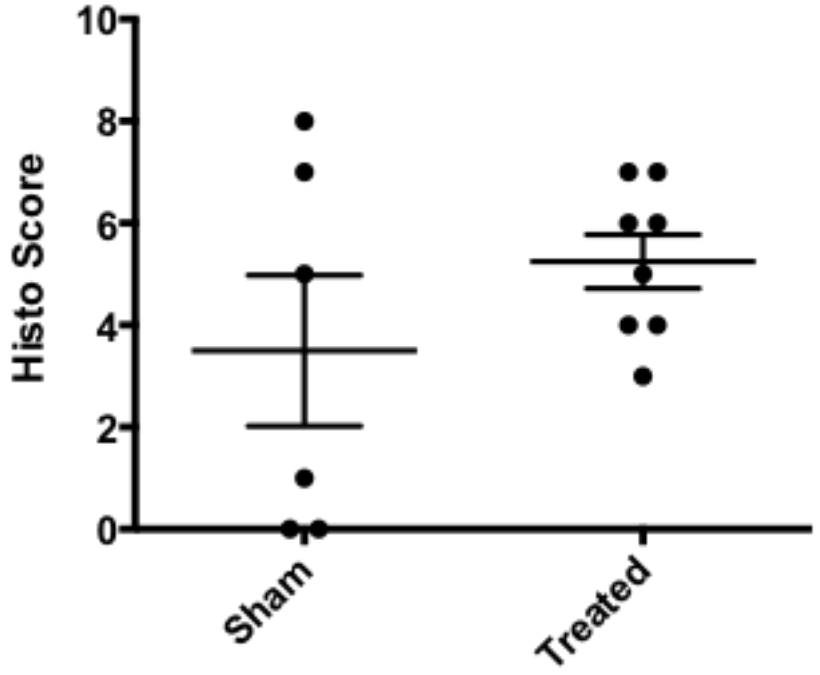

Figure 4.10 Mouse weights. There is a statistically significant difference in the weight of treated mice from the midpoint (20 weeks) to the end of the experiment. SB- sham before treatment, SM-sham midpoint, SE-sham end of experiment, TB- treated mice before treatment, TM-treated midpoint, TE-treated end. (C,D) Plasma estradiol and testosterone concentrations

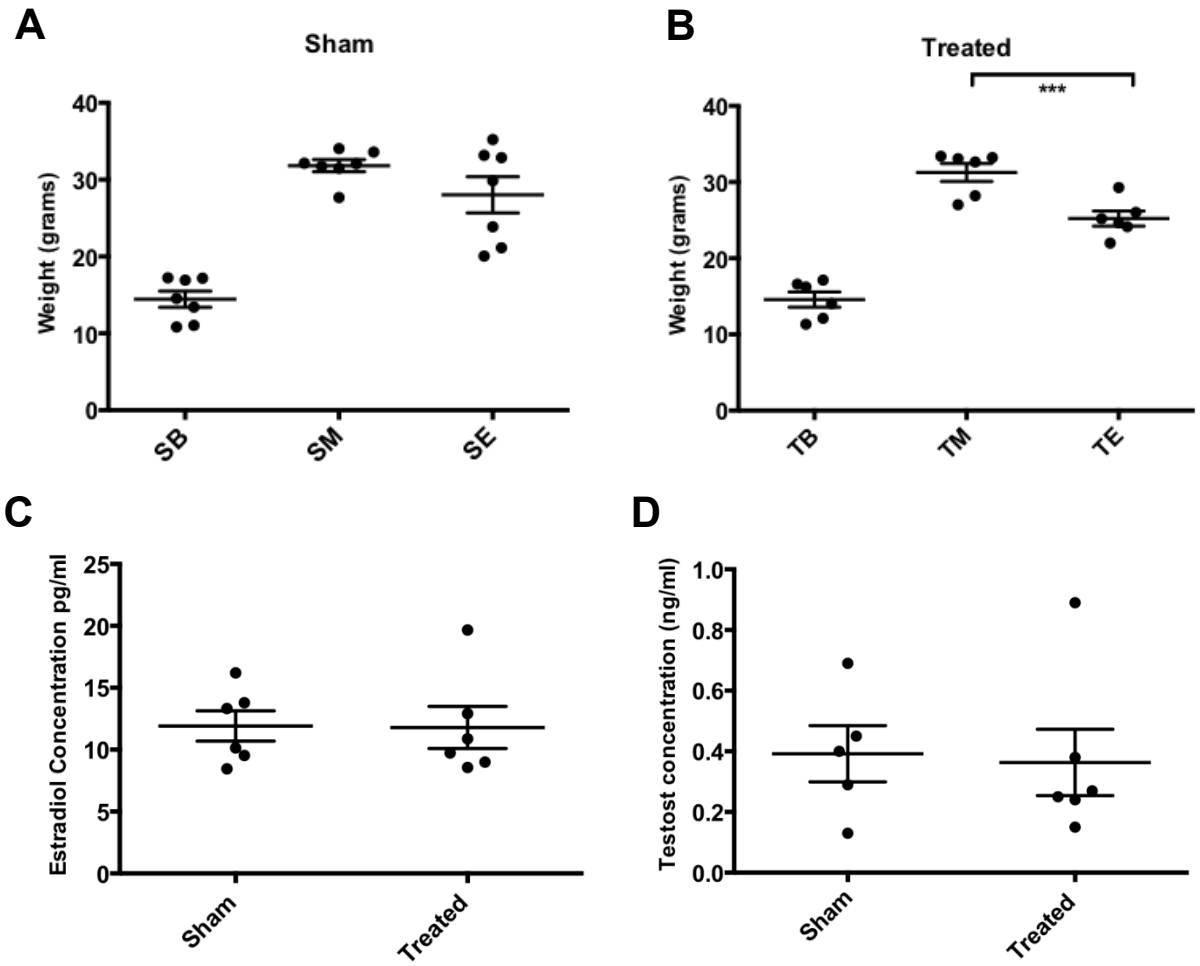

Figure 4.11 PCA plot of fecal sample distribution and clustering according to microbial community content. Key: Blue (BC)- control initial, Green (BT)-transfer initial, Turquoise (MC)-control midpoint, Pink (MT)-transfer midpoint, Purple (NC)- control necropsy, Red (NT)- transfer necropsy. The letter indicates the litter that each mouse came from (A, B, C, D, E)

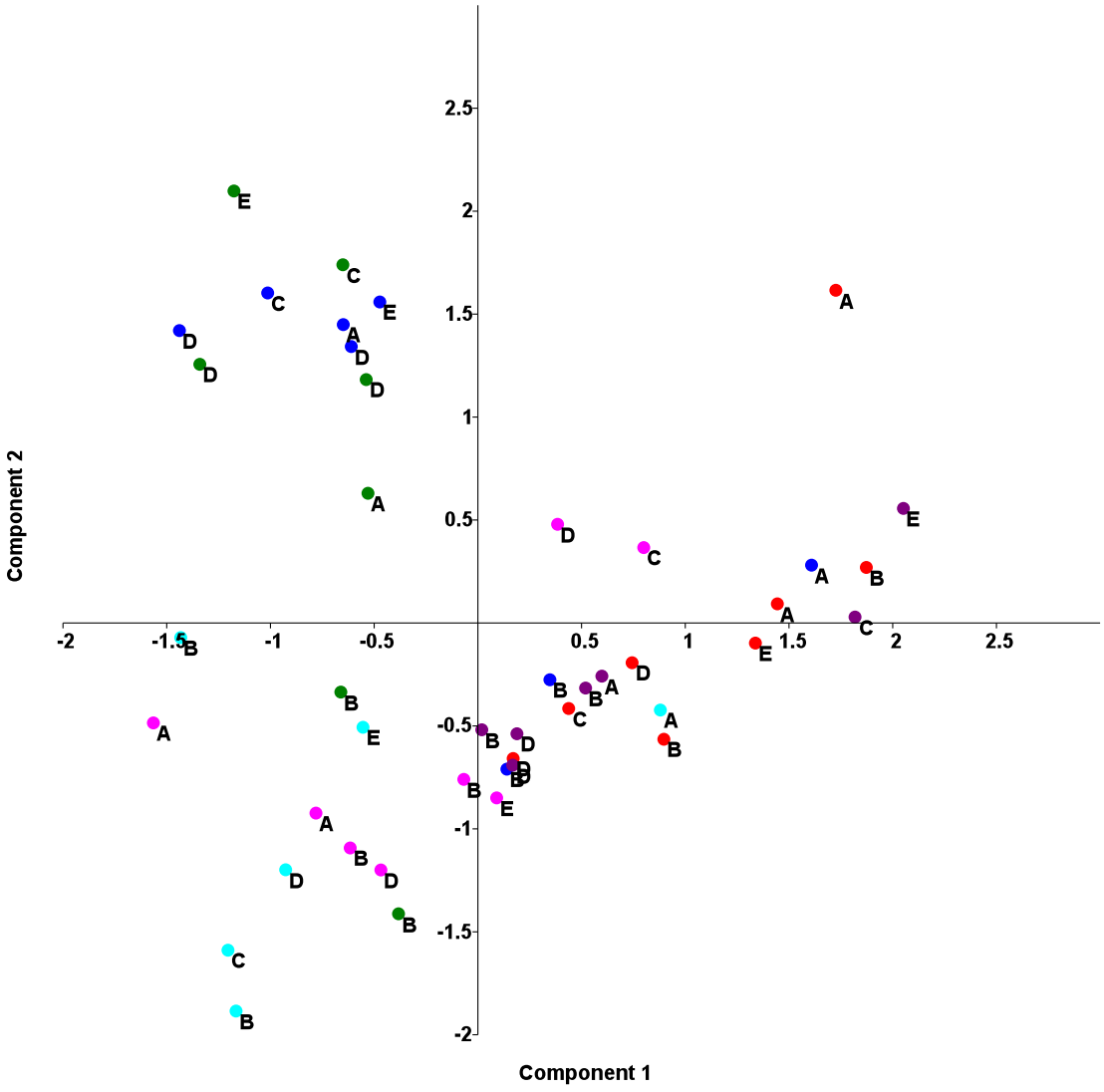

Figure 4.12 Plot of OTU changes of specific bacterial groups at times before the transfer (BC, BC), at the midpoint when mice were 20 weeks (MC, MT), and at necropsy (MC,NT). Note the decline in Lactobacillus in the treated samples at necropsy, compared to the control necropsy samples

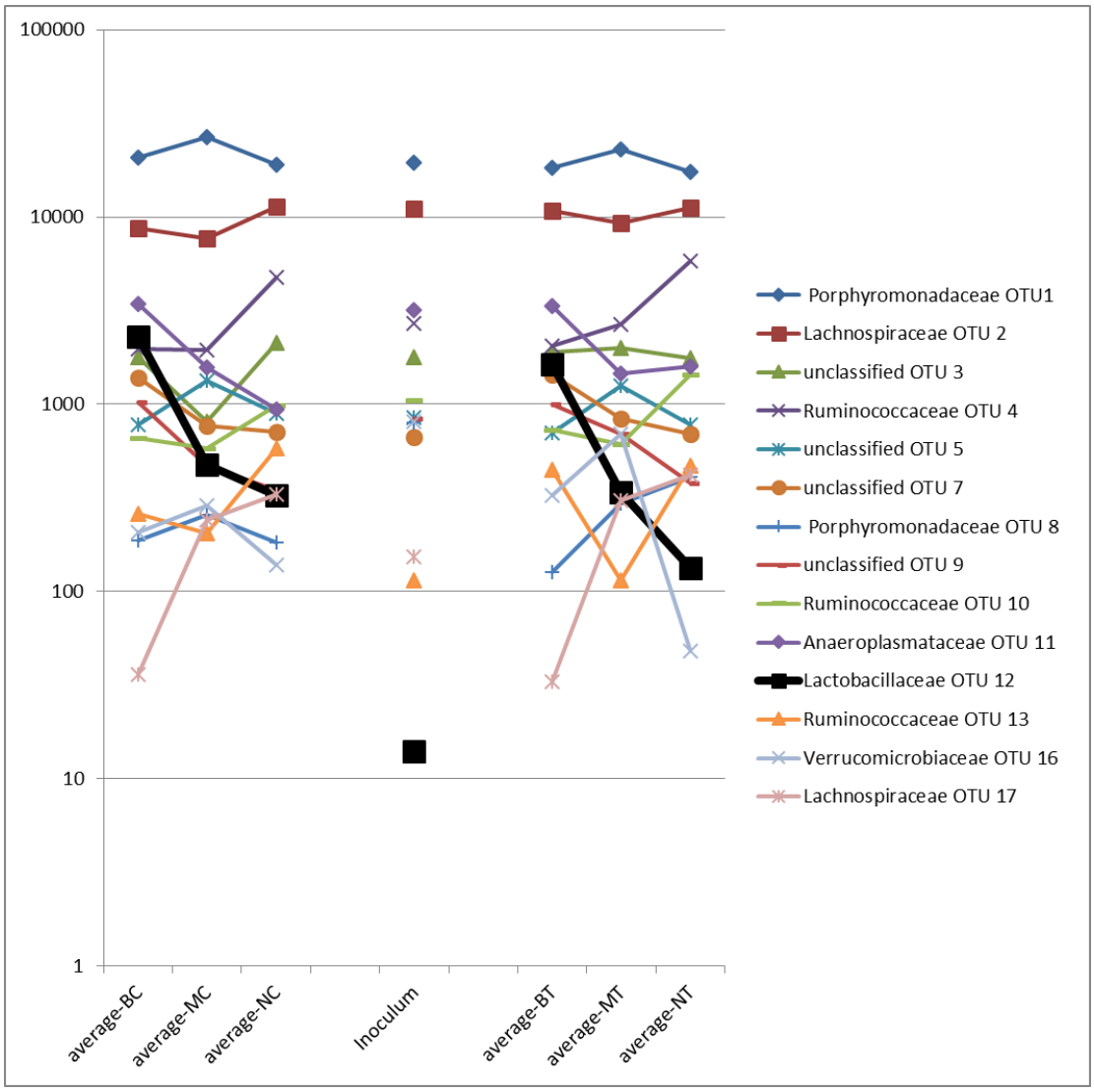

Table 4.1 OTU Values. Each OTU was compared to the inoculum separately; control and treated mice were combined for the initial sample. P values are in bold are significant after correction for multiple comparisons. At the midpoint (20 weeks), mice that received the transfer had a microbial community that looked different from the control group.

Operational Taxonomic Unit	Bacterial Family	Control and Transfer Initial	Control midpoint	Transfer midpoint	Control necropsy	Transfer necropsy
OTU001	*Porphyromonadaceae*	**0.002**	ns	**0.003**	**0.0008**	ns
OTU002	*Lachnospiaceae*	**4.3 x 10-6**	ns	**0.0001**	**0.0032**	ns
OTU003	unclassified (order Clostridiales)	0.041	ns	ns	ns	0.029
OTU004	Ruminococcacaceae	**8.3 x 10-5**	ns	**1.2 x 10-5**	**0.0027**	**0.0086**
OTU005	unclassified (phylum *Bacteroidetes*)	**0.002**	ns	0.0176	ns	ns
OTU008	*Porphyromonadaceae*	ns	ns	**0.0041**	ns	0.0181
OTU009	unclassified (phylum *Firmicutes*)	**0.0013**	ns	ns	ns	ns
OTU010	*Ruminococcaceae*	**3.5 x 10-5**	0.024	**2.7 x 10-6**	0.0111	**0.0009**
OTU012	*Lactobacillaceae*	**0.019**	ns	ns	0.0228	ns
OTU013	*Ruminococcaceae*	ns	ns	0.0255	ns	ns
OTU014	*Ruminococcaceae*	**0.0009**	ns	**0.0001**	ns	ns
OTU016	*Verrucomicrobiaceae*	ns	ns	ns	0.0358	0.0448
OTU017	*Lachnospiraceae*	0.0123	ns	**0.0094**	0.0072	ns
OTU018	*Bifidobacteriaceae*	0.0107	ns	ns	ns	ns
OTU021	unclassified (class Clostridia)	ns	**1.2 x 10-5**	**6.0 x 10-11**	**2.8 x 10-10**	**4.6 x 10**
OTU033	*Ruminococcaceae*	ns	ns	**2.6 x 10-10**	ns	ns
OTU042	*Lachnospiraceae*	ns	0.03	ns	ns	ns

BIBLIOGRAPHY

BIBLIOGRAPHY

1. **Borody, T. J., and J. Campbell.** 2012. Fecal microbiota transplantation: techniques, applications, and issues. Gastroenterol Clin North Am **41:**781-803.

2. **King, C., and N. Sarvetnick.** 2011. The incidence of type-1 diabetes in NOD mice is modulated by restricted flora not germ-free conditions. PLoS One **6:**e17049.

3. **Langford, D. J., A. L. Bailey, M. L. Chanda, S. E. Clarke, T. E. Drummond, S. Echols, S. Glick, J. Ingrao, T. Klassen-Ross, M. L. Lacroix-Fralish, L. Matsumiya, R. E. Sorge, S. G. Sotocinal, J. M. Tabaka, D. Wong, A. M. van den Maagdenberg, M. D. Ferrari, K. D. Craig, and J. S. Mogil.** 2010. Coding of facial expressions of pain in the laboratory mouse. Nat Methods **7:**447-449.

4. **Markle, J. G., D. N. Frank, S. Mortin-Toth, C. E. Robertson, L. M. Feazel, U. Rolle-Kampczyk, M. von Bergen, K. D. McCoy, A. J. Macpherson, and J. S. Danska.** 2013. Sex differences in the gut microbiome drive hormone-dependent regulation of autoimmunity. Science **339:**1084-1088.

5. **Salomon, B., L. Rhee, H. Bour-Jordan, H. Hsin, A. Montag, B. Soliven, J. Arcella, A. M. Girvin, J. Padilla, S. D. Miller, and J. A. Bluestone.** 2001. Development of spontaneous autoimmune peripheral polyneuropathy in B7-2-deficient NOD mice. J Exp Med **194:**677-684.

6. **Xu, M. Q., H. L. Cao, W. Q. Wang, S. Wang, X. C. Cao, F. Yan, and B. M. Wang.** 2015. Fecal microbiota transplantation broadening its application beyond intestinal disorders. World J Gastroenterol **21:**102-111.

CHAPTER 5

Investigating the Role of Sex Hormones in Spontaneous Autoimmune Peripheral Neuropathy: A pair of pilot studies

ABSTRACT

NOD.B7-2$^{-/-}$ mice develop Spontaneous Autoimmune Peripheral Polyneuropathy, with clinical signs and histopathologic lesions similar to those described in humans with AIDP. SAPP occurs mainly in female mice, while male mice are less affected. In order to further the understanding of SAPP, investigation focused on the effect of direct manipulation of hormones that differentiate males and females. Two pilot studies were conducted in parallel with each other. Females were used for the ovariectomy study and males for the testosterone blocking study. We employed novel techniques (in the Mansfield lab) to evaluate the effects of testosterone and estrogen in the onset and severity of SAPP. The hypothesis was that removing the ovaries from females would protect them from SAPP, and that blocking the action of testosterone via subcutaneous injection of the androgen receptor blocker, Flutamide, would render male mice more susceptible to SAPP. Mice that underwent ovariectomy did not develop disease at any lower rate or decreased severity compared to mice that had the sham surgery. Both groups of male mice exhibited clinical signs consistent with SAPP. However, frequent paw-licking was also noted in both groups. This has not previously been a prominent feature in male mice with SAPP. Female mice should be ovariectomized at an earlier age. Going forward, the Flutamide study should be repeated, with a different vehicle for drug delivery.

These pilot studies will provide information on sample size, feasibility, and time commitment required for undertaking repeat studies on larger scale.

INTRODUCTION

NOD.B7-2$^{-/-}$ mice develop a spontaneous peripheral nerve disease called Spontaneous Autoimmune Peripheral Polyneuropathy (SAPP). Beginning at 20 weeks of age, mice begin experiencing difficulty walking. By 32 weeks of age, almost 100% of females and 30% of males are affected (1). Clinical signs include splayed hind limbs, overgrown toenails, and in severe cases, flipped hind limbs. Earlier studies have confirmed that the disease causes pain; mice often exhibit a facial grimace, and less commonly, tremors.

The currently accepted theory regarding SAPP and diabetes is that both of the diseases have similar pathogeneses, with different target organs—the pancreas for diabetes and the peripheral nerves for SAPP (1) . In the NOD WT mouse, it has been shown that the gut microbiota can upregulate plasma testosterone concentration, which protects the mice from diabetes. Markel and colleagues transferred male cecal contents into female weanling mice and observed an 80% reduction in the development of diabetes in the female mice, while the transferred mice went on to develop the disease at the regular rate of occurrence. Measurements of plasma testosterone showed that female mice that were protected from diabetes had higher levels of testosterone than their affected counterparts (2). These findings make it apparent that sex hormones play a role in SAPP—that is the most significant difference between the male and female species.

In humans, the majority of autoimmune diseases occur in females. The balance of sex hormones is thought to have a strong immunomodulatory effect on autoimmune disease. Research studies are focused mainly focused on the prototypical rheumatic autoimmune diseases, Systemic Lupus Erythematosus (SLE) and Rheumatoid Arthritis (RA). Information regarding hormonal influence is slim for Multiple Sclerosis (MS), and even less so for GBS. Current research suggests that estrogen increases the production of the proinflammatory cytokines Interleukin-1(IL-1),Interleukin-6 (IL-6), and Tumor Necrosis Factor alpha (TNFa) (3). It

also decreases antigen presentation and polarizes the immune system toward a T-helper 2 (Th2) response. In New Zealand Black/New Zealand White (NZB/NZW) models of SLE, consistently elevated levels of estradiol speed disease onset and is associated with increased mortality (4). Those mice that undergo oopharectomy have a later disease onset and milder disease severity (5).

In contrast to the proinflammatory effects of estrogen, testosterone fosters a more calming immune profile. It magnifies the production of the anti-inflammatory cytokine IL10, while decreasing the expression of proinflammatory cytokines (3). In addition, it polarizes the immune system toward a T helper-1 (Th1) response by the activation of CD8 T cells. In the NZB/NZW mouse model of SLE, intact male mice lived longer and had a later disease onset than their castrated littermates. Once the influence of testosterone was removed via castration, its protective effects were lost and the mice readily succumbed to the disease (5). As a result of this, the hypothesis is that blocking the effect of testosterone with the androgen receptor antagonist, Flutamide, will have a similar effect.

In prior studies using the NOD.B7-2$^{-/-}$ mice to investigate SAPP, male mice are always less severely affected than their female counterparts, both in number and disease severity. Males that eventually develop SAPP do so at a later age; they have never reached a humane endpoint secondary to SAPP. These observations further add support to our agreement with published literature that shows testosterone to be protective in autoimmune diseases. This chapter presents findings from two pilot studies that were run in parallel with each other to investigate the role of estrogen and testosterone in the development of SAPP.

RATIONALE

Ovariectomy

The purpose of this study was to remove the influence of estrogen from the immune response and protect female mice from SAPP. The rationale was that using ovariectomy (OVX) to remove the major source of estrogen from female mice at 11 weeks of age would greatly reduce SAPP compared to female mice that received sham surgery. The expectation is that ovariectomized female NOD.B7-2$^{-/-}$ would be protected from developing SAPP. We hypothesized that sham surgery mice would develop clinical and histological features associated with SAPP.

Hypothesis: Ovariectomy will provide protection from SAPP in NOD.B7-2$^{-/-}$ mice.

Blocking Testosterone with Flutamide

The rationale for this study was that since diabetes and SAPP are thought to have a similar pathogenesis, and testosterone was protective for NOD WT mice with diabetes, the same would hold true for the B7-2$^{-/-}$ mice and the development of the autoimmune disease SAPP. Thus, if the influence of testosterone was removed from male mice, they would develop SAPP at a rate comparable to females of the same strain.

Hypothesis: Blocking the binding of testosterone to its cognate receptor is sufficient to abrogate protection from SAPP in NOD.B7-2$^{-/-}$ male mice.

RESULTS

Ovariectomy Study

Open Field Test (OFT)

When mice were compared longitudinally to each other within treatment groups, over the course of the experiment, there were significant decreases between the means of number of rears at multiple time points. Sham mice had a statistically decreased mean at 25 weeks, when compared to 14 weeks of age (Figure 5.2, A). OVX mice had statistically significant differences in the number of rears at 23, 25, 28, and 30 weeks of age, when compared to 14 weeks of age (Figure 5.2, B). When sham mice were compared to OVX mice at each time point, there was a significant increase in the mean between groups at 14 weeks of age (Figure 5.3, A) and 23 weeks of age (Figure 5.3, E). At 23 and 28 weeks of age, 67% (8/14) of the OVX mice did not rear in the open field test (Figure 5.3, E and G).

Mice in this experiment showed the classic signs of dyskinesia (including foot clasping) when held up by their tails (Figure 5.4). When sham mice were compared to OVX mice at each time point, both groups were free of dyskinesia up until 20 weeks of age. At that time, it was present in 27% (3/11) of mice (Figure 5.5, D). The sham mice remained free of similar motor deficits until 25 weeks of age, when 40% (2/5) of mice were affected (Figure 5.5, E). Once the dykinesia appeared in a group, it remained present throughout the duration of the experiment.

Deficits in the pencil grip test first appeared in OVX mice at 14 weeks of age, with 8% (1/13) of mice affected (Figure 5.6, B). When grip deficits were first observed in the sham treated mice at 25 weeks of age, 60% (3/2) of mice were affected (Figure 5.6, E). Seventy-five percent (9/12) of the OVX mice were unable to grip the pencil with their hind limbs at 23 and 28 weeks of age (Figure 5.6, E and F); this decreased to 50% by 30 weeks (Figure 5.6, G). All of

the mice that received sham surgery had grip deficits at the end of the experiment (Figure 5.6, G).

Pain was present in animals in this experiment, but it was not a prominent feature. The facial grimace was first noticed in the OVX group, in 7% (1/14) mice (Figure 5.7, D). The first grimace in the sham was observed at 28 weeks of age, with 20% (1/5) of mice affected (Figure 5.7, F).

A heat map with combined occurrences of dyskinesia, grip test deficits, and facial grimace revealed that there were more severe phenotyping deficits in the mice that received ovariectomy. In addition, there was an earlier onset of deficits compared to the sham group (Figure 5.8).

Histopathology

The differences between the means of overall histopathology scores were not statistically significant (Figure 5.9, A). However, there was a trend toward decreased scores in OVX group of mice, compared to sham mice. All mice in the sham group had moderate to severe inflammatory lesions in the evaluated peripheral nerve sections. In the OVX group, there were four mice that had no detectable lesions in their dorsal root ganglion, brachial plexus, or sciatic nerve.

Testosterone

Mice that underwent ovariectomy had a trend toward higher plasma testosterone than their sham surgery counterparts.

Flutamide Study

Open Field Test (OFT)

When mice were compared longitudinally to each other within treatment groups, over the course of the experiment, there were significant decreases between the means of numbers of rears, at multiple time points. Compared to the initial testing time point at 16 weeks of age, sham mice had a statistically decreased mean at every other testing time point in the experiment, except 18 weeks (Figure 5.10, A). Flutamide treated mice had statistically significant differences in the number of rears at 24, 26, 28, and 30 weeks of age, when compared to 16 weeks of age; there were also significant differences at the 28 and 30 week time points, compared to 18 weeks (Figure 5.10, B). When sham injected mice were compared to Flutamide injected mice at each time point, there was a slight trend toward increased rears at 18 and 21 weeks of age (Figure 5.11 B, C).

Dyskinesia was first observed at 21 weeks of age in 33% (2/8) of sham treated mice (Figure 5.12, C). Mice treated with Flutamide did not begin to show dyskinesia until 26 weeks of age, at which time, 26% (2/7) mice were affected. At the conclusion of the study, there were more sham mice with deficits in this test than treated mice. Eighty-six percent (6/7) of sham mice were affected, compared to 29% (2/7) of mice that received Flutamide injection (Figure 5.12, E).

Grip test deficits were first apparent in the sham injected mice, with 50% (4/4) of mice affected at 21 weeks of age (Figure 5.13, C). The Flutamide treated mice first showed deficits at 24 weeks of age, with 57% (4/7) mice affected (Figure 5.13, D). By the time the sham injected mice were 26 weeks of age, 100% (7/7) of them had grip deficits, which persisted throughout the duration of the experiment (Figure 5.13, E-F). At the 28 week time point, 86% of the

Flutamide treated mice had deficits, which were also present at the conclusion of the experiment, at 30 weeks of age (Figure 5.13, F and G).

The facial grimace was first observed at 21 weeks of age in both groups, with 25% (2/8) the sham mice, and 29% (2/7) of the Flutamide injected mice affected (Figure 5.14, C). The grimace persisted throughout the rest of the experiment. At the conclusion of the study, 71% (5/7) of sham mice and 86% (6/8) showed a facial grimace (Figure 5.14, E).

Paw-licking was a prominent clinical sign exhibited while mice were in the open field testing cage. It was seen at the first testing time point of 16 weeks in 8% (1/8) of the sham injected mice (Figure 5.15, A). Flutamide treated mice first exhibited paw-licking at 21 weeks, with 14% (1/7) mice exhibiting the behavior (Figure 5.15, C). Paw-licking was present in both experimental groups to some degree, for the duration of the experiment.

A heat map with combined occurrences of dyskinesia, grip test deficits, facial grimace, and paw-licking revealed that there were more severe phenotyping deficits in the sham injected mice (Figure 5.16). Between 24 and 30 weeks of age, 5 different mice (out of 8) showed deficits in all four testing parameters at one point or another, whereas none of the Flutamide treated mice ever did. Mice treated with Flutamide were also affected, but none of those mice showed all four clinical signs during one particular testing week. Five of the seven mice did show a total of three deficits between 24 and 30 weeks of age.

Histopathology

With the exception of three mice in this study, all other mice had no detectable inflammatory infiltrates or architectural changes within the dorsal root ganglion, brachial plexus, or sciatic nerve (Figure 5.17 A). One mouse in the sham treated group had a histo score of 7 (severe). Of the mice that received the Flutamide injection, there was one that had a score of 6 (moderate), and a second with a score of 1 (mild).

Estradiol

There was no significant difference in plasma estradiol concentration between the sham injected and Flutamide injected mice with samples available for analysis.

MATERIALS AND METHODS

Mouse Breeding and Handling

All experimental protocols and procedures were approved by the Institutional Animal Care and Use Committee at Michigan State University (06-12-107-00). All mice used in the experiments described here were originally obtained from The Jackson Laboratory (Bar Harbor, Maine). PCR assays obtained from Jackson Laboratories were used to confirm mouse genotypes both before and after experiments (http://jaxmice.jax.org/pubcgi/protocols/protocols.sh?objtype=protocol &protocol_id=346).The mice were bred and reared in a specific pathogen free colony, and singly house at a containment facility (OVX experiment) and in the breeding colony (flutamide experiment) in sterilized, filter-topped cages, with sterile bedding, that were changed once a week. Mice were fed a diet of Irradiated Harlan Teklad 7913 chow (Harlan Teklad, Indianapolis, Indiana, USA) and given free access to sterilized water. Animal technicians and experimental handlers wore standard personal protective equipment for non-infectious animals.

Ovariectomy

Once the surgical area was prepared (Figure 5.1, A), mice were removed from their home cage and sterile lubricant was placed in their eyes. They were the placed on a sterile surgical board in ventral recumbency, and anesthetized with 5-6% isofluorane delivered through a nose cone (Figure 5.1, B). The lumbar area over the both ovaries was shaven and cleaned with alcohol, followed by a betadine solution. To expose the ovaries a small longitudinal incision was made bilaterally through the skin and underlying muscle, over the area of both ovaries. The ovary was located within the ovarian fat and remove using a probe. Sterile scissors were used to remove the ovary from the uterine horn, which was then placed back into the abdominal cavity. This procedure was repeated on the other side to remove the remaining ovary. The

incision was closed with tissue two tissue staples that were removed one week later. The mice were placed in a recovery cage under a warm light, and allowed to breathe room air. Once they were awake, they were placed back in their home cage to finish recovering. The mice were given a subcutaneous injection of Ketoprofen 24 hours post-surgery, at a dose of 5mg/kg. Necropsy examination of the reproductive tract was made to confirm successful surgery for each mouse (Figure 5.1, C). Fifteen mice were ovariectomized and 5 received the sham surgery.

Open Field Test (OFT)

Mice were placed in the open field test and observed every two weeks for signs of motor deficits. The test was performed with modifications from (6). The mice were videotaped for 60 seconds while they moved freely about the field (plastic rat cage). At the end of the 60 seconds, they were help up by their tails and evaluated for dyskinesia, which included the clasping reflex. The open field testing cage was disinfected using 70% ethanol in between each mouse.

Presence or absence of a facial grimace was evaluated from the open field test videos. This protocol was modified from Langford, et.al (7). The mice received a score of 0 if there was no grimace present, and a score of 1 if there was a grimace. A grimace was identified by the following features: squinted eyes, flattened ears, and puffed cheeks. The presence or absence of paw-licking (Flutamide study) was also assessed.

Histopathology

Hematoxylin and eosin stained sections of tissue from the dorsal root ganglion, brachial plexus, and sciatic nerve were examined. Scoring was based on the degree of inflammation present in each section. Those sections that had a mild degree of inflammation were assigned the number 1. Moderate inflammation was given a score of 2, and severe inflammation was given a score of 3. Cells composing the infiltrate were recorded along with any other

architectural changes, such as myelin loss. Scores from the tissues were added together for a final histopathology score. Each mouse was then given an overall histopathology score as follows: A total score of 1-3 was classified as mild, 4-6 as moderate, and 7-9 as severe. The slides were blinded and read by an ACVP board certified veterinary pathologist (BJG).

Hormone ELISA Assays

ELISA assays for estradiol and testosterone were performed on thawed plasma. The assays were provided in kits from CALBIOTECH (Spring Valley, California, USA). Blood was collected at necropsy and centrifuged at 10rpm for 120 seconds. The plasma was removed with a pipette, aliquoted into 50µl samples to avoid multiple freeze-thaw cycles, and stored at -80ºC until it was time to run the assay. The samples were run in duplicates.

Estradiol

The samples were thawed on wet ice prior to use, and all reagents were removed from the refrigerator and brought to room temperature prior to use. 25 µL of the standards and samples were dispensed into their respective wells. Estradiol enzyme conjugate in the amount of 100µL was then added and the wells were gently mixed on a shaker for 20 seconds. The samples were incubated at room temperature for 2 hours, and the liquid was subsequently removed from the wells. The wells were washed with wash buffer 3 times and blotted on absorbance paper after each wash. Then, 100µL of tetramethylbenzidine (TMB) reagent was added to the wells and incubated at room temperature for 30 minutes. The reaction was halted by the addition of 50µL of Stop Solution in each well. The wells were mixed gently on the shaker for 30 seconds. The absorbance was read at 450 nm with A Universal EL800 Microplate Reader (BioTek Instruments, Inc., Winooski, VT). The absorbance values were interpolated and fitted to the standard curve using GraphPad Prism 6.

Testosterone

The samples were thawed on wet ice prior to use. 25 µL of the standards and samples were dispensed into their respective wells. 100µL of Testosterone-HRP Conjugate Reagent was placed into wells, followed by 50µL of rabbit anti-Testosterone. The samples were mixed well using a shaker, and incubated at room temperature for 1 hour. The wells were then rinsed with wash buffer 3 times, followed by the addition of 100µL of TMB reagent. The samples were mixed gently for 5 seconds and allowed to incubate for 15 minutes at room temperature. Stop Solution was added to the wells and mixed on the shaker for 30 seconds. The absorbance was read at 450 nm with A Universal EL800 Microplate Reader (BioTek Instruments, Inc., Winooski, VT). The absorbance values were interpolated and fitted to the standard curve using GraphPad Prism 6.

Flutamide Preparation and Injection

Flutamide (Sigma-Aldrich) was administered at a dose of .25mg/kg. It was stored in an amber colored lab bottled, wrapped in aluminum foil at room temperature. Immediately before dosing the mice, 25 uL of flutamide in DMSO was placed into a sterile falcon tube, and brought up to a volume of 5mls with 0.9% NaCl (physiologic saline). 0.3 mLs of the solution was drawn up into a tuberculin syringe. Sham injected mice received 25uL of the vehicle (DMSO) in physiologic saline solution. The procedure for drawing up the solution is the same as for the Flutamide treated mice. Mice were treated 3 times per week.

An animal handle removed the mouse from its cage and restrained it while tenting the scruff immediately behind its head, over the neck area. The researcher delivering the treatment removed the cap from the needle and inserted it, bevel up, into the subcutis of the tented area of skin. Once the bevel was completely in, the plunger was pressed at a steady rate to deliver

the test article solution. The bevel was slowly retracted from the subcutis and the needle/syringe combo was disposed of in a designated sharps container.

Statistical Analysis

The open field test over time, within groups was analyzed using a one-way ANOVA, with Holm-Sidak's multiple comparisons test. Dykinesia, grip deficits, grimace, and paw licking were analyzed using Fisher's exact test. Histopathology and ELISA data were analyzed with Mann-Whitney test. All statistical tests were performed using GraphPad Prism, version 6 (La Jolla, CA, USA).

DISCUSSION

The major finding in the ovariectomy pilot study was that the OVX mice were not protected from developing SAPP. In fact, they had just as many clinical deficits as the mice that received the sham surgery. Moreover, dyskinesia, deficits in the grip test, and grimace responses were all noted first in the OVX mice. Although the facial grimace was not seen until later in the experiment compared to the rest of the evaluated clinical parameters, it was still present first in the OVX mice. The fact there were significant decreases in the means of rears over time, within each treatment group is not surprising. Mice tend to become less active as time progresses. However, the significant difference in the mean rears at 23 weeks of age is of interest; at this particular time point, as well as 28 weeks of age, there were a large number of mice that did not rear at all in the open field test. In addition, at 28 weeks, 75% of the OVX mice also had grip deficits.

The histopathology findings are similar to those described for SAPP. There was a trend toward higher histo score numbers in the sham mice, which is what was expected at the beginning of the study—however, based on the clinical disease presentation, and what is known from previous studies regarding the positive correlation of clinical signs and nerve inflammation, it is feasible to think that the OVX mice would have higher histo scores. It is worthy to note that despite clinical parameters consistent with SAPP, there were four OVX mice that did not have any peripheral nerve inflammation (these mice brought the average of the histo scores down for the group). It is though that these mice with zero histopathology scores may have been "protected" from inflammation by the removal of estrogen and increased testosterone. Two of the mice had plasma testosterone levels near the maximum for the group (~0.7 ng/mL), while others had levels near the lower end for the group (~.3 ng/mL). Overall, the OVX mice had higher testosterone levels than mice given the sham surgery.

Four of the mice with no ovaries had no peripheral nerve inflammation, but clinical signs of disease. With these findings, we wonder if there are other cells in the peripheral nerves of the OVX mice that are responsible for the manifestation of clinical signs in the absence of inflammation. Can pain be responsible for the clinical signs in those mice? It has been reported that the pain pathways for male and female mice are different. Specifically, microglial cells are responsible for pain in male mice, while lymphocytes drive the female pain response (8) . Through a series of experiments with induced nerve injury, Sorge and colleagues were able to show that treatment with glial inhibitors was able to reverse pain in male mice (9). In the case where lymphocytes are not present to regulate disease, microglial cells may play a role. Recall from the age screen study where inflammation only precedes the onset of clinical signs in a small percentage of mice. Could it be that the removal of the ovaries in these mice would have caused them to develop disease at a much later time?

Situations like the aforementioned scenario where 2 of the 4 OVX mice with clinical signs (but no inflammation) have increased testosterone, spark the debate regarding “group effect” versus “each animal as its own case study”. While some in the research community may be tempted to dismiss the findings due to the fact that only two mice had testosterone levels near the maximum for the group, instead of all four, it is worth it to remember these occurrences, and the fact that it could have some potential bearing on the reason why there was no inflammation present in the face of clinical signs. It is not customary in scientific research to evaluate each mouse as its own case; rather, the group effect is preferred. Here, we make the case that for mechanistic studies involving spontaneous diseases, a longitudinal approach that examines each mouse as its own entity in addition to the group effect might be more informative.

This experiment concluded when the mice were 30 weeks of age, rather than the desired time point of 40 weeks, because the sham control mice reached a humane endpoint.

From previous studies with the B7-2$^{-/-}$ mice, expectations were in place for onset of clinical disease and inflammation. In hindsight, more mice should have been included in the control group. More surgically treated mice were used because of the potential to lose a few as a result of the surgery. We didn't lose any mice secondary to surgery.

The hypothesis was that if estrogen did indeed play a major role in the age of onset and severity of SAPP, then removing both ovaries from the mice would confer protection. Despite being ovariectomized at 11 weeks of age, mice still showed clinical signs and histopathologic lesions consistent with SAPP. In conclusion, the hypothesis is rejected with the thought that ovariectomizing the NOD.B7-2$^{-/-}$ mice at an earlier age may yield different results than those yielded from this pilot study. Despite the fact that the hypothesis was rejected, this pilot study has valuable insight into the correlation of clinical signs with histopathology findings, and provided the opportunity for training personnel in OVX surgery.

The results of the testosterone receptor blocking with Flutamide study were the opposite of what we expected. There was no clear separation of the experimental groups based on clinical signs or histopathology lesions. Unexpectedly, mice treated with the vehicle (DMSO) showed more frequent clinical signs than Flutamide treated mice. In addition, paw-licking in the open field test was a prominent feature seen in both groups of mice. Similar to the phenomenon seen in the previous experiment, with the exception of the grimace response, the sham treated mice were the first to exhibit dyskinesia, grip deficits, and paw-licking. Surprisingly, 86% of sham treated mice showed dyskinesia, compared to only 29% of Flutamide treated mice. Up until these experiments, dyskinesia was associated with inflammatory infiltrates in both female and male mice; males tend to show less severe dyskinesia. Even more surprising was the large number of mice that had grip deficits at the end of the study (sham-100%, flutamide-86%). With these clinical results, it was fully expected to see severe inflammation, consistent with SAPP in the dorsal root ganglion, brachial plexus, and sciatic nerves of these mice. Pain was also a

prominent feature of the clinical disease presentation in both groups of mice. At the conclusion of the experiment, 71% of sham injected mice and 86% of treated mice had a facial grimace. The absence of inflammation in all but one mouse per group in the face of overt clinical signs provides more support that there are other mechanisms at work in this experiment, which leads back to the microglial-neural crosstalk as a facilitator of pain (9).

The clinical disease manifestation seen in this study is unlike any other seen over the years involving male mice in the Mansfield Colony. It is clear that the clinical signs are not being mediated by the classical inflammatory infiltrates of lymphocytes and plasma cells seen in SAPP. Because both the sham and treated mice exhibited such robust clinical signs, we have to take into account the effect that the drug delivery vehicle may have had. The frequent paw-licking is reminiscent of mouse behavior after administration the formalin test for noxious stimuli has been administered. A directly toxic dose and toxic effect on mice is not present within the literature, however, the amount of DMSO used was so small, that toxicity is unlikely. A total of 25μL (in 5mL 0.9NaCl) was used for a total of 7 mice. The same amount was used for the sham injected mice.

Initial efforts in this pilot study were aimed at establishing a working dose of Flutamide suitable to see a distinct difference in estrogen concentration once testosterone was removed. However, the group sizes of mice available at the time would only allow for one drug dose; anything less would compromise statistical power. The use of a 60 or 90 day slow release subcutaneous pellet was considered, but ultimately decided against due to concerns about each mouse receiving the same amount of “slow release” each day.

We hypothesized that blocking the binding of testosterone to its cognate receptor would be sufficient to abrogate protection from SAPP in NOD.B7-2$^{-/-}$ male mice. While the clinical signs are suggestive of SAPP, they occurred in greater frequency in the sham treated mice that received no drug. It is a possibility that the small amount of DMSO used to dissolve the

Flutamide may have had adverse effects. With this considered, the hypothesis is rejected and another pilot experiment is presented in Chapter 6 to investigate the possibility of toxicity secondary to DMSO.

ACKNOWLEDGEMENTS

We would like to thank Dr. Laura McCabe and Regina Irwin for consultation and discussion regarding the ovariectomy and Flutamide pilot experiments. In addition, we extend sincere gratitude to Sandy Raehtz for technical assistance with surgeries.

APPENDIX

Figure 5.1 Ovariectomy setup.(A) Surgical setup for ovariectomy. (B) Mouse on surgical board being anesthetized with Isofluorane through a nose cone. The dorsum is shaven in preparation for the surgery. (C) Reproductive tract from ovariectomized and sham mice. The OVX reproductive tract is smaller than the reproductive tract from the sham mouse.

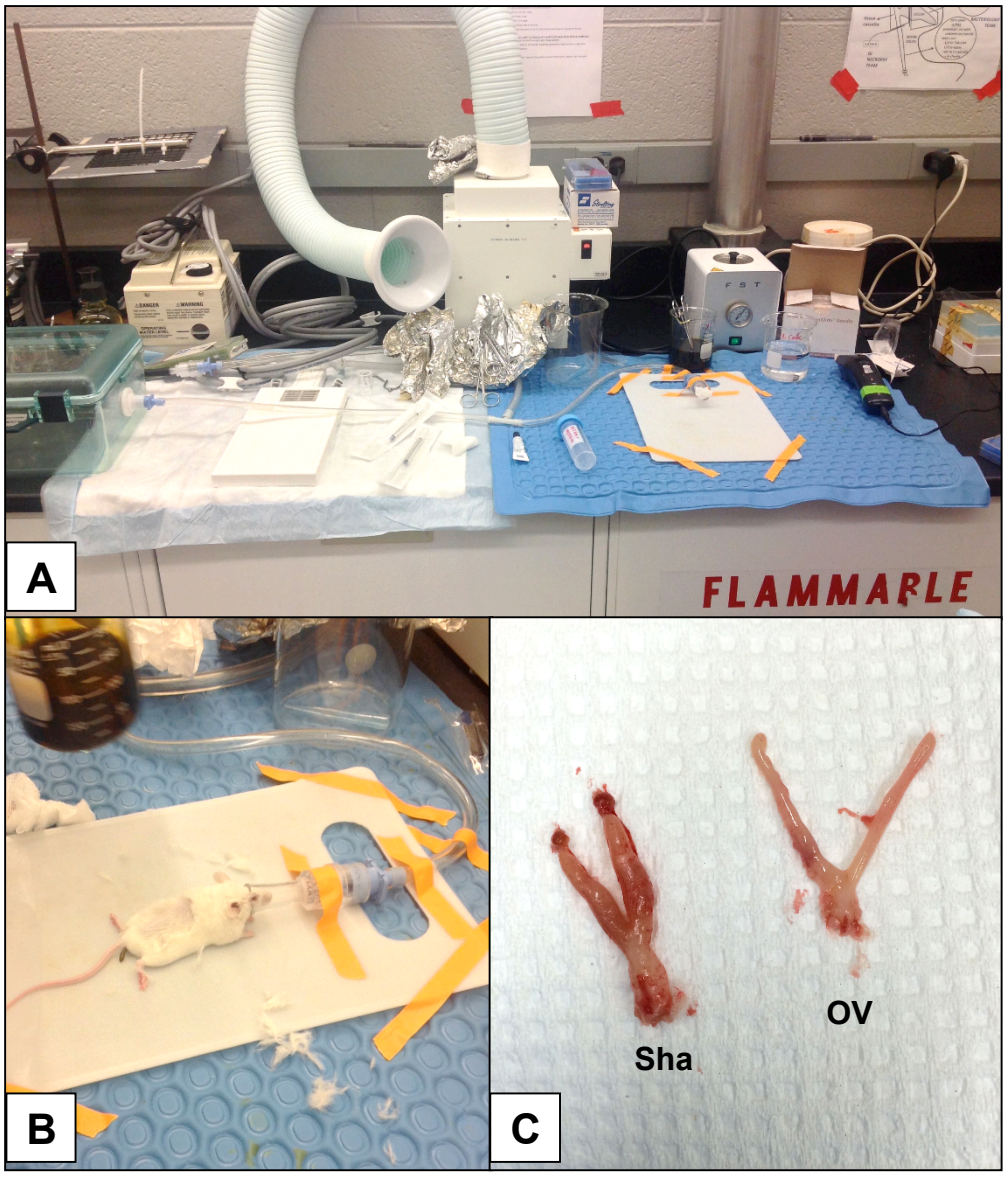

Figure 5.2 Number of rears over time. (A) Sham mice showed a constant decline over time, with a significant decrease in the mean between weeks 14 and 25. (B)

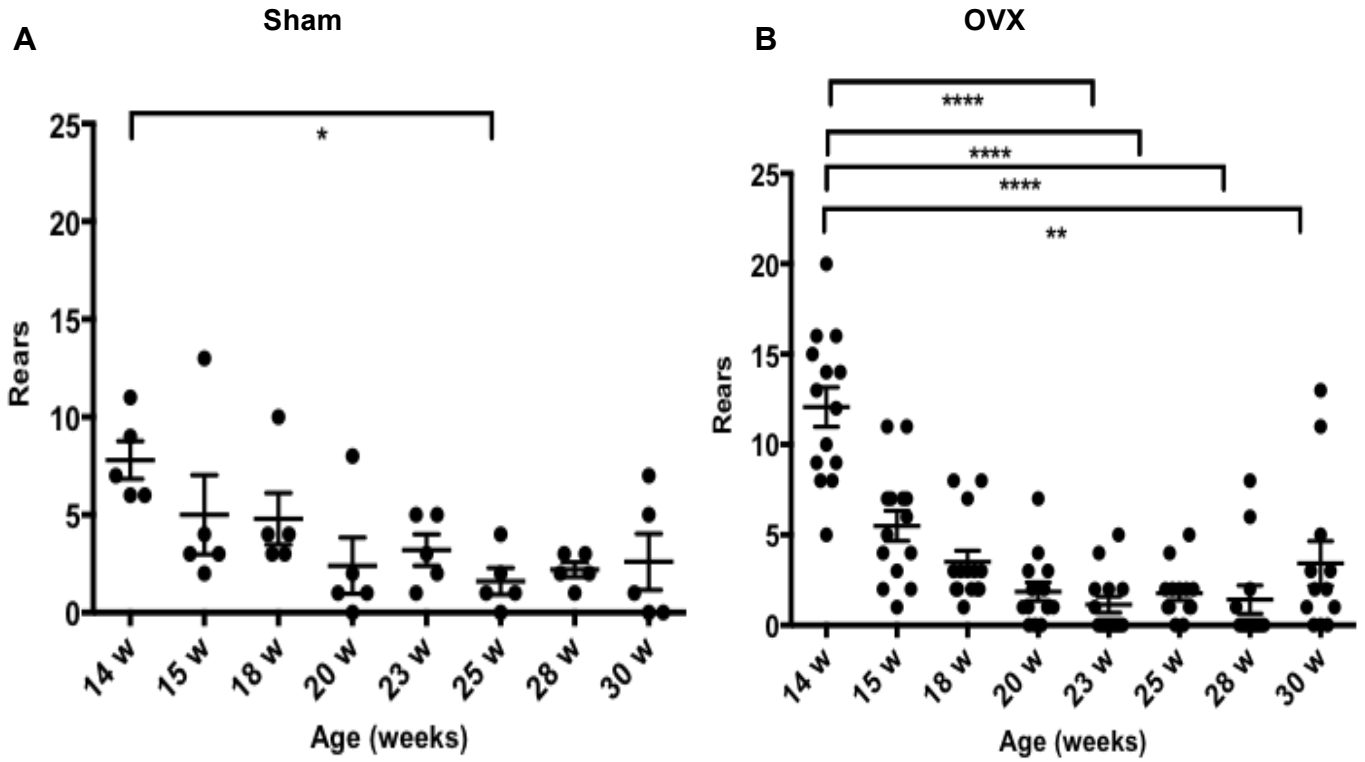

Figure 5.3 Rears at each time point, with comparisons between experimental groups. Time points before clinical disease onset (A-C). Time points at clinical disease onset (D-H). A significant difference between the means is present at 14 weeks (A) and 23 weeks (E).

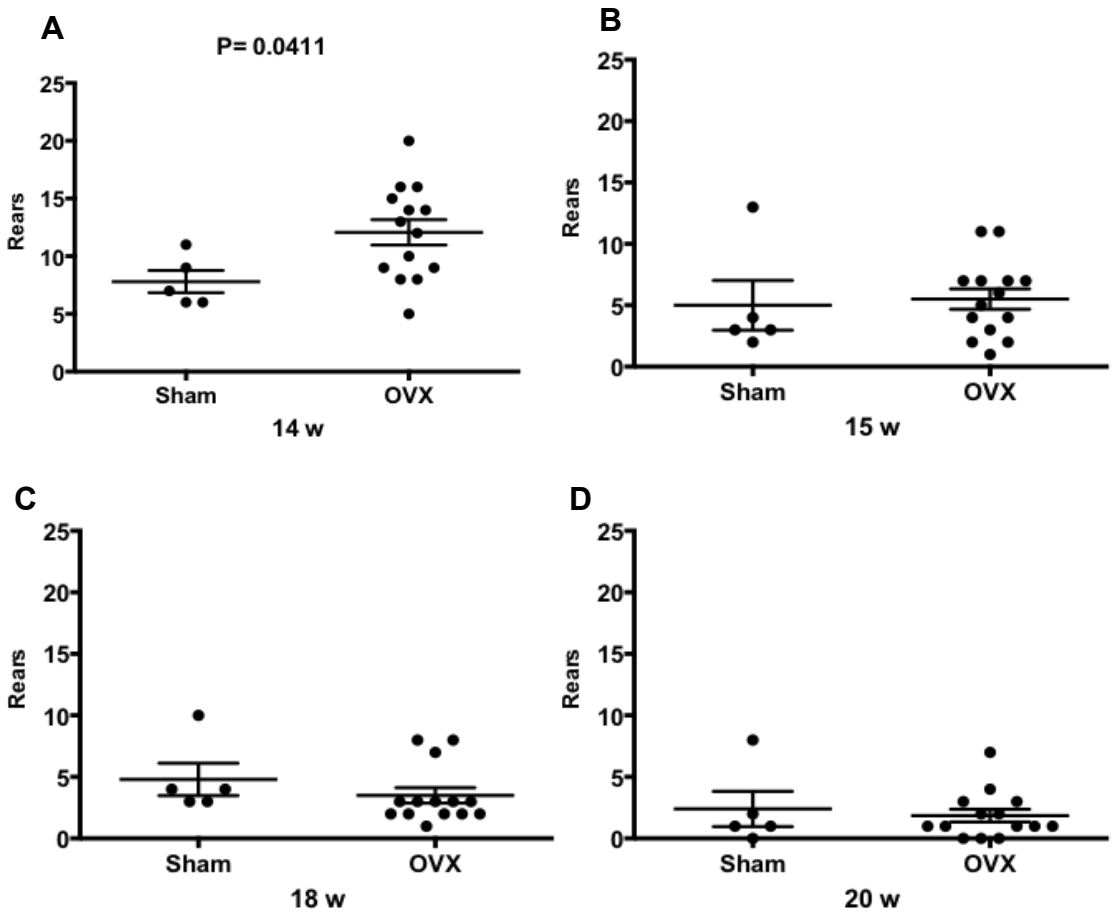

Figure 5.3 (cont'd)

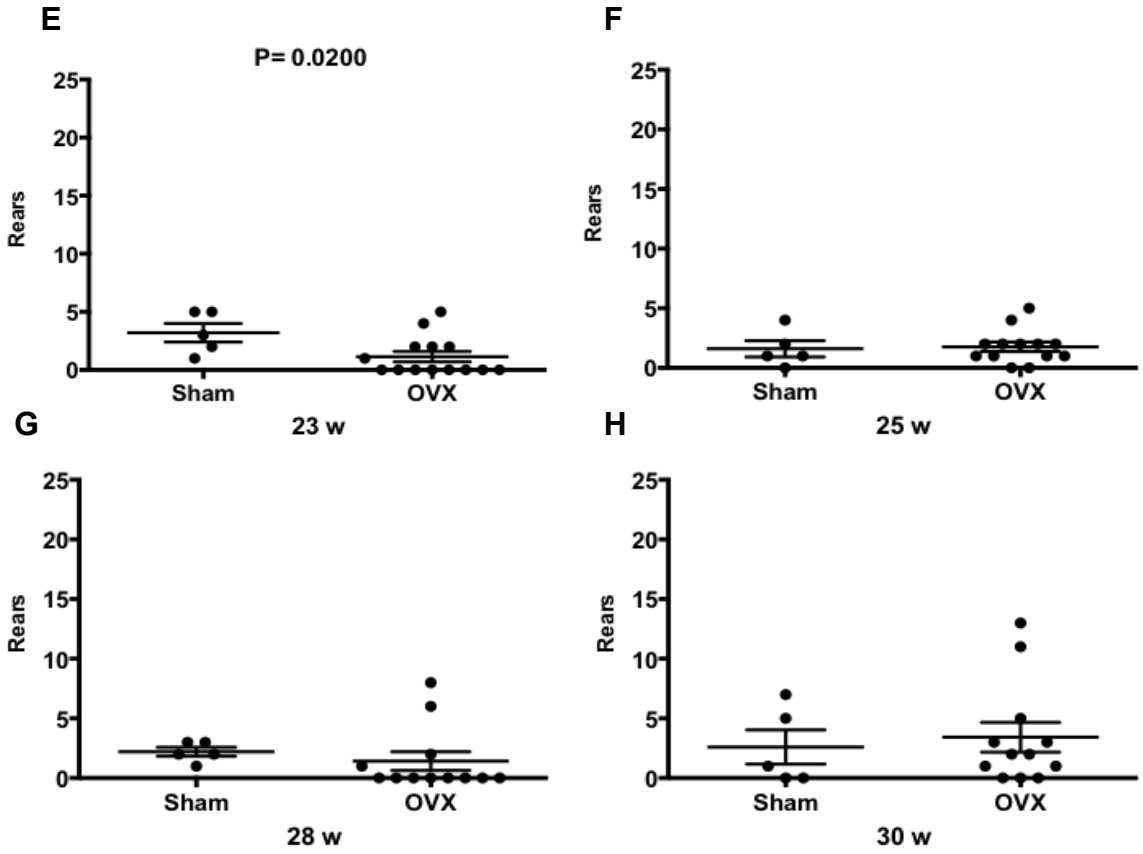

Figure 5.4 SAPP affected mouse clinical signs, the clasping reflex (A) and severe dyskinesia with twisted torso (B).

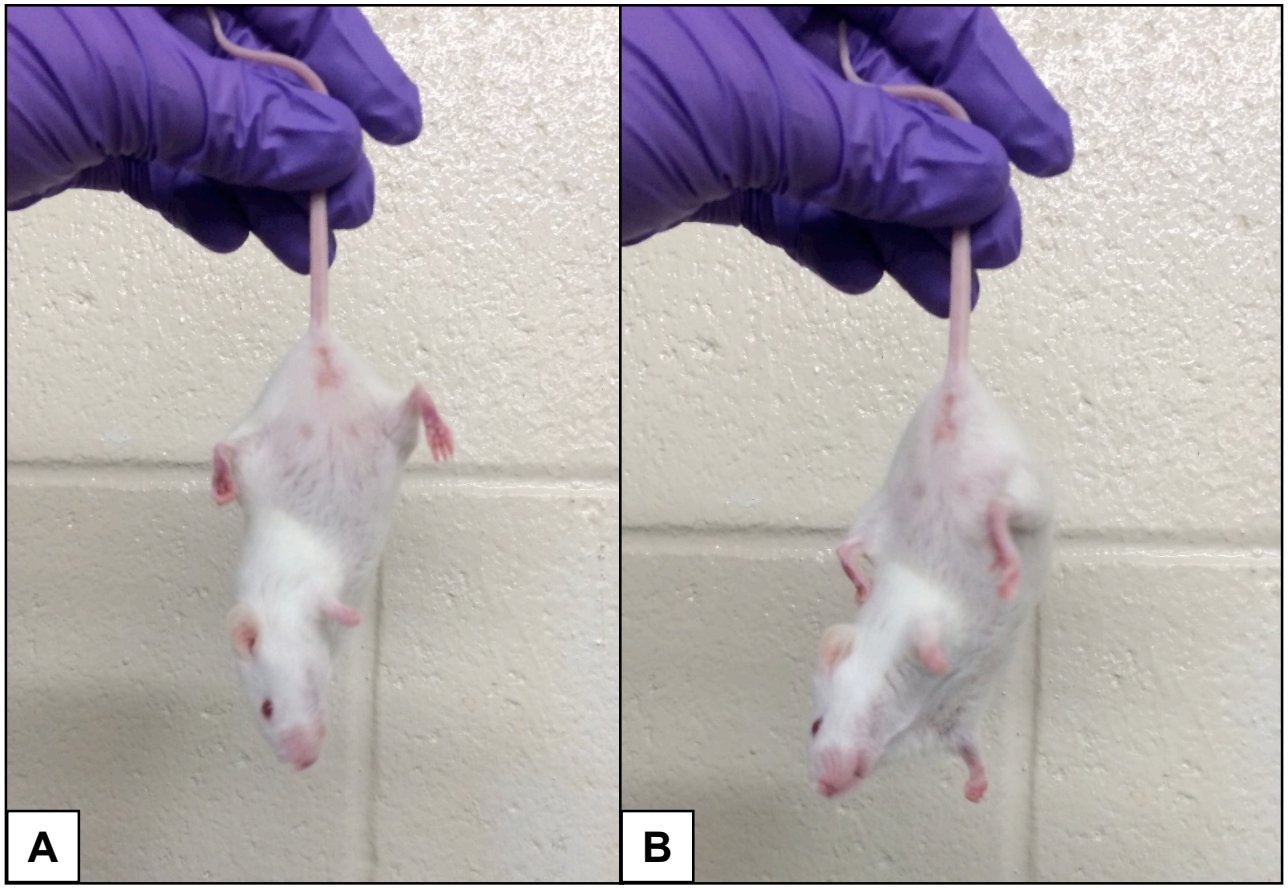

Figure 5.5 Dyskinesia at each time point, with comparisons between experimental groups. Time points before clinical disease onset (A-C). Time points at clinical disease onset (D-H). Note that dyskinesia was first seen at 20 weeks of age in the OVX mice (D) and not until 5 weeks later in the sham group (E).

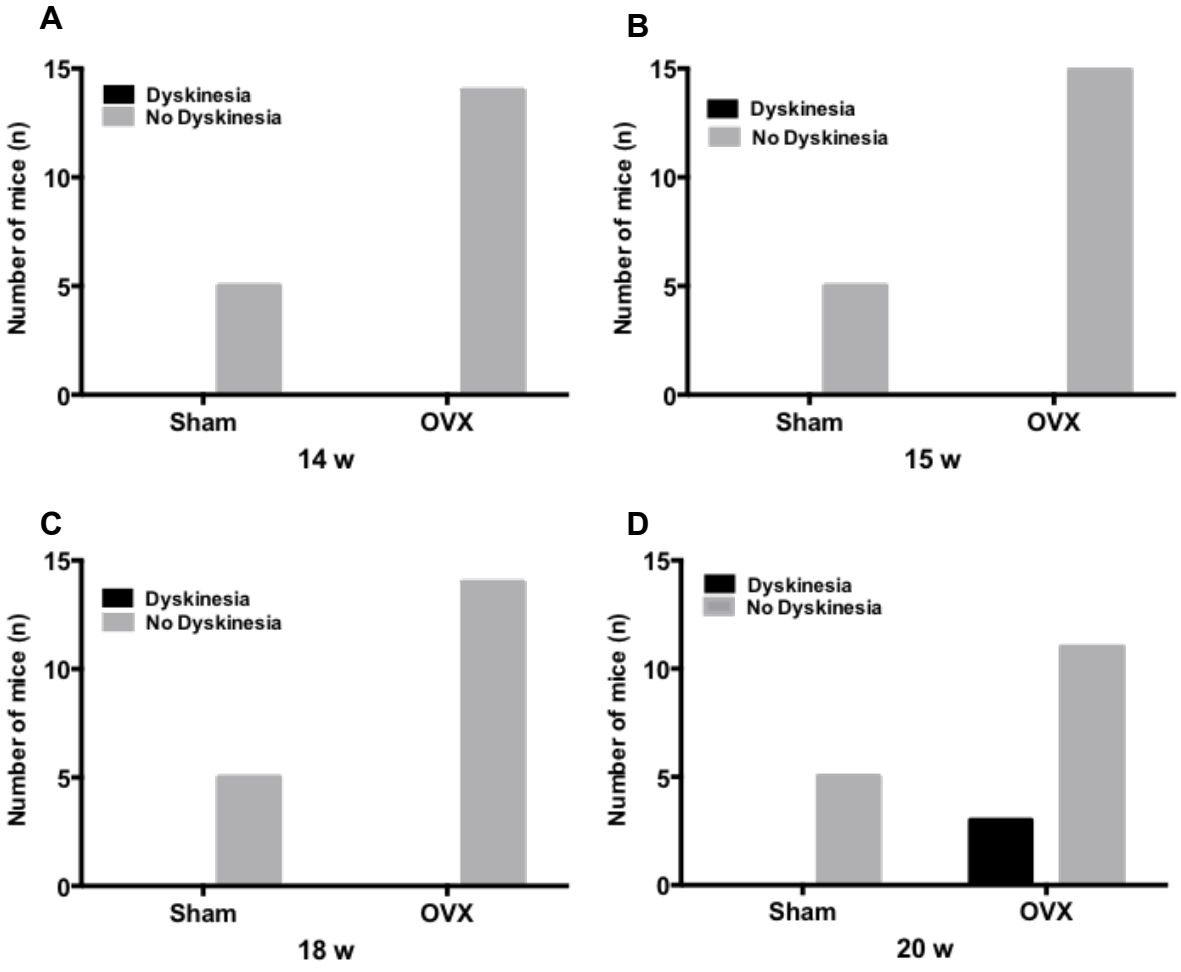

Figure 5.5 (cont'd)

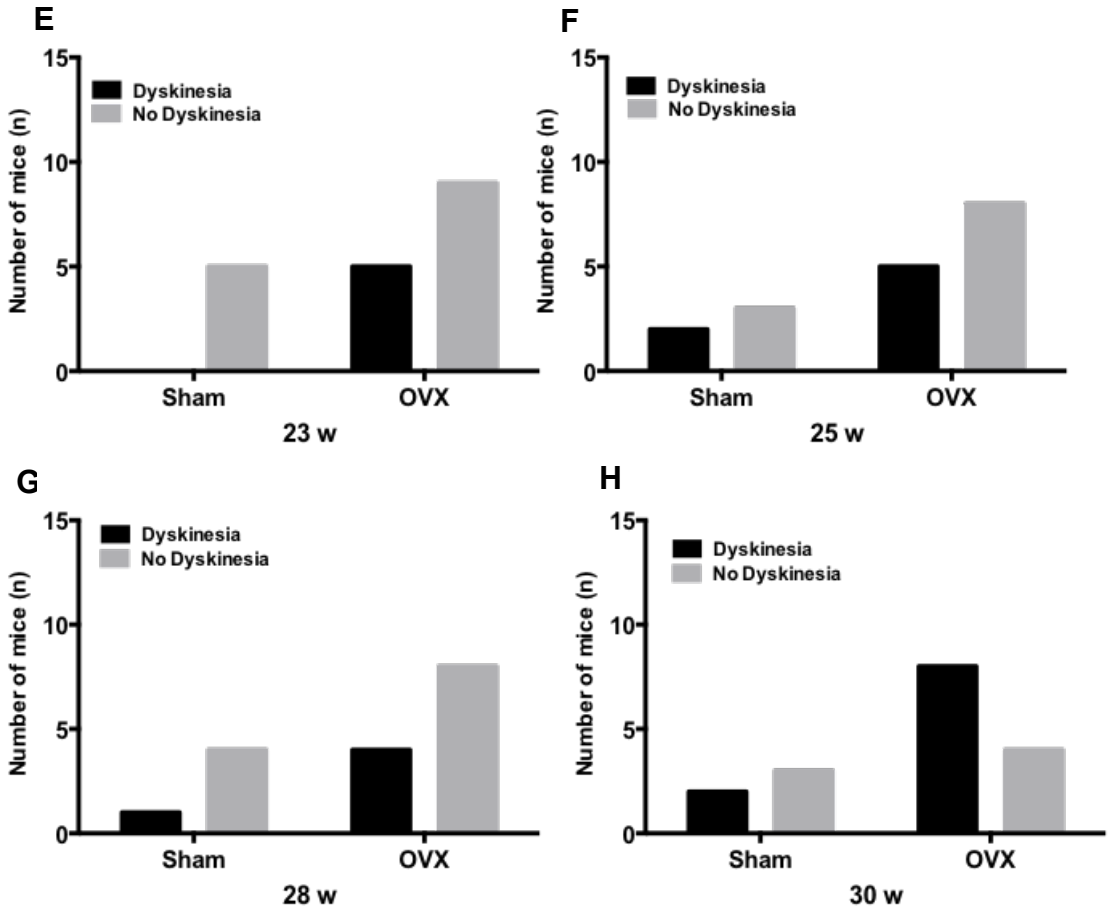

Figure 5.6 Evaluation of hind limb grip at each time point, with comparisons between experimental groups. Time points before clinical disease onset (A-C). Time points at clinical disease onset (D-H). Note that a grip deficit was first seen at 14 weeks of age in the OVX mice (A) and not until 25 weeks of age for sham mice (E). The majority of OVX mice had deficits at 25 and 28 weeks (E and F). All of the sham mice showed deficits at 30 weeks (G).

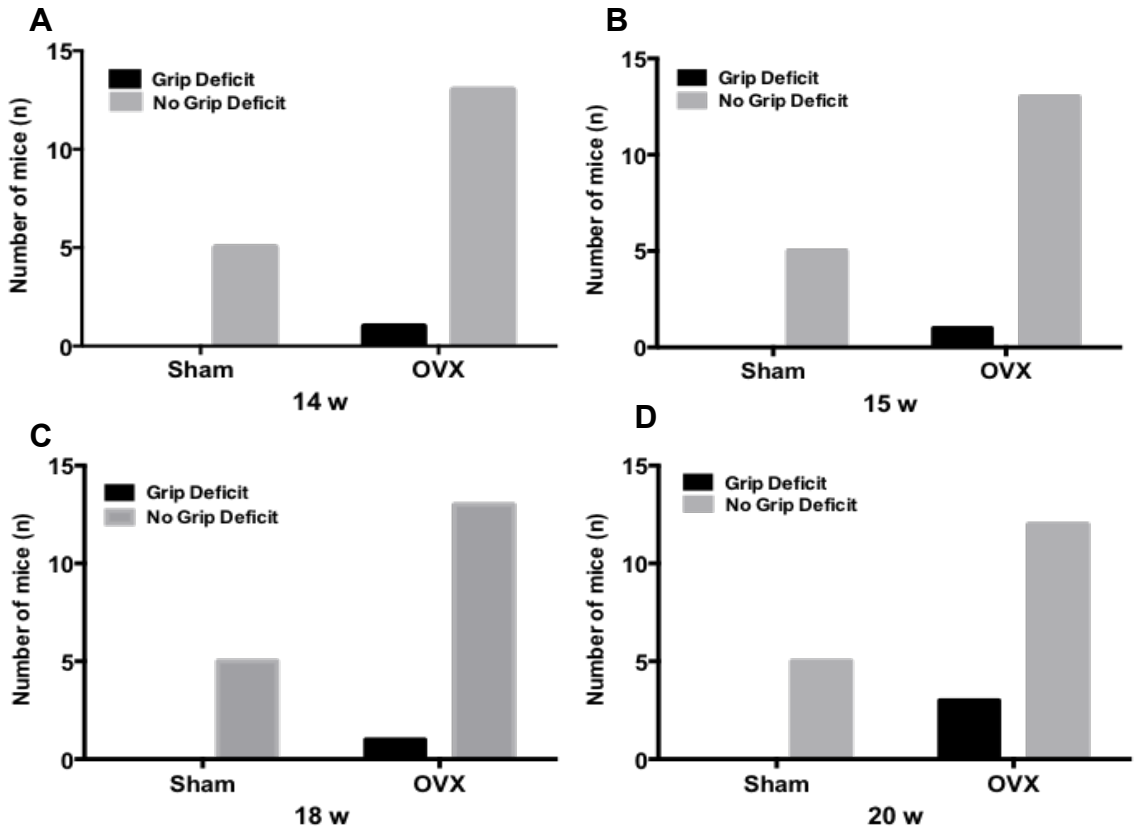

Figure 5.6 (cont'd)

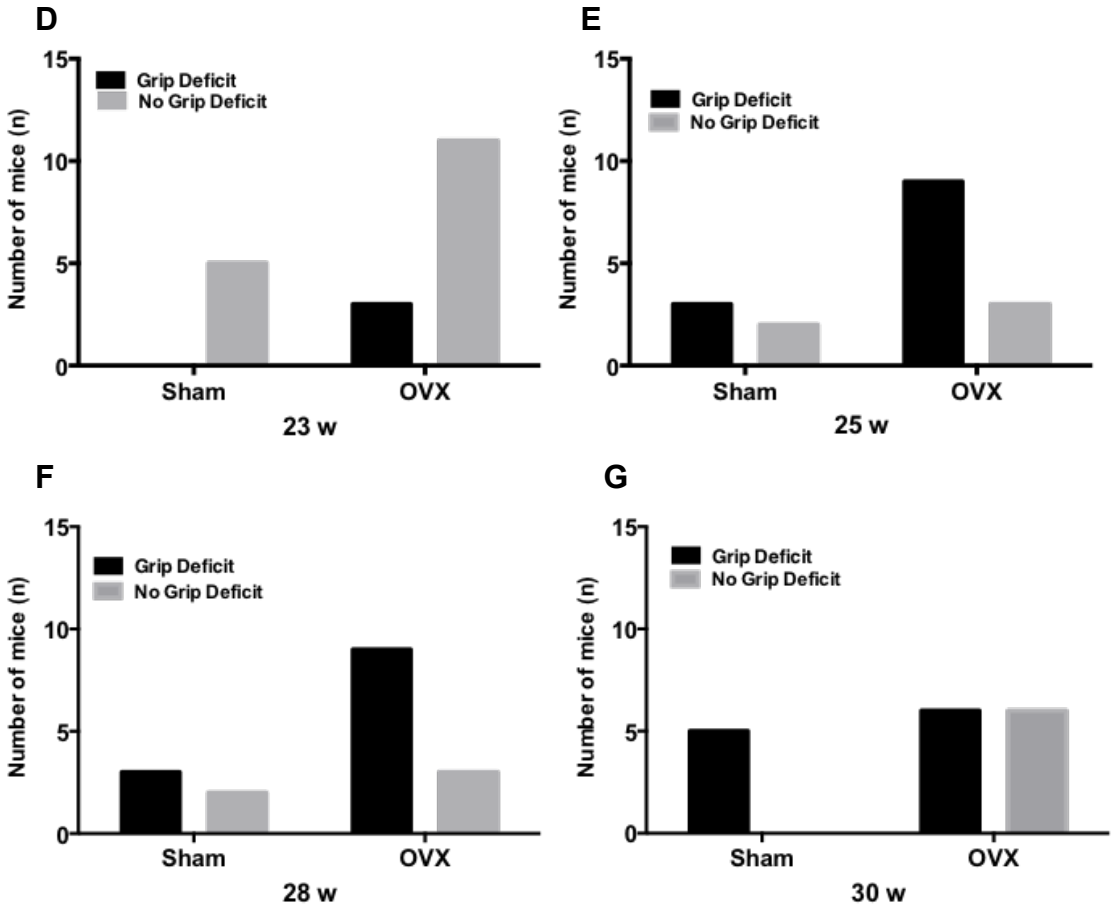

Figure 5.7 Evaluation of pain by facial grimace response at each time point, with comparisons between experimental groups. Time points before clinical disease onset (A-C). Time points at clinical disease onset (D-H). The grimace was first observed at 20 weeks of age in the OVX mice (D) and not until 28 weeks of age for sham mice (F).

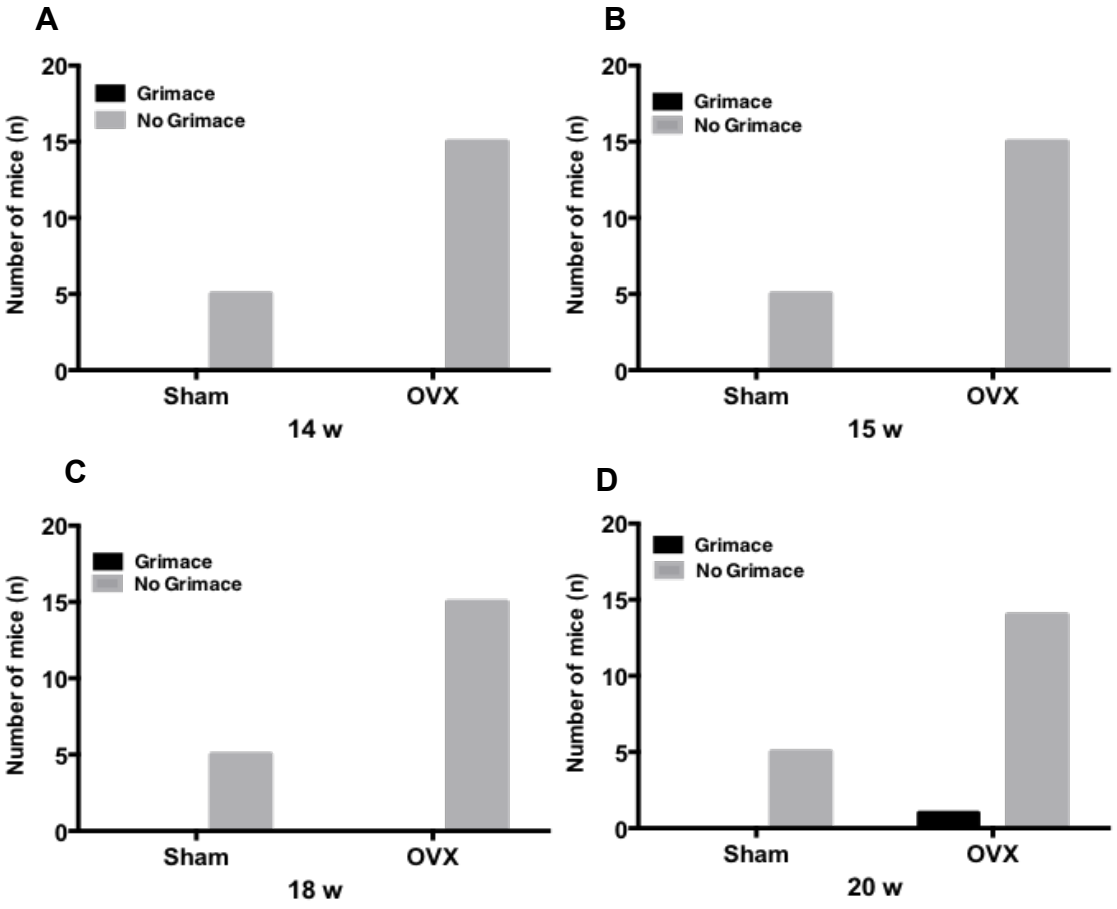

Figure 5.7 (cont'd)

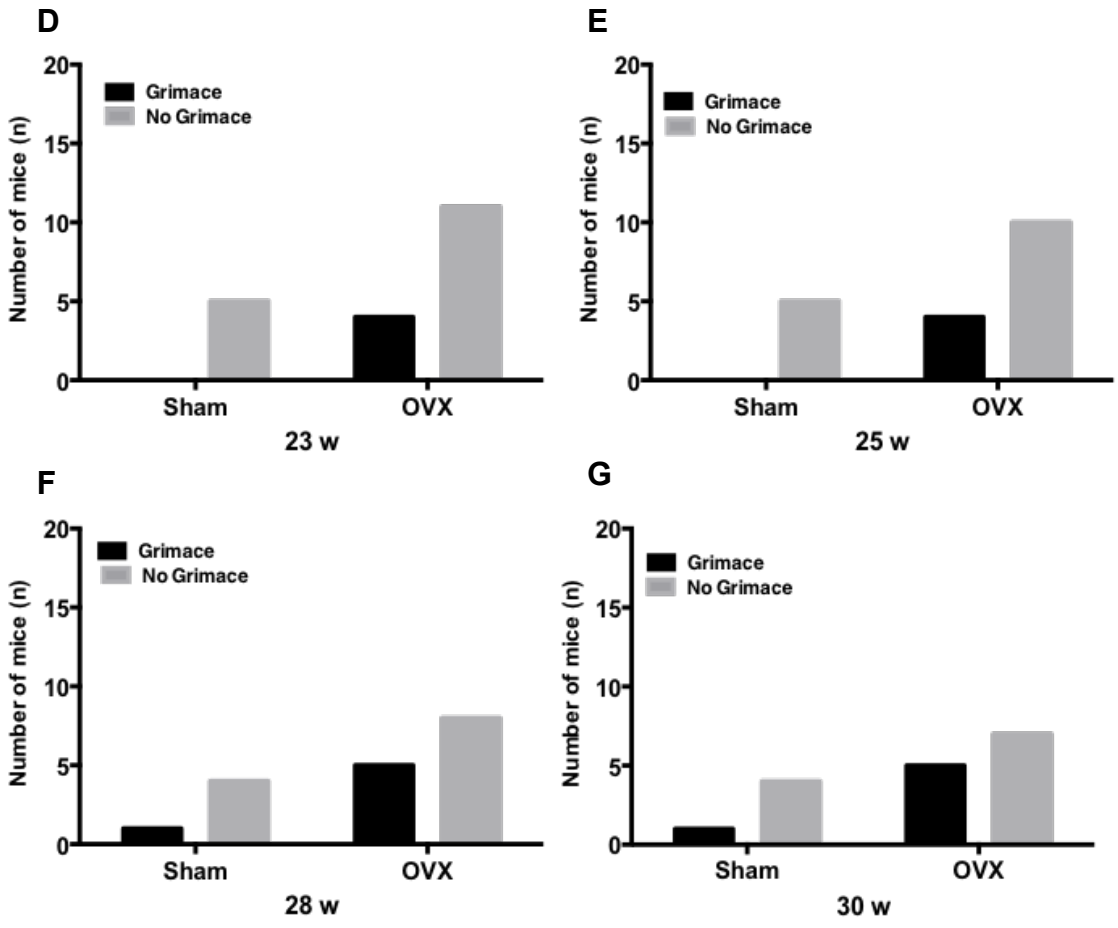

Figure 5.8 Heat map of combined phenotyping test results. Dyskinesia, grip test, and grimace are included. OVX mice are shaded in peach. Overall, they have more heavily blue shaded areas, which occur at earlier time points than for the sham mice.

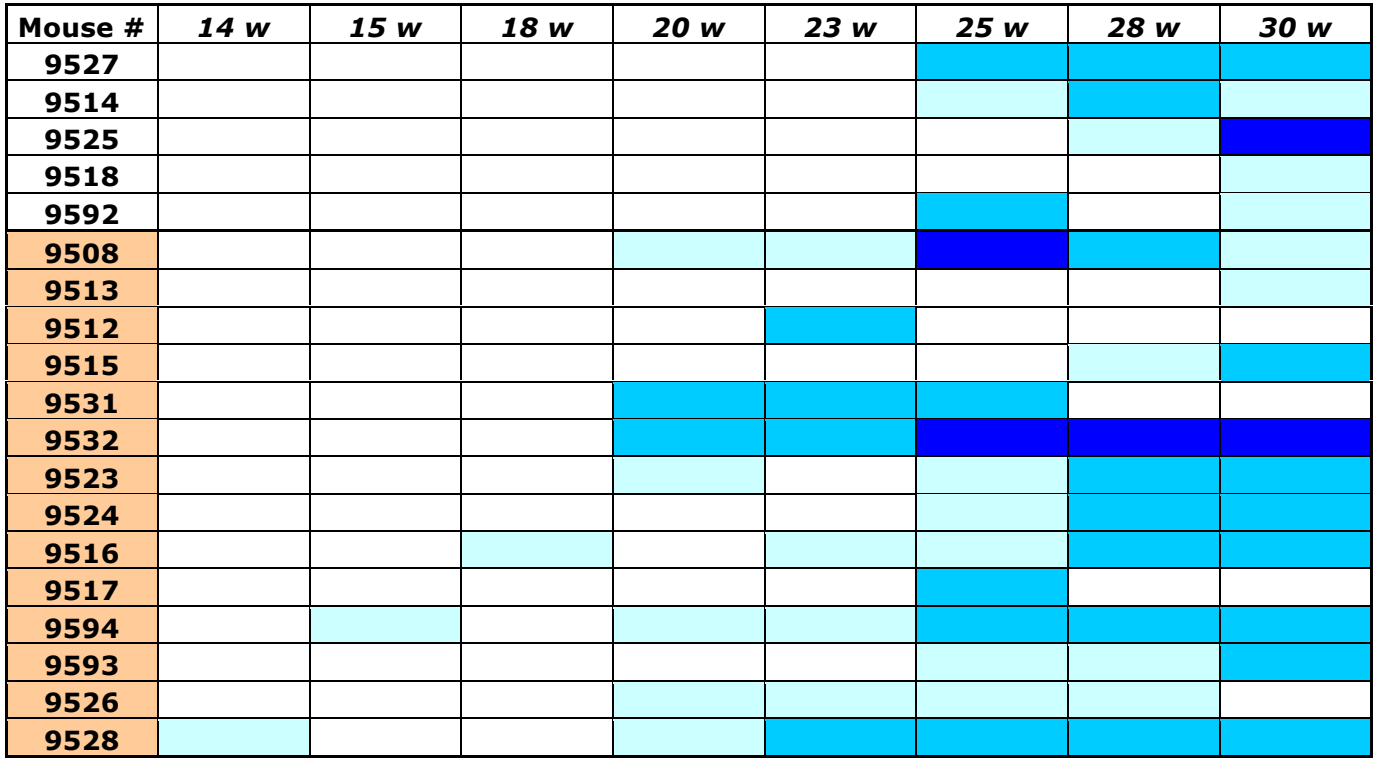

Color	# of signs
	1
	2
	3

Figure 5.9 Histopathology scores (A) Scatterplot of histopathological scores of the dorsal root ganglion, the sciatic nerve, and the brachial plexus. Note the trend toward increased histo scores in the sham treated mice. At the conclusion of the study, four OVX mice did not have any inflammation in the peripheral nerve. Testosterone plasma concentrations. OVX mice have a trend toward higher testosterone levels than sham treated mice (B).

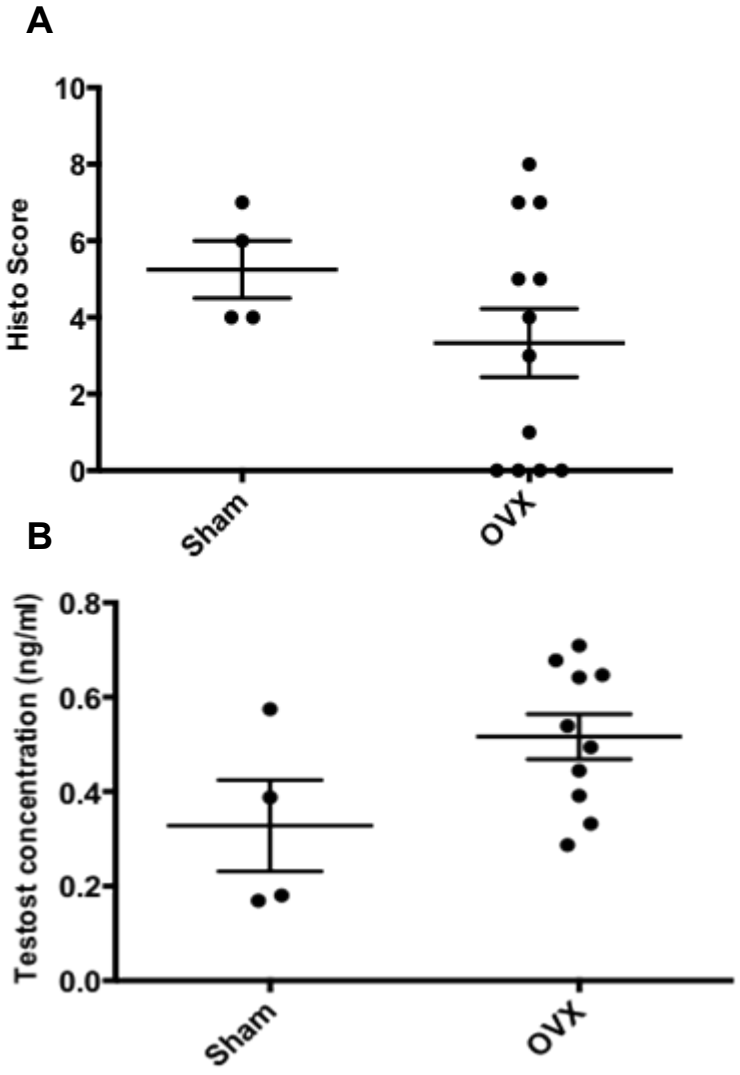

Figure 5.10 Number of rears over time. Both sham (A) and treated (B) mice showed a constant decline over time, being active at the beginning of the study and decreasing as the experiment progressed.

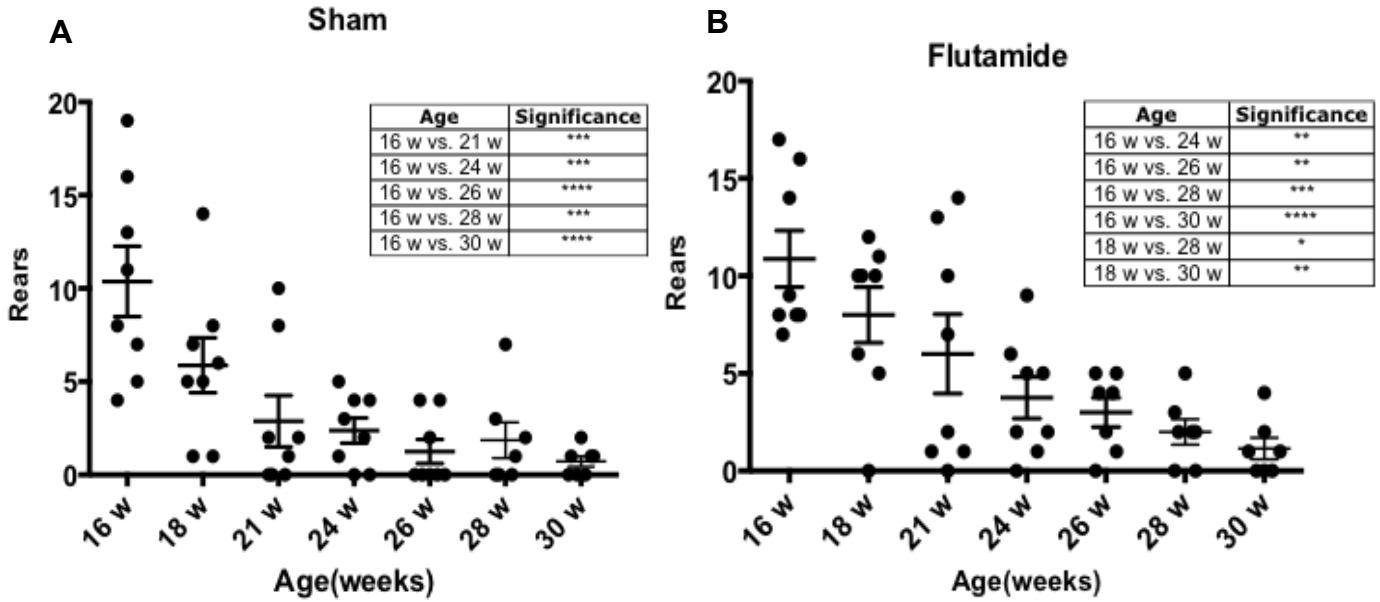

Figure 5.11 Rears at each time point, with comparisons between experimental groups. There is no significant difference between the means; however, at 18 weeks (B) and 21 weeks of age (C), Flutamide treated mice have a trend toward increased rears.

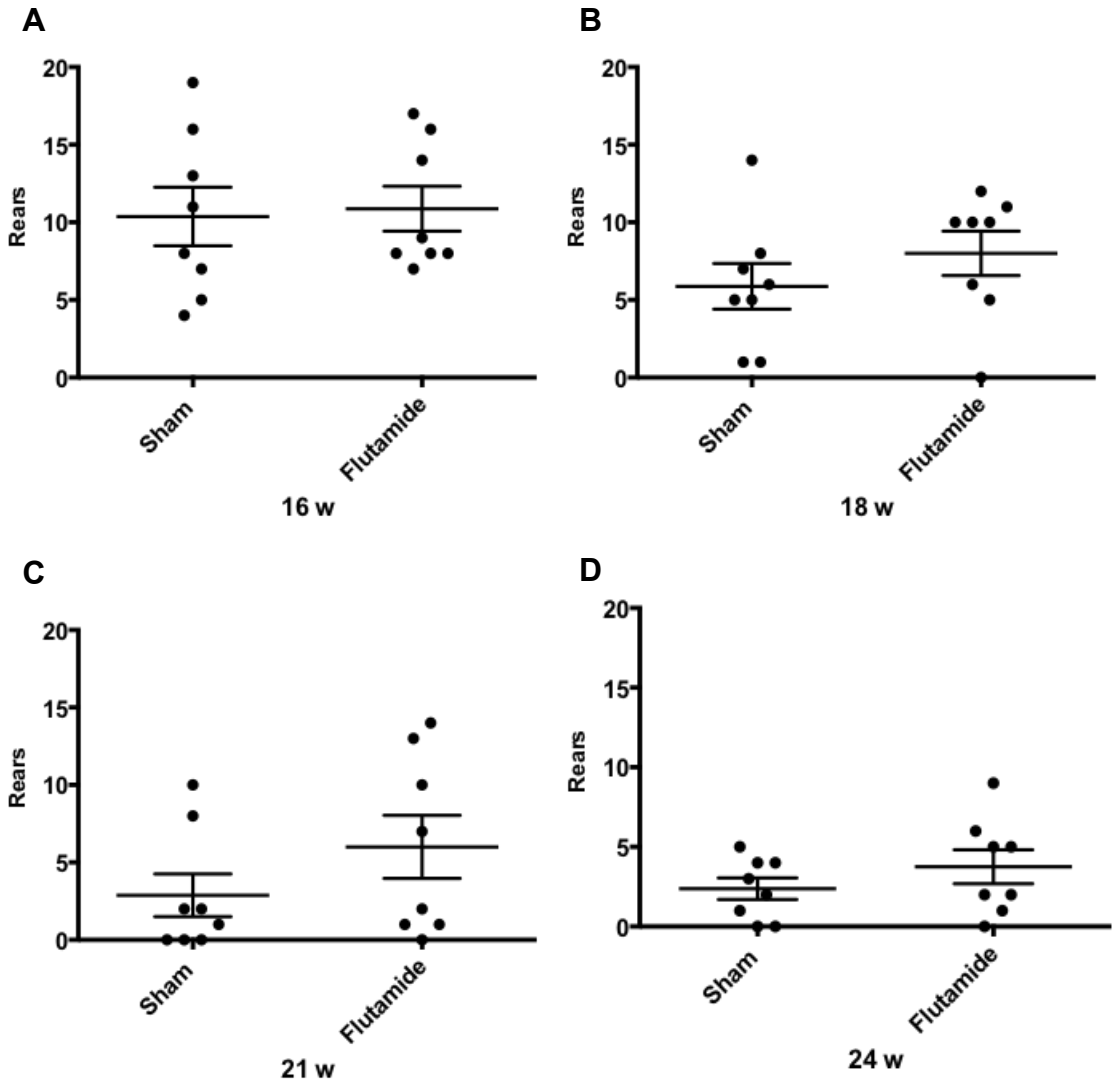

Figure 5.11 (cont'd)

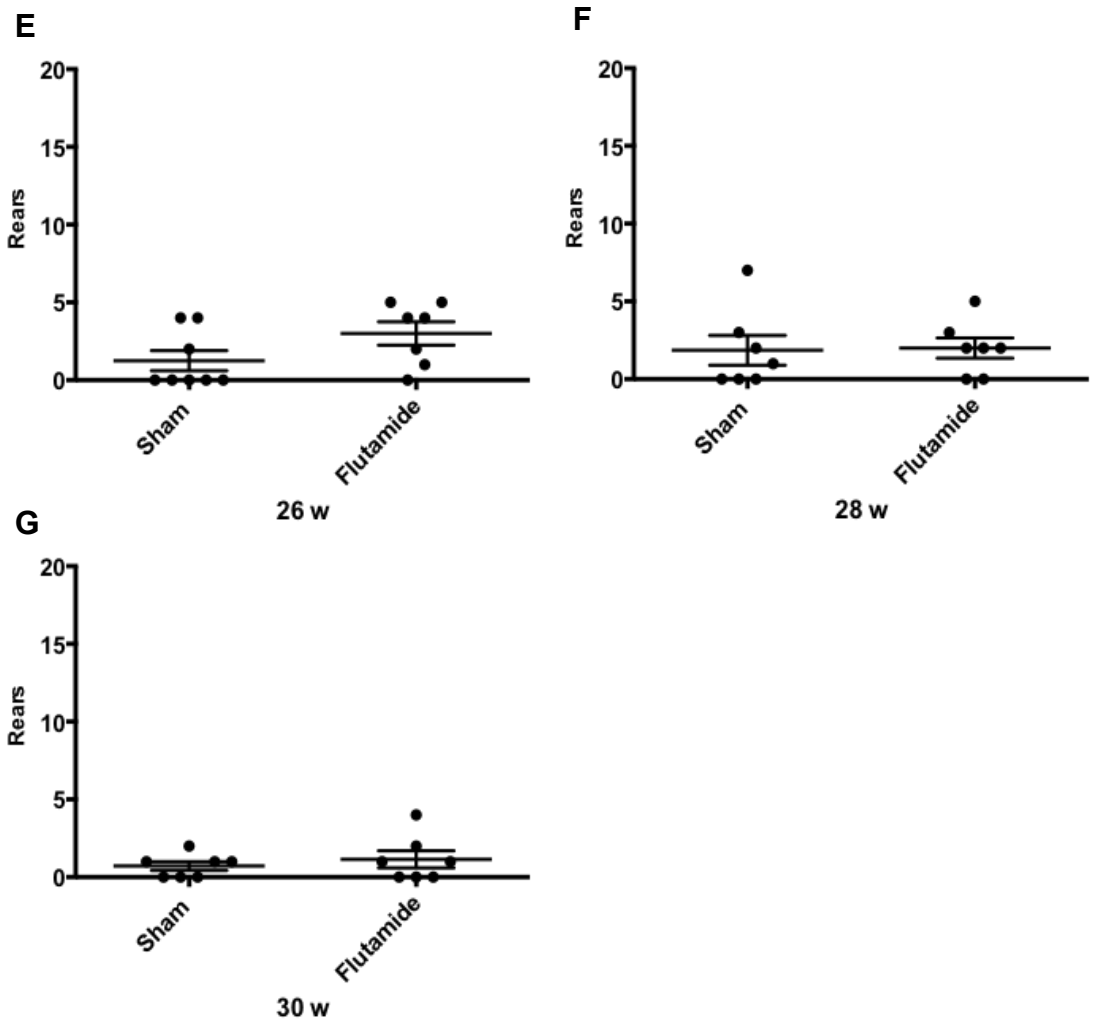

Figure 5.12 Dyskinesia at each time point, with comparisons between experimental groups. Dyskinesia was first seen at 21 weeks of age in the sham injected mice (D) and not until 26 weeks later in the Flutamide treated group (E).

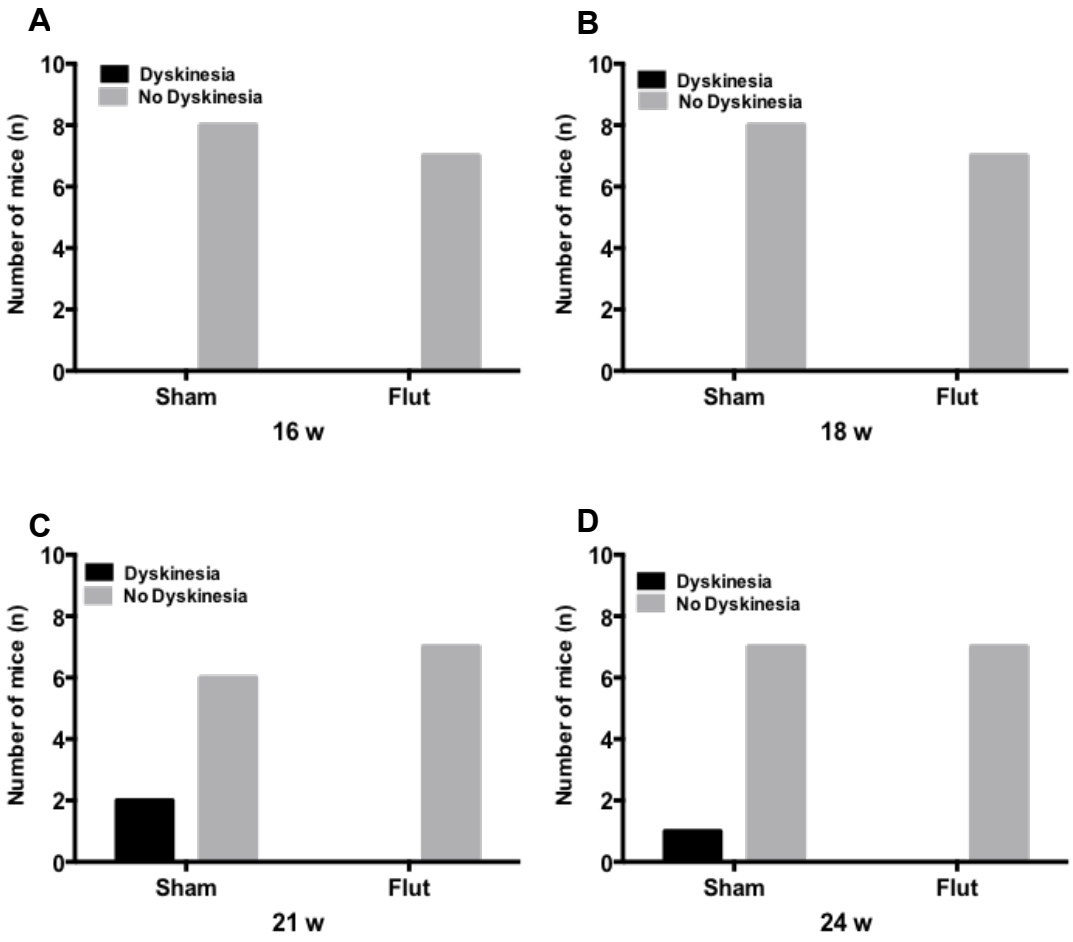

Figure 5.12 (cont'd)

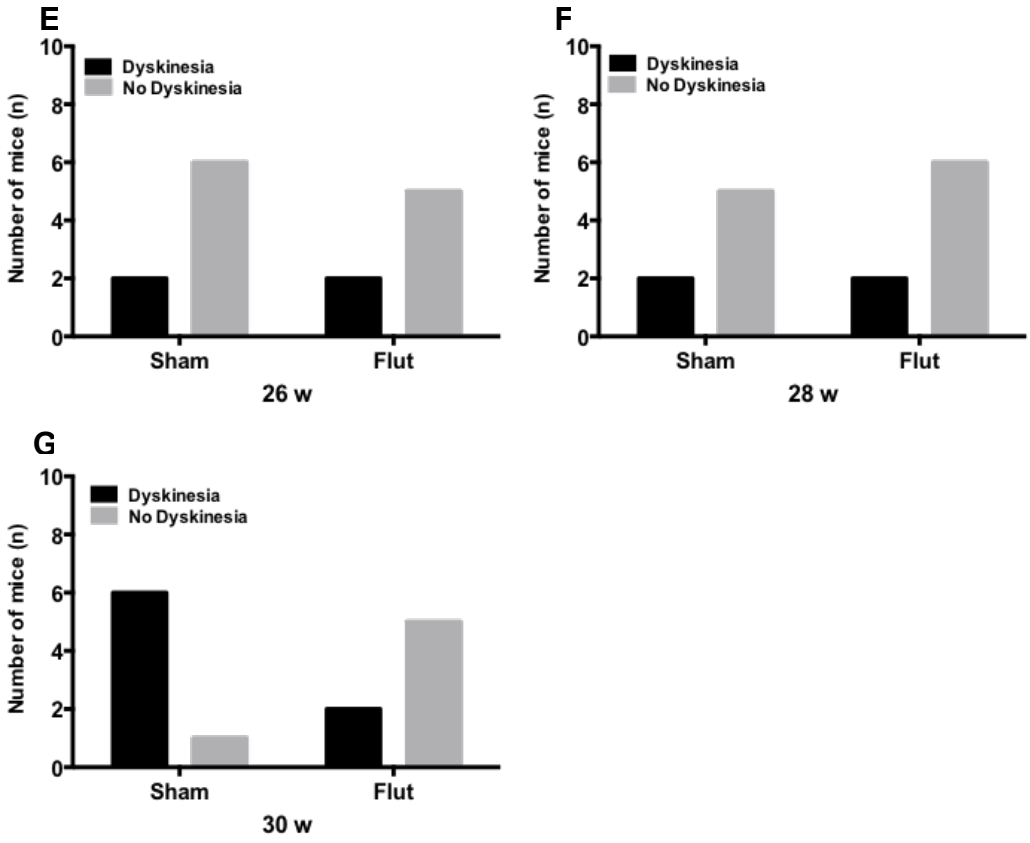

Figure 5.13 Hind limb grip at each time point, with comparisons between experimental groups. The grip deficit was first seen at 21 weeks of age in the sham mice (C) and 24 weeks of age for Flutamide treated mice (D). At 26 weeks, 100% of sham mice had grip deficits (E). At 28 weeks, 86% of the Flutamide treated mice had deficits (F).

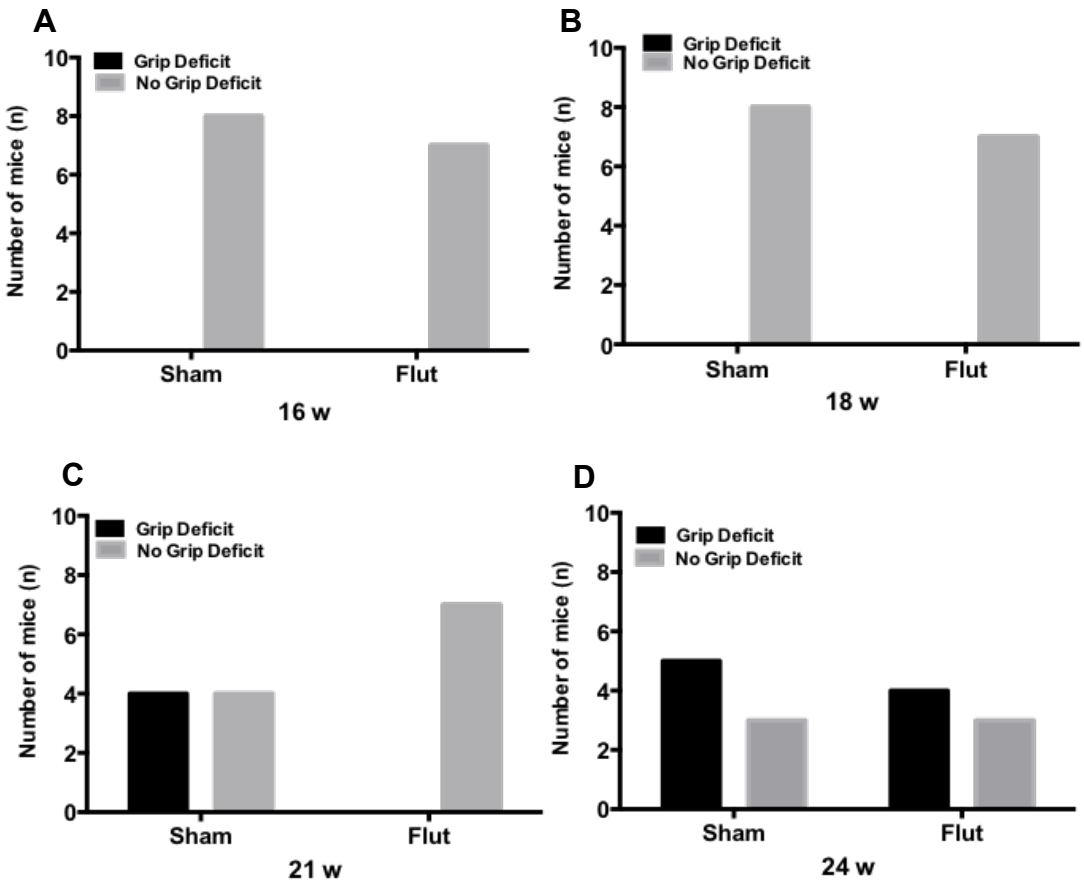

Figure 5.13 (cont'd)

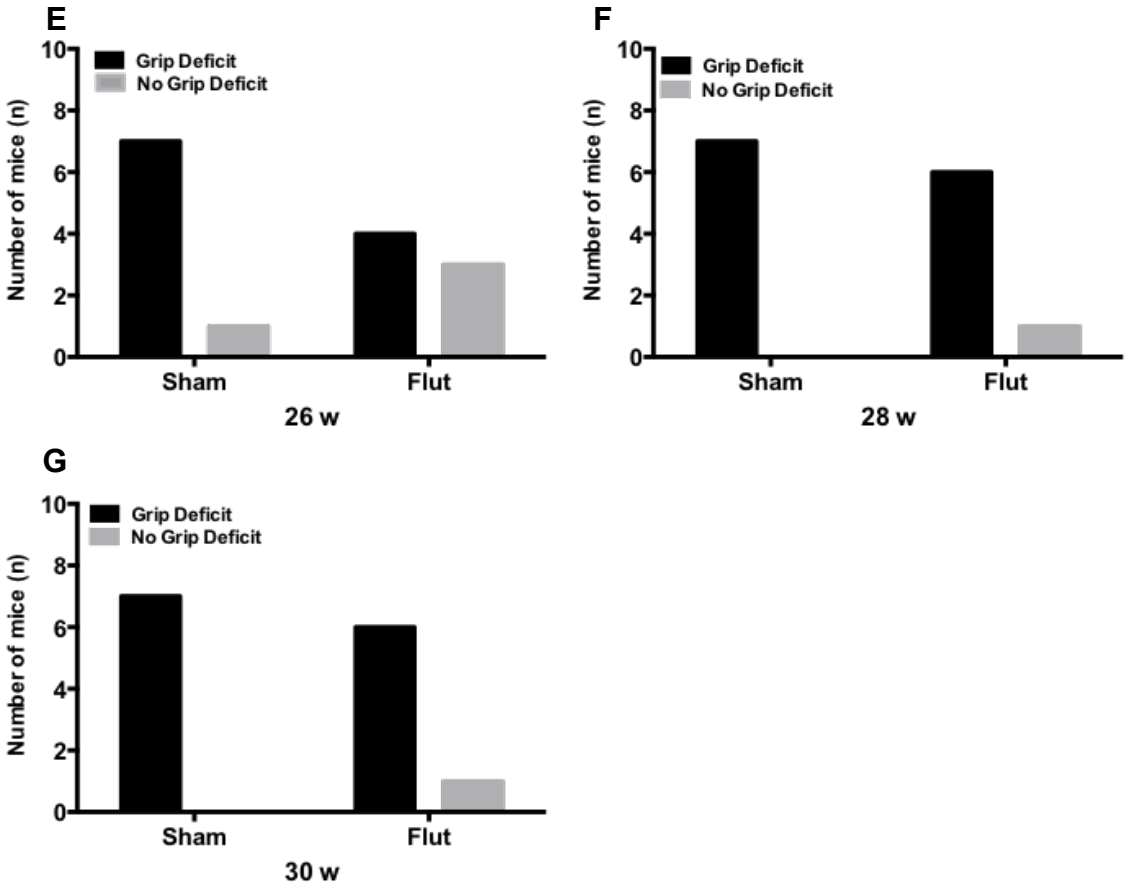

Figure 5.14 Facial grimace response at each time point, with comparisons between experimental groups. The grimace was first seen at 21 weeks of age in the sham injected mice (D) and at 24 weeks of age in the weeks in the Flutamide treated mice (F).

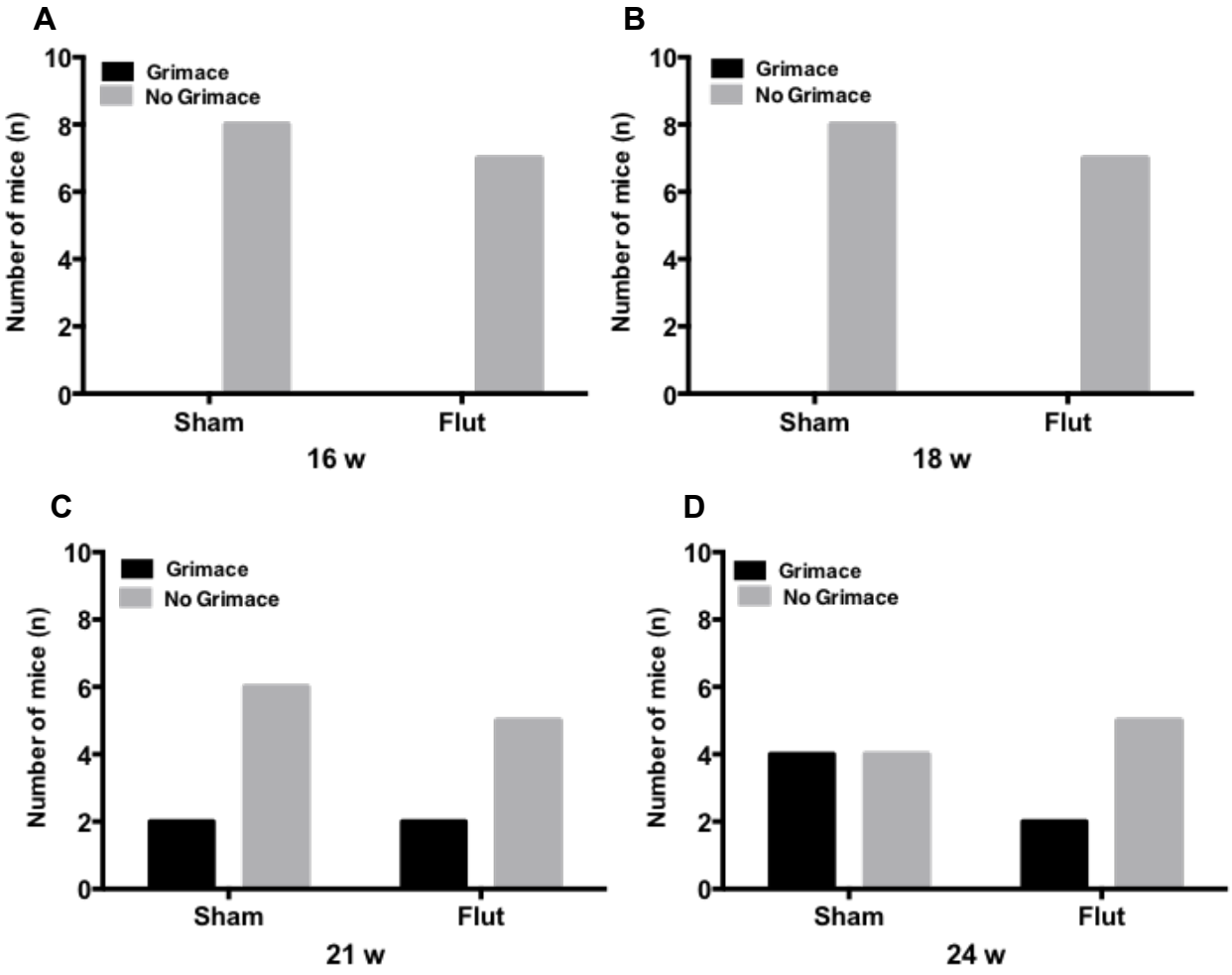

Figure 5.14 (cont'd)

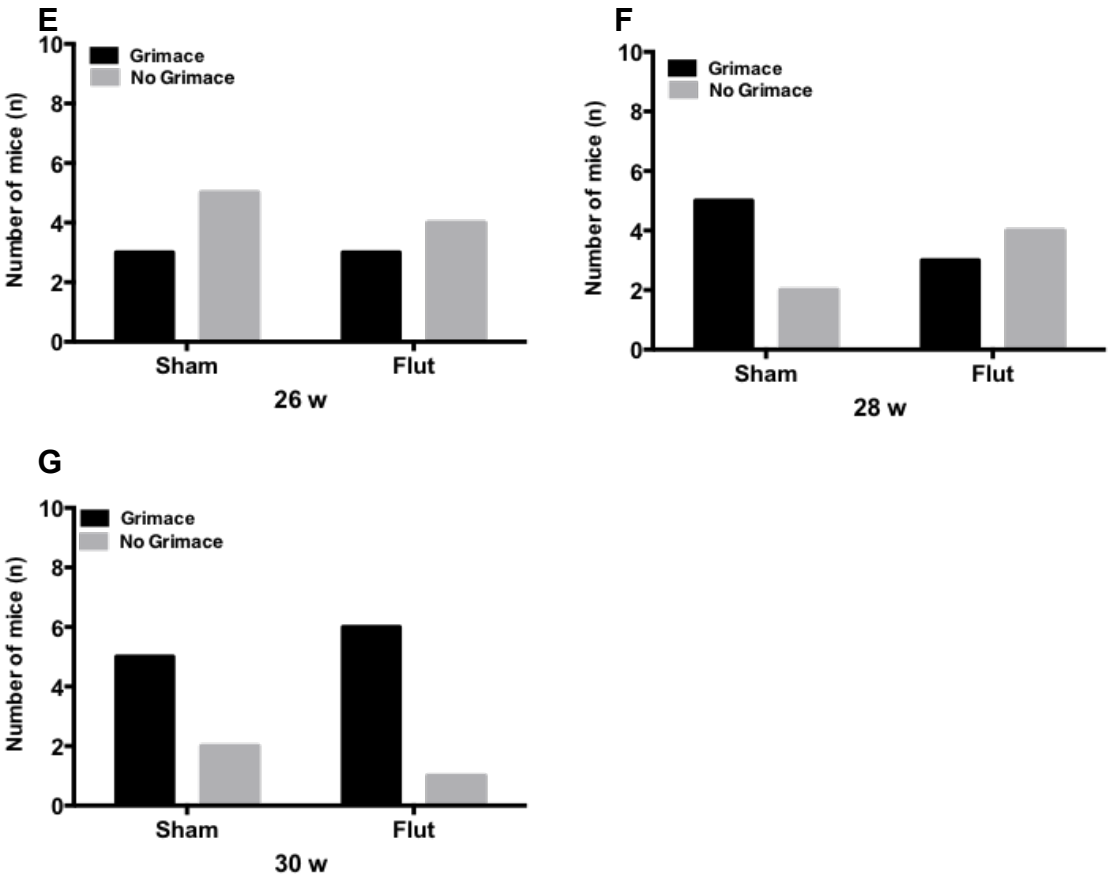

Figure 5.15 Paw licking at each time point, with comparisons between experimental groups. It was first seen at 16 weeks of age in the sham injected mice (A) and at 21 weeks of age in the weeks in the Flutamide treated mice (F).

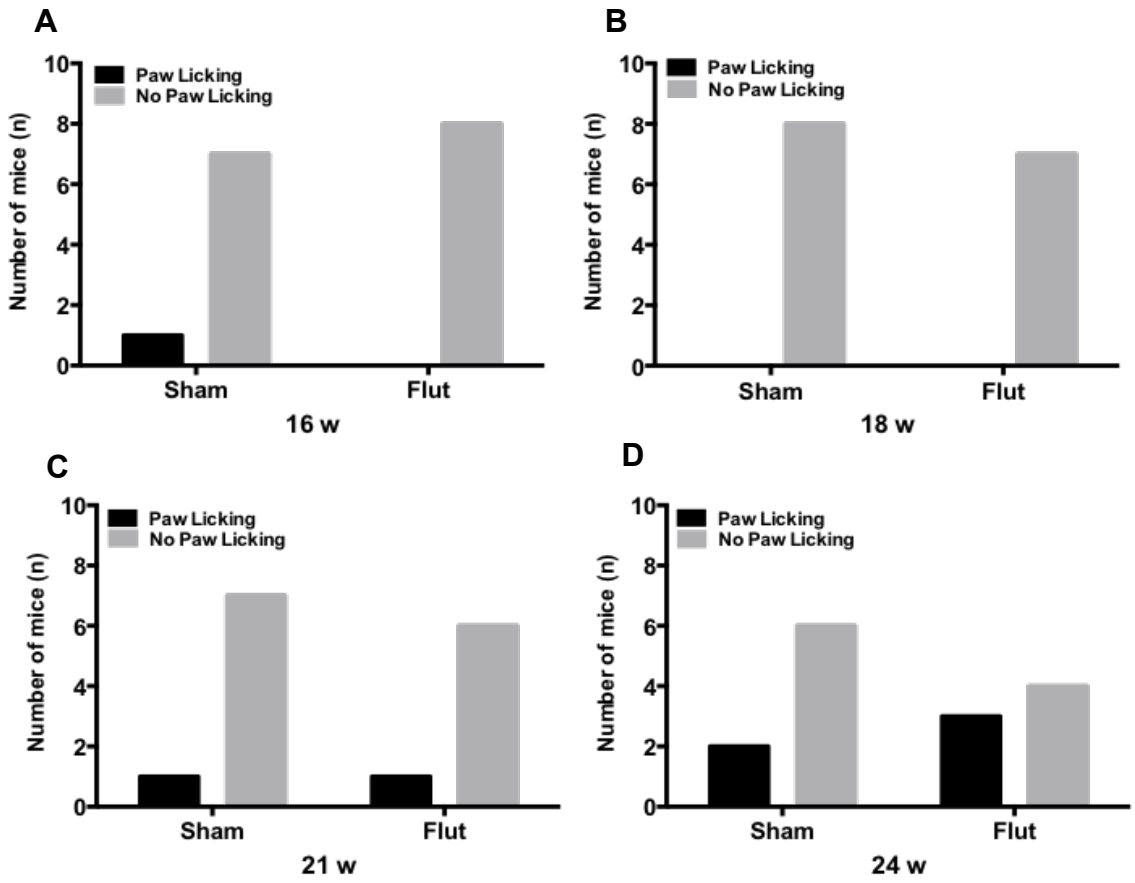

Figure 5.15 (cont'd)

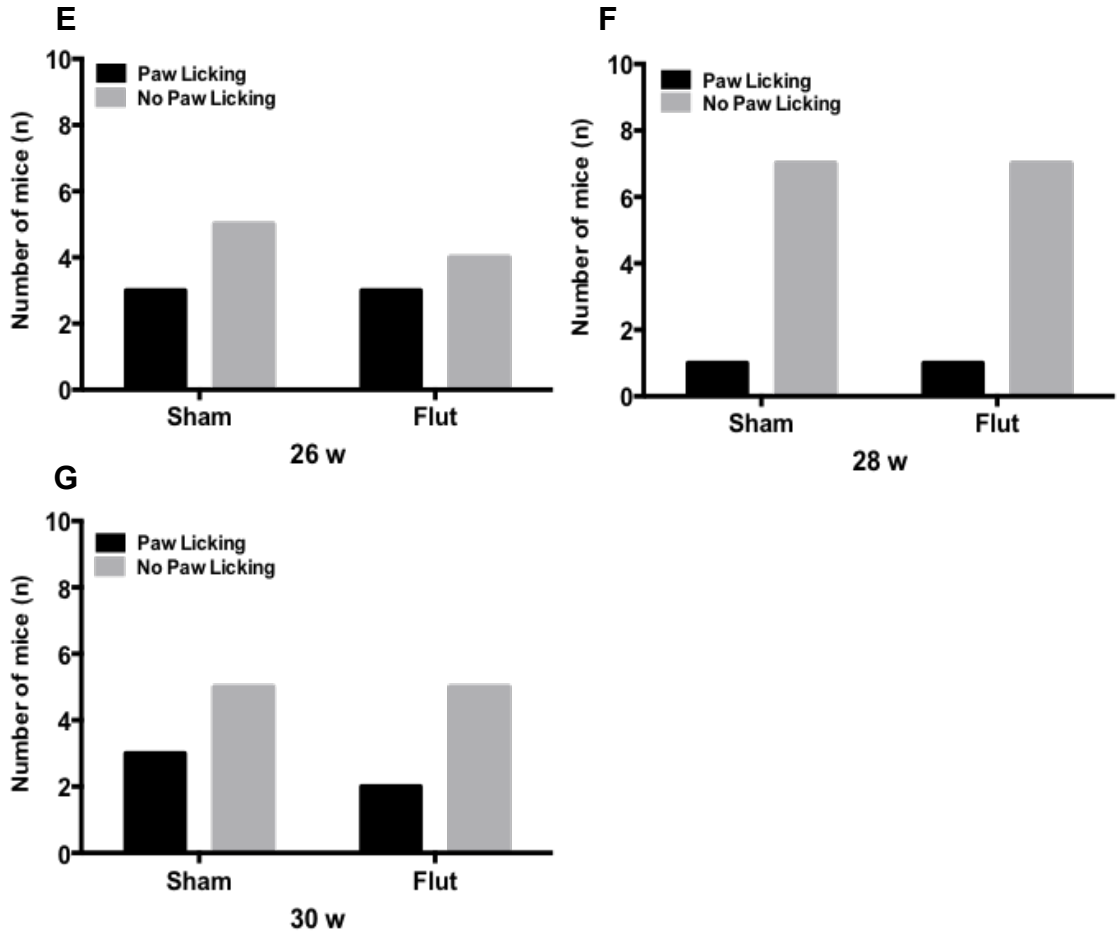

Figure 5.16 Heat map of combined phenotyping test results. Dyskinesia, grip test, grimace, and paw licking are included. Flutamide treated mice are shaded in light blue. The black shaded boxes denote mice that were humanely euthanized.

Mouse #	*16 w*	*18 w*	*21 w*	*24 w*	*26 w*	*28 w*	*30 w*
9505							
9510							
9507							
9519							
9588							
9521							
9590							
9530							
9506							
9509							
9511							
9520							
9522							
9589							
9529							

Color	# of signs
	1
	2
	3
	4

Figure 5.17 Histopathology and Estradiol of Flutamide treated males. (A) Histopathology (B) Estradiol

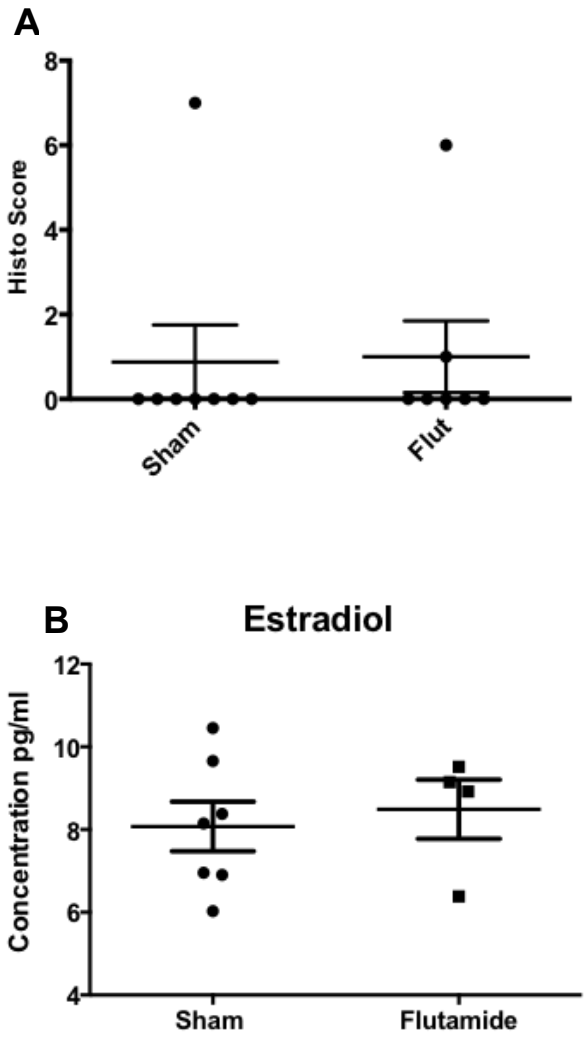

BIBLIOGRAPHY

BIBLIOGRAPHY

1. **Salomon B, Rhee L, Bour-Jordan H, Hsin H, Montag A, Soliven B, Arcella J, Girvin AM, Padilla J, Miller SD, Bluestone JA.** 2001. Development of spontaneous autoimmune peripheral polyneuropathy in B7-2-deficient NOD mice. The Journal of experimental medicine **194:**677-684.

2. **Markle JG, Frank DN, Mortin-Toth S, Robertson CE, Feazel LM, Rolle-Kampczyk U, von Bergen M, McCoy KD, Macpherson AJ, Danska JS.** 2013. Sex differences in the gut microbiome drive hormone-dependent regulation of autoimmunity. Science **339:**1084-1088.

3. **Gonzalez DA, Diaz BB, Rodriguez Perez Mdel C, Hernandez AG, Chico BN, de Leon AC.** 2010. Sex hormones and autoimmunity. Immunol Lett **133:**6-13.

4. **Siiteri PK, Jones LA, Roubinian J, Talal N.** 1980. Sex steroids and the immune system--I. Sex difference in autoimmune disease in NZB/NZW hybrid mice. J Steroid Biochem **12:**425-432.

5. **Zandman-Goddard G, Peeva E, Shoenfeld Y.** 2007. Gender and autoimmunity. Autoimmun Rev **6:**366-372.

6. **Brooks SP, Dunnett SB.** 2009. Tests to assess motor phenotype in mice: a user's guide. Nature reviews Neuroscience **10:**519-529.

7. **Langford DJ, Bailey AL, Chanda ML, Clarke SE, Drummond TE, Echols S, Glick S, Ingrao J, Klassen-Ross T, Lacroix-Fralish ML, Matsumiya L, Sorge RE, Sotocinal SG, Tabaka JM, Wong D, van den Maagdenberg AM, Ferrari MD, Craig KD, Mogil JS.** 2010. Coding of facial expressions of pain in the laboratory mouse. Nat Methods **7:**447-449.

8. **Bordon Y.** 2015. Neuroimmunology: A painful difference between the sexes. Nat Rev Immunol **15:**469.

9. **Sorge RE, Mapplebeck JC, Rosen S, Beggs S, Taves S, Alexander JK, Martin LJ, Austin JS, Sotocinal SG, Chen D, Yang M, Shi XQ, Huang H, Pillon NJ, Bilan PJ, Tu Y, Klip A, Ji RR, Zhang J, Salter MW, Mogil JS.** 2015. Different immune cells mediate mechanical pain hypersensitivity in male and female mice. Nat Neurosci **18:**1081-1083.

CHAPTER 6

FUTURE DIRECTIONS

This body of work has provided a substantial amount of additional information regarding SAPP. In Chapter 2 we presented data that documents the occurrence of novel clinical signs of SAPP, as well as the presence of inflammation prior to the onset of clinical disease in a small proportion of mice. In chapter 4, we investigated the role of the microbiota in the onset and severity of SAPP. We were also successful in transfer of cecal contents to weanling mice via oral gavage. We believe that the expected gut microbial community changes will be seen once the analysis of bacterial sequences from time points closer to the transfer are complete. Chapter 4 focused on altering the immunological parameters of the disease, with experiments that neutralized cytokine antibodies and generated heterozygote mice. Chapter 5 included 2 pilot studies run in parallel with each other to remove sex hormone influence from male and female mice.

Considering all that has been learned throughout the studies presented in this thesis, there is still more to investigate, including:

1. a more detailed description of the disease using a battery of phenotype tests that provide **quantitative** measures
2. reproducible blockage or reversal of SAPP
3. proof that without the presence of gut microbiota, SAPP does not occur

Phenotype tests with quantitative measures.

Motor function

The open field test is the “bread and butter” to mouse phenotyping. It provides video that can be analyzed after the study is over, as opposed to many other tests that require a decision in real time. Real-time experimental calls have been a point of debate and contention in recent literature because as there is no way to revisit them later or have a quality assurance done. The open field alleviates this potential pitfall because it is available for multiple people to review—there should be no significant differences in interpretation from person to person. As is

the case with anything in research, there is always an effort to improve upon existing techniques. In discussions with other researchers that use the open field test in their experiments, many researchers have suggested testing the mice under red light, instead of white light (personal communication). Filming mice in their home cages is also an option. It reduces the amount of anxiety triggered by unfamiliar spaces and scents; however, it presents the need for far more monetary and personnel resources. The feasibility of this decreases with experiments that have large samples sizes of mice.

As mentioned in Chapter 2, we have replaced the task of "footprinting" with ventral plane imaging (VPI), which is a fairly novel technique used to measure various aspects of mouse gait. The grip strength meter is an ideal instrument that measures the amount of force generated by a mouse when it pulls on a bar that is attached to the apparatus. This is an ideal test for the NOD.B7-2$^{-/-}$ mice because as they begin to develop SAPP, the amount of strength in their forelimbs and hind limbs will decrease. The grip strength meter can be adapted for the front or back of the mouse. This test should replace the pencil grip test and the hang test used our in prior studies, as mild deficits can be difficult to call with the pencil grip test, and some mice with moderate mild to moderate SAPP are able to adapt to hanging on the wire (hang test).

Sensory disturbances

While the grimace test is effective, it can be subjective if the facial expression is mild. In the original descriptive paper, it is graded on a scale of 0-2. Because of the subtlety of the expression with a score of 1, we modified the test with an "all or none" approach. Mice were given a score of 0 if there was no response, and a score of 1 if there was a grimace. In addition to this test, von Frey Hairs and hot/cold plate tests can be used to assess pain in these mice. It is clear from our work that they indeed do experience pain, but additional tests would allow us to measure the severity and follow the progression (or regression).

Germfree mice

We have started a germfree mouse project in collaboration with the University of Michigan, and have reached the stage where embryos have been removed from dams and frozen at -80°C. Moving forward, embryos will be transplanted into mice in germfree isolators and delivered via cesarean section to avoid passing through the vaginal canal, risking the potential of microbial inoculation. Allowing those pups to flourish will provide a definitive answer as to whether or not the intestinal microbiota plays a crucial role in the development of SAPP. The experiment would need to run for at least 35 weeks to answer this question.

Regulatory cytokines

The experiment done with neutralizing antibodies against IL-17 and IFNγ should be repeated, with a few key changes:

- There should be an experimental group that doesn't receive any injections
- I-17 and IFNγ should be administered for longer period of time
- Only female mice should be used

The role of B7-2

The role of B7-2 as a costimulatory molecule is well rehearsed in current immunology texts and review publications. However, it is evident from our work that mice with only one allege coding for the B7-2 gene results in two separate diseases in heterozygote mice. At this point, we have concluded that the disease is either diabetes or SAPP, but not both. This begs the question of “What other portion of the immune system is affected?” It is clear that the B7-2 molecule does not determine a specific target organ for inflammation. Our focus then shifts to pancreas and the sciatic nerve. The “common denominator” in those organs are Schwann cells. They are found in peri-islet areas in the pancreas and form the myelin that covers axons in the peripheral nervous system. They both share a common antigen, so it is not wrong to assume that each organ would be attacked equally by the immune system. If that is the case, then why

is there not both pancreatic and peripheral nerve inflammation in the NOD WT, NOD.B72$^{-/-}$, and NOD.B7-2$^{+/-}$ mice? There are several missing pieces to the NOD immunoregulatory derangements in general, but in the case of the heterozygote mice, one has to wonder if the amount of CD86 protein present makes a difference in the target organ differentiation. To this end, it would be worth it to measure the amount of CD86 protein present in all three of the aforementioned strains of mice. At the same time, it would be imperative to keep clinical records of disease outcome, including the age of onset and human endpoint in the mice: 1) diabetes 2) SAPP 3) diabetes and SAPP 4) no disease. This data would provide further insight into the clinical disease course.

Gene Expression Studies

Studies that incorporate bacterial gene expression are necessary to complete the microbial community portion of this work. While the 16S sequencing has given us insight into the bacteria that are present in the gut when the mice are weanlings, 20 weeks old, and 36 weeks old, it would be worth it to understand if there is a difference in gene expression between mice that develop SAPP and mice that do not. For this answer, weekly samples can be taken from mice in the colony, from weanling age, through adult hood at various intervals. Samples from 15 female mice and 15 male mice would be sufficient to develop baseline data, which can be compared and contrasted to data gathered from mice in future mechanistic studies. Once this information is gleaned, we can begin to investigate the regulatory role, if any, of various gene differences on sex hormone production and systemic inflammation, through the bacterial gene knockdown studies. In contrast to the process for DNA extraction used for sequencing where samples could be frozen before extraction, fecal samples would need to be processed immediately after collection for the gene expression analyses. Experimental groups of weanling mice for gene expression studies should consist of:

- Female mice transferred with donor male cecal contents
- Female mice given test vehicle

- Male mice transferred with female donor cecal contents
- Male mice given test vehicle

Earlier Ovariectomy Timepoint

In order to see the desired effect of ovariectomy and removal of estrogen influence, mice should be ovariectomized at an earlier time point. The two time points proposed are weanling age (3 weeks) and reproductive age (6 weeks). In addition, equal sample sizes of mice should be used.

Castration for Removal of Testosterone Influence

Castrating male mice removes the effects of testosterone without the side effects of possible toxicity. The downside to investigating SAPP this way is that there is no way to add it back naturally. If an androgen receptor blocker, such as flutamide, was used as the test article, it could be withdrawn at any time and endogenous testosterone would be able to bind to its receptor.

Data Analysis (group vs individual)

Evaluating the mice over time, for each individual parameter may yield valuable information that can be masked when evaluating mice as a group. The statistics may be a bit difficult to handle because of all of the different parameters, but it is worth the effort; even a small difference in response can be promising. The NOD.B7-2$^{-/-}$ mice are inbred—they are the same, yet different. Finally, because of the difference in pain pathways between male and female mice, it may be appropriate to use only females in studies in which pain will be evaluated.